EFFECT OF AGGRESSIVE GAS ON SEPARATION PROPERTIES OF CARBON MOLECULAR SIEVE HOLLOW FIBER MEMBRANES

A Thesis
Presented to
The Academic Faculty

by

Shweta Karwa

In Partial Fulfillment
Of the Requirements for the Degree
Doctor of Philosophy in the
School of Chemical and Biomolecular Engineering

Georgia Institute of Technology

May 2016

EFFECT OF AGGRESSIVE GAS ON SEPARATION PROPERTIES OF CARBON MOLECULAR SIEVE HOLLOW FIBER MEMBRANES

Approved by:

Dr. William Koros, Advisor
School of Chemical and Biomolecular Engineering
Georgia Institute of Technology

Dr. Dennis Hess
School of Chemical and Biomolecular Engineering
Georgia Institute of Technology

Dr. Pradeep Agrawal
School of Chemical and Biomolecular Engineering
Georgia Institute of Technology

Dr. Paul Jason Williams
Shell International Exploration and Production (US) Inc.
Shell Technology Center (Houston)

Dr. David Bucknall
School of Materials Science and Engineering
Georgia Institute of Technology

Date Approved: December 10th, 2015

Dedicated to my parents and siblings. I love you.

ACKNOWLEDGEMENTS

This PhD has been a real learning experience - it has given me time to think about life philosophies, taught me to deal with problems, and really made me an adult. It is an understatement to say I have learned the value of patience, perseverance and hard work through this often stressful venture.

I want to deeply thank my parents for molding me into who I am today and for always believing in me. They have instilled in me a desire to achieve, and I am indebted to them for their unconditional love and immeasurable sacrifices. My awesome siblings Shruti and Anand have always been there for me, pushing me to do my best every day. I am indeed blessed.

Funding support from Shell Global Solutions is greatly appreciated. Dr. Jason Williams and Dr. Joseph Mayne have provided invaluable advice and I am truly glad for the incredible interactions over teleconferences and meetings we have had over the last 4 years. I am also grateful to my committee members, Dr. Pradeep Agrawal, Dr. Dennis Hess and Dr. David Bucknall for their technical insight and feedback in my thesis. Their valuable suggestions and comments have been very useful in shaping this work.

It has been a pleasure to work with the Koros group, and all members past and present deserve acknowledgement. I wish to particularly thank Ruben Kemmerlin and Dr. Nitesh Bhuwania for their guidance during the initial years of my PhD.

I would like to thank all my friends, both in the U.S. and in India. I have survived grad school because of all the good times with them. They have always been eager for

weekend getaways, stimulating conversations, long trips and have made my life wonderful. I would especially like to thank Dr. Aritra Sengupta, for helping me through every step of my PhD, and without whose support I would be a different person.

Outdoor Recreation at Georgia Tech and the Student Government Association have been great in getting me involved in campus life as a grad student. They have given me the space and the mental capacity to compartmentalize work and hobbies, and have immensely added to my experience at Georgia Tech.

Most importantly, I want to sincerely thank my advisor Dr. William Koros for everything. He has been around in times I could not have imagined myself go through, and has been a great influence. It is marvelous to see his devotion to work, his energy and humbleness. He has encouraged me through good and bad times alike, always leading by example. It has been a privilege to work with him.

TABLE OF CONTENTS

LIST OF TABLES

LIST OF FIGURES

SUMMARY

Natural gas is gaining importance in the industry as a clean fossil fuel, and its demand is expected to increase from 111 trillion cubic feet in 2008 to increase to over 169 trillion cubic feet by 2035. With the above scale of operations for natural gas production, there is a vast requirement for processing and purification of natural gas. Carbon dioxide (CO_2) and hydrogen sulfide (H_2S) are acid gases commonly found in raw natural gas streams that must be removed prior to consumer use. While absorption based purification techniques are popular in the industry for this purpose, they are also high cost and high energy consuming processes. Thus, tremendous energy and cost saving possibilities exist in the natural gas business if a more energy efficient gas separation process such as membrane separation can be used more extensively.

A practical membrane separation process is considered in this study for removal of CO_2 from natural gas in the presence of H_2S. Carbon molecular sieve (CMS) materials derived from Matrimid® and 6FDA:BPDA-DAM have been used for this particular separation. Hollow fiber CMS membranes created from the above polymers show substructure collapse, which increases the separation layer thickness, thereby reducing productivity significantly. To prevent this substructure collapse, a proof of concept pre-pyrolysis treatment called V-treatment has been shown earlier to be effective. Optimization of this V-treatment for CMS from both the polymers has been done in this study. The exposure time, exposure temperature, and concentration of treatment agent have been optimized and shown to prevent collapse, thereby producing membranes with productivity higher than untreated samples. Most importantly, it was proven that this method is scalable.

Details of interaction of H_2S with CMS membranes were also clarified in this work and found to be different for CMS starting from different precursors. In addition to the measured changes in transport performance, analytical characterization techniques including FT-IR and TPD prove that H_2S conditions CMS membranes by chemical interaction. The H_2S conditioning leads to a permanently reduced permeance through the CMS membrane, thereby making the membrane less attractive for industrial use. To prevent this conditioning, a novel method, called chlorine fixation, for neutralizing the reactive edges of the CMS was explored. Chlorine reacts with the carbons in the CMS membranes and renders the sample less sensitive to the incoming H_2S. Although this resulting membrane starts with a lower, yet industrially acceptable permeance, it is partially resistant to H_2S.

Combining the V-treatment and chlorine fixation together was checked for enhancement of separation properties, after long exposure to H_2S. This is also done while adding no extra steps in the production of CMS membranes, therefore retaining the time and cost of the entire process. Like all CMS membranes, aging is a problem faced by the V-treated membranes.

The current study focuses on benchmarking the performance of CMS membranes in a sour gas feed, and considerations related to mitigating the condition of the membranes must be studied in further detail. This work establishes a framework for providing a potentially practical hollow fiber membrane technology for aggressive gas separation.

CHAPTER 1 INTRODUCTION

Natural gas has become increasingly important over the last few years as a clean fossil fuel [1]. Due to its better burning efficiency, natural gas results in lower carbon dioxide (CO_2) emissions [2] and produces significantly lower quantities of other atmospheric pollutants such as sulfur dioxide (SO_2), nitrogen oxides (NO_x), and particulate matter.

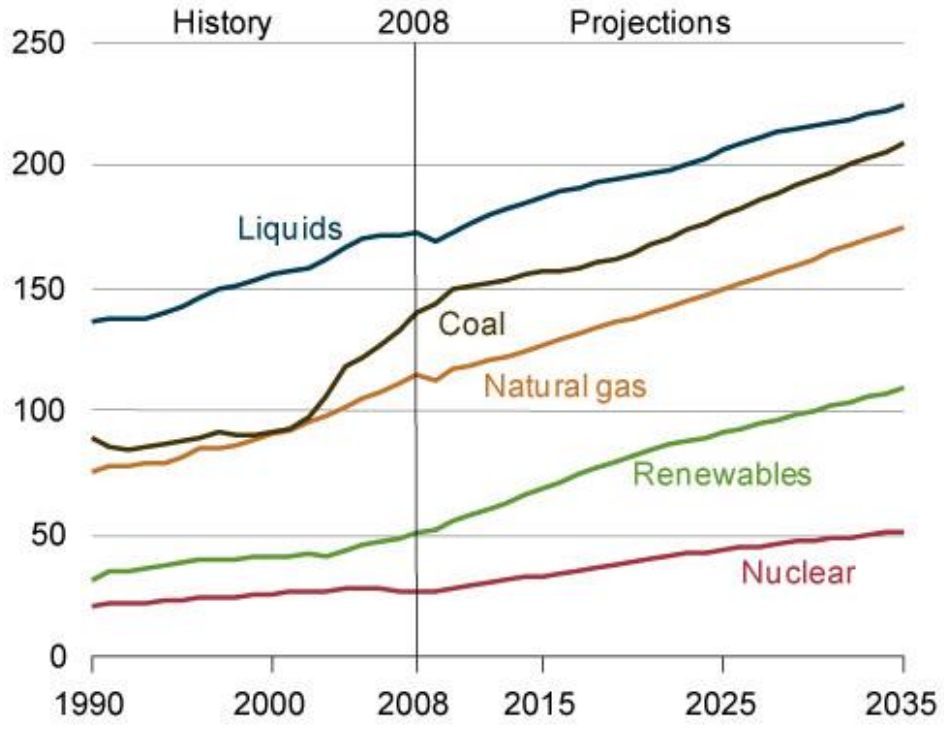

Figure 1: World energy consumption by fuel source, 1990-2035 in BTU [3]

The International Energy Outlook 2011 predicts a 40 % increase in natural gas consumption in the next 20 years [4]. The annual global consumption of natural gas, shown in Figure 1, exceeded 111 trillion cubic feet (Tcf) in 2008, and is expected to increase to

over 169 Tcf by 2035 [5]. The U.S. consumption of natural gas alone is expected to increase from 26.2 Tcf (26.9 quadrillion BTU) in 2013 to 29.7 Tcf (30.5 quadrillion BTU) in 2040, as shown in Figure 2. With a demand this high, there is also a requirement to economically and efficiently extract natural gas from many reservoirs and purify it to a serviceable standard.

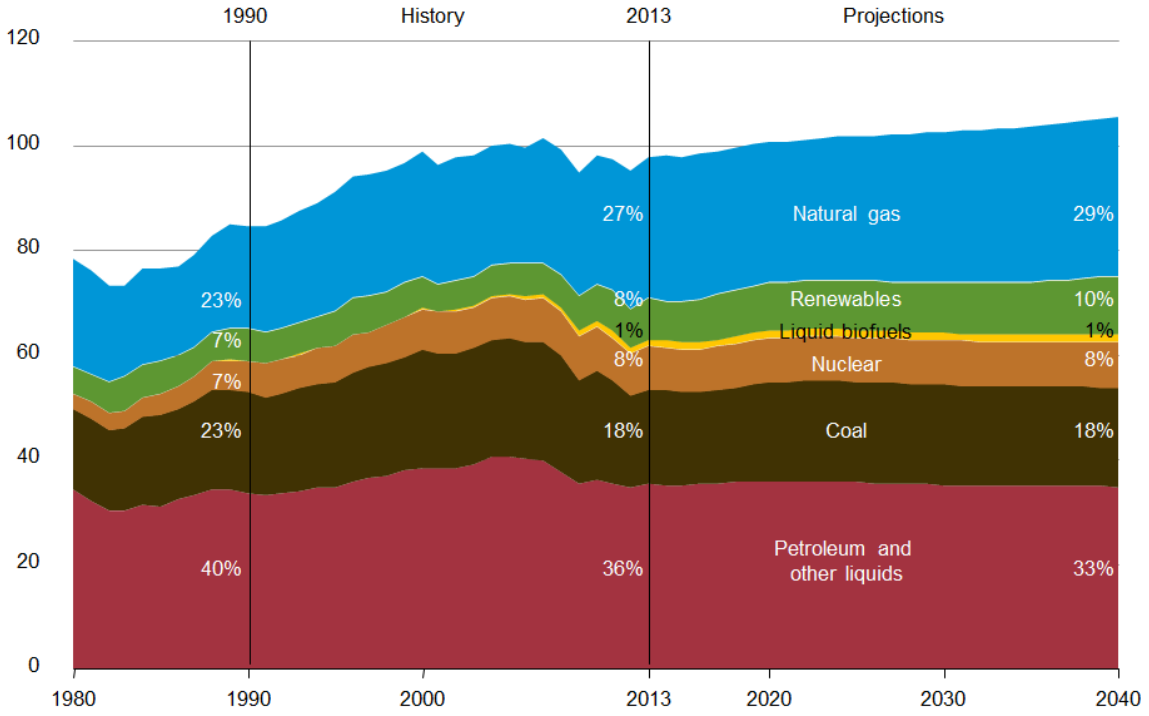

Figure 2: U.S. energy consumption by fuel source, 1980-2040 in BTU [6]

Raw natural gas comprises mainly methane (CH_4) with varying levels of contaminants such as carbon dioxide (CO_2), water (H_2O), hydrogen sulfide (H_2S), higher hydrocarbons, and inert gases including nitrogen (N_2) and helium (He). Not only do these impurities increase compression cost for processing of the natural gas, but they also

decrease its heating value. Moreover, the concentration of these corrosive (CO_2) and toxic (H_2S) contaminants must be reduced below a specified level meet the US pipeline quality standards, listed in Table 1 [7].

Table 1: US pipeline regulations [5]

Component	**Specification**	**Concentration found in U.S. natural gas wells**
CO_2	< 2 %	< 1 – 40%
H_2O	< 120 ppm	
H_2S	< 4 ppm	< 4 ppm – 5%
C_{3+} content	950-1050 Btu/scf; Dew point: < -20°C	0 – 20%
Inerts (N_2, He, etc.)	< 4 %	> 4%

Acidic gas contaminants comprising CO_2 and H_2S are particularly detrimental, as they are present in significant quantities in many reserves. In their 2007 report [8], Total notes that nearly 40 % of the world's gas reserves contain levels of CO_2 and H_2S that pose obstacles to development, overcoming which is a key challenge for oil companies. In some areas of the world like the Middle East, Canada and the Far East, oil and gas fields can contain a significant amount (up to 35%) of H_2S in the raw natural gas stream [9, 10]. In the US alone, 13% of proven natural gas reserves contain elevated levels of both CO_2 and H_2S [11]. There is increasing interest in producing sour fluids as sweet gas reserves mature over time. Many sour reservoirs are deemed to be prolific producers, which can lead to

large volumes of hydrocarbon resources for markets which can absorb the additional costs incurred by the production of sour gas [12].

As noted earlier, the acid gases CO_2 and H_2S also cause corrosion of transport equipment and pipelines, compressors, pneumatic equipment and transmission lines. The term "sour gas" is used specifically when natural gas contains significant amounts of H_2S, while "acid gas" can refer to any natural gas containing considerable amounts of both CO_2 and H_2S. When natural gas contains H_2S exceeding 5.7 milligrams of H_2S per cubic meter (~ 4 ppm), it is called 'sour gas,' indicating that H_2S has a foul smell of rotten eggs. Removal of sulfur impurities from natural gas is called "sweetening", again to signify that the pungent smell is eliminated from sour gas.

Apart from the unpleasant smell, also as noted above, H_2S is highly toxic as a gas by itself. Very low concentrations of H_2S can be harmful or fatal to human beings. Table 3 provides toxicological information of H_2S [4].

Table 2: Toxicological information of H_2S [4]

Specification	**Concentration of H_2S**
OSHA Permissible Exposure Limit (PEL)	10 ppm
OSHA Permissible Exposure Limit (PEL) ceiling	20 ppm
Lethal Concentration (LC_{50})	800 ppm / 5 minutes

Because of the low permissible exposure limit (PEL = 10 ppm) and lethal concentration of H_2S (LC_{50} = 800 ppm), removal of H_2S from natural gas is a high priority [4]. It is essential to reduce the concentration of H_2S below 4 ppm for it to be safe and non-

corrosive to transportation equipment and industrial handling. Since H_2S is so toxic and corrosive, sour gas needs to be handled extremely carefully, both on the lab scale and industrially.

1.1 Gas Separation Overview

Separation processes as a whole make up 40-70% of operational costs and capital in industry [13]. Therefore, the natural gas industry is always seeking more efficient separation technologies [5].

1.1.1 Existing Technologies for Separation

Common natural gas sweetening process and removal of acid gases like CO_2 include absorption into liquids, adsorption onto solids such as pressure swing absorption (PSA) and temperature swing adsorption (TSA), chemical conversion, and cryogenic distillation.

The most common of these sweetening processes are amine and physical absorption, accounting for nearly 70 % of all the techniques used for treating raw natural gas. Amine absorption is a very efficient process where large streams of raw natural gas are treated with liquid amine (such as monoethanolamine, diethanolamine, diisopropanolamine, diglycolamine, or methyldiethanolamine) to remove both CO_2 and H_2S [14]. A typical amine absorption process for acid gas removal is shown in Figure 3. The sour gas is fed into the amine absorption column (contactor), where the methane is stripped of the acid gases and "sweetened."

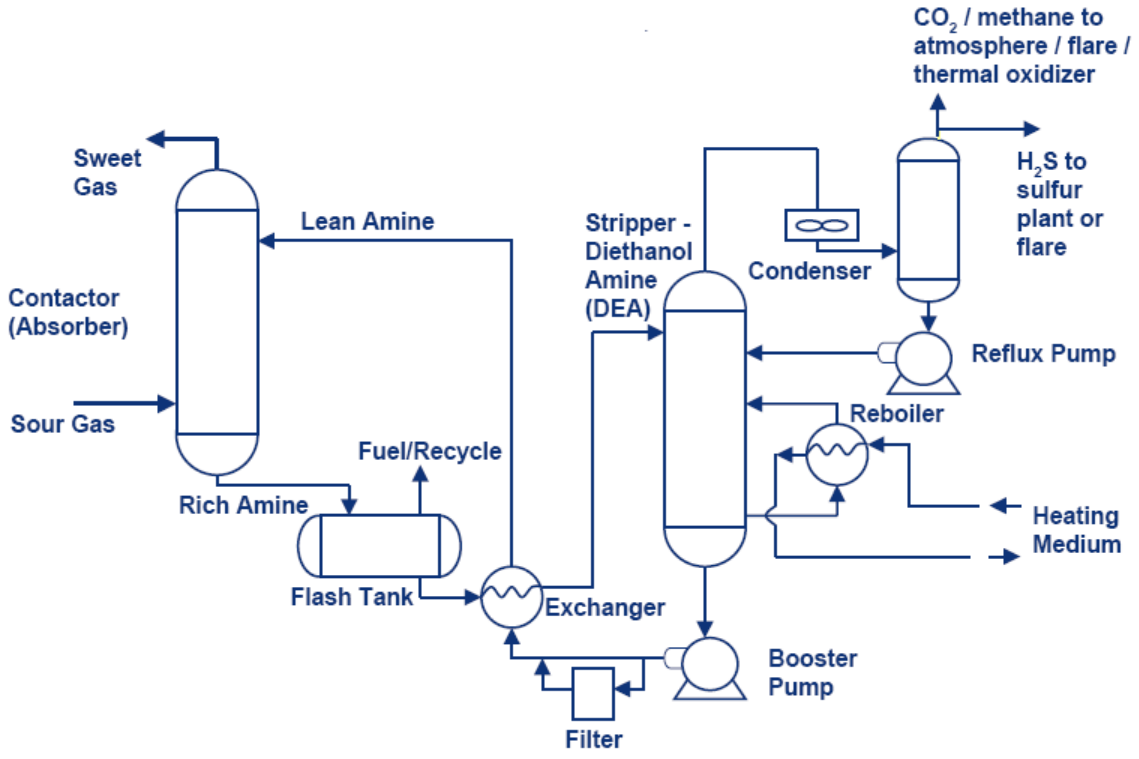

Figure 3: Typical amine absorption process for removal of acid gases in natural gas processing [15]

When the amine solution gets saturated, it is thermally regenerated to flash off the acid gases in the stripper. Plants handling large volumes of sour gas containing greater than about 200 ppm H_2S usually use this amine-based technology for acid gas removal. Amine treatment, however, is a capital and energy intensive process. It has high costs associated with maintenance, operation, and regeneration of amine. The size of the equipment is proportional to the mass of the material to be absorbed, and therefore the capital cost of such a thick walled and complex equipment is also high. Additionally, the material cost for the amines used and the cost of thermally-driven regeneration of amine solvent, and the relatively high maintenance for it, leads to large expenditure to the companies [5].

Chemical treatments are used for streams containing less than 100 ppm of H_2S. Processes like scavenging or sulfur recovery processes like Sulfa-Scrub, Sulfa-Check, Chemsweet, Suertron 600, solid iron sponge or solid zinc oxide are used as an alternative or as a polishing step following absorption processes [14-19]. In these techniques, H_2S is chemically adsorbed on a solid and the adsorbed gas is converted to a waste product that is less harmful. However, many of the scavenged waste products present considerable disposal problems and can comprise toxic waste.

Cryogenic or high pressure distillation processes are used for removal of N_2 from CH_4 since these gases are both very similar to each other in size, or for olefin/paraffin separation. Cryogenic distillation is a very cost intensive process, since the gases must be cooled to very low temperatures, in large feed streams, and is not profitable to use in gas streams with higher percentages of N_2. Olefin/paraffin separations in the petrochemical industry are currently carried out by high pressure distillation processes, which are very energy intensive as well [20, 21]. All of these traditional processes can, in principle, be replaced by membrane alternatives.

1.1.2 Membrane separation of gases

While amine absorption is still the primary method used for acid gas separation, polymeric membranes have gained importance recently [22]. A summary of the development of membrane gas separation technology was made by Baker [23]. He has shown the evolution of membrane starting from Graham's Law of Diffusion in the mid 1800's to the development of anisotropic membranes, and spiral wound and hollow fiber configurations were advances in the technology. Since then different kinds of membranes (zeolites and polymers) have been explored for O_2/N_2, H_2/N_2 and H_2/CH_4 separations by

different companies. Medal first started using polyimide membranes for CO_2/CH_4 separation in 1994.

Membrane-based gas separation has grown significantly as a business, and substantial growth in the future is projected. As an alternative or a supplement to amine absorption, membrane technology offers high efficiency, reduced environmental impact and good scalability for natural gas purification [14]. Membrane processes also benefit from the fact that the driving force of this separation i.e. the pressure difference is essentially "free", which comes from existing natural gas well pressures typically in excess of 1000 psi. In addition, the compact and modular design of membrane systems leads to process intensification. They also have a smaller environmental footprint. The relative sizes of a membrane unit and the amine absorption unit can be observed in Figure 4. The membrane unit (circled in green) is shown relative to the large columns of the amine absorption unit that it replaced when the amine unit had to be decommissioned due to corrosion. Membrane units are normally skid-mounted and modular, involve fewer moving parts, and can provide outstanding separation surface area-to-volume ratios.

Figure 4: A skid-mounted membrane unit (circled in green) was installed to replace a bulky amine absorption process (in background)

The membrane separation market is continuing to grow, and it is predicted to be 30% for natural gas purification by 2020 (Figure 5). Membranes have been primarily used for air separation, CO_2 removal from natural gas, and hydrogen separation. Polymeric membranes like cellulose acetate and polyimides are used for gas separations because of their relatively easy processability. Hybrid membrane-absorption processes also offer high value as a separation process setup. These are particularly useful when the concentration of contaminants like CO_2 and H_2S are very high, making the membrane separation step ideal for bulk contaminant removal and the secondary absorption can be used to fine tune the concentration to meet pipeline regulations.

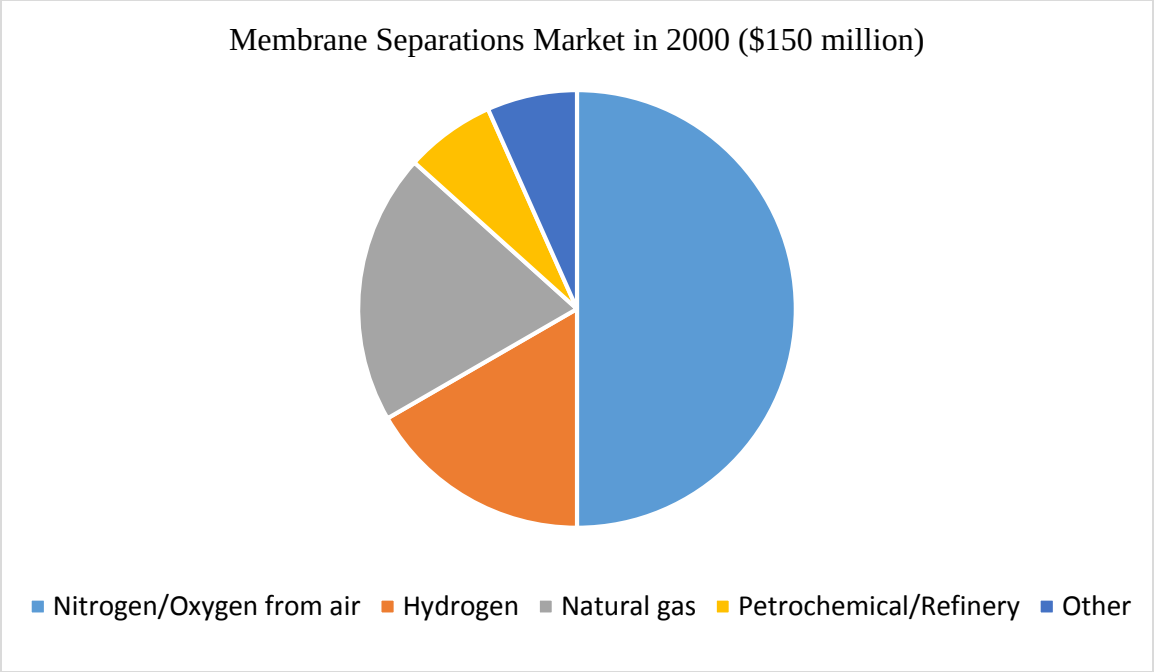

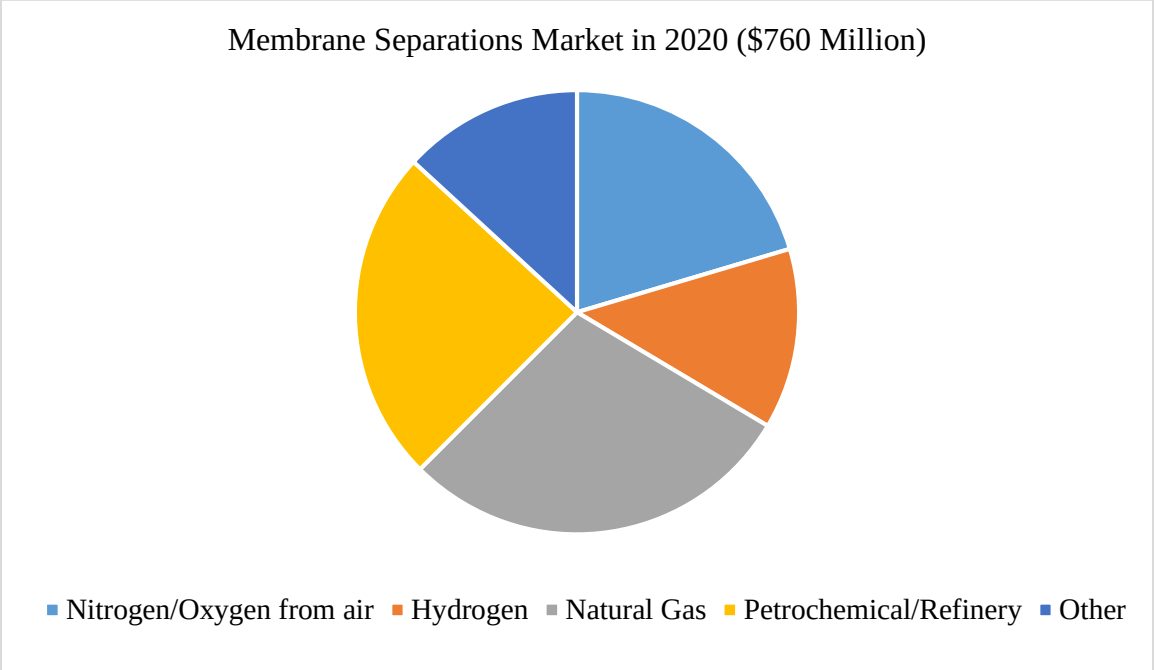

Figure 5: Membrane separation market share in year 2000 and projection for year 2020 for different areas of separation [23, 24]

If membrane separation replaces amine absorption, that will reduce natural gas cleanup and its environmental impact. The cost saving would ultimately transfer to the end user, making it easier for people to access natural gas, and easier for oil and gas companies to provide natural gas to consumers who don't have access to low cost fuel. For all these encouraging reasons, this work will focus on membranes to purify natural gas.

1.1.3 Why Carbon Molecular Sieves (CMS)

For a membrane to be economically viable industrially for separation, it has to have the following characteristics:

- High flux through the membrane
- High selectivity for application specific gases
- Mechanical durability
- Economical to produce on large scale
- Adequate tolerance to process pressures and temperatures
- Stability towards all components of the feed gas

Traditionally, polymeric membranes have been used for gas separation. Industrially synthesized polymers also have been used for O_2/N_2 separation widely. Polymeric membranes have excellent processability, are easy to handle and low cost to produce and maintain. Many researchers have used polymeric membranes even for natural gas purification; however, polymeric membranes have faced two major hurdles that hinder broader industrial use. Robeson [25, 26] has showed that for various gas separations, solution processable polymers are limited by an "upper bound". The upper bound for CO_2/CH_4 separation is shown below in Figure 6.

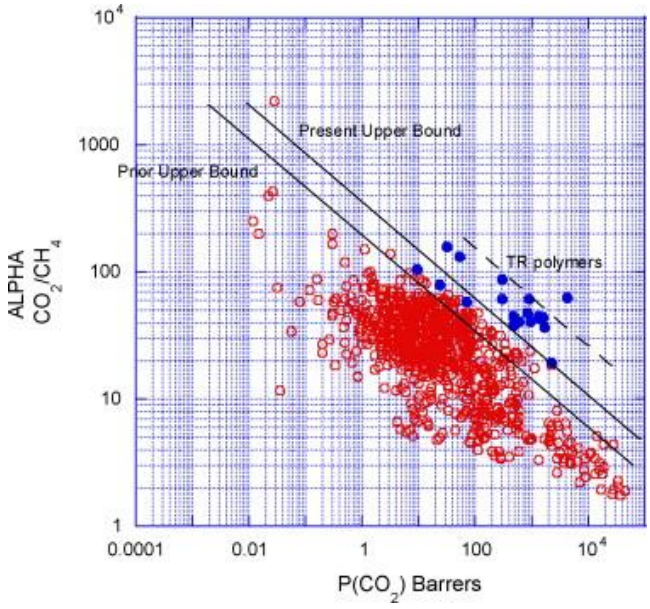

Figure 6: Robeson's upper bound for CO_2/CH_4 separation using polymeric membranes [26]

As researchers produce newer polymers with higher fluxes (permeabilities shown on the x-axis), those polymers exhibit lower efficiencies of separation (CO_2/CH_4 selectivity on the y-axis). When new polymers are synthesized with properties that are tuned to give higher selectivities, their productivities are low. Ideally, membranes that can give high throughput as well as high separation efficiency are desired. For this reason, it is wise to explore other membrane materials with desired transport properties. It is reasonable to pay some price for using these newer suited membranes for separation in terms of cost, mechanical strength and ease of industrial processability; however, the cost is always an issue.

Another problem that polymer membranes often have to face is plasticization under high pressures of some gases [27]. When the polymer membrane is subject to a high pressure of a highly sorbing feed gas, as would be in the case of natural gas with high levels of acid gases, they undergo plasticization. Plasticization is a phenomenon in which high feed pressure of a highly condensable gas such as CO_2 and H_2S, causes the polymer chains to swell up, thereby reducing selectivity.

Polymer membranes are, of course, not the only candidates used for gas separation using membrane technology. Metal organic frameworks, ceramics, zeolites, and activated carbon have been studied by researchers; however, due to their mechanical processability and lower cost, polymer membranes and materials derived from polymer membranes have a distinct advantage over other materials.

Carbon Molecular Sieves are a relatively new class of materials, which can overcome both these drawbacks of polymers. Carbon molecular sieves (CMS) are made by controlled thermal decomposition of polymers in inert atmosphere at high temperature, which show higher permeability and selectivity than regular polymer membranes. Additionally, CMS membranes avoid the plasticization problem, since the basic structure of CMS is rigid. Because of these reasons, this thesis will focus on CMS membranes. CMS membranes, their synthesis, structure, and properties are discussed in more detail in Chapter 2.

1.1.4 Why hollow fibers

Membranes can be produced in several different morphologies – plate and frame, dense films, spiral wound and hollow fiber morphology shown in Figure 7. The dense film morphology is the most effective to use during the fundamental study of a material.

However, dense films offer low throughput membranes and are not commercially attractive for large scale operation that require high rate of output. On the other hand, hollow fiber membranes provide a high surface area to volume ratio and can also be manufactured with smaller selective layers and are much more industrially relevant. Moreover, hollow fiber modules exhibit good gas flow distribution and have the facility for cross flow.

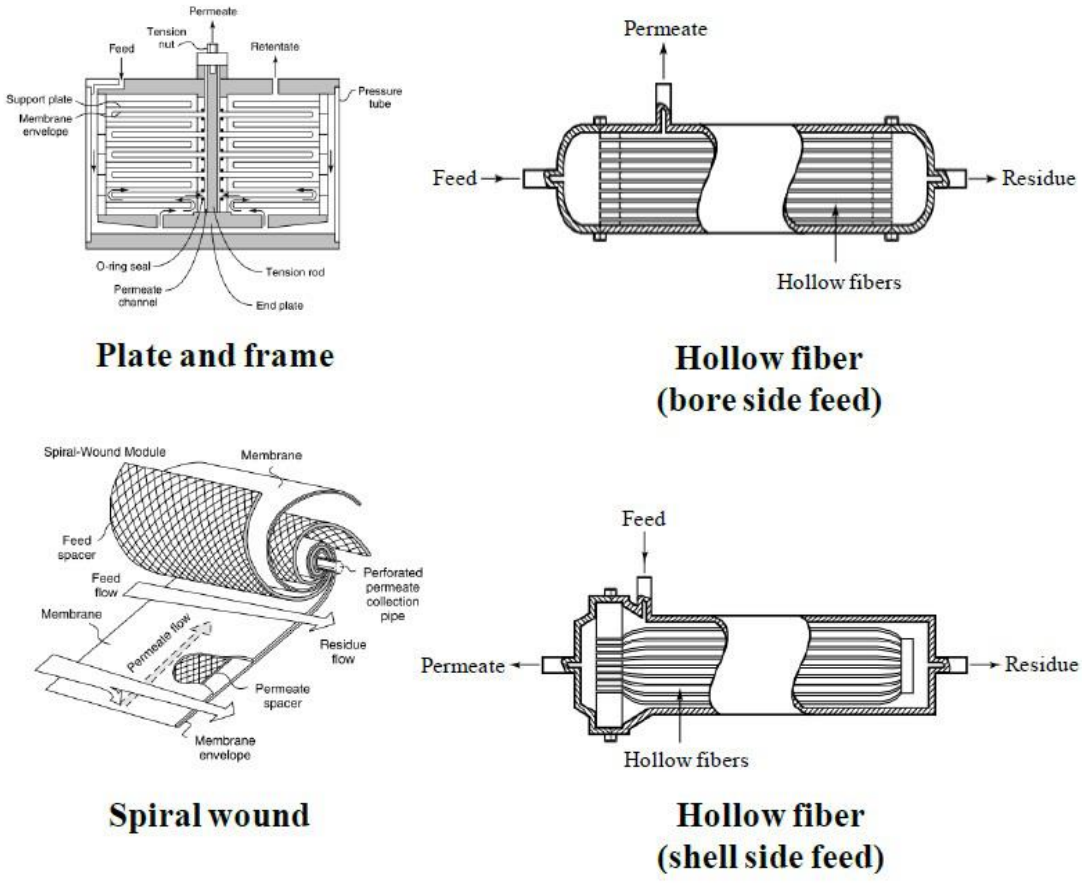

Figure 7: Different configurations of membranes commonly used in industry [23]

Asymmetric hollow fibers are thin cylindrical membranes, and can be spun in a continuous process. They have a very thin skin layer which is dense and responsible for the separation of gases. Beneath the skin layer is a highly porous and mostly unselective part that serves as support for the skin layer, and is referred to as the porous sub-structure. The support has a very open interior and provides minimal resistance to mass transfer through it [28]. Specifically for CMS membranes, the asymmetric hollow morphology is preferred over homogeneous flat sheets from a practical point of view because of better strength and flexibility, due to the selective "skin" layer supported by the porous sub-structure. Such small diameter, cylindrical morphologies provide high surface area-to-volume ratios, with the ability to withstand large transmembrane driving force pressure differences.

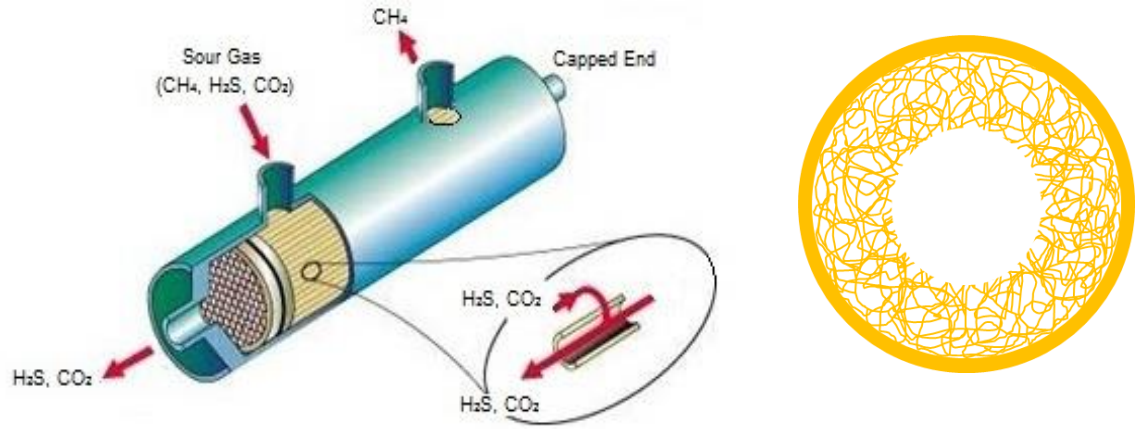

Figure 8: Illustration of an asymmetric hollow fiber setup for sour gas separation (left - adapted from [29]) and cross section of asymmetric hollow fiber (right)

Hollow fibers offer very high fluxes per unit volume, since their surface area-to-volume ratio can be as high as 10,000 m^2/m^3 for fibers with small diameters, which favors hollow fiber membranes for industrial use.

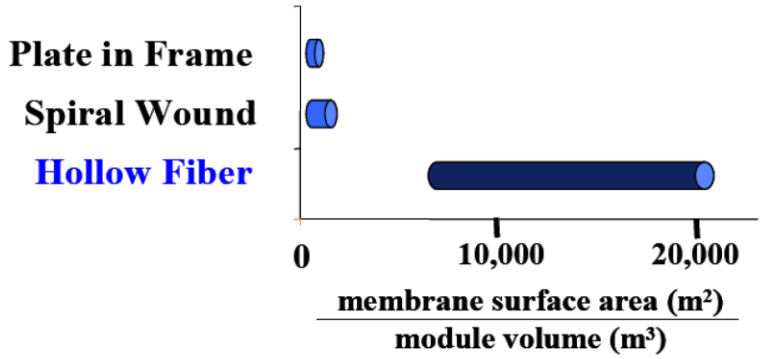

Figure 9: High surface area to volume ratio of hollow fibers when compared to dense films and spiral wound membranes [30]

The skin layer thickness of these membranes can be as low as 100 nm – 1 micron, and the outer diameter of the membrane can be of the order of 250 microns. A more in depth discussion of production and properties of these hollow fiber membranes is provided in Chapter 3.

1.2 H_2S removal with CO_2

CO_2 removal from CH_4 by membrane separation has been studied in detail, since CO_2 is the most commonly found contaminant in natural gas and that there are many CO_2 contaminated reserves throughout the world. However, little academic research has considered H_2S/CH_4 separation because H_2S is highly toxic and corrosive. The subsequent disposal of H_2S after separation is also relatively more difficult. Handling and safety regulations for H_2S are stringent both industrially and academically, so H_2S separation from CH_4 still remains a subject of industrial research much more than academic research due to the large risk involving dealing with H_2S. There is even less academic research on

removing both H_2S and CO_2 from CH_4; however, as the world's natural gas reserves are used, sour gas sweetening is increasingly important to provide the world with clean natural gas. Recall, as noted earlier, almost 40% of the world's remaining reserves are contaminated with sour gas [8], so efficient separation technology for sour gas sweetening has become increasingly important.

Most academic research has focused on removal of H_2S from CH_4 using rubbery polymers and only considers feeds with low percentages of H_2S. While rubbery polymers such as polyether-block-amide show high H_2S/CH_4 separation properties, they have low CO_2/CH_4 separation efficiency and industrially unappealing mechanical properties. Cellulose acetate has been shown to perform well for both the separations with some pre-treatments, however it cannot function well under high acid gas feed conditions due to plasticization [15]. Glassy polymers on the other hand have excellent CO_2/CH_4 separation but low H_2S resistance and H_2S/CH_4 separation efficiency. Removal of CO_2 and H_2S simultaneously has been studied very less, and is typically unimpressive for an industrially relevant process.

It is therefore important to study CMS membranes, a relatively new class of materials which show promising properties, for simultaneous separation of CO_2 and H_2S from CH_4. In this work, all the above factors have been given careful consideration before choosing CMS as the material of choice. As advanced materials, CMS membranes show very promising properties in the fundamental studies with homogeneous dense films as well as in hollow fiber morphology. Therefore, CMS hollow fiber membranes will be used in this work for separation of H_2S and CO_2 from CH_4.

1.3 Specific Aims and Hypotheses

The overarching goal of this project is to understand the key fundamental and practical principles to allow producing a purified product of CH_4 by separating its acid gas contaminants, CO_2 and H_2S, using CMS hollow fiber membranes. The process should have a high throughput and high efficiency, at high pressures of sour gas. We have taken care to ensure the process can be made scalable to large sizes.

There are two major issues with achieving this goal:

1) *Substructure collapse*: Good permeabilities and selectivities were achieved for CMS dense films by tuning important factors during the final pyrolysis; however, for the CMS hollow fibers a major drop was observed in permeance. It was seen that a significant difference exists in the effective separation layer thickness between precursor fibers and their resultant CMS fibers. SEM results showed that the deviation was essentially due to the collapse of the porous substructure of the precursor fiber as shown in Figure 10. When hollow fibers are pyrolyzed, the pores that supports the skin layer collapse to form a dense thick layer that adds additional resistance to mass transfer through the membrane. This leads to lower permeance (P/l) than expected through the CMS hollow fiber membrane, where P is the intrinsic permeability and l is the separation thickness.

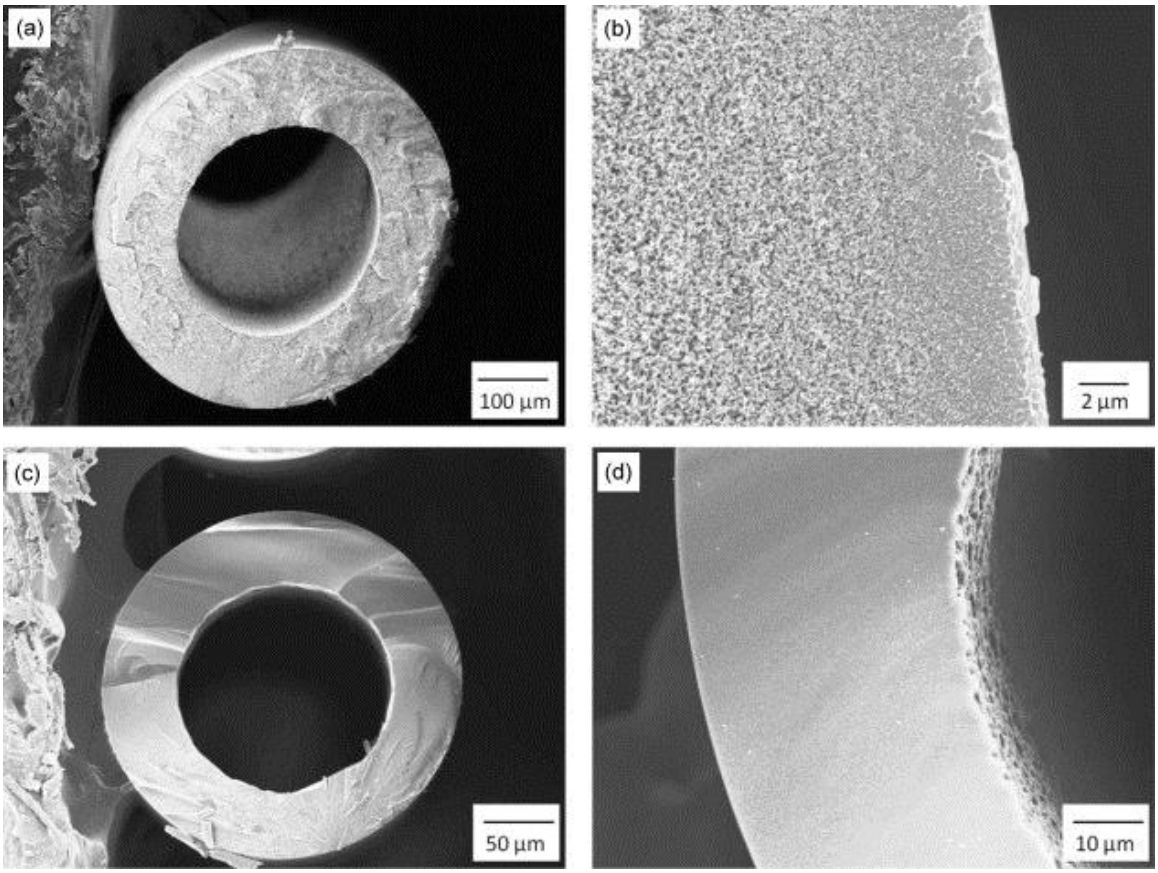

Figure 10: SEM images of the Matrimid® precursor fiber (a) and (b) and resultant CMS fiber (c) and (d) [31]

The Koros group has developed a process referred to as V-treatment that prevents collapse of the porous substructure in the precursor fiber during pyrolysis; however, this process has not been explored in depth for CMS membranes made from the polyimide 6FDA-BPDA:DAM. It has also not been used for CMS membranes for H_2S removal. This process prevents the CMS hollow fiber from collapse by maintaining the selective skin layer thickness similar to that of the precursor fiber. This results in especially high permeances, and similar selectivities as compared to the collapsed CMS hollow fibers. This V-treatment process will be used extensively in this project.

2) *H_2S poisoning*: Once CMS membranes are formed, they are tested for productivity with various gases like CO_2, CH_4, H_2S, etc. It was expected that the CMS membranes would be stable to all these gases at operating pressure and temperature. Preliminary H_2S/CH_4 separation data showed attractive productivities and efficiencies; however, it was observed that the flux of gases through the CMS membranes dropped with exposure to H_2S. A significant change was seen as the membranes were continually exposed to moderate levels of H_2S (10/90 H_2S/CH_4 feed at 50 psia at 35 °C) [32]. This change in properties suggests that H_2S interacts with the CMS membranes and effectively "poisons" the membrane. Since there is hardly any literature available that studies CMS in presence of H_2S, this project will study the interaction of H_2S and CMS material to understand the dynamics, and propose methods to deal with H_2S conditioning.

A plan was drawn to address these two main issues separately, and then combine their results to give a membrane that yields high fluxes, and at the same time is resistant to the aggressive nature of H_2S. This thesis plans to test following hypotheses to solve the challenges mentioned above.

Hypothesis 1: V-treatment would be able to prevent sub-structure collapse for CMS membranes made from 6FDA-BPDA:DAM. The process will be done on fibers from 6FDA:BPDA-DAM and an optimization will be performed with respect to time, concentration and temperature required for the V-treatment process.

Hypothesis 2: H_2S reduces the permeance of CMS fibers, by lowering the sorption and diffusion coefficients of the CMS membranes. This will be tested by measuring the permeance of CO_2 and CH_4 through the CMS fibers before and after conditioning with

H_2S. Sorption experiments will be conducted to determine if the sorption coefficient has been changed. H_2S interaction with CMS will be understood through characterization.

Hypothesis 3: Interactions of H_2S with CMS can be controlled by functionalizing CMS. The CMS will be reacted with some dopants to study whether the fixation of dopant atoms can make the CMS inert to H_2S.

The overarching goal of this study is to advance the ability to engineer and understand CMS asymmetric hollow fiber membranes with a focus on natural gas purification by removing impurities like CO_2 and H_2S from the primary CH_4 constituent. This goal can be broken down into following three objectives:

Aim 1: V-treatment: *Engineer the asymmetric hollow fiber membranes to achieve superior separation properties.*

Aim 2: H_2S conditioning: *Obtain a fundamental understanding of interaction of H_2S with carbon molecular sieves.*

Aim 3: Stabilization against H_2S: *Engineer CMS hollow fiber membranes to resist aggressive sour gas feed conditions and characterize the membranes, to optimize separation performance.*

By the end of this endeavor, this work will provide a fundamental understanding of how H_2S affects CMS membranes. It will also explore the possibility of doping a CMS hollow fiber membrane with chlorine to make it adequate to perform a primary bulk separation of methane from CO_2 and H_2S. The experimental techniques developed in this

work will contribute to development of new techniques for membrane separation. The final part will also assess whether the impact of H_2S on CMS membranes is reversible or irreversible.

CHAPTER 2 THEORY AND LITERATURE REVIEW

Membrane based separation relies upon the basic fact that different materials (in this case gases) have different fluxes through membrane. CMS is a special form of carbon that has been used for separation that, like polymers, separates by a combined sorption diffusion process; however, CMS shows unusual ability to perform molecular sieving based on entropic factors in the diffusion process.

2.1 Transport through membranes

Membranes are usually used as selective barrier materials for gas transport. Gas mixtures on the feed side of the membrane come in contact with the upstream face of the membrane, and then one or more of the gas species in the mixture selectively passes through the membrane to the downstream side (called the permeate side). This process results in the enrichment of the rejected species to remain in the upstream, which is therefore called retentate side. Figure 11 shows various different types of membranes that exist, which follow different mechanisms for selectively transporting molecules through them. For example, if a membrane has large pores, the transport is defined by the size of the pores and the mean free path of the molecules diffusing through the membrane at the given temperature and pressure. When the pores are much larger than the mean free path of the gas molecules, viscous flow occurs. On the other hand, when the size of the pores is smaller than the mean free path of the molecule, diffusion takes place through Knudsen diffusion mechanism in which the separation is based on the molecular weights of the gases [33]. The Knudsen selectivity is defined as $\alpha_{A/B} = \sqrt{\frac{M_B}{M_A}}$, where $\alpha_{A/B}$ represents the

selectivity of the gas A over the gas B. For gas pairs with similar molecular weights, like O_2/N_2 or H_2S/CH_4, the Knudsen selectivity is fairly low.

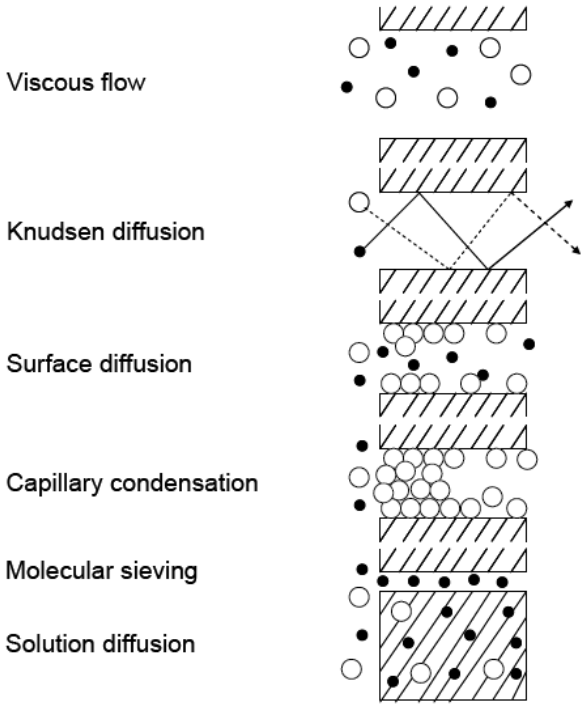

Figure 11: Various mechanisms for selective mass transfer of gases through membranes [34]

Selective surface diffusion is used with materials that can preferentially adsorb certain species over others. Once the species have been adsorbed, they diffuse across the surface from one sorbed site to the other [35]. Here the separation efficiency depends on the physicochemical nature of the pore surface and the pore size.

Molecular sieving transport occurs when penetrating molecules are separated based on size, relying on the pore structure of the membranes. Diffusion through these pores requires activation energy for the molecules to overcome repulsion from the walls, and

even small changes in the size of pores can result in significant differences in the activation energy required for diffusion. Therefore, size-selective molecular sieving allows the smaller molecule(s) to pass through the membrane resulting in efficient separation [35-37]. In the solution-diffusion transport process, the size (diffusivity) and condensability (solubility) selective factors interact to determine which component(s) pass through the membrane the fastest [35]. If the membrane does not have pores, separation takes place by sorption-diffusion mechanism; however, even with ultramicroporous (<7Å) pores, sorption diffusion mechanism controls transport.

2.1.1 Sorption-diffusion mechanism

Transport through polymeric membranes is defined by a sorption diffusion mechanism, illustrated in Figure 12.

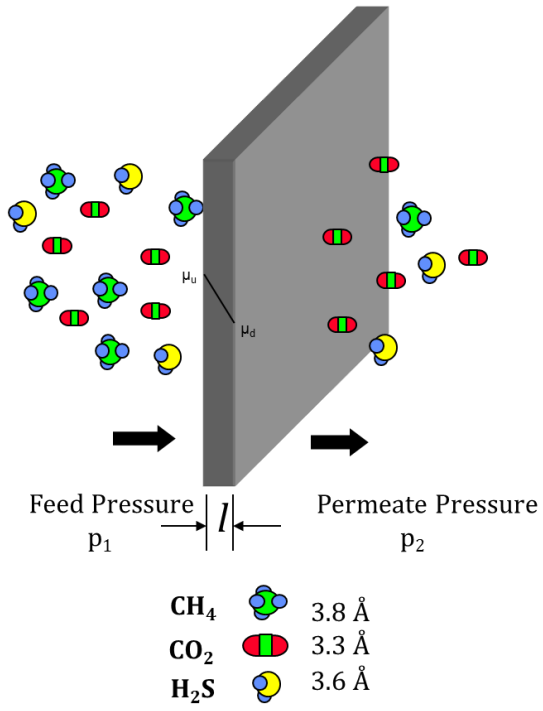

Figure 12: Schematic representation of $CO_2/H_2S/CH_4$ by the solution-diffusion process

The high chemical potential side of the membrane is called the upstream, and the low chemical potential side is called the downstream. During the transport process, the penetrant gas first sorbs (or dissolves) into the membrane on the upstream side, then diffuses through the membrane from the high chemical potential to the low chemical potential side under the chemical potential gradient, and then desorbs from the membrane on the downstream. The fact that different penetrant molecules have different sorption and diffusion coefficients through the membrane, can make them faster or slower than one another. In this case, smaller penetrants like CO_2 and H_2S are the faster gases, and the larger CH_4 is the slower gas. This difference in the rate of the transport is what causes the separation to occur.

At temperatures below and above the glass-transition temperature (T_g) of the polymer, details of for gas transport can be somewhat different. An amorphous polymer is in a rubbery state when it is above its T_g, or glassy state when it is below T_g [38]. As shown in Figure 13, all amorphous polymers have a specific volume (V) which is a combination of the volume occupied by the polymer chains (V_o) and the free volume around the polymer chains (FV). The polymer changes from glassy regime to rubbery regime at the T_g, and glassy polymers have extra unoccupied free volume as compared to rubbery polymers.

Glassy and rubbery polymers exhibit similar but somewhat different transport behavior due to the fact that the former are not in a state of true thermodynamic equilibrium. The polymer chains in rubbery polymers are more flexible and have short relaxation times, so diffusion discrimination is low and sorption is the dominant factor for

selective gas transport through these membranes. Glassy polymers on the other hand, have relatively more rigid polymer chains with longer relaxation times, which leads them to having the extra free volume. Penetrant molecules can potentially sit in long-lived segmental packing defects (holes) with somewhat lower intrinsic diffusion mobilities depending on the kinetic diameter of the gas as well as polymer chain packing and mobility [38].

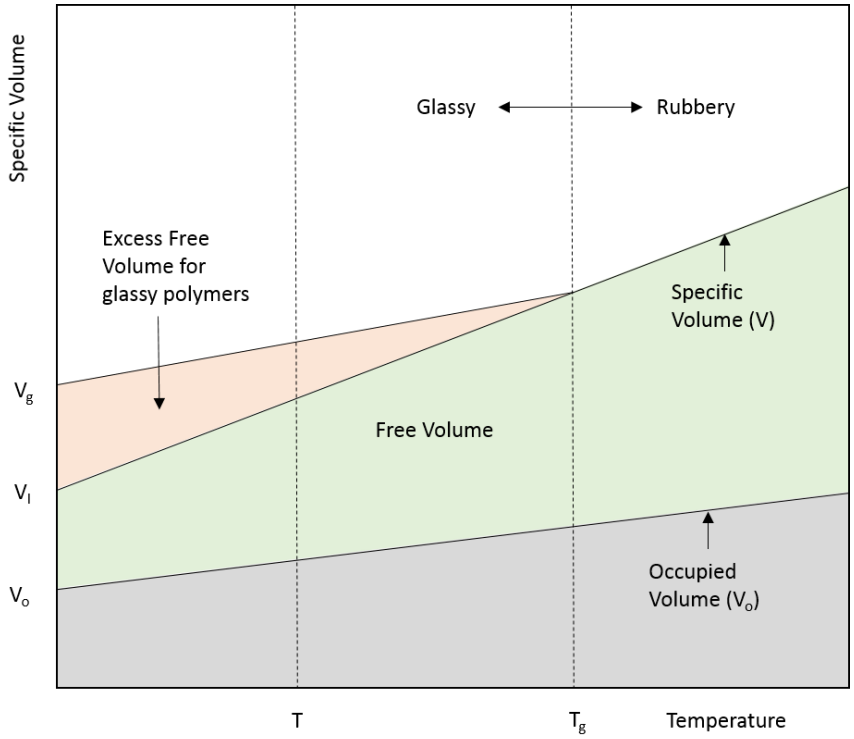

Figure 13: Glassy polymers vs rubbery polymers as a function of temperature. Adapted from [1].

2.2 Carbons and Carbon Molecular Sieves

Typically, polymer precursors are pyrolyzed to yield either coke or char. Precursors that pass through a liquid or rubber phase on pyrolysis and form graphitizable carbons, usually lead to coke. Precursors that do not fuse during pyrolysis and form non-graphitizable carbons lead to formation of char [1 – 3].

A model of hexagonal graphite with layers of carbon atoms (called lamellae) that are stacked parallel to each other, is shown in Figure 14. The layers are arranged in an alternating A-B-A-B type of sequence. Structure of carbon forms are loosely based on this model, for both the graphitizable (anisotropic) and non-graphitizable (isotropic) carbons [1, 2].

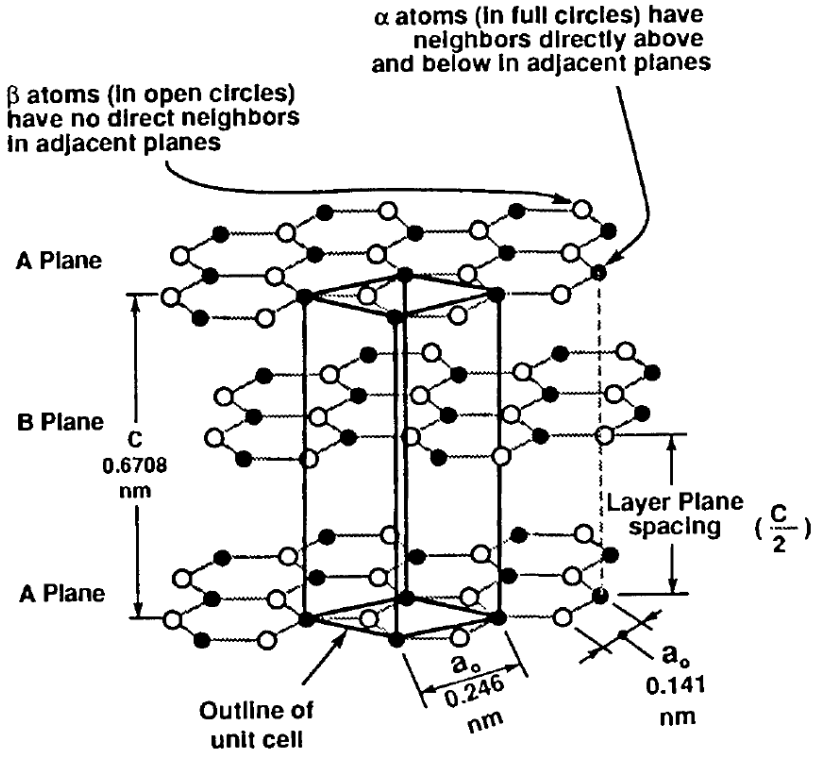

Figure 14: Crystal structure of graphite with A-B-A-B stacking sequence and unit cell [39]

Isotropic carbons have more structured arrangement, in that they largely have parallel stacks of these graphitic layers, and can thermally rearrange to increase order. Anisotropic carbons on the other hand, have a more random stacking, with lamellae that are imperfectly arranged. In addition to the lamellae of carbon not being in a perfect arrangement, anisotropic carbons could also have other hetero atoms like nitrogen, oxygen, sulfur and hydrogen. The imperfections in the stacking array and shift from true lattice structure lead to formation of packing defects that contribute to the porosity of the carbon material.

Carbon molecular sieves (CMS) are a class of carbons where the pores of the material are approximately of the same order of magnitude as the size of typical gas molecules, ranging from the sizes of He, CO_2, CH_4 to bigger molecules like C_2H_6, C_3H_8 and SF_6. They are formed by the thermal decomposition of polymers in inert and controlled atmosphere at high temperature. Figure 15 illustrates how CMS is envisioned with graphene like sheets randomly stacked on top of each other, giving it an amorphous long range structure. It is comprised of disordered and highly disoriented, sp^2 hybridized condensed hexagonal sheets, with pores formed from packing imperfections. The parts where the edges of the graphene sheets come together are called ultramicropores, which look like small slit like windows with width dimension less than 7 Å. The larger open spaces of size 7-20 Å are called micropores and are responsible for most of the free volume in the CMS that accommodates equilibrium sorption. When placed in succession, the ultramicropores connect the micropores, so the ideal pore structure of CMS can be visualized as shown in Figure 16 [37].

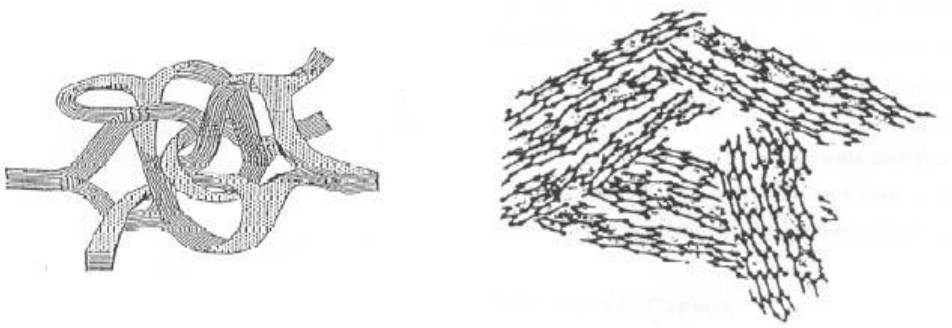

(a) (b)

Figure 15: CMS structure with (a) Sheets of carbon amorphously stacked and (b) stacking imperfections give rise to pores.

Due the comparable size of the gas molecules to the pores, the separation occurs by molecular sieving where the smaller gas molecules can pass through and the larger gas molecules are held behind. However, CMS is amorphous, and therefore does not have a fixed pore size. Instead, there is a distribution of pore sizes that arise from the imperfect packing. There are two major peaks in the distribution, making it look like a bimodal distribution.

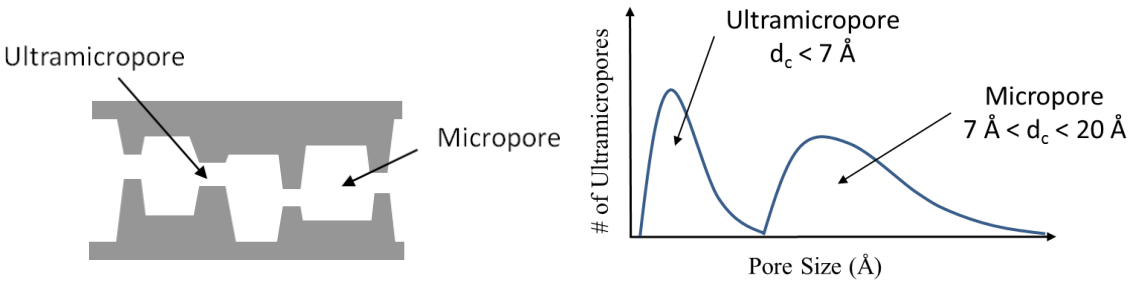

Figure 16: (a) Idealized pore structure of CMS membrane, (b) Idealized bimodal pore size distribution in CMS structure

In this simple model, the micropore galleries provide sorption sites, while the constricted ultramicropores provide the sieving effect by selectively allowing smaller molecules to pass through, thereby resulting in high separation efficiency. The combination of micropores and ultramicropores allow a CMS membrane to achieve both high permeability as well as high selectivity.

Unlike zeolites or other porous membranes of a definite pore structure, CMS is not crystalline. The disordered and amorphous structure of CMS makes it difficult to conclusively characterize the pore dimensions by X-ray diffraction (XRD), high resolution microscopy or other techniques useful for zeolites [37, 40-42]. Gas sorption experiments can provide some information related to the larger micropores [37, 43-45], but cannot completely enlighten us about the size distribution of the ultramicropore responsible for molecular sieving.

2.2.1 Transport in CMS membrane

Transport in CMS materials occurs by molecular size sieving, but can still be modeled in terms of sorption-diffusion mechanism [37, 46, 47]. The permeation relies on the diffusivity of each penetrant molecule (which itself relies on the size and shape of the gas molecule) and solubility of the molecule in the material. Larger micropores not only provide sorption sites for penetrant to sorb onto, and gas transport takes places by a jumping mechanism from one sorption site to the next along the concentration gradient. Since micropores are large and long, they also provide longer diffusion jump lengths further promoting high permeability through the membrane. Similar sized molecules can be effectively separated based on differences in their activation energy for diffusion, termed

‘energetic selectivity’. Ultramicropores on the other hand are much smaller, and are comparable to the size of the penetrant gas molecules. They restrict the diffusion through membranes, since gas molecules have to overcome the repulsive interaction with the ultramicropores windows to execute a jump. These windows can effectively restrict the rotational degrees of freedom and internal vibrations of certain gas molecules in a given mixture. Unlike conventional polymeric membranes, CMS membranes can therefore provide this high ‘entropic selectivity’ because of their rigid ultramicropore windows. This capability allows effective discrimination between gas species via a molecular sieving effect, and ultimately leads to separation [37, 46, 47]. When combined together, the micropores and ultramicropores provide high permeability as well as high selectivity through the membrane [37, 48, 49].

A membrane can be characterized in several ways, and important terminology for gas separation is discussed below. The two main criteria are: 1) Permeability and 2) Selectivity.

2.2.1.1 Permeation

According to the sorption-diffusion mechanism, gas molecules sorb at the upstream, diffuse through the membrane under a chemical potential gradient, and desorb at the downstream [1]. It is assumed that the fluid on either side of the membrane is in equilibrium with the membrane material at the gas-membrane interface. While pressure drops across the membrane, the pressure within the membrane is essentially constant at the high pressure (upstream) value. The driving force based on the chemical potential gradient across the membrane is expressed as a concentration gradient [50]. This description of the assumptions is demonstrated in the Figure 17 below.

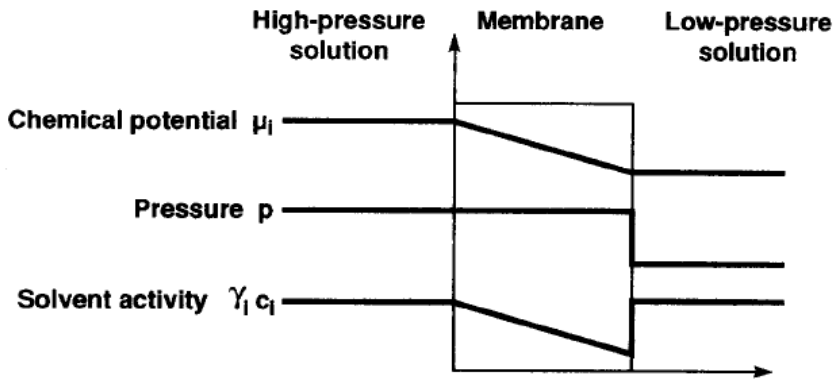

Figure 17: Assumptions in solution-diffusion model for membrane transport [50]

Permeability is the measure of intrinsic productivity of a membrane material, and equals the flux normalized by the membrane thickness and the partial pressure difference (or fugacity) across the membrane. It can further be represented as a product of a kinetic factor, i.e. the average diffusion coefficient (D_A), and a thermodynamic factor, i.e. the average sorption coefficient (S_A) [1, 38]. This relationship can be derived by representing the flux (N_A), in the absence of any bulk flow effect, using Fick's first law of diffusion [1, 33] as shown in the equation (1).

$$P_A = \frac{N_A \times l}{\Delta p_A} = -D_A \frac{dC_A}{dx} \frac{l}{\Delta p_A} \tag{1}$$

where P_A is the permeability, N_A denotes the flux through the membrane, l is the membrane thickness, and Δp_A is the transmembrane partial pressure difference, C_A is the concentration of the component A, and D_A is the concentration dependent diffusion coefficient. In cases where non-ideal gas phase effects exist, which are common for sour

gas feeds at high pressures, the partial pressure difference is simply replaced by the transmembrane fugacity driving force difference for each component. Permeability is measured in units of Barrer which is given by:

$$1\ Barrer = 10^{-10}\frac{cm^3_{STP} \times cm}{cm^2 \times s \times cmHg} \tag{2}$$

In the case of homogeneous dense film membranes, the membrane thickness can be determined fairly easily. For asymmetric membranes however, the thickness l cannot be readily and accurately determined, so the term permeance is used, which is the permeability divided by the thickness, $P_A/\ l$. Permeance is usually reported in gas permeance units (GPU).

$$\left(\frac{P}{l}\right)_A = \frac{N_A}{\Delta p_A} \tag{3}$$

$$1\ GPU = 10^{-6}\frac{cm^3_{STP}}{cm^2 \times s \times cmHg} \tag{4}$$

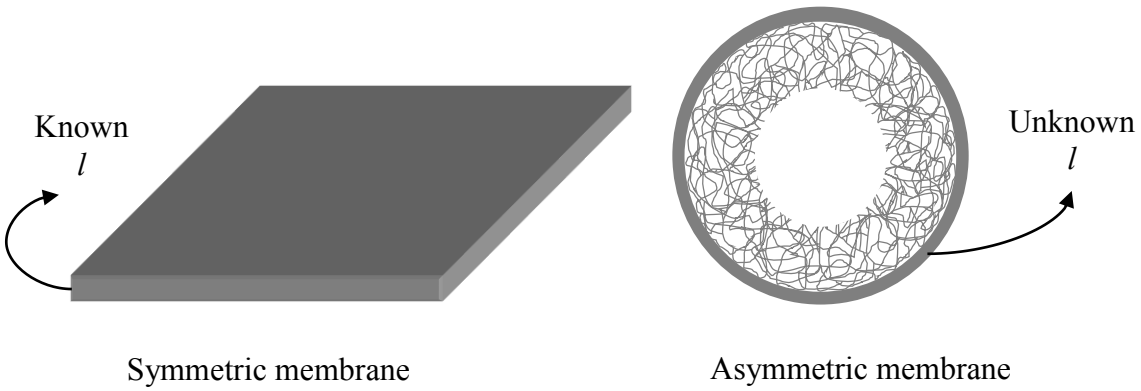

Figure 18: Representation of dense film and hollow fiber membranes

Equation (1) can be split between diffusive part and sorptive part, and written in a combined manner as equations (5) and (6) respectively.

$$D_A = \frac{\int_0^{C_{A,u}} D_A \, dC_A}{C_{A,u}} \tag{5}$$

$$S_A = \frac{C_A}{p_A} \tag{6}$$

Putting the above two equations together, and substituting in equation (1) we get

$$P_A = D_A \times S_A \tag{7}$$

Therefore, permeability of a gas A can be written as product of the sorption coefficient of the gas in the material, S_A, and the diffusion coefficient of the gas through the material, D_A. The diffusion coefficient represents a kinetic factor or a mobility factor, which depends

on the size, shape and kinetic energy of the molecule. The sorption coefficient represents a thermodynamic factor, and for the case of molecular sieves, the sorption coefficient is determined by the condensability of the gas penetrant, detailed chemical nature of the carbon surface, and the porosity in the material.

The sorption coefficient can be calculated from the sorption curve corresponding to a particular gas and a particular membrane. For CMS, the sorption coefficient is the pressure normalized concentration of gas at an equilibrium pressure. Selectivity is the separation efficiency of the membrane, which indicates the capacity of the membrane to separate one gas from another. It is the ratio of the permeabilities (or permeances) of the permeate side mole fraction to the feed side mole fraction of the diffusing gas when the downstream pressure is low compared to the feed pressure, as it is in the current work. If *x* and *y* are the mole fractions corresponding to upstream and downstream respectively for fast gas A and slow gas B, the selectivity can be given by the permeabilities components as:

$$\alpha_{A/B} = \frac{(P/l)_A}{(P/l)_B} = \frac{P_A}{P_B} = (\frac{S_A \times D_A}{S_B \times D_B}) \tag{8}$$

In a mixed gas feed the selectivity is given as:

$$\alpha_{A/B} = \left(\frac{y_A/y_B}{x_A/x_B}\right) \tag{9}$$

When required, deviations from ideal gas behavior must be accounted for.

2.2.1.2 Sorption

As shown above, the sorption coefficient of a gas A describes the amount or concentration of gas (C_A) taken up by the membrane material at a given pressure (p_A) at equilibrium as represented in the following equation.

$$\mathbb{S}_A = \frac{C_A}{p_A} \tag{10}$$

Sorption depends on the interaction of the gas with the membranes and its condensability. In glassy polymers, a dual mode sorption model is used to describe the sorption [1, 38]; however, for molecular sieving materials such as zeolites and CMS, sorption is modeled as Langmuir sorption which uses a finite number of sorption sites and rigid saturable capacities [37, 51]. The concentration of molecules dissolved in packing disruptions, or so-called holes or microvoids, (C_H) is related to p_A by the Langmuir isotherm:

$$C_H = \frac{C'_H\, b\, p}{1 + bp} \tag{11}$$

where, C'_H is the Langmuir saturation constant and b is the Langmuir affinity constant. In CMS membranes, the majority of the penetrant molecules are sorbed in the larger pores (micropores) [37] characterized by dimension d_{tv} in Figure 19. The smaller ultramicropores have a higher repulsive interaction energy of the molecule sitting in it, as compared to that of the molecule sorbed into the larger micropores.

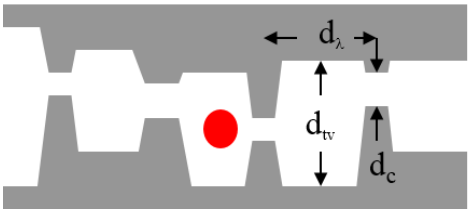

Figure 19: Representation of sorption sites in CMS membranes (adapted from [37])

The Langmuir isotherm accounts for site saturation, the rate of sorption being proportional to the product of the penetrant concentration in the gas phase and the amount of available sorption sites, which reaches dynamic equilibrium with the desorption rate. The Langmuir isotherm, although simple, offers a useful visualization of sorption process in CMS [51].

In case of multi-component mixtures, competitive sorption occurs, with both species seeking the sorption capacity. For each component *i* in the mixture, similar expressions can be derived based on Langmuir sorption model in CMS membranes.

$$C_{Hi} = \frac{C'_{Hi}\, b_i\, p_i}{1 + \sum b_i\, p_i} \tag{12}$$

2.3 Formation of CMS hollow fiber membranes

This study focuses on the asymmetric hollow fiber configuration of CMS membranes due to its industrial scale-up advantage as explained earlier in Chapter 1. To form the asymmetric CMS hollow fiber membranes, asymmetric polymeric hollow fiber membranes must first be formed, followed by pyrolysis to convert the fiber to a CMS hollow fiber membrane. This section explains the theory of the experimental techniques

used in synthesis and characterization of CMS membranes. Subsequent sections will discuss the work done in this area by previous researchers.

2.3.1 Hollow Fiber Spinning Theory

The asymmetric precursor hollow fiber membranes used in this study were formed by a dry-jet/wet-quench spinning process, which uses a polymer solution (dope) prepared as described by Clausi and Koros [52]. Dope composition can be described in terms of a ternary phase diagram as shown in Figure 20. The dope composition is chosen so that the viscosity and rheology of the dope are conducive to the spinning process, while also providing an asymmetric morphology. Spinnability is strongly influenced by the molecular weight of the polymer and its concentration in the dope, e.g. a higher molecular weight of the polymer will yield a highly viscous dope at the same polymer concentration. Similarly, a higher concentration of the polymer yields a more viscous dope when the molecular weight is held constant. Additionally, the ratio of solvents to that of non-solvents in the dope should be adjusted in order to keep the dope in the 1-phase region, but very close to the binodal line, so that an asymmetric fiber morphology can be created. The binodal line separates the 1-phase solution (dope) and the 2-phase solution (polymer after phase separation.)

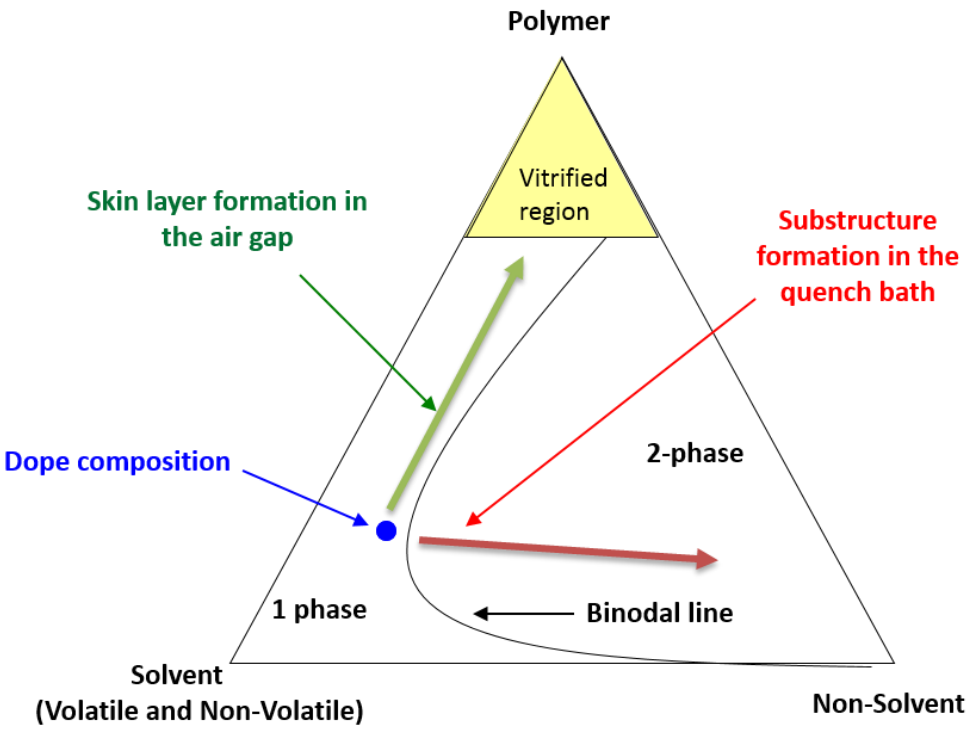

Figure 20: Ternary phase diagram illustrating the formation of polymeric asymmetric hollow fiber membrane, adapted from [27].

In the dry-jet/wet-quench spinning process used in this work, the dope and a bore fluid are co-extruded through a spinneret into an air-gap before being quenched in an aqueous bath. A basic representation of the dry-jet/wet-quench spinning process can be found in Figure 21. In the air gap, a thin dense nascent skin layer is formed due to rapid evaporation of the volatile solvents. As the concentration of the solvent decreases in the air gap, it drives the dope composition toward the vitrified region (following the path of the green line indicated by the "Skin Layer Formation" arrow in Figure 20). Once the fiber enters the quench bath, the non-solvent (water) diffuses into the nascent fiber, where the dope phase separates and forms a porous substructure beneath the skin (indicated by the red line indicated by the "Substructure Formation" arrow in Figure 20). In this way a dense

selective skin layer with a porous support structure can be formed, with the desirable asymmetric morphology. After phase separation in a water quench bath, solidified fibers are collected by a take-up drum.

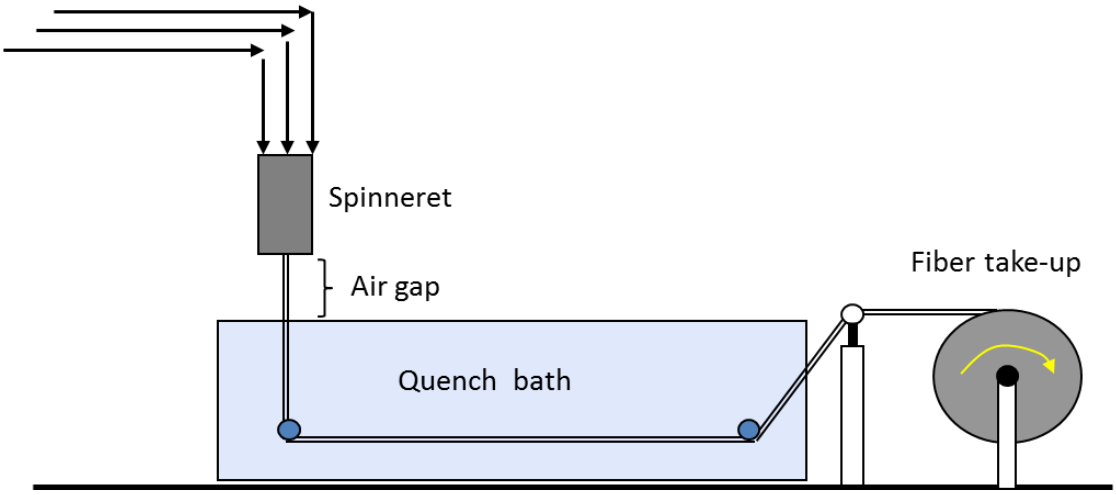

Figure 21: Schematic of dry-jet/wet-quench spinning process. Dry-jet/wet-quench spinning is the process used to produce polymer precursor asymmetric hollow fiber membranes.

Following completion of the spinning process a solvent exchange process is performed to avoid collapse of the porous substructure. The solvent exchange process is an extremely important step in the membrane fabrication process [28, 53], without which the hollow fiber membranes may densify. The porous precursor fibers contain water after they have been on the take up drum. If they are subjected to high temperatures, for instance during drying or pyrolysis, evaporation/boiling of the water causes significant changes in the structure and properties of the fiber, and of the resulting CMS membrane. The high capillary forces associated with removal of water within the small radii of the pores close to the skin can cause densification of the structure in this region, which will result in a less

permeable membrane [28]. This can be prevented by the solvent exchange process, which replaces the water that is present in the porous substructure of the precursor fiber with a fluid having a lower surface tension, e.g. methanol or hexane.

2.3.2 Pyrolysis process

Polymer precursors (polymer fibers in this case) are pyrolyzed in a controlled environment to form CMS membranes [15]. For asymmetric CMS hollow fiber, gas separation occurs primarily in the intrinsic CMS dense skin, not in the supportive highly porous support layer. As noted earlier, the dense layer of asymmetric CMS corresponds to a molecular sieving structure having a bimodal pore distribution (Figure 16 (b)). The pore structure and distribution is in the order of Angstroms and can be altered using several different parameters [54], such as: choice of polymer precursor, pyrolysis temperature protocol, pyrolysis atmosphere, and post-pyrolysis treatment. These key parameters have been discussed in the following sections.

2.3.2.1 Polymer precursor

The choice of the polymer precursor is the first important parameter in CMS membrane fabrication. Koresh & Soffer [55] pioneered the production of defect-free CMS hollow fiber membranes from cellulose fibers. They showed that polymers should not melt or flow before they decompose in order to be suitable as precursors for CMS membrane production. Many different thermosetting polymers including cellulose derivatives, phenolic resins, polyfurfuryl alcohol, poly(vinylidene)-based polymers, polyacrylonitrile and polyimides have since been used in CMS membrane fabrication [49, 56-62]. Since polyimides have high glass transition temperature, processability, mechanical strength and

good intrinsic separation performance, they have the preferred polymers as precursor materials for many researchers [49, 54, 61].

The intrinsic properties of the polymer precursor affect final CMS properties. The most important precursor properties include chemical structure, which determines the fractional free volume (FFV), chain mobility, glass transition temperature, and the composition and amount of volatile products evolved during pyrolysis all [49, 63]. Williams researched the effect of the fractional free volume of the starting polymer in CMS fabrication. The separation performance of CMS membranes derived from the precursors with different fractional free volumes, exhibited difference in permeabilities and diffusivities. These results were attributed to the differences in FFV of the starting polymers, where the polymer with the higher FFV had higher permeability and diffusivity [49].

Various gas pairs have been studied with CMS derived from these polyimides. Steel [37] studied a commercially available polymer Matrimid® and an in-house polyimide 6FDA:BPDA-DAM. These polymers were pyrolyzed at two pyrolysis temperatures, 550°C and 800°C, using identical pyrolysis conditions. Matrimid®-based CMS membranes were more selective and less permeable compared to 6FDA:BPDA-DAM-based CMS at both the temperatures. This difference is attributed to the different chemical structures of the two polyimides. The bulky -CF_3 groups in 6FDA:BPDA-DAM hinder the packing of the polymer chains leading to a higher fractional free volume compared to Matrimid®. CMS derived from a higher FFV polymer precursor leads to an intrinsically more open CMS structure with higher permeability. While Matrimid® evolves volatiles such as CO, CO_2, etc., 6FDA:BPDA-DAM also evolves fluorinated compounds, such as CHF_3 and trace HF

in addition to CO, CO_2, etc. This leads to higher microporosity which contributes to a more permeable CMS structure. Vu [64] and Kiyono [62] reported a similar trend for CMS hollow fibers fabricated from these two polyimides. Rungta [65] studied CMS dense film membranes derived from these two polyimides for ethane/ethylene separation and report a similar trend. Recent studies by Xu [66] have compared the asymmetric CMS hollow fiber separation performance for Matrimid® and 6FDA:BPDA-DAM precursors for various gas pairs. Their performances are as follows:

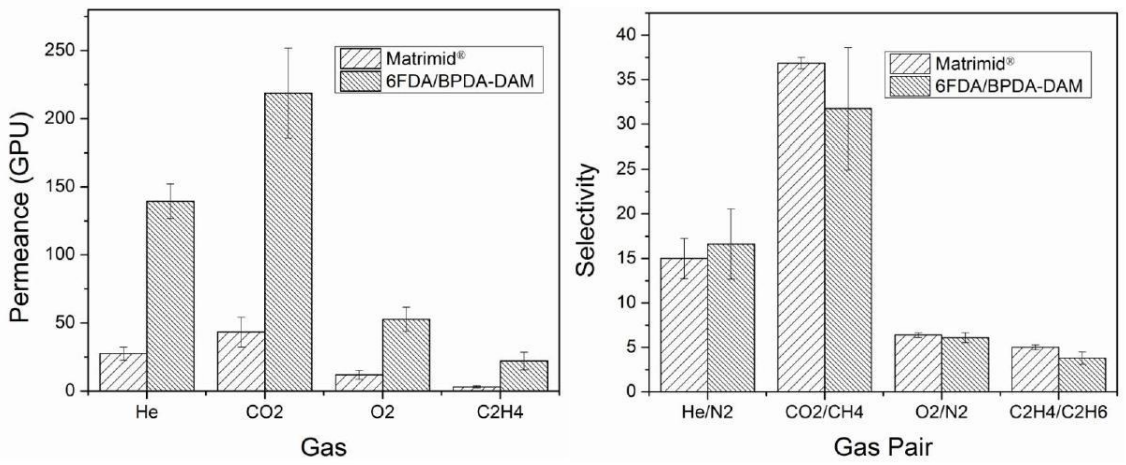

Figure 22: Permeance and selectivity of CMS hollow fiber membranes derived from Matrimid and 6FDA:BPDA-DAM precursors for various gas pairs, adapted from [66].

In this study, the two polyimides Matrimid® and 6FDA:BPDA-DAM have been chosen as starting materials to derive CMS membranes for ethylene/ethane separation. Preliminary investigation of the three precursors and their viability in forming CMS membranes for CO_2/CH_4 separation in presence of H_2S will be discussed in section 4.2.7. Differences in the separation properties and morphology of CMS membranes resulting from the 2 precursors are shown in Figure 22.

2.3.2.2 Pyrolysis temperature and protocol

The process of pyrolysis has several features that can affect the final pore structure of the resulting CMS material. Parameters such as the pyrolysis temperature, heating ramp rate and thermal soak time at the final pyrolysis temperature can influence the tuning of the micropores and the ultramicropores of the CMS structure.

Final pyrolysis temperature is the highest temperature to which the precursor is heated during the pyrolysis process. The pyrolysis temperature is chosen such that it lies between the decomposition temperature for the polymer and the graphitization temperature, typically in the range of ~500-1000°C [1, 3]. Researchers have shown that an increase in pyrolysis temperature typically results in lower permeability and higher selectivity in general, possibly due to a more compact CMS with smaller average pore sizes [37, 65], as shown in Figure 24. Steel [37, 67] reported that with increasing the pyrolysis temperature, both O_2 and CO_2 permeabilities decreased along with an increase in O_2/N_2 and CO_2/CH_4 selectivity for CMS membranes derived from Matrimid® and 6FDA:BPDA-DAM, as shown in Figure 23.

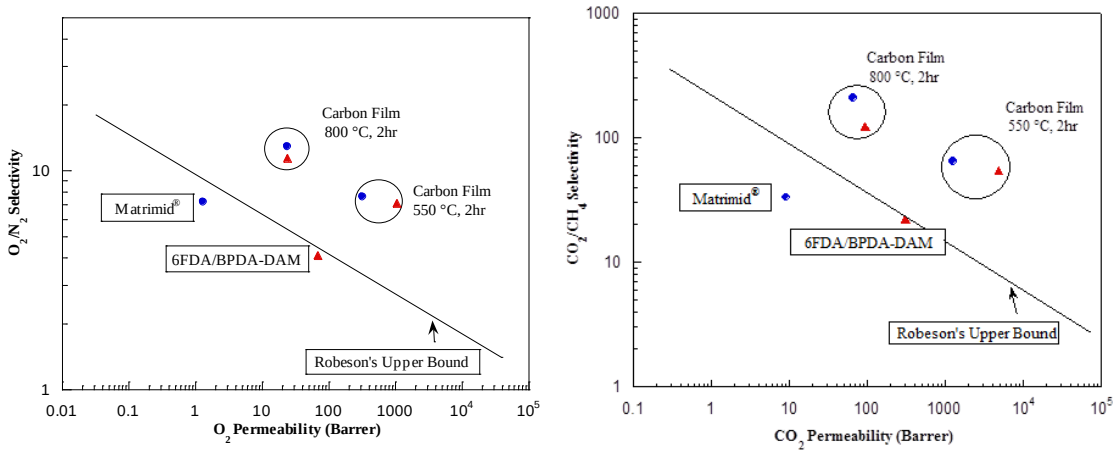

(i) (ii)

Figure 23: Effect of final pyrolysis temperature on (i) O_2/N_2 separation and (ii) CO_2/CH_4 separation [37].

The role of different heating ramp-rates [47] and thermal soak times [67, 68] for tuning the CMS separation performance has also been studied. However, for the purpose of this study, only the optimization of final pyrolysis temperature is considered to achieve the right combination of permeance and selectivity. The optimum condition was chosen from previous studies for simplification.

Kemmerlin from the Koros group used 500 °C for pyrolyzing Matrimid® for application in exposure to sour gas. This part will be discussed in Section 5.2 in detail.

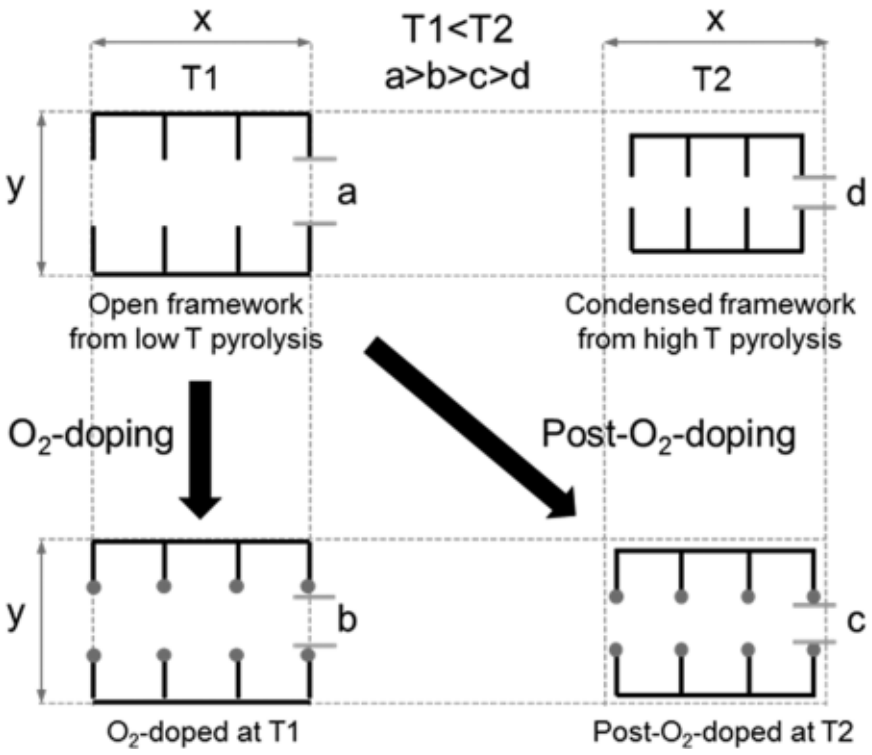

Figure 24: Illustration of effect of final pyrolysis temperature and oxygen doping on the size of ultramicropore structure of the CMS membranes [69].

2.3.2.3 Pyrolysis atmosphere

Pyrolysis is described as the decomposition of a precursor in a controlled environment at high temperature. Therefore, pyrolysis atmosphere is critical in controlling the intrinsic CMS structure and its resulting separation performance. Pyrolysis can be carried out either in a more or less inert atmosphere or in vacuum. Geiszler performed a detailed study of pyrolyzing 6FDA:BPDA-DAM under both vacuum and inert atmosphere of He and Ar, and reported that gas permeances were higher for inert environment as compared to vacuum [70, 71].

Even slight variation in the composition of the inert atmosphere can lead to a large change in the resulting separation properties of CMS. Williams hypothesized that the

amount of oxygen present in the inert purge gas can affect the resulting CMS separation performance [49]. Kiyono *et al.* studied this hypothesis by investigating the importance of this oxygen concentration, and called it 'oxygen doping.' Her results of oxygen doping on Matrimid® and 6FDA:BPDA-DAM precursors for CO_2/CH_4 separation are shown in Figure 25.

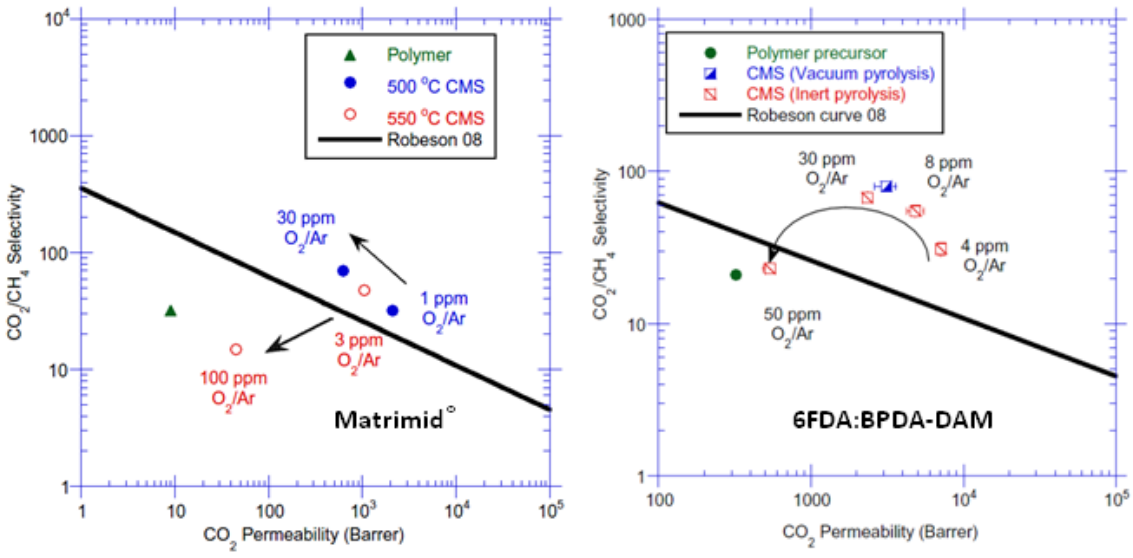

Figure 25: Effect of oxygen doping on CO_2/CH_4 separation performance in Matrimid® and 6FDA:BPDA-DAM dense films [72].

The hypothesis is that at elevated temperatures during pyrolysis, the oxygen present in the inert gas tends to selectively chemisorb at the ultramicropore sites, which have been shown to be ~17 times more reactive than the basal plane, thus allowing for carefully tuned separation performances [73]. The cartoon of how it changes the ultramicropores is shown in Figure 24, where it shows that the oxygen doping can lower the average ultramicropore size.

This work will utilize oxygen doping as well as probe into one other dopant molecule for doping the reactive ultramicropores, and changing the concentration to find an optimum, as discussed in Chapter 6. While an optimum from of 30 ppm as suggested by Figure 25 is used in this work, there is room for further optimization.

2.3.2.4 Pre-pyrolysis treatment of polymer precursor

Polymer precursors are often subjected to pre-treatment before they are pyrolyzed. The purpose of pre-treatment is to pre-arrange and stabilize the polymer material before undergoing the high-temperature pyrolysis, by altering its chain mobility and morphology. There can be two types of pre-treatments: thermal pre-treatment and chemical pretreatment. Several pre-treatments have been used to condition the polymer precursor prior to pyrolysis. Thermal stabilization by pre-oxidation of precursor for cross-linking the polymer structure has been done by many researchers in the past [58, 59, 74, 75]; however, oxidative pre-treatment still needs further optimization for effective end use.

Chemical modification of the polymer precursor has also been used in many cases. Chemical crosslinking as well as soaking the polymers in different alcohols has been studied by Tin *et al.* [76], showing an increase in selectivity due to increased structural re-organization of solvent treated precursors. While this increase is attributed to smaller pores due to the structural re-organization, the fundamental causes have not been explored.

A novel pre-pyrolysis treatment called ‘V-treatment’ has been developed by Bhuwania in the Koros group. This pre-treatment aims to resolve the collapse of the porous substructure in the asymmetric CMS hollow fibers, but providing structural support to the

pores. This work will use and study this V-treatment technique extensively, and will be discussed in Chapter 4.

2.3.2.5 Post-pyrolysis treatment of CMS

Researchers have studied different thermochemical post-treatments to tailor the pore dimensions and distributions of CMS membranes. Several common techniques used are chemical vapor depositions (CVD), post-pyrolysis thermal treatment, post-oxidation and coating of CMS membranes [54]. Low temperature post-oxidation has been the most commonly used method, where CMS membranes are heated in oxidative atmosphere *after* an inert atmosphere pyrolysis to increase the pore volume. While oxygen doping is performed during the pyrolysis process with trace amounts of oxygen, post-oxidation is performed after the pyrolysis. This typically leads to an increase in the permeability of CMS membrane [77]. Soffer *et al.* investigated chemical vapor depositions post-oxidation techniques extensively for cellulose derived CMS fibers [78].

A recent study has been done by Singh *et al.* [79], where a post-pyrolysis oxygen doping concept referred as 'Dual Temperature Secondary Oxygen Doping (DTSOD)' has been developed. In this process, the CMS membranes are exposed to trace amounts of oxygen at higher temperature for a brief period of time after the final pyrolysis temperature has been reached. The reaction mechanism assumed to be similar to the oxygen doping mechanism. Similar to the oxygen doping, excessive amounts of oxygen in the DTSOD will lead to excessively tuned ultramicropores. DTSOD concept has been applied to ethylene/ethane separation as well [69].

The current work will not particularly assess or apply a post treatment process.

2.4 Membranes for separation of H_2S

As noted earlier, in the natural gas industry, the chief application of gas separation membranes is bulk CO_2 removal. Most often, this separation is performed using glassy polymers like cellulose acetate (CA), which is considered to be the industrial standard. Most researchers have used dense film type membranes for this separation, reporting performance values in terms or permeabilities with the unit Barrer. For raw natural gas contaminated with low-concentration H_2S, CA has been employed industrially. Bhide et al. have used values of 8.9 Barrer for the CO_2 permeability coefficient and 21 for the CO_2/CH_4 selectivity of CA, while giving values for H_2S/CH_4 selectivity of CA as 19 with a H_2S permeability of 8.1 Barrer [14]. Ternary mixed gas data (65% CH_4, 29 % CO_2, 6% H_2S) has been reported at 10 atm for CA as selectivity of 22 for CO_2/CH_4 and 19 for H_2S/CH_4, and permeabilities of 2.43 Barrer for CO_2 and 2.13 Barrer for H_2S by Chatterjee et. al. [80]. Although challenging, it would be very [81]attractive if the H_2S/CH_4 selectivity could be increased significantly to upgrade sour gas streams to pipeline quality. Also, CO_2- and H_2S-induced plasticization is expected to pose a significant problem for aggressive sour gas separations using most glassy polymeric membranes.

Rubbery materials have been the main focus of the limited amount of high-concentration H_2S gas permeation data that has been reported. H_2S/CH_4 selectivities up to 74 with a permeability of 199 Barrer for H_2S have been reported with rubbery poly(ether urethane urea) membranes, using a ternary mixture containing 70.8% CH_4, 27.9% CO_2, and 1.3% H_2S at 10 atm. The flexible polyether units containing commercially available rubbery polymer PEBAX™ has been found to give H_2S/CH_4 selectivities between 50 and 60 with H_2S permeabilities up to 695 Barrer [80, 82]. Although the numbers are impressive,

rubbery polymer membranes do not perform as well for CO_2/CH_4 separations and are difficult to form into thin selective layer. The CO_2/CH_4 selectivity for these materials are generally around 15 with permeabilities comparable to advanced glassy polyimide membranes such as Matrimid® [80, 82-84]. In addition, it is unlikely that rubbery polymers possess the mechanical integrity, chemical or thermal stability to withstand the high feed pressures, acid gas concentrations and temperatures encountered in aggressive sour gas separations applications.

In the area of acid gas separations – namely bulk CO_2/CH_4 separations – the majority of recent activity has focused on glassy polymers. Polyimides have received much attention because of their thermal stability, mechanical robustness, and exceptional intrinsic CO_2/CH_4 separation properties [85]. The commercially available polymer Matrimid® is a glassy polyimide that has been studied intensively for CO_2/CH_4 separations. This polymer exhibits favorable selectivity, permeability but with limited resistance to penetrant-induced plasticization. While excellent dense film separation properties are a key element to the viability of membrane materials, processability and spinnability are equally important to membrane commercialization. Researchers have shown that the polyimides discussed above can be used to form defect-free asymmetric hollow fiber membranes with industrially acceptable skin layer thicknesses, outside diameters and production rates.

Rubbery polymers show very good performances in separating H_2S from CH_4 at low H_2S levels, and yet glassy cellulose acetate is an industry standard for H_2S/CH_4 separation. In fact, however, both CA and rubbery polymers have inferior mechanical properties and exhibit poor performance in separating CO_2 from CH_4 under aggressive feed conditions. It is therefore questionable to use rubbery polymers when both H_2S as well as

CO_2 have to be separated from CH_4. On the other hand, glassy polymers like polyimides show good productivity and selectivity for CO_2/CH_4 separation when they are made plasticization resistant, but perform poorly in separating H_2S from CH_4.

Kraftschik in the Koros group has shown that crosslinked polymers referred to as PEGMC can be plasticization resistant and show a favorable separation performance with H_2S/CH_4 and CO_2/CH_4 of 24 and 29 respectively [24, 86]. When these crosslinked polymers were treated with PDMS, even better separation properties were observed. Selectivity of H_2S/CH_4 was as high as 29 and CO_2/CH_4 was greater than 50 for a feed gas containing 5% H_2S, 45% CO_2, 50% CH_4. The goal of this study was to examine whether CMS can exceed this performance.

Achoundong *et al.* reported a GCV-modified CA membrane that is shown to be very stable under aggressive feed gas conditions of high acid gas concentration at high pressures. This material had CO_2 permeability of 139 Barrers and H_2S permeability of 165 Barrer which are more than one order of magnitude higher than neat CA values [15, 87]. The selectivities of this material were also very attractive with CO_2/CH_4 at 33 and H_2S/CH_4 at 39. However, GCV-modified CA membranes have only been formed into dense film morphology and it is difficult for this material to be economically manufactured into high-quality high-throughput fiber membranes. Nevertheless, it is also represents performance that CMS is targeted to beat in this work.

2.5 Summary

CMS materials have been shown to exhibit excellent gas separation properties that surpass the Robeson upper bound. CMS derived from numerous polyimide membranes and

have been used for separation of various gas pairs like CO_2/CH_4, ethylene/ethane, propylene/propane etc. The structure of the CMS can be tuned by several parameters, like the starting polyimide, pyrolysis temperature, pyrolysis atmosphere (doping), as well as pre and post treatment processes.

CMS have not been studied for separation of H_2S from CH_4. The fact that CMS materials do not plasticize at high pressures of aggressive gases may be advantageous in this particular application.

CHAPTER 3 MATERIALS AND METHODS

This work uses Carbon Molecular Sieve membranes hollow fibers, which were made by pyrolyzing polymeric membranes in controlled environments at high temperatures (500 °C - 800 °C). The polymers used in this work were polyimides Matrimid® and 6FDA:BPDA-DAM. These polyimides were formed into a viscous dope, which was extruded from a spinneret in a spinning process to create hollow fiber membranes. The hollow fiber membranes were dried from a total of 6 spins and stored in a bag for 1-2 years and used periodically for making CMS membranes. Some of the polymer hollow fibers were V-treated in batches before pyrolysis under a desired atmosphere and temperature, to produce CMS membranes. The CMS hollow fiber membranes were then tested for gas separation performance. The specific procedures and formulations are described in detail the following sections.

3.1 Polymer Selection

As mentioned in Chapter 2, polyimides have been shown to be good precursors for formation of CMS membranes. A proof of concept was shown on the commercially available Matrimid® 5218 and then extended to the in house synthesized polymer 6FDA:BPDA(1:1)-DAM.

Matrimid® is the commercial name for BTDA-DAPI polyimide, and it was purchased from Huntsman International LLC. The chemical structure of Matrimid® and the name BTDA-DAPI are shown below. It has a molecular number of 71,200 Dalton and a 3.6 polydispersity index (M_w/M_n).

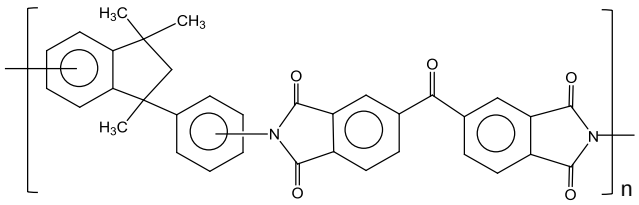

Figure 26: Structure of Matrimid®
BTDA : 3,3',4,4'-benzophenone tetracarboxylic dianhydride
DAPI: 5(6)-amino-1-(4'aminophenyl)-1,3-trimethylindane

Matrimid® was selected as a starting polymer for this work for the following reasons:

1. It has been shown to exhibit good separation properties both in polymeric form as well as in the CMS form.
2. It is a commercially available and a relatively inexpensive polyimide.
3. It is a good standard to measure the performances of other polymers against.
4. It has attractive permeability and selectivity for CO_2/CH_4 separation.

The other polymer, 6FDA:BPDA-DAM is an essentially colorless to light yellow in-house synthesized polyimide in the Koros lab and then produced by Akron Polymer Systems Inc. using a standard synthesis procedure [27]. The chemical structure of 6FDA:BPDA-DAM is shown in Figure 27.

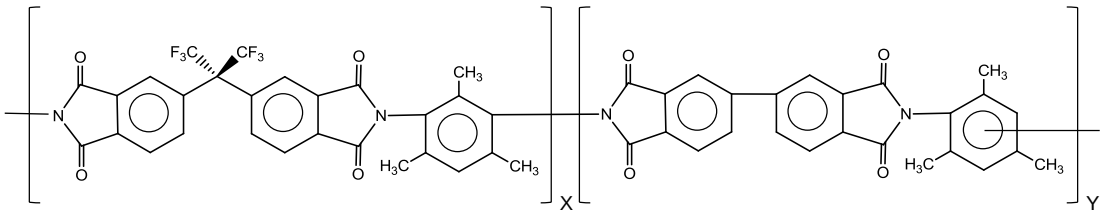

Figure 27: Structure of 6FDA:BPDA-DAM
FDA: 4,4'-(hexafluoroisopropylidene) diphthalic anhydride
BPDA: 3,3'-4,4'-biphenyl tetracarboxylic acid dianhydride
DAM: 2,4,6,-trimethyl-1,3-phynelene diamine

The 6FDA:BPDA-DAM sample synthesized had a molecular weight of 163,000 Dalton and a polydispersity index of 1.8, which is lower than that of Matrimid®. The 6FDA:BPDA-DAM was used as an extension of work done on Matrimid® for the following reasons:

1. It has been considered previously in literature for the desired CO_2/CH_4 separation.
2. 6FDA:BPDA-DAM has high matrix free volume, due to the bulky $-CF_3$ packing disrupting groups on the polymer chain. High free volume leads to a higher permeability of all gases through the membrane.
3. Although more expensive than Matrimid®, its high permeability compared to Matrimid® strikes a good balance between price and productivity.

Other 6FDA based polymers were considered, however bearing in mind the applicability and scalability and cost of this process, they were not studied further for this work.

3.2 Hollow fiber membrane formation

As mentioned previously in Chapter 1, it is important to form hollow fiber membranes for industrial purposes as opposed to dense film membranes, because hollow fibers provide a much larger surface area-to-volume ratio. Hollow fiber membranes also have a thin separation skin layer, which reduces the diffusion barrier. Moreover, fibers tend to be more flexible than flat sheets/dense films in the CMS form, yet resistant to failure from a trans-membrane pressure difference. In the Koros group, hollow fibers are prepared in house, and the procedure for it is described in the following sections.

3.2.1 Dope formation

A dope is formed from the above polymers to form hollow fibers. Workable dopes are viscous solutions, comprising the polymer, selected solvents (high volatility and low volatility) and non-solvents to reach a composition near the binodal line on a ternary phase diagram. The low volatility solvent used generally is N-methylpyrrolidine (NMP), since it is a strong solvent for the polyimides of interest and is relatively ecofriendly and safe to use. Tetrahydrofuran (THF) is used as the volatile solvent which rapidly evaporates in the air gap, resulting in the formation of the nascent defect free skin layer. Ethanol is used as a non-solvent, so that the precipitation process occurs quickly once the dope contacts the water quench bath. The dope compositions for both the polymer precursors Matrimid® and 6FDA:BPDA-DAM have been well studied in the past and were optimized by Xu for these polymers [52, 88]. Table 3 represents the dope compositions adopted for spinning in this study.

Table 3: Dope composition for Matrimid® and 6FDA:BPDA-DAM polymer spinning

Component	**Matrimid®**	**6FDA:BPDA-DAM**
Polymer	26.2	18
NMP	53	50.5
Ethanol	14.9	15
THF	5.9	10
LiNO3	-	6.5
Total	100	100

The polymer is dried for 24 hours at 120 °C to remove any absorbed moisture. The dope is made by adding the least volatile solvent first and progressing to the most volatile solvent in a dried clean jar. The polymer is then measured out in weighing pans and added to this mixture of solvents. The jar is sealed with electrical tape and stirred vigorously until all the polymer is at least wet with the solvent. This mixture is set on a pair of rollers, slowly rolling the dope jar for at least 3 weeks. This ensures uniform contact of the solvent with the polymer, causing the dissolution of the polymer in the solvent and promoting a uniform viscous dope formation.

The dope should resemble thick honey at the use temperature. After at least three weeks of rolling, when it looks uniform, the dope is ready for spinning.

3.2.2 Spinning process

Spinning a dope into a hollow fibers has elements of both science and art to attain defect free fibers. Practice, skill and extreme attention to detail required for spinning. A spinning is assembly is shown in Figure 28.

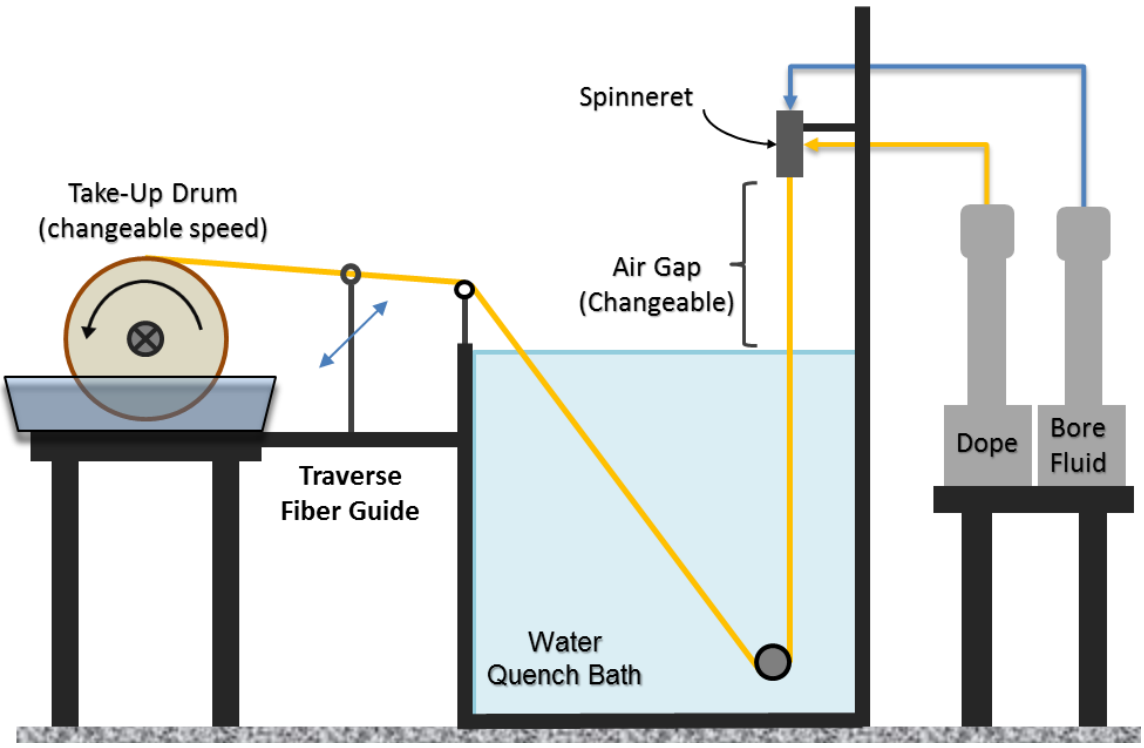

Figure 28: Schematic of a spinning assembly containing the dope, spinneret, quench bath and take up drum.

The dope is filled into a 1000 mL syringe pump (ISCO Inc., Lincoln, NE) and allowed to degas at 60 °C overnight. A bore fluid, which is a mixture of NMP and water, is then loaded into a separate 500 mL syringe pump. The dope prepared from the polymer (refer to the previous section) is co-extruded with a bore fluid through a circular die spinneret, at a separate fixed flowrates. The bore fluid, as the name suggests, used to form the bore of the hollow fiber.

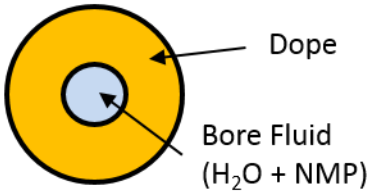

Figure 29: Cross section of a spinneret. The dope is extruded from the annular ring and forms the fiber, and the bore fluid is extruded from the center making it hollow.

The dope is maintained at a desired temperature by using heating tapes around the syringe pumps and the spinneret, and the tubing connecting the two. The dope line and the spinneret also contain micro filters of 20 μm and 2 μm, so that any possible polymer particles, dust specs and other fragments do not ruin the intended spin. The spinneret is a custom made precise cylindrical piece of apparatus with concentric cavities for the flow of the polymeric dope on the outside and the bore fluid on the inside, as shown in Figure 29. The co-extruded polymer solution is allowed to fall through an air gap into a water quench bath at a temperature lower than that of the dope. When the dope is in the air, the volatile solvent from the outermost layer of the dope evaporates, leaving a dense but thin nascent skin layer. Once the dope contacts the water in the quench bath, it undergoes precipitation due to phase separation (influx of water and outflow of solvent) forming a solid porous substructure beneath the dense skin of the fiber. This fiber is collected on a spinning drum and allowed to roll in water until most solvent removal is complete. Once the polymer has completely precipitated, the fibers are collected from the drum and subjected to a process called solvent exchange. This above method is called the dry jet – wet quench method of spinning.

Spinning is a complex process which has many variables like dope composition, dope temperature, extrusion rate, take up rate, air gap. Varying any of these can lead to difference in morphology of the obtained fiber. For example, a higher air gap will lead to a thicker separation skin layer as compared to smaller air gap and a higher take up rate for the same extrusion rate will lead to a fiber with smaller outer radius.

The best defect free hollow fiber membranes were achieved with the following values of the variables: air gaps 5 cm and 10 cm. Similar spins were done to obtain Matrimid® fibers too.

Table 4: Spinning parameters for successful defect free 6FDA:BPDA-DAM fibers obtained in this work

Parameter	**Component**	**Value**
Bore Fluid Composition	NMP	
	Water	
Air gap		5 cm, 10 cm
Take up rate		30 m/min
Dope Temperature		60 °C
Quench bath temperature		50 °C
Extrusion rate	Dope	180 mL/hr
	Bore Fluid	60 mL/hr

3.2.3 Solvent exchange and drying

Solvent exchange is a process that is performed on the wet polymer fibers prior to drying. After the spinning process, the fibers are still wet and are allowed to sit in deionized water for 3 days before beginning the solvent exchange process, refilled with fresh DI water

every day. The solvent exchange process progressively changes the liquid environment around the fibers from less volatile and high surface tension liquids (water), then methanol, then volatile and low surface tension (hexane), so that the solvent can be removed from the polymer fibers. This process minimizes capillary forces experienced by the fiber if a high surface tension liquid like water were allowed to dry directly. If this step is skipped there is a possibility that the porous substructure of the wet fiber will collapse and form a dense wall due to the strong capillary force of drying water. The two solvents we use are chosen taking care that the polymer itself does not dissolve in these solvents. Methanol and hexane, in that order, were used to perform solvent exchange on our fibers. The fibers were removed from the water bath and were immersed in methanol for 20 minutes. The methanol was then replaced by fresh methanol another two times, for 20 minutes each. Similarly, after methanol, the fibers were immersed in hexane thrice for 20 minutes each. After the third soak in hexane, the fibers were ready to dry. The fibers were placed on an aluminum foil, and excess hexane was soaked by Kimwipes. They were then dried in a convection oven at 120 °C for 12 hours. Once they were dry, the fibers were stored in a Ziploc bag with a desiccant alongside.

3.3 V-treatment

V-treatment is a pretreatment process performed on dry polymer fibers before pyrolysis, in order to prevent collapse of the porous substructure during the pyrolysis. The process was discovered by Bhuwania in the Koros group and has been optimized in this work.

The procedure of V-treatment is as follows: polymer hollow fibers are soaked in VTMS solution for 24 hours, then exposed to 100% RH (relative humidity) air in a glove

bag for 24 hours. The 100% RH conditions are achieved by running air through a water bubble column, then filling that air into the glove bag before sealing it. (Note: humid air is not continuously flown through the glove bag for 24 hours.) Once the fibers have been exposed to humidity, they are dried in a vacuum oven at 150 °C under active vacuum for 24 hours. The theory of how the substructure collapse is prevented by this V-treatment process, has been discussed in Chapter 4. An optimization has been performed on this treatment for 6FDA:BPDA-DAM fibers, so it is advisable to read Chapter 4 before using this method.

3.4 Pyrolysis

Pyrolysis is a key step in the production of a CMS hollow fiber membrane. Pyrolysis of fibers involves exposure to high temperatures in a controlled environment. A typical pyrolysis set up is shown in Figure 30.

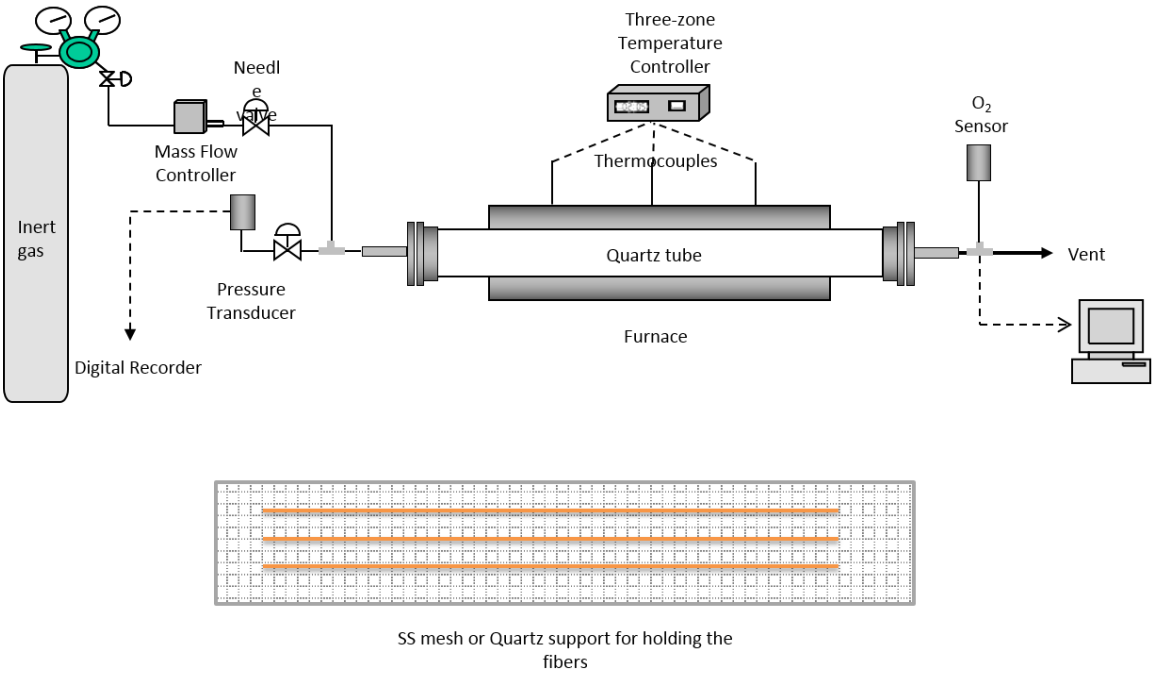

Figure 30: Schematic of a typical pyrolysis set up for producing CMS membranes containing a furnace, quartz tube, temperature controller and oxygen sensor.

The pyrolysis set-up used for the study was similar to the previously reported systems [89] and consists of a three-zone furnace (Thermocraft, Inc., model # XST-3-0-24-3C, Winston-Salem, NC) connected to a multichannel temperature controller (Omega Engineering Inc., Stamford, CT). The three zones were connected to three channels of the temperature controller, each attached to a thermocouple. A quartz tube (National Scientific Co., 55 mm ID and 4 feet long, Quakertown, PA) was used to hold the fibers in the furnace. An assembly of a metal flange with silicon O-rings (MTI Corporation, model EQ-FI-60, Richmond, CA) was used on both ends of the quartz tube. An oxygen analyzer (Cambridge Sensotec Ltd., Rapidox 2100 series, Cambridge, England) was integrated to monitor oxygen concentration during the purge of the setup and the pyrolysis process. The flow rate of the purge gas was controlled with a mass flow controller (Alicat Scientific, part

number MC-500 SCCM-D). In the case of chlorine fixation, the flowrate of the purge was controlled by a needle valve or metering valve and measured by a mass flow meter (Alicat Scientific, part number MS-500 SCCM). Burnout of the tube was performed between experiments, where the quartz tube and wire mesh were rinsed with acetone and baked in air flow of 500 sccm at 800 °C to remove any residue which could affect subsequent runs [90].

The precursor fibers were placed on a support plate, and loaded horizontally into a quartz tube. Two different supports for the fibers were used: a wired stainless steel mesh and a quartz plate. The stainless steel mesh was acquired from McMaster Carr, Robbinsville, NJ, and loosely bound separately with thin stainless steel wires.

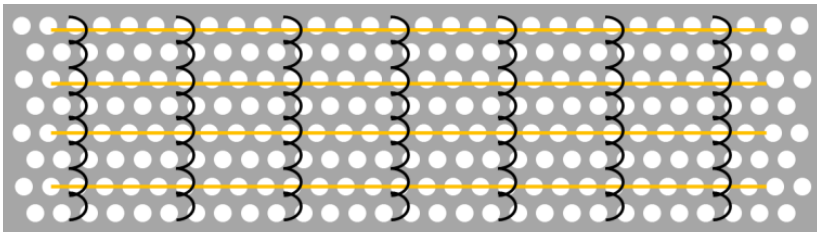

Figure 31: Stainless steel mesh with fibers loaded, woven through stainless steel wires. The fibers do no touch each other during pyrolysis.

The quartz plate was custom made with channels and ordered from United Silica Products, Franklin, NJ (as shown in Figure 32), to allow diffusion of volatile by-products evolved during pyrolysis. This quartz plate was used for dense film and some cases of hollow fiber pyrolysis.

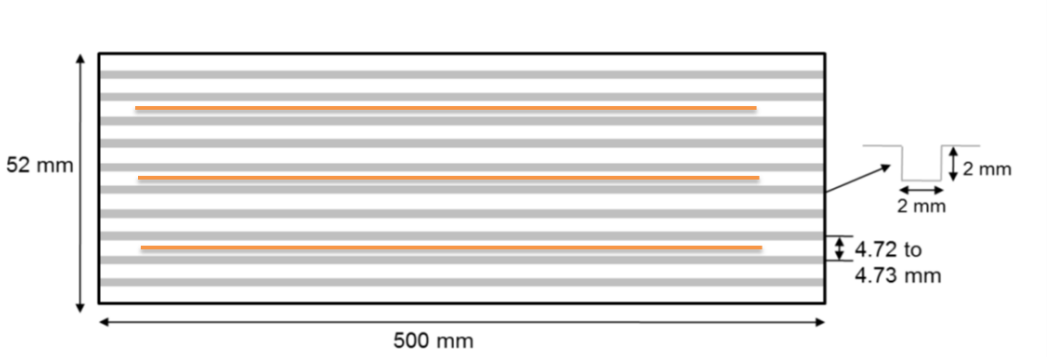

Figure 32: Custom made quartz plate with fibers loaded in the grooves. The fibers do no touch each other during pyrolysis.

Pyrolysis temperature, ramp rate, thermal soak time and pyrolysis atmosphere are important factors affecting pore structure of carbon membrane. These steps can be individually changed to tune the properties of the resulting CMS structure.

3.4.1 Pyrolysis temperature

The final pyrolysis temperature T_{max}, is the maximum temperature to which the sample is heated during pyrolysis. This final temperature significantly affects the structure of the carbon, as discussed in Chapter 2. For higher pyrolysis temperature, the permeability through the CMS membrane typically drops. This is often accompanied by increase in the selectivity of the gas pair passing through the membrane. This happens because with higher temperature the CMS structure gets more time and energy to conform to a thermodynamically stable densified state, which produces a tightened CMS structure as shown in Figure 24 of Chapter 2. Because the sizes of the ultramicropores are reduced at higher pyrolysis temperature, it is harder for the larger gas molecules (like methane) to pass through them; however, smaller gas molecules (like CO_2 and H_2S) can still permeate through the tightened ultramicropores, thereby increasing the selectivity. Practically, a

tradeoff exists between permeability and selectivity when they are controlled solely by the final pyrolysis temperature.

A final temperature is chosen depending on the application – by estimating where the permeance and selectivity is desired. In this case, for the aggressive gas separation with CO_2 and H_2S are to be separated from CH_4, a study of different temperatures was done.

3.4.2 Ramp rate

The ramp rate is chosen to be industrially viable, and yet slow enough that the membrane has enough time to provide enough time for heat transfer and removal of the species leaving the polymer during the pyrolysis process. Changing ramp rates can also influence the selective CMS morphology. For example, for a higher ramp rate of say 10 °C/min, the CMS structure can start by being very open. However, it is not as thermodynamically stable as the CMS produced with lower ramp rates, and shows significant aging. In our case, we use a standard ramp rate of 3.85 °C per minute, and have not changed this variable to tune properties of the CMS.

3.4.3 Soak time

Soak time refers to the period that the membrane is allowed to sit at the final pyrolysis temperature. Similar to the final pyrolysis temperature, longer soak times can tighten the CMS structure. In this work, a soak time of 2 hours was used for all pyrolysis temperatures, and was not varied to tune properties of the CMS.

A combination of pyrolysis temperature, ramp rate and soak time gives a pyrolysis protocol for performing the pyrolysis experiments. The standard protocol typically used is shown in Table 5. The time required in step 5 is calculated with a ramp rate of 3.85 °C/min.

Table 5: Heating protocol for pyrolysis

Step no.	**$T_{initial}$ (°C)**	**T_{final} (°C)**	**Time (min)**
1	Room Temperature	50	20
2	50	250	15
3	250	T_{max} – 15	Calculate with 3.85 °C/min
4	T_{max} – 15	T_{max}	60
5	T_{max}	T_{max}	120

3.4.4 Pyrolysis atmosphere

Pyrolysis atmosphere refers to the gas composition surrounding the polymer during the pyrolysis process. For pyrolysis, the gas atmosphere around the sample needs to be mostly oxygen free. If enough oxygen were present, at very high temperatures the polymer would simply combust to CO_2 and H_2O instead of decomposing to the desired CMS. In the presence of other gases, which may become even mildly reactive, at high temperatures a chemical reaction may occur with the polymer, which may or may not be desired. The most commonly used pyrolysis atmospheres have been Nitrogen and Argon gases. Nitrogen is very neutral until very high temperatures and Argon, being an inert gas, does not react at conceivable temperatures. Pyrolysis atmosphere is also an important factor that can be tuned in a variety of ways to give dramatically different results.

In this study, inert atmosphere was achieved by putting the sample into a quartz tube of the required length, sealing it on both the ends and purging UHP Argon gas continuously through an inlet into it until all the air inside is replaced and the oxygen level

is the minimum achievable. Oxygen level can be monitored by attaching the oxygen sensor at the end of the quartz tube. Pyrolysis shouldn't be started until the oxygen reading shows less than 1 ppm of oxygen level if "UHP" (ultra-high purity) conditions are desired. Even a small leak can rapidly pollute the inert atmosphere, and it is nearly impossible to completely eliminate minute leaks. So it is advised that the inert gas is flown continuously through the pyrolysis tube until the end of the pyrolysis and cooling to room temperature has occurred.

The pyrolysis atmosphere can also be altered to tune the properties required for the final application. If a dopant molecule is added to the pyrolysis atmosphere, it can react with the reactive edges at the ultramicropores of the CMS membrane. Oxygen as a dopant has been studied by Kiyono and has used in the past by many researchers to obtain the optimum properties of the CMS membranes [72]. We have proposed to use chlorine as a dopant in the work discussed here.

In this work, ultra-high purity (UHP) Argon from Airgas (has 99.9% Argon, less than 1 ppm oxygen content) was used in many cases. This is indicated as UHP Ar in the results section. Other dopants in the levels of parts per million mixed in Argon, have also been used, and will be indicated in the results section. A list of all the gases used for pyrolysis atmosphere is listed here, with their abbreviations used in the results section

1. UHP Ar (Ultra High Purity Argon)
2. 30 ppm O_2 (30 ppm of O_2 in Argon)
3. 5 ppm Cl_2 (5 ppm of Cl_2 in Argon)
4. 15 ppm Cl_2 (15 ppm of Cl_2 in Argon)
5. 30 ppm Cl_2 (30 ppm of Cl_2 in Argon)

3.5 H_2S laboratory

This work considers the effect of H_2S on CMS membranes, and deals with pure gas H_2S as well as mixed gas containing H_2S. Because H_2S is highly toxic, a special laboratory is dedicated to ensure its safe handling [19]. The permeation boxes and sorption systems are enclosed in a large ventilated cabinet made of Plexiglass (Figure 34) as a secondary containment section to prevent H_2S exposure if a leak was to occur in any system. This cabinet is connected to an overhead exhaust duct with negative pressure so that it is constantly pulling the air from the cabinet, and is connected to a 16 feet vertical packed bed H_2S scrubber (Indusco Environmental Services, Inc) on the rooftop. A solution of 20 - 25 weight % sodium hydroxide (NaOH) is pumped from the lab to the spray headers to neutralize the acid gases released from the experimentation systems.

$$H_2S + 2\,NaOH \rightleftharpoons Na_2S + 2\,H_2O$$

$$CO_2 + H_2O \rightleftharpoons H_2CO_3$$

$$H_2CO_3 + NaOH \rightleftharpoons NaHCO_3 + H_2O$$

$$NaOH + NaHCO_3 \rightleftharpoons Na_2CO_3 + H_2O$$

Figure 33: Reactions of NaOH solution with acid gases CO_2 and H_2S for scrubbing

The main feed vales for permeation and sorption systems are pneumatically-actuated, and are controlled from a computer outside of the cabinet by a LabVIEW® program for additional safety; the downstream actuated valves are programmed to shut

down when the downstream pressure reaches the maximum transducer pressure (100 torr) to avoid over-pressurization that may damage the transducers or to prevent unintended release of high amounts of H_2S.

Figure 34: Cabinet as secondary enclosure for safe H_2S handling. Permeation and sorption systems are enclosed inside the cabinets.

Several Honeywell H_2S sensors are placed in the lab, two inside the fume cabinets and three outside in the ambient air, to ensure safety of the users. Additionally, individual H_2S sensors are worn by lab members while entering the lab. Gas cylinders containing H_2S and flammable gases are stored in a gas cylinder cabinet (Matheson Tri-Gas®) with ventilation

to the rooftop acid gas scrubber. Moreover, access to the lab is restricted to members who have undergone and maintained a respirator safety certification for H_2S handling. Members are required to wear a gas purifying respirator at all times while working in the lab.

3.6 Permeation

Permeation is a procedure used to test the separation properties of the membrane. There are different ways to set up a permeation test, but they all follow the same basic idea. The membrane is subjected to a gas at the upstream, and passage of a test gas or gases through it, allows determination of the pressure and thickness normalized flux as a "permeability" measured in Barrers. When a permeation test is done on hollow fibers, the throughput is referred to as permeance and is measured in terms of Gas Permeance Units [GPU]. The calculations are described in more detail in Chapter 2

3.6.1 Module Fabrication

For testing fibers, a small scale module is fabricated by a method described earlier [68]. The membrane is made into a module by sealing together several Swagelok parts. The seal is made by the ferrule set which presses against the inside of the joints of the Swagelok fittings. The female NPT parts on both the ends are then packed with Teflon "worms", with a small orifice left for the fibers which will be inserted. Once the Teflon worm is packed into the NPT, the fiber is inserted carefully through the module, and the fibers ends are allowed to protrude out of both the ends to cover the Male NPT fitting attached to a small piece of Tygon tubing. The ends are then sealed using a desired epoxy and then the male NPT fitting is fixed into it. The module is left for the epoxy to set (the time varies depending on which epoxy is used) before the Tygon tubing at the ends are broken off to reveal a clean end with a bore of the fiber open to atmosphere.

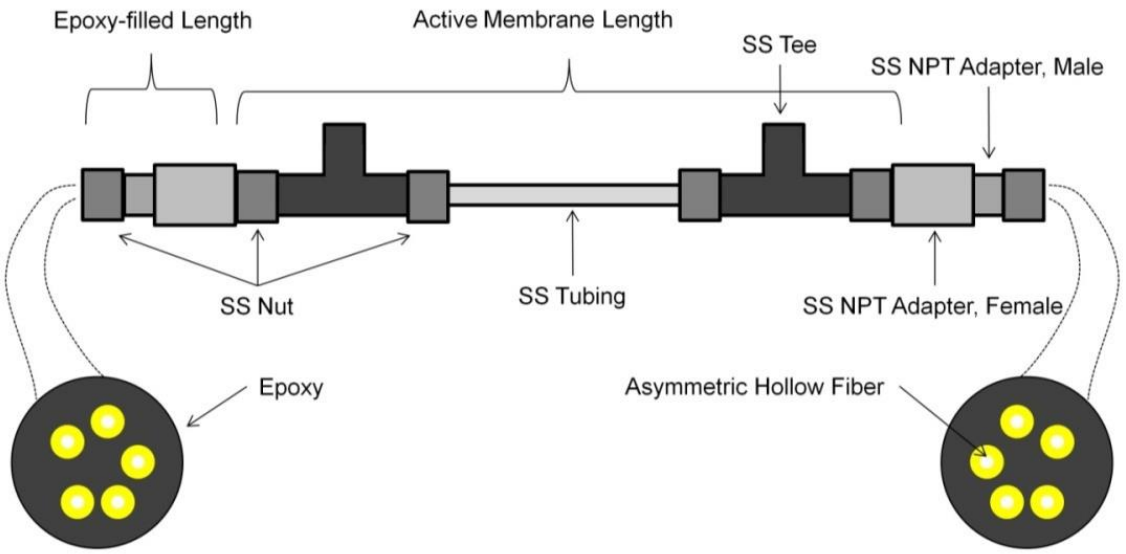

Figure 35: Lab scale hollow fiber membrane module for testing. Stainless Steel components are used for all parts to prevent corrosion by acid gases [24].

Once the module is ready, it can be attached to a permeation box. There are different types of permeation boxes: the two major types being constant pressure permeation and constant volume permeation.

3.6.2 Constant pressure permeation

To use a constant pressure system, the membrane is attached to a gas feed line, called the upstream. The gas from the upstream comes in contact with the membrane, and partially permeates through it at a certain rate (which is what needs to be calculated,) and emerges on the other side of the membrane, which is called the downstream. The downstream of the membrane is attached to a bubble flow meter or a digital flow meter so that the volumetric flow rate of the gas leaving the membrane can be measured. The dV/dt, volumetric flow rate, is then used to calculate the permeance of the membrane (essentially

telling us how fast the membrane will allow a gas to flow through it.) The formula used for this is:

$$\frac{P}{l} = \frac{(5.28 \times 10^7)\,(\frac{dV}{dt})}{A \times T \times (p_f - p_{atm})} \tag{13}$$

Where:

P/l = Permeance [=] GPU

$\frac{dV}{dt}$ = Permeate flow rate [=] cc(STP)/sec

T = Temperature [=] K

A = Membrane area [=] cm^2

p_f = Feed pressure [=] psia

p_{atm}= Atmospheric Pressure [=] psi

The permeance P/l of the membrane is measured by a term called GPU:

$$GPU = 10^{-6}\frac{cm^3_{STP}}{cm^2 \times s \times cmHg}$$

This setup is ideal for a membrane with high throughput. A schematic of the system is shown in Figure 36.

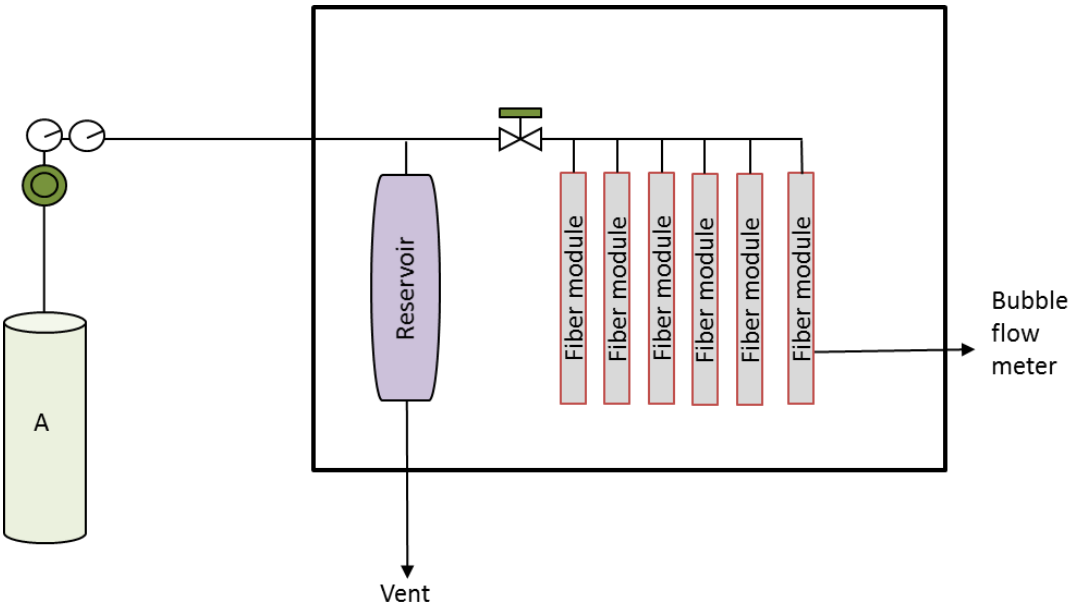

Figure 36: Constant pressure permeation system for hollow fiber membrane modules

3.6.3 Constant volume permeation

Constant volume systems are ideal for membranes with low throughput, which is hard to measure by a bubble flow meter or digital flow meter. In such systems, the membrane is attached to a gas feed line, again called the upstream. The gas from the upstream comes in contact with the membrane, and passes through it at a certain rate (which is what needs to be calculated,) and emerges on the other side of the membrane at a vacuum, which is called the downstream. The downstream of the membrane, in this case, is a constant volume of a known value, and it is attached to a sensitive pressure transducer. As the gas from the upstream starts permeating through the membrane and to the downstream, the pressure in the downstream starts increasing. The increasing pressure with respect to time (dp/dt) is recorded from the pressure transducer on a computer. This value of dp/dt is then used to calculate the permeance (essentially indicating how fast a particular gas can pass through the membrane.) Slow membranes can be measured very efficiently in this

system, and it has the capacity to expand the downstream volume so that there is some control in the researcher's hands. A schematic of the system is shown in Figure 37.

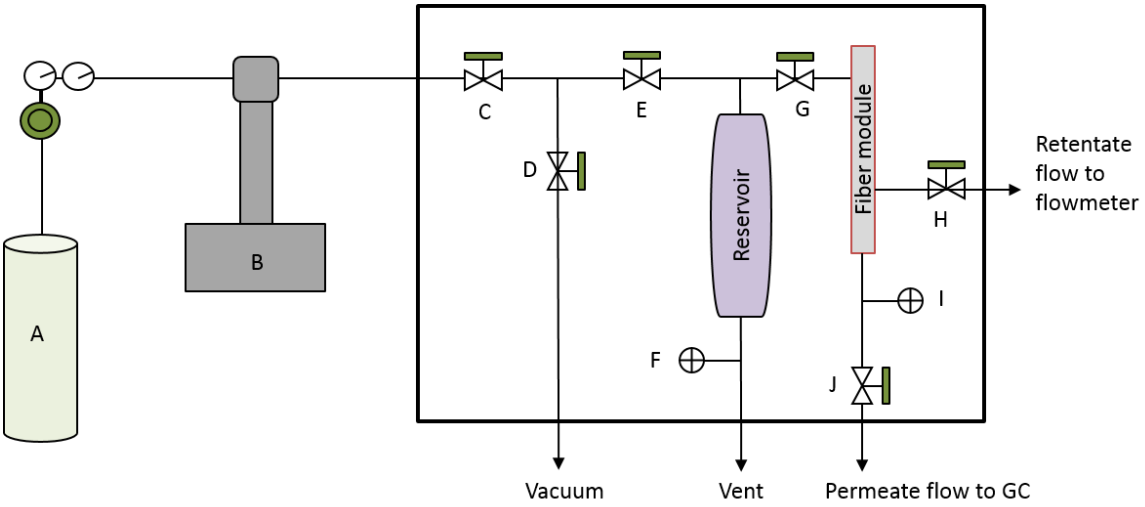

Figure 37: Schematic of a constant volume permeation system for testing pure and mixed gas

Table 6: Components for permeation system in the H_2S laboratory

Components	**Vendor**
A: Gas cylinder	Praxair
B: Syringe Pump	1015 mL D Series Syringe Pump (Teledyne Isco)
C: Feed Input Valve	Swagelok Double Sealed Bellows Valve
D: Upstream/Downstream Isolation Valve	Swagelok Double Sealed Bellows Valve
E: Feed Isolation Valve	Swagelok Double Sealed Bellows Valve
F: Upstream Pressure Transducer	Honeywell (2000 psia max. pressure)
G: Pneumatically-actuated Feed Valve	Swagelok Pneumatic Actuated Bellows Valve
H: Retentate Valve	Swagelok Double Sealed Bellows Valve
I: Downstream Pressure Transducer	MKS Instruments, Inc (50 or 100 Torr)
J: Pneumatically-actuated GC Valve	Swagelok Pneumatic Actuated Bellows Valve

To control the temperature inside the permeation system, a temperature controller is installed on the outside of the system and a fan is installed inside the system. For all measurements performed in this work, the permeation system was maintained at 35°C.

These permeation systems were slightly modified from the typical systems that are used for testing non-toxic gases, since H_2S-containing gases require a more robust design to ensure user safety [91]. The most important change to note is that pneumatically activated feed and GC sampling valves are used instead of manual bellows valves. These can be controlled from a computer outside the fume hood that contains the system, via a LabView (National Instruments Corp.) code, which also records the upstream and downstream pressure data with time. This reduces the risk of exposure to H_2S and can also protect sensitive system elements from over-pressurizing. A detailed construction of these systems can be found in other theses [15].

These systems can be used to do two types of test: pure gas tests and mixed gas test.

Pure gas testing: Only one gas of interest is fed to the upstream at a given time. Starting with the least condensable gas, a pure gas test of all gases of interest can be done to obtain intrinsic permeances. The pure gas permeances can then be used to calculate the intrinsic pure gas selectivity. This helps to calculate the time required for each gas to reach steady state. However, this is not how the membrane will be used industrially, and hence has no industrial application. The permeance is calculated as:

$$\frac{P}{l} = \frac{(6.949 \times 10^4)\left(\frac{dp}{dt}\right)V_d}{A \times T \times \Delta p} \tag{14}$$

Where:

P/l = Permeance [=] GPU

V_d = Downstream volume [=] cm^3

T = Temperature [=] K

A = Membrane area [=] cm^2

Δp = Transmembrane Pressure difference [=] psia

Mixed gas testing: In this case, the system is fed a set composition of a mixture of the gases of interest. Mixed gas permeation set up and testing is much more complex than pure gas permeation. Since the fast gas can permeate through the membrane much faster than the slow gas, it can lead to depletion of the fast gas in the upstream of the membrane, causing concentration polarization. To prevent concentration polarization, the stage cut of a mixed gas feed must be carefully maintained. The upstream gas also has to be bled out at a small flow rate so as to keep the upstream composition constant. It is the measure of the relative flow rates of calculated as follows, and ideally should be maintained at or less than 1% for mixed gas permeation tests.

$$Stage\ Cut\ \% = \frac{n_{permeate}}{n_{feed}} \times 100 \quad (15)$$

The feed gas is fed at the shell side of the membrane, and a countercurrent flow configuration is used for mixed gas permeation testing. For non-H_2S containing mixed gas feeds, a digital mass flowmeter (FMA Series, Omega Engineering, Inc.) was used to measure the retentate flow rate.

However, for H_2S containing mixed gas feeds, the procedure is significantly more challenging. H_2S is a toxic gas, and flow meters may expose the user to it and hence cannot be used for retentate flow measurement.

$$\frac{P}{l} = \frac{(6.949 \times 10^4)\, y_i \left(\frac{dp}{dt}\right) V_d}{A \times T \times (x_i p_{up} - y_i\, p_{down})} \quad (16)$$

Where:

x_i = upstream mole fraction of component *i*

y_i = downstream mole fraction of component *i*

The permeation is continued until steady state is reached, and then the permeate gas is diverted to a gas chromatograph (GC) (Varian 450-GC, Agilent Technologies) in order to determine its composition. The permeate gas composition is tested until steady state operation is confirmed. A more accurate result can be obtained by substituting the pressure by fugacity of the gas. The fugacity coefficients are calculated by using the Peng Robinson equation of state, which is well suited for natural gas feed.

In this work, most tests were done in constant volume permeation boxes.

3.7 Sorption

Sorption is a term used to collectively describe absorption and adsorption in the membrane. Sorption experiments are done so that the amount of any given gas that dissolves or "sorbs" into the CMS membrane can be measured, and to calculate what kind of sorption selectivity the membranes has for our gases of interest. In this particular project, it is also useful to study whether the H_2S chemically affect the sorption capacity of CO_2 and CH_4 on the CMS membranes.

Sorption tests are done in this study by using a pressure decay sorption test. The fundamental of this test is a simple mole balance to obtain the concentration versus pressure isotherm. A gas is fed into a closed chamber with the CMS sample at a certain pressure,

and then as the gas slowly sorbs into the CMS membrane, the overall pressure of the gas in the chamber decays until it equilibrates. This sorbed gas, at different pressures, can then be used to determine the sorption isotherm for the gases. In the case of CMS samples, the sorption isotherms follow the Langmuir isotherm.

Similar to the permeation systems, to ensure corrosion resistance in the H_2S lab, sorption systems are made completely with stainless steel. The set up for this experiment is as originally described by Koros and Paul [92]. The design for the sorption set up was slightly modified to better suit the safety requirement of the H_2S lab. A schematic of the system is shown in Figure 38. The two main compartments of the system are the reservoir (space between valves A and C) and the sorption cell E.

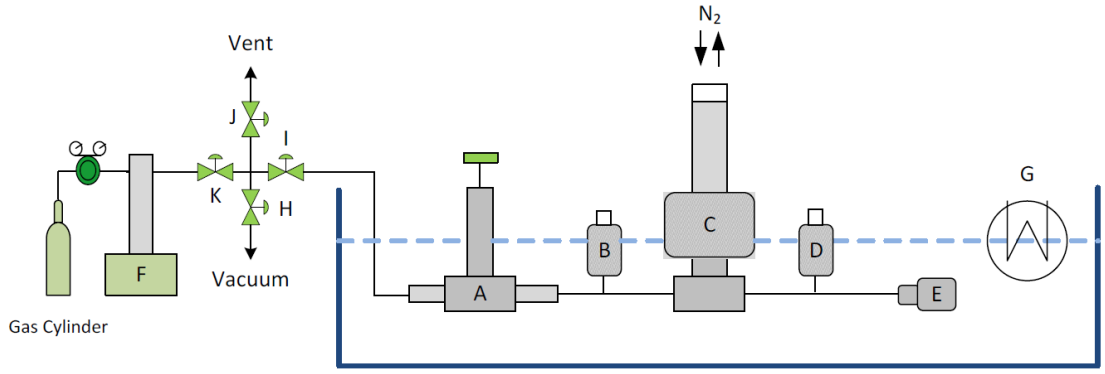

Figure 38: Sorption system in the H_2S lab [15]

Dried sample is weighed and loaded into the sorption cell E. The reservoir and the cell of known volumes are kept in an oil bath to maintain constant temperature. The system is evacuated for 24 hours before any sorption test is started. Desired pressure of gas is fed to the reservoir, while the pneumatic valve C is kept closed. The reservoir isolation valve A is then closed to shut it off from the gas cylinder. A LabVIEW® program records the

pressure versus time data until equilibration. After the pressure equilibrates, the pneumatic valve C opens very briefly for 1-3 seconds to let the gas from the reservoir into the sample cell, and then closes again. Right after this is done, the reservoir and sample cell pressure should be equal to each other. However, the gas slowly sorbs into the sample and after a few hours the sorption process reaches equilibrium. The difference between the two pressures is used to calculate how much gas was sorbed into the CMS sample. The formula to calculate the amount of gas sorbed into the CMS material is given by:

$$n_p = \frac{1}{RT}\left[(V_C - V_{CMS}) \times \left(\frac{p_{C,i}}{z_i \times p_{C,i}} - \frac{p_{C,f}}{z_f \times p_{C,f}}\right) + V_R \times \left(\frac{p_{R,i}}{z_i \times p_{R,i}} - \frac{p_{R,f}}{z_f \times p_{R,f}}\right)\right] \quad (17)$$

$$C_{S,i} = 22412.7 \times n_p / \left(\frac{m_s}{\rho_s}\right) \quad (18)$$

Where,

n_p = moles of penetrant gas, *i*, sorbed [=]

V_C = Sample cell volume [=] cm^3

V_{CMS} = Volume of sample $= \frac{m_s}{\rho_s}$ [=] cm^3

$p_{C,i}$ = initial pressure of sample cell [=] psi

$p_{C,f}$ = final pressure of sample cell [=] psi

$p_{R,i}$ = initial pressure of reservoir [=] psi

$p_{R,f}$ = final pressure of reservoir [=] psi

z = compressibility factors associated with initial and final pressures of gas

$C_{S,i}$ = concentration sorbed into sample at STP [=] $cm^3_{gas}/ cm^3_{sample}$

Once a sorption value in units of (cc of gas/cc of sample) is obtained, a higher pressure of gas is then then added to the reservoir, and the same process is repeated for higher pressures. A sorption test is a very important test, and can help us determine how a certain gas molecule interacts with the CMS membrane.

3.8 Characterization techniques

3.8.1 Scanning Electron Microscopy (SEM)

SEM has been used to take a look at the cross sections of both the polymeric precursor hollow fiber, and CMS hollow fiber membranes. The SEM LEO 1530 has been used, equipped with a thermally assisted field emission gun and operating voltage 8 kV. All fibers were coated with gold before SEM.

3.8.2 Fourier Transform Infra-Red Spectroscopy (FTIR)

FTIR-ATR spectroscopy was conducted using a Bruker-Tensor 27 spectrometer (Bruker Corp.) with a MVP 2 Series™ ATR attachment (Harrick Scientific Products, Inc.). The system was continuously purged with N_2 and spectra measurements consisted of 128 scans with a resolution of 4 cm-1. Dense films were the preferred sample medium, but powder were also measured by using the ATR attachment.

3.8.3 Thermogravimetric Analysis

Thermogravimetric analysis is used to measure residual solvent content, weight losses associated with pyrolysis, and polymer degradation temperatures in fiber and powder samples. The instrument used was a TGA Q500, TA Instruments. A heating rate

similar to the pyrolysis protocol from Table 5 was used for all TGA experiments. The sample compartment was purged with UHP Argon at a flow rate of 30 mL/min for all TGA experiments.

3.8.4 Solid-state NMR

Solid-state NMR spectra were measured at the Georgia Tech NMR center by Johannes Leisen using a high resolution Bruker AV3-400 solid-state spectrometer. The spectrometer operated at 1H frequency of 400 MHz.

3.8.5 X-ray photoelectron spectroscopy (XPS)

XPS is performed on carbon fibers as well as powders to determine the bonding of chlorine in CMS membranes. The spectra were acquired using a Thermo K-Alpha XPS (Thermoscientific) with a monochromatic Al Kα line, operating under ultra-high vacuum conditions. A spot size of 400 μm was used for powder sample, while 70 μm was used for fiber samples. Survey XPS scans were obtained over the B.E. range (0-800 eV) with a step size of 0.01 eV and high resolution scans typically at 20 eV pass energy.

3.8.6 Thermally Programmed Desorption (TPD)

Thermally programmed desorption was carried out to find whether the H_2S is released from the CMS sample. A Micromeretics TPD was used from the Jones group. The sample was heated up to 120 °C to evaporate any moisture in the sample. It is then cooled down and heated up to 550 °C (final pyrolysis temperature) at a ramp rate of 10 °C/min. Helium was used as a carrier gas for all experiments.

CHAPTER 4 MEMBRANE FORMATION

Xu *et al.* [88] showed that CMS hollow fibers from Matrimid® (as shown in Figure 10) and 6FDA:BPDA-DAM precursors showed differing degrees of porous support layer collapse. The collapse of substructure results in a low permeance, which is an obvious concern for scale up of membrane separation. A proof of concept process to prevent the substructure collapse was developed by Bhuwania from the Koros group. This chapter clarifies factors enabling this V-treatment process, and reports its optimization for V-treatment on Matrimid® and 6FDA:BPDA-DAM hollow fiber membranes.

4.1 Pyrolysis conditions

4.1.1 Choosing temperature

As described in the Section 2.3.2.1, intrinsic properties of the polymer precursor impact the properties of the CMS structure. These intrinsic properties for Matrimid® lead to a much tighter CMS structure than 6FDA:BPDA-DAM in terms of permeation and selectivity. Also from Section 2.3.2.2 that describes the pyrolysis temperature and protocol, it is known that a higher pyrolysis temperature leads to tightening of the pores of any CMS. The pore structure in Matrimid® starts out "tighter", and as will be seen later in Chapter 5, is affected significantly by H_2S; so the lowest feasible pyrolysis temperature was chosen to provide the most open Matrimid® derived CMS. The glass transition temperature (T_g) and decomposition temperature (T_d) of Matrimid® are 305 °C and 425 °C respectively. To ensure that the Matrimid® is transformed to a practical CMS, a temperature (500 °C) above

the decomposition temperature was chosen as the final pyrolysis temperature. This temperature gives the highest permeance of CO_2. Previously, Kiyono showed that Matrimid® CMS membranes are more tunable using oxygen doping at 500 °C. Similarly, Kemmerlin used 500 °C final pyrolyzing temperature to explore effect of H_2S on CMS membranes. For these reasons, 500 °C was chosen as the pyrolysis temperature for Matrimid® related experiments in this work. Experiments were also performed at 550 °C, 600 °C and 650 °C pyrolysis temperatures as a comparison for permeation data and to be consistent with Bhuwania's work. Additionally, a few experiments were carried out at 800 °C to examine the effect of using different pyrolysis system supports on the CMS properties. Not only for this work, but for future applications, it was felt wise to combine these studies in an integrated series with a well-controlled starting material.

For 6FDA:BPDA-DAM, optimization was done by both Kiyono [62] and Bhuwania [90] to identify and optimum pyrolysis temperature (550 °C) with respect to optimum permeance and selectivity for CO_2/CH_4 separation. This 550 °C temperature was chosen for use in the current study using 6FDA:BPDA-DAM.

4.1.2 SS mesh vs quartz tube

As a control study, since at the outset of this work, the conditions that would be used were not decided, any effects due to the support material used to hold the precursors during pyrolysis was considered. Pyrolysis experiments were performed at temperatures ranging between 500 °C to 800 °C, and it was observed that an SS mesh had negative effect on permeance for Matrimid® derived CMS fibers at higher temperatures.

From literature it is known that at high temperatures near 800 °C, Chromium (Cr) from the stainless steel alloy exhibits significant vapor pressure [93, 94]. This vaporized

Cr can deposit on the pores of CMS hollow fibers and plugs them, thereby producing a lower CO_2 permeance than with pure quartz supports. Although not a main focus of this work, this effect of Cr was found to also show more dramatic effect in the more challenging separations like N_2/CH_4, where size selectivity is more difficult to achieve. The expected permeance should equal the permeability divided by film thickness. Xue Ning has studied N_2/CH_4 separation using CMS dense films from Matrimid® using quartz support plates [95]. Her data shows that the intrinsic permeability of the Matrimid® pyrolyzed at 800 °C in UHP Ar is 6.78 Barrers, which translates to 0.17 GPU of N_2 permeance. Work done here for the pyrolysis of Matrimid® hollow fibers was done at 800 °C on an SS mesh gave N_2 permeances four times lower than the expected value. Conversely, when the pyrolysis mesh was substituted with a quartz plate instead of a stainless steel support, expected permeances were achieved.

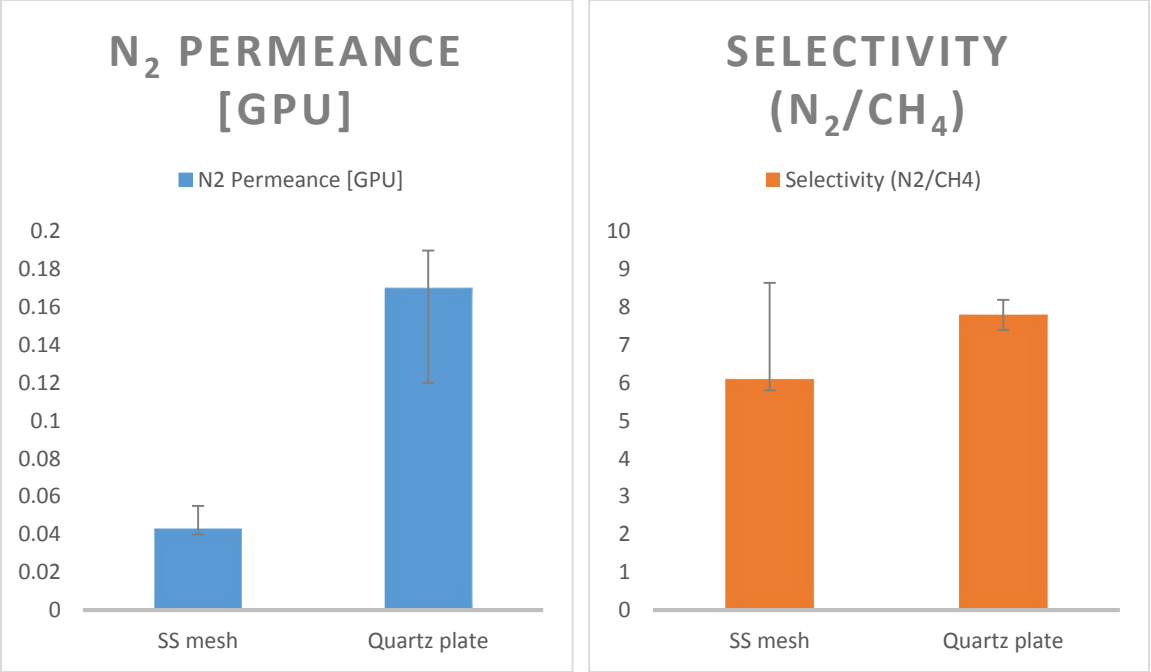

Figure 39: Permeance of N_2 and selectivity N_2/CH_4 using two different pyrolysis supports at 800 °C under UHP Ar, tested with pure gas at 100 psi and 35 °C.

XPS was performed on these fibers pyrolyzed at high temperatures and the presence of a chromium peak was observed. This supports the hypothesis that the vapor pressure of chromium at high temperatures is detrimental to the gas transport of slow gases. At low temperatures like 500 °C to 600 °C, the vapor pressure of Cr is very low above such stainless supports and does not cause a *significant* difference in the permeance, especially in the case of faster gases like CO_2 (as shown in Figure 30.)

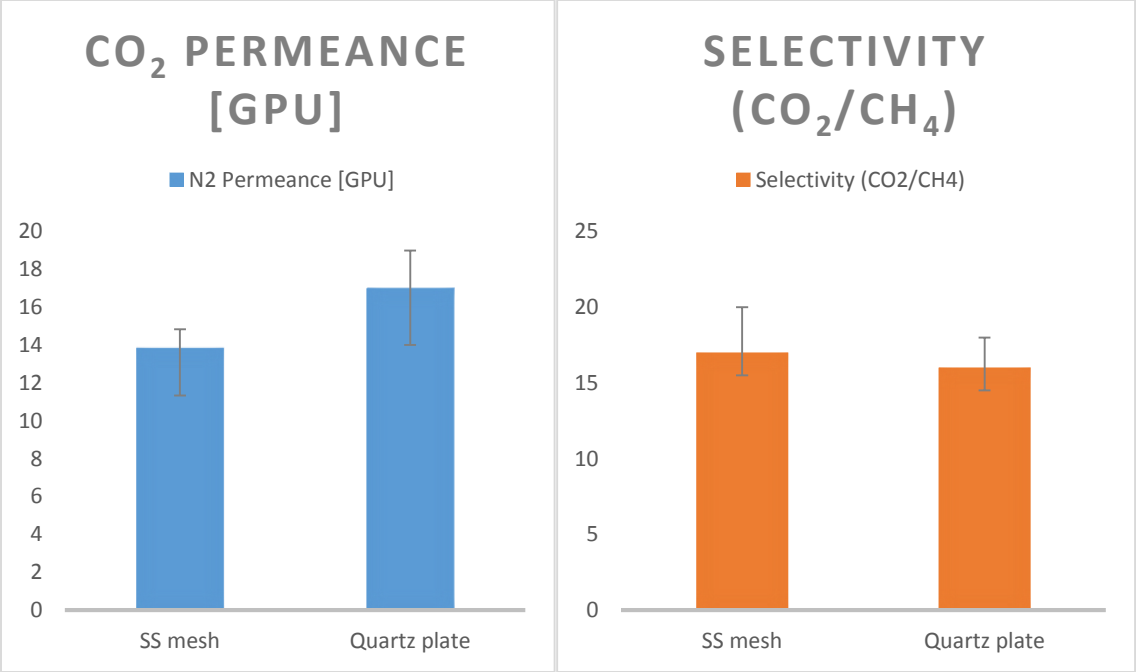

Figure 40: Permeance of CO_2 and selectivity CO_2/CH_4 using two different pyrolysis supports at 500 °C with UHP Ar atmosphere, tested with pure gas at 100 psi and 35 °C. No particular evidence is seen as lost.

Therefore most experiments done in this range of temperatures were performed on SS mesh with UHP Argon. Experiments involving Cl_2 in the pyrolysis atmosphere were performed on quartz mesh, since chlorine caused the SS mesh to break down.

4.2 V-treatment

As mentioned earlier, V-treatment is a method that was discovered by Bhuwania from the Koros group, to suppress the porous substructure collapse of the hollow fiber membranes [96]. This treatment provided higher permeance of CMS hollow fiber membrane; however, at the time of the commencement of this study, the exact mechanism of V-treatment was unknown and some questions remained regarding the mechanism of

V-treatment at the completion of Bhuwania's work. To answer these questions, additional studies were done in the current PhD project.

Of course, defect free fibers had to be spun before the V-treatments could be performed on fibers. Matrimid® fibers obtained from Bhuwania were initially used and then spun using the same conditions. The precursor polymer properties of the green (polymer) fibers are shown in the following table. Additionally, fibers were spun for this work from the polymer 6FDA:BPDA-DAM, which as noted earlier, leads to a more intrinsically open CMS structure. The fibers were proven to be defect free by comparing the O_2/N_2 selectivity to that of the dense film data (shown in parenthesis), the measured permeances at 35 °C set a baseline case for comparing permeances.

Table 7: Separation performance of defect free Matrimid® and 6FDA:BPDA-DAM asymmetric hollow fibers, tested with pure gas at 50 psi and 35 °C. O_2/N_2 selectivity of dense films, shown in parenthesis, is cited from previous work [37, 66]

Polymer	(O_2/N_2)	P/l CO_2 [GPU]
Matrimid®	6.3 ± 0.2 (6.7)	23 ± 6
6FDA:BPDA-DAM	3.99 ± 0.07 (4.1)	63 ± 8

A study of how the VTMS affects the permeance and selectivity of a Matrimid® hollow fiber was being carried out by Bhuwania at 550 °C and 650 °C. Matrimid® hollow fibers were also spun several times for this work, and defect free hollow fiber membranes were obtained. As noted earlier, the current work focused first on pyrolysis of Matrimid® fibers at 500 °C. This lower temperature was chosen to create CMS with more open structures that could ultimately be useful for H_2S applications. First, however, detailed CO_2

and CH_4 benchmarks at 500 °C were needed. The transport properties for CO_2 and CH_4 are shown in Figure 41, comparing the permeance of CO_2 in the green fiber (polymer precursor fiber), CMS hollow fiber pyrolyzed at 500 °C and CMS hollow fiber with V-treatment pyrolyzed at 500 °C.

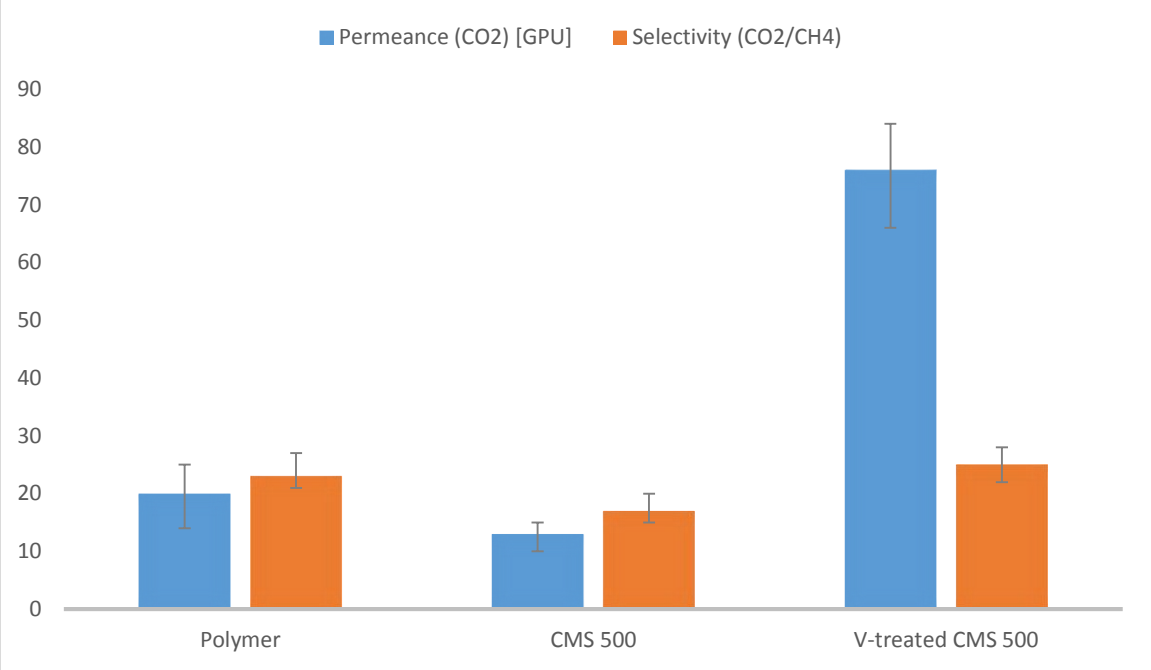

Figure 41: Gas transport properties for Matrimid® polymer fibers, CMS fibers and V-treated CMS fiber pyrolyzed at 500 °C. Tested with pure gas feed at 50 psi at 35 °C.

It was seen that the untreated CMS fibers pyrolyzed at 500 °C showed lower performance than even the polymer fibers. This result can be explained in terms of the substructure collapse of CMS hollow fiber, similar to what is shown in Figure 10. When the Matrimid® fibers were V-treated, no substructure collapse was seen and hence the permeance increased 5 times compared to the untreated CMS fibers. This was also

confirmed with an SEM image of the fiber where the porosity of the substructure could clearly be seen in Figure 42.

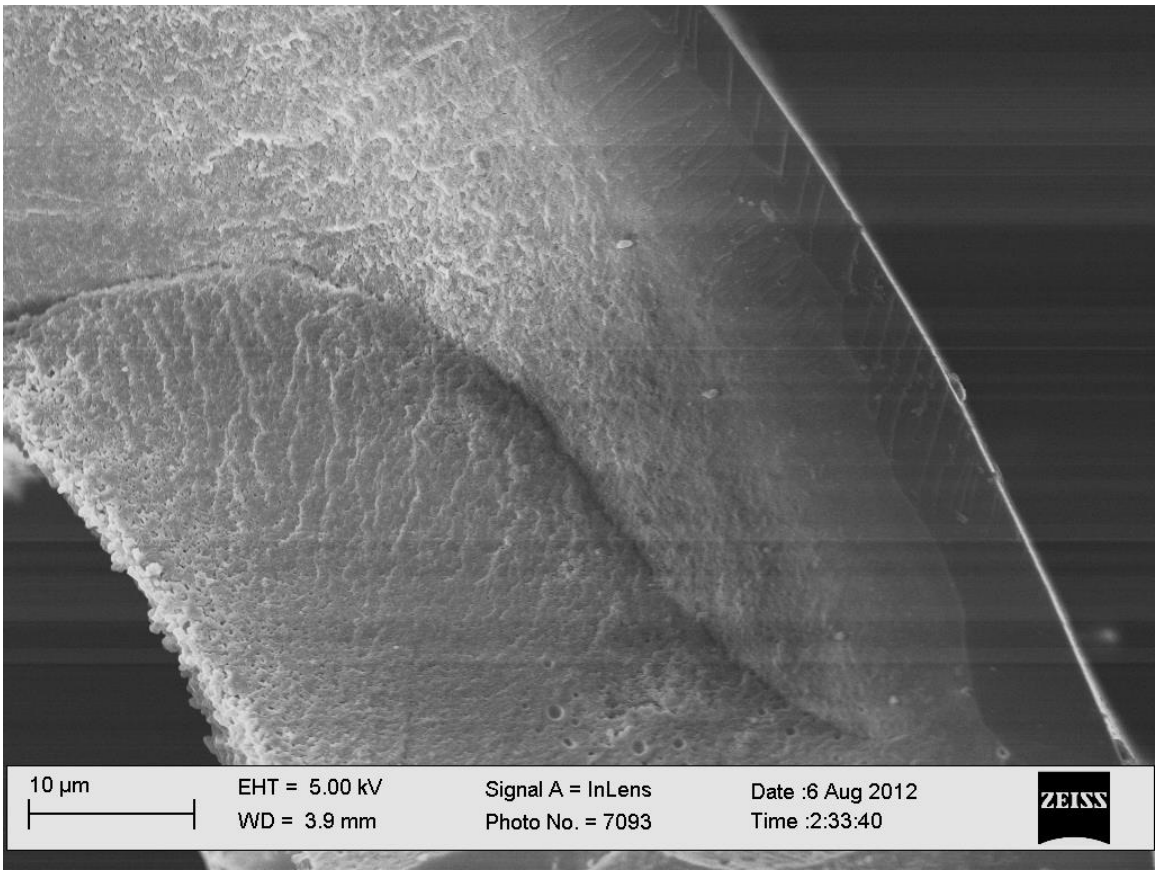

Figure 42: SEM image of V-treated Matrimid® fiber pyrolyzed at 500 °C in UHP Argon shows intact porours substructure.

The comparison of CO_2 permeances in the above three cases shows that V-treatment obviously provides superior permeance, experiments were planned identify the most optimum V-treatment conditions.

4.2.1 Clarifying key V-treatment parameters

While the main features of V-treatment mechanism were felt to be understood at the onset of the current project, work done here helps support the hypothesis by Bhuwania and to extend it for practical use [96]. As discussed, improved understanding of the actual V-treatment mechanism emerged while doing this work in parallel with that of Bhuwania. This section considers the exact temperature at which V-treatment occurs, as well as the time required for soaking the fiber in VTMS to achieve the anti-collapse during pyrolysis.

The procedure of V-treatment at the time of initiation of the current project was to immerse the polymer precursor hollow fibers in 100% VTMS in a closed vessel and to heat them to 200 °C, where "grafting" was said to occur. The VTMS grafted fibers were wiped off with Kimwipes to remove the remaining liquid and then dried under vacuum to evaporate excess VTMS. Once the fibers were dry, they were pyrolyzed with UHP Ar to the final pyrolysis temperature.

4.2.1.1 Temperature

It was demonstrated by Bhuwania that when fibers were treated with VTMS up to a temperature below the T_g of Matrimid®, it resulted in no collapse of the substructure. Clearly the fiber containing the VTMS experienced a wide range of temperature during pyrolysis, suggesting that the VTMS was grafting or otherwise chemically interacting with the polymer at an unidentified high temperature. Identifying the main V-treatment temperature window was desirable from a practical scale-up perspective as well as understanding the detailed mechanism of the V-treatment. To achieve this insight, the temperature to which the fibers had to be heated in the presence of VTMS was explored. This was intended to identify the minimum temperature required prior to pyrolysis, for the

fiber to exhibit no collapse. A different procedure had to be used to observe the particular temperature at which this change occurred, to decouple it from the pyrolysis heating protocol. To attempt to ensure that the fibers were soaked at exactly the intended temperature without combining with the pyrolysis heating, a solvent exchange was performed with acetone right after the V-treatment procedure. This was intended to extract any remaining VTMS from within the bore and pores of the fiber before the pyrolysis process was started.

To implement the above idea, different samples of Matrimid® fibers were heated in a vacuum oven, each to a different indicated temperature for 1 hour while being soaked in 100% VTMS. The fibers were V-soaked and heated in a closed vessel to different temperatures (100 °C, 130 °C, 150 °C, 200 °C) to find the temperature range where the modification appeared to be happening. The hypothesis was that heating up to 'x' °C would result in collapse, while up to 'y' °C would result in no collapse, which would clearly identify a particular preferred temperature. After solvent extraction with acetone, the fibers were pyrolyzed at 550 °C with UHP Argon. The result is observed from SEM images of the pyrolyzed fibers shown in Figure 43, which show the morphology of the substructure.

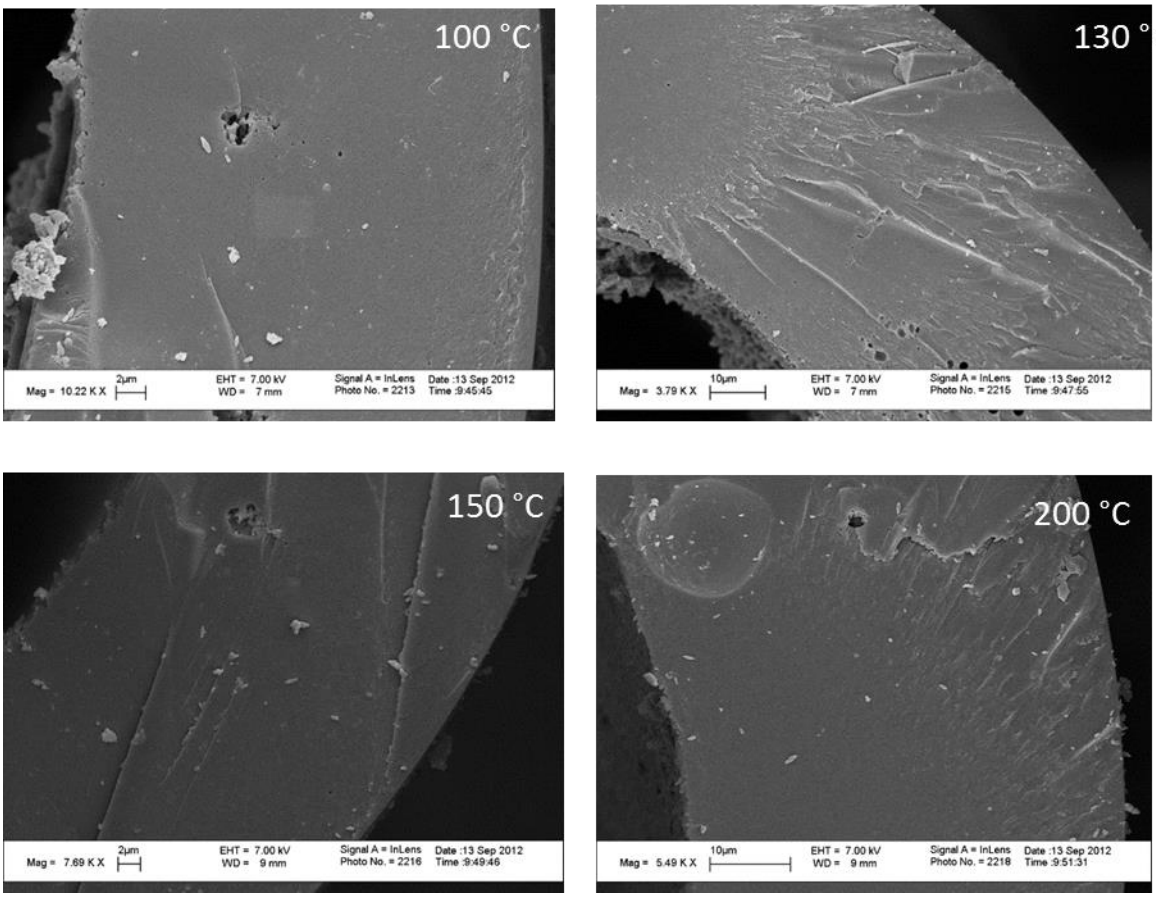

Figure 43: V-treatment performed at different temperatures before performing solvent extraction to determine what timeperature is best suited for V-treatment

Surprisingly, the SEM images showed that the porous substructure of the V-treated fibers collapsed, regardless of the temperatures at which the V-treatment "grafting" was performed. This result clearly indicated that a particular temperature of "V-grating" was *not the key to the process*. This indicated, in fact, that when the VTMS was extracted using acetone, the V-treatment does not form the silica oligomer at any of the temperatures used. In a parallel study by Bhuwania, ^{13}C NMR showed no modification in the Matrimid® precursor structure before and after V-treatment. The combination of these parallel insights suggested *a non-grafting process* during the temperature driven pyrolysis process. In

collaboration with Bhuwania, the picture of the oligomers is hypothesized to be formed during the process of V-treatment, which were generated with essentially "zero" vapor pressure. While these compounds had negligible vapor pressure and *could not be extracted* by pulling vacuum, they could be easily extracted by acetone. Since the temperature of the V-treatment appeared irrelevant in this stage of the soak, the procedure of the soak was changed to room temperature instead of 200°C. This clearly would simplify the ultimate scale up of the process.

4.2.1.2 Time

Another important parameter was the time allowed for the V-treatment, so experiments were done to identify the time the V-treatment needed for completion at room temperature. To ensure that the fibers were soaked for the intended time, solvent exchange was performed with acetone after the V-soaking of the fibers. This extracted any remaining VTMS from within the bore and pores of the fiber.

Procedure: Matrimid® fibers were soaked with VTMS at room temperature for 'x' time (different amounts of time ranging from 1 min to 6 hours). Soaked fibers were removed from VTMS and immersed in Acetone for 30 mins to quench the VTMS interaction with the polymer fibers. They were then removed from acetone, dried with Kimwipes and pyrolyzed to form CMS, following the 550°C temperature protocol. The results of this experiment were assessed by looking that the SEM images of the pyrolyzed fibers, shown in Figure 44.

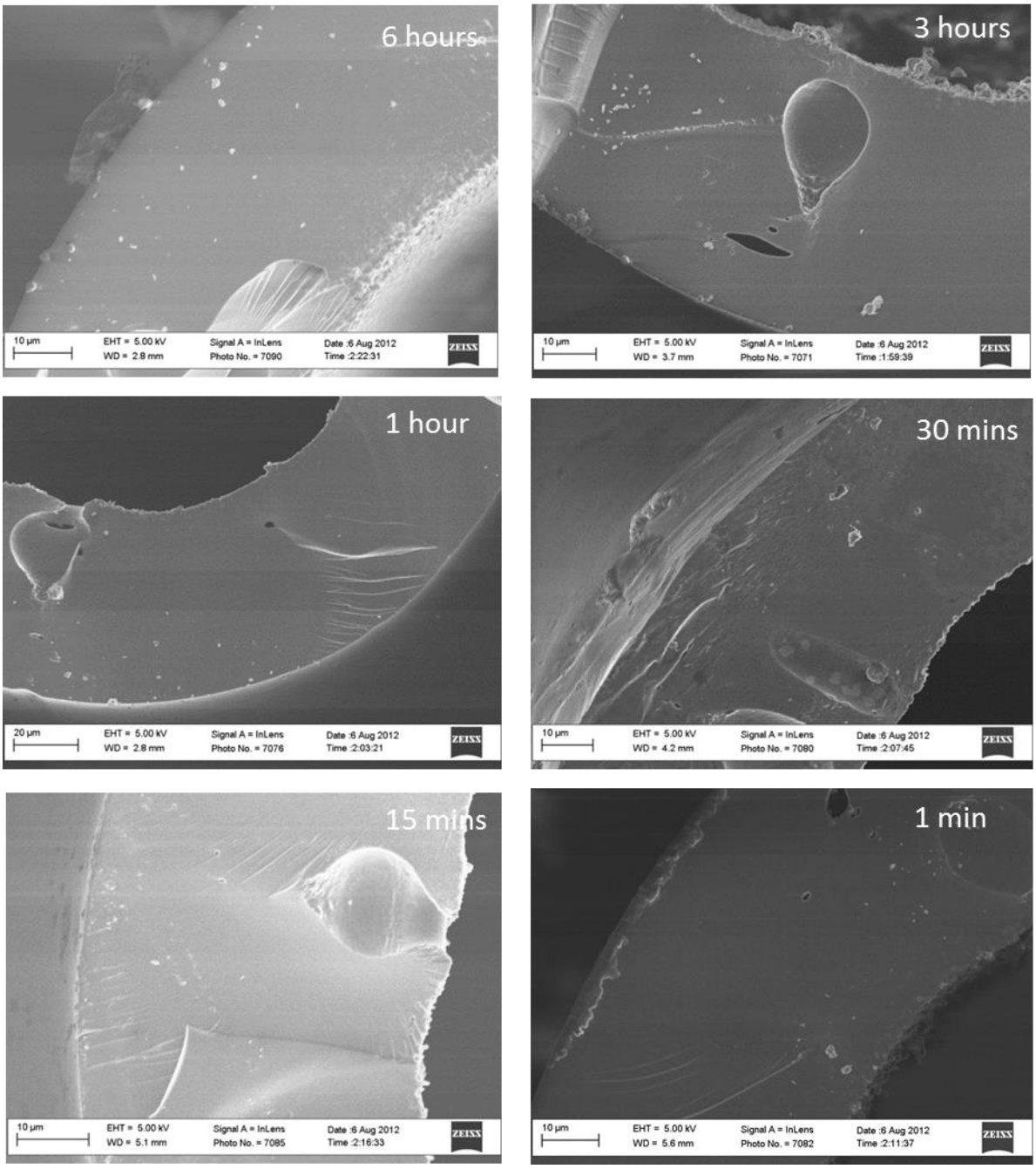

Figure 44: V-soak done on fibers for different amounts of time before washing with acetone to quench the process

The SEM images again clearly indicated collapse in all cases. However, it had been seen before in previous experiments that V-soak at times greater than 2 hours was enough

to yield the expected results. This raised questions regarding the "grafting" concept, per se in Bhuwania's work, and led to modification of the V-treatment hypothesis.

The two experiments above showed that restricting the V-treatment to particular times or temperature by quenching in acetone led to collapse of the substructure. This observation indicated that the acetone extracted the VTMS before it was allowed to perform the function of anti-collapsing agent. This information contributed to shape the understanding of the V-treatment mechanism. In conjunction with Bhuwania's research it was found that the V-treatment does *not chemically modify the polymer or the carbon structure*. In fact it does not react with the substrate at all. However, a key factor in the process of V-treatment is the exposure of the VTMS to humid environment for an organo-silica layer to form. This mechanism is explained in the next section.

4.2.2 Clarification of Actual Mechanism of V-treatment

With Bhuwania in the lead of this part of the study, a mechanism was developed for explaining how the V-treatment prevents the collapse of the substructure of hollow fibers. A more detailed explanation can be found elsewhere [90, 96]. While this work was the focus of Bhuwania's final discovery, contributions make here were valuable in clarifying details of this novel process.

Silanes are known to undergo hydrolysis at room temperature and polycondensation to give a complex organo-silica homogeneous gel [97-99]. The hydrolytic polycondensation reaction of vinyltrimethoxysilane (VTMS) is shown in Figure 45. This polymerization of VTMS gives a silsesquioxane structure with a backbone structure consisting of siloxane bonds and carbon-carbon bonds. This gel has a relatively

low degree of siloxane bonding, and therefore resembles an oligomer more than a polymer. The silsesquioxane forms a flexible gel, which is soluble in organic solvents and does not alter the mechanical properties of the fibers.

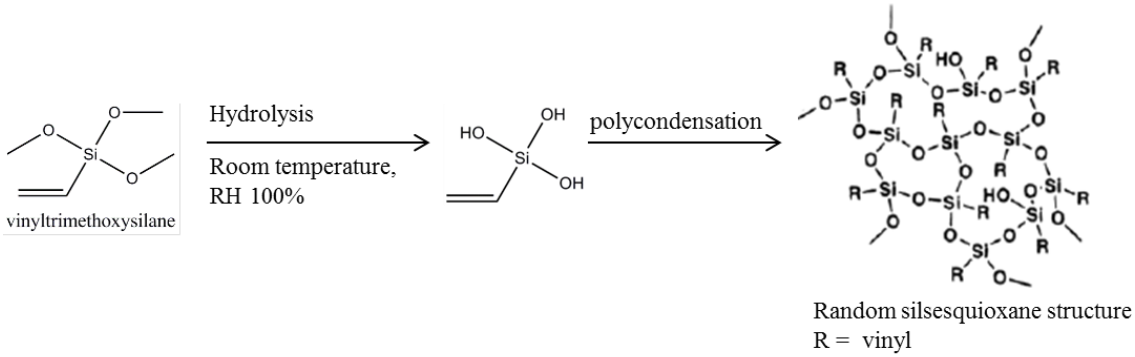

Figure 45: Mechanism of V-treatment: poly condensation and forming oligomer [90].

In the current V-treatment process (schematic of which is shown in Figure 46), the pores of precursor hollow fiber are saturated with VTMS by soaking them in a VTMS solution. The V-soaked fibers are kept in a glove bag to expose them to a controlled 100% relative humidity atmosphere for hydrolysis. The oligomerization occurs simultaneously, giving rise to the silsesquioxane gel. When these fibers are pyrolyzed to high temperatures in a furnace, this gel provides mechanical support to the porous substructure, not allowing the polymer matrix in the substructure to collapse. After the pyrolysis, an asymmetric CMS hollow fiber membrane is obtained with its thin selective skin layer and the porous supporting structure intact. The gel also forms an additional undesirable silica layer on top of the selective skin of the CMS hollow fibers, represented by the graphic in Figure 47.

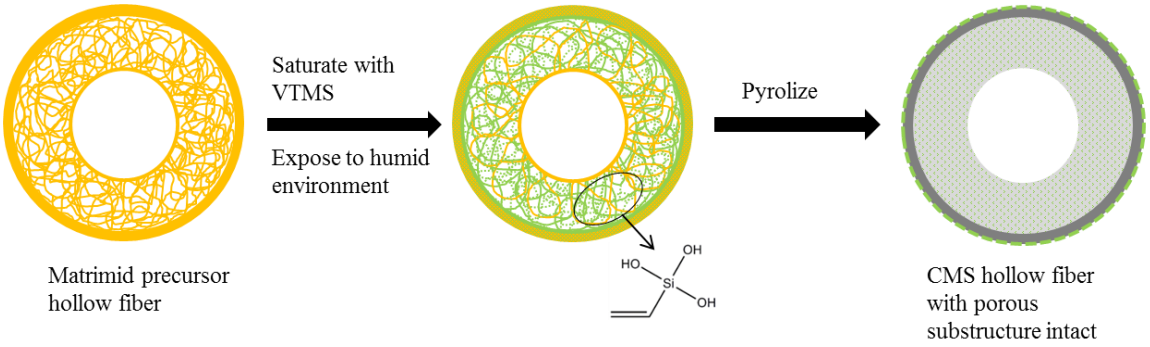

Figure 46: Hypothetical process of V-treatment inside a fiber during pyrolysis.

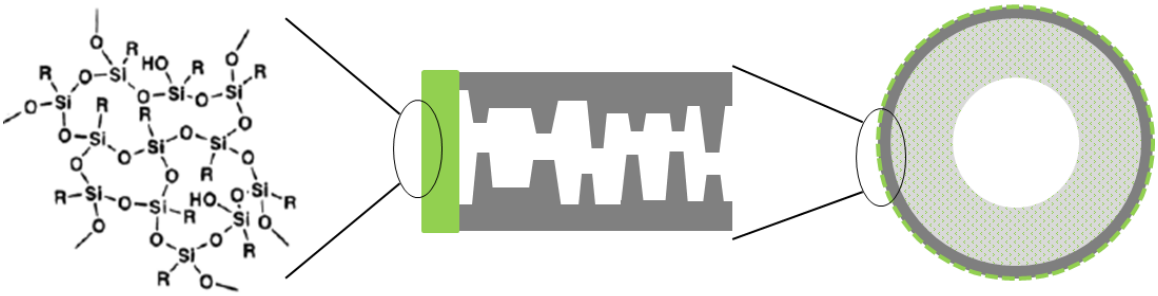

Figure 47: Silica layer that prevents collapse on the skin layer of the CMS fiber.

While the outermost silica layer is porous, it still adds a non-selective resistance for gas transport through the membrane. Due to the silica layer deposition, only limited increase in gas permeance was observed in the membrane. An open question remained regarding the presence of any silica within the ultramicropores of the thin selective layer. XPS sputter ion etch by Bhuwania suggests that minimal silica is actually is present in the selective CMS layer [90].

4.2.3 KOH etching

To reduce the amount of silica deposited on the surface of the CMS fibers, an optimization of concentration of VTMS in the V-treatment on Matrimid® fibers was explored by Bhuwania. The results shown in Figure 48 indicate that 10% VTMS in hexane gives the best permeance for Matrimid® derived CMS fibers pyrolyzed at 650 °C, without any loss in selectivity. Hexane was chosen as a solvent since it is already used in the post spinning process for solvent exchange. Using hexane for diluting the VTMS means that V-treatment can be integrated into the solvent exchange process, thereby adding no extra steps to the entire process of making testable CMS hollow fibers.

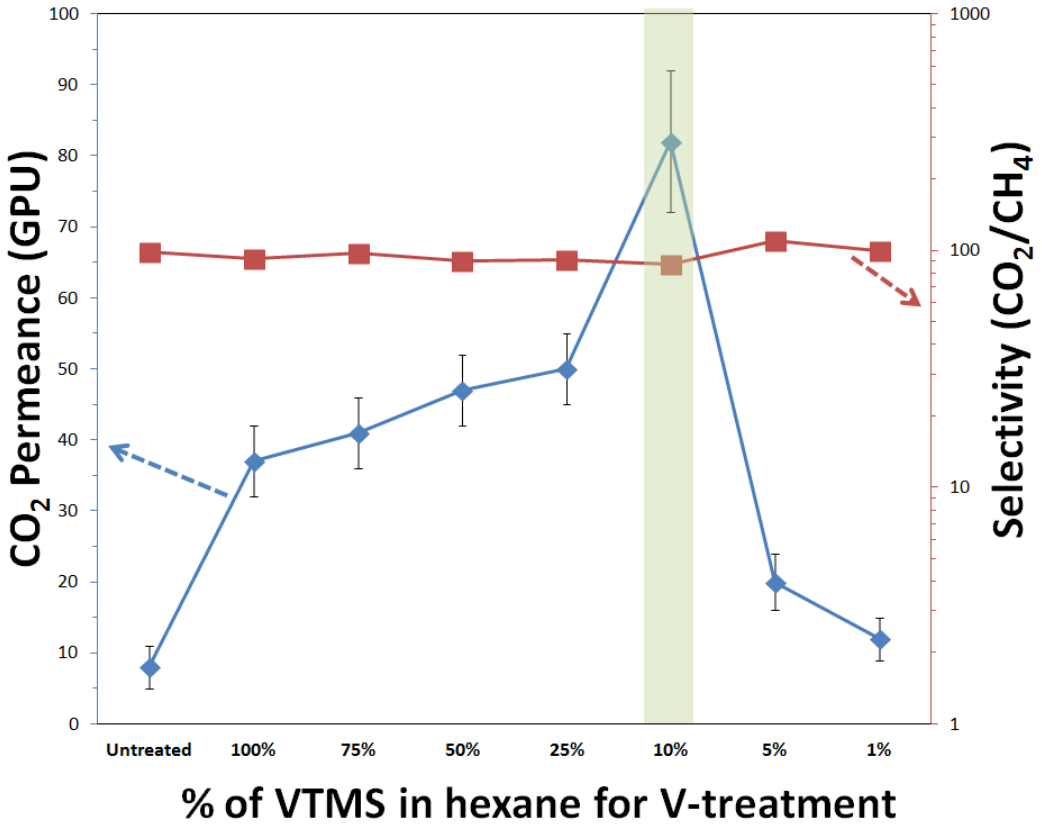

Figure 48: Separation performance for different VTMS concentrations in hexane for CMS hollow fibers of Matrimid® pyrolyzed at 650 °C in UHP Argon. Pure gas feed was used for testing at 100 psi and 35 °C [90]

The same concentration of 10% hexane was then used in this work for pyrolysis at 500 °C. The transport properties are shown in Figure 49. It is seen that 10% hexane also gives slightly better performance for Matrimid® fibers pyrolyzed at 500 °C. Moreover, significant savings will result in the amount of VTMS used.

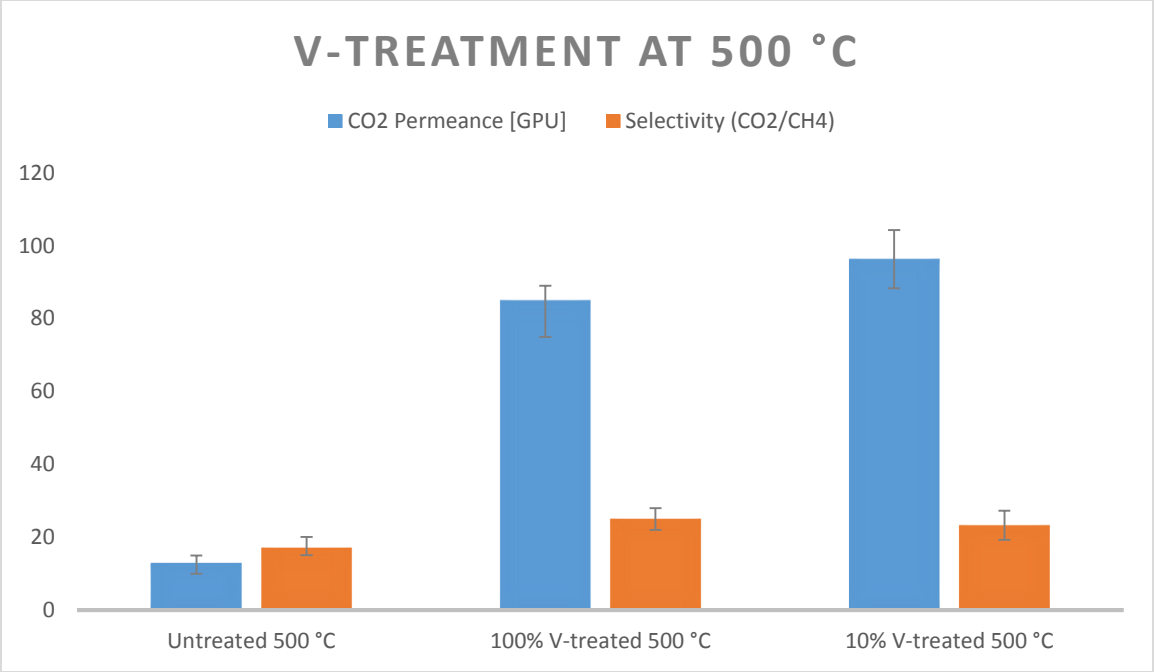

Figure 49: Gas transport properties of Matrimid® hollow fibers pyrolyzed at 500 °C in UHP Argon, tested with pure gas at 100 psi and 35 °C

While V-treatment demonstrates a great improvement in permeance, it has the potential to improve much more if the effects of the unnecessary externally deposited silica film (Figure 47) can be avoided. In order to reduce this deteriorating effect of the silica, an attempt was made to etch off the silica and/or carbon scum with an etching agent in a post pyrolysis process.

Hydrofluoric acid is an obvious choice for etching of silica; however, it is dangerous to handle and difficult to scale up, so it was avoided in this project. Sodium hydroxide and potassium hydroxide are also typically used to etch silicon from substrates for different end uses [100, 101], and to etch the organo-silica film off of our CMS membranes, the strongest agent of this type was used.

Procedure: Matrimid® precursor fibers (shown in Figure 50) were taken from the shelf and soaked in 10% VTMS solution for 12 hours. They were then exposed to 100% RH air, and dried under vacuum for 24 hours. At this stage the organo-silica layer had already formed inside and outside the fibers. Pyrolysis was done on these fibers at 600 °C under UHP Argon to obtain CMS fibers with an intact porous substructure. At the time, 600 °C was used for consistency with Bhuwania's work that was being completed. The role of the organo-silica gel of providing mechanical support to the substructure was completed, and it was ready to be etched off. For the etching process, these CMS fibers were submerged in KOH solution and sonicated for 4 hours. They were then washed with DI water and dried in vacuum at 150 °C for 3 hours. The hypothesis was that the KOH would etch the silica and be washed from fibers, leaving a CMS fiber without the extra resistive layer.

The permeances of the fibers were measured after the KOH etch, and the results are represented in Figure 51.

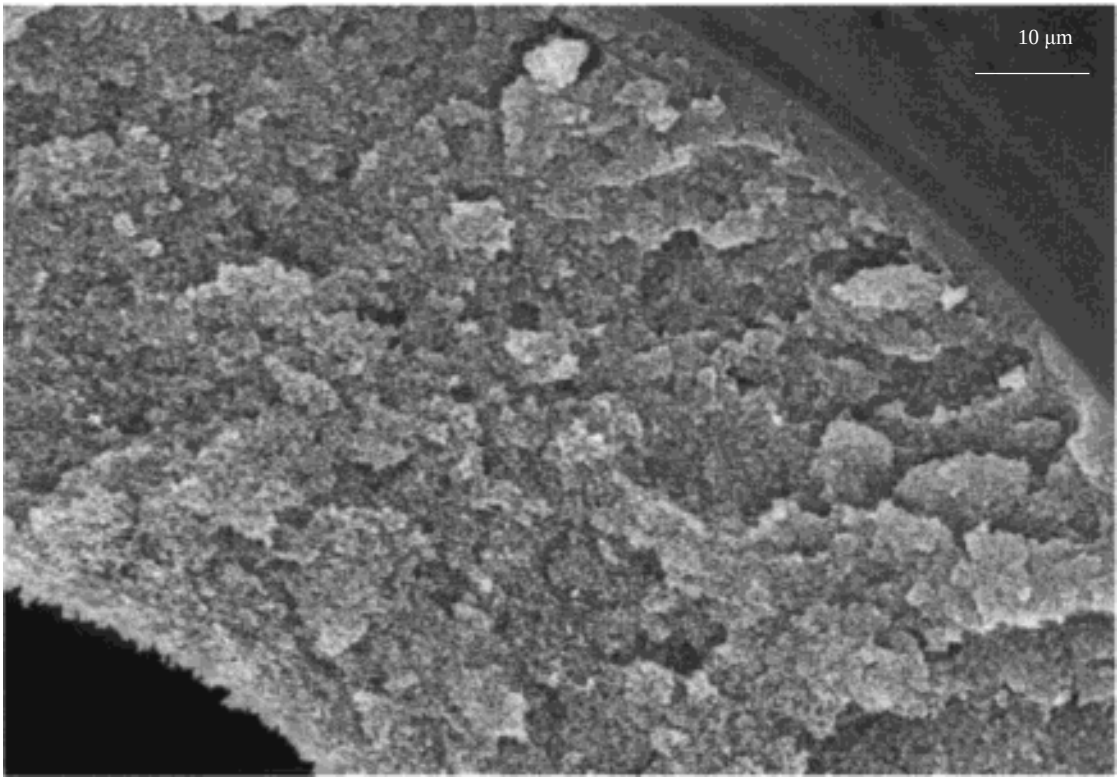

Figure 50: SEM image of cross section of Matrimid® precursor hollow fiber membrane

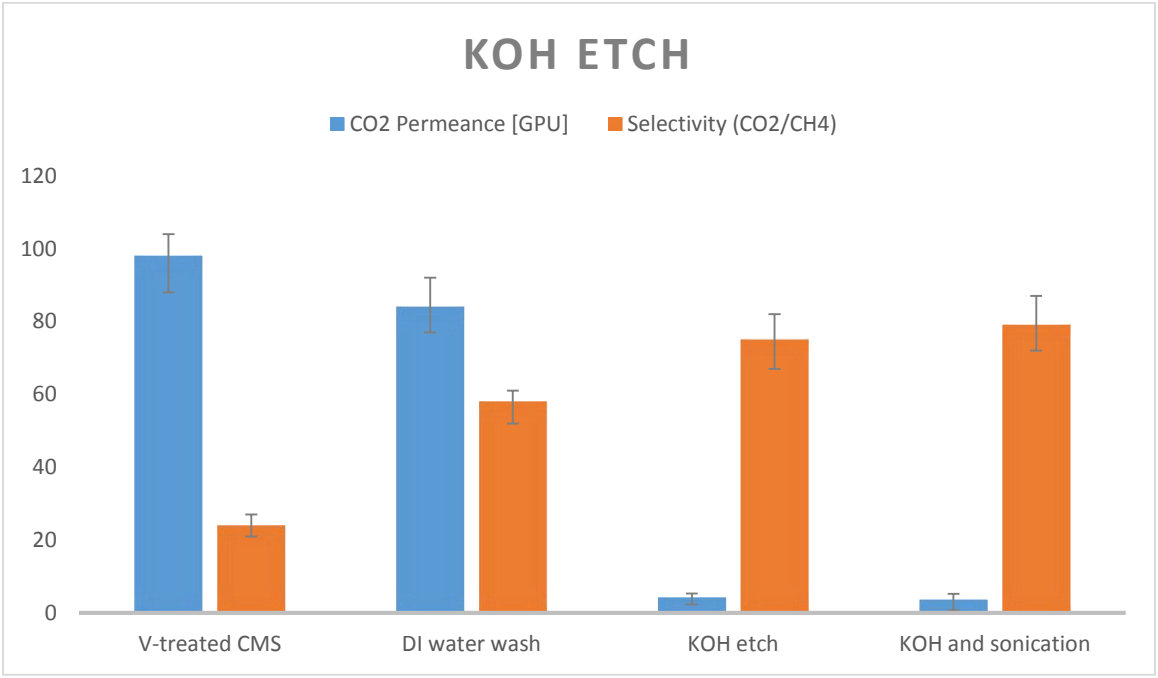

Figure 51: Effect of KOH etching on performance of CMS fibers pyrolyzed at 500 °C under UHP Argon, pure gas test at 50 psi and 35 °C

Clearly, the permeance decreased after this etching process. The drop in permeance is presumably caused when the KOH breaks the silica gel down into smaller siloxanes after etching; however, these siloxanes were not removed from the CMS fibers under the conditions tested in this work. The KOH may plug the pores of the CMS membrane (Figure 52), which may also be one of the causes of the reduced permeance. In any case, this initially reasonable idea appeared to have considerable problems.

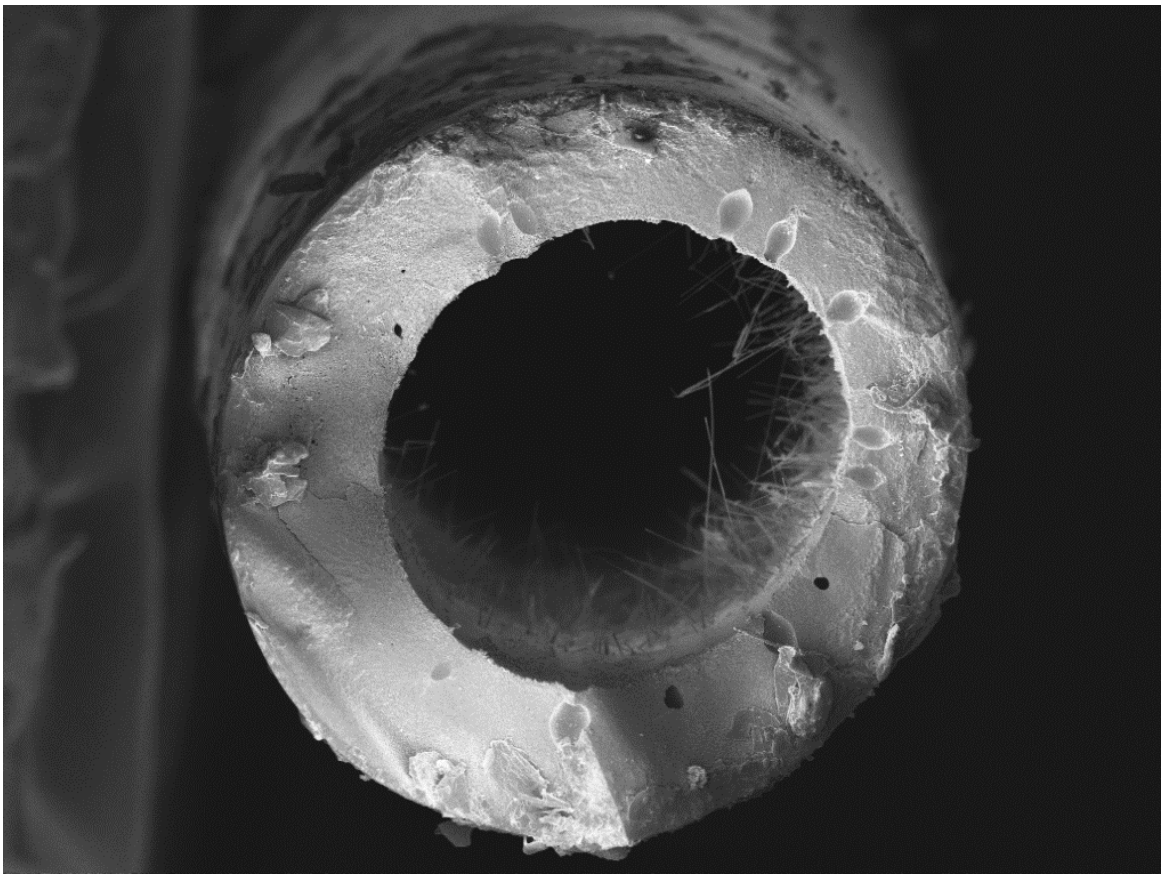

Figure 52: Matrimid® CMS hollow fiber after KOH etching was performed

Fortunately, while the KOH etch wasn't successful in removing or reducing the silica layer, the problem was circumvented by a simple washing method described in the section 4.2.4. This approach was different from the undesirable acetone liquid immersion extraction method described earlier in section 4.2.1.1.

4.2.4 Washing

For removing the excess silica layer on the skin of the fibers, a scalable washing method was proposed instead of etching that is reported in the previous section. This method consisted of washing the VTMS from the surface of the fibers *before* pyrolysis. The hypothesis was that the VTMS that remained on the fibers after soaking the fibers in 10% VTMS solution, could be washed with a solvent that can dissolve VTMS.

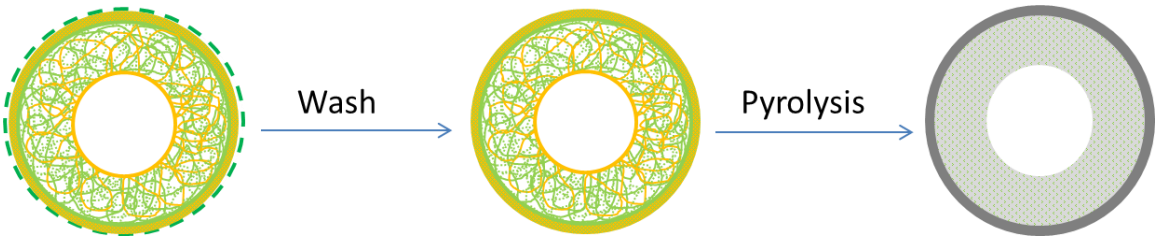

Figure 53: Hypothesis for washing the excess silica layer from the skin layer of the polymer hollow fiber.

Procedure: Matrimid® precursor fibers were soaked in 10% VTMS solution in hexane for 24 hours. After removing them from solution, they were immediately washed 2-3 times with a solvent of choice, using a squirt bottle. These washed fibers were exposed to 100% humidity in a glove bag for 24 hours, and dried under vacuum at 150 °C overnight. The dry fibers were then pyrolyzed in UHP Argon at 650 °C.

Experiments were performed using solvents such as acetone, hexane and water. An additional experiment was done using hexane for washing the VTMS, and then immediately depositing the fiber in water to quench the possible diffusion of VTMS out of the porous substructure, through the skin.

The mechanical properties of these fibers were similar to the regular V-treated fibers. These washed fibers did not stick to each other during pyrolysis. To check if the washing method is successful in reducing the excess VTMS from over the skin layer, permeance data was used. This is a proof of concept study to show that permeance can be increased with adding a washing step.

These experiments were repeated for CMS hollow fibers from Matrimid® pyrolyzed at 650 °C for consistency with Bhuwania's work, and the results for those are as follows:

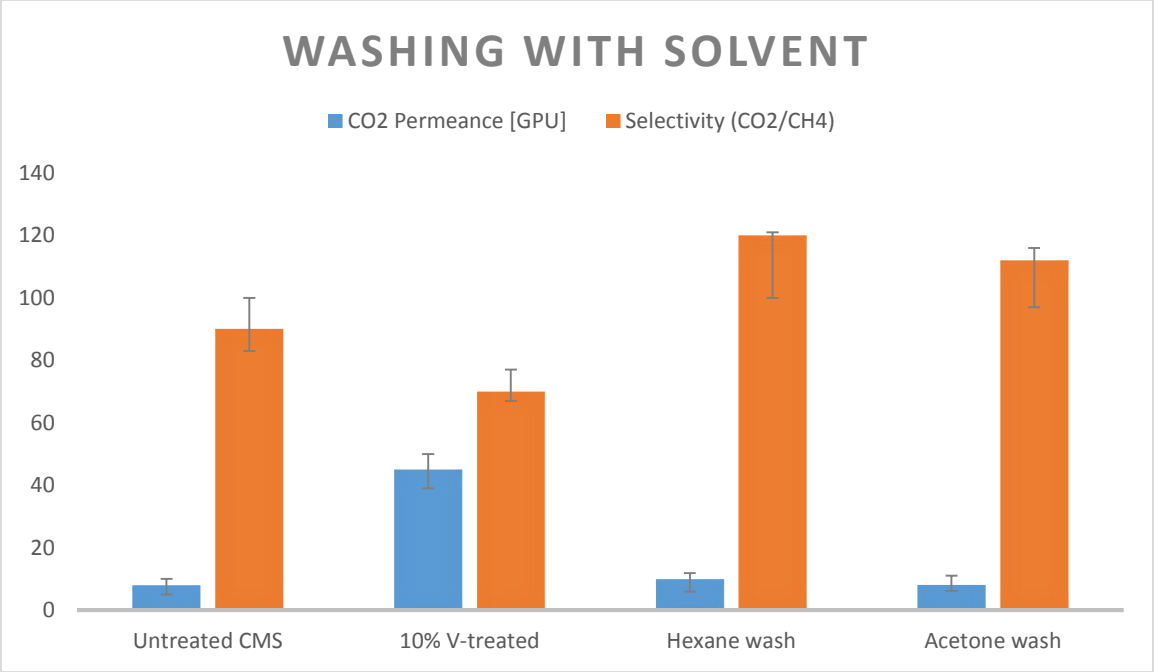

Figure 54: Transport properties of Matrimid® derived CMS fibers after washing with solvents compared to an untreated and a V-treated control, pyrolyzed at 650 °C under UHP Argon, pure gas at 100 psi and 35 °C.

Conclusion: Washing with solvent removed the VTMS from substructure, and acted like the liquid solvent extraction described in sections 4.2.1.1 and 4.2.1.2. After washing with solvent, the substrate behaved like non-V-treated hollow fiber and demonstrated collapse. Since washing with solvent extracted the anti-collapse agent completely from the fiber, the next logical step was to wash the organo-silica with a solvent containing a smaller percentage of VTMS.

The procedure followed was the same as above, where the washing was done with a lower percentage of VTMS solution in hexane. This ensured that there was still some VTMS left in the fibers at the time of pyrolysis.

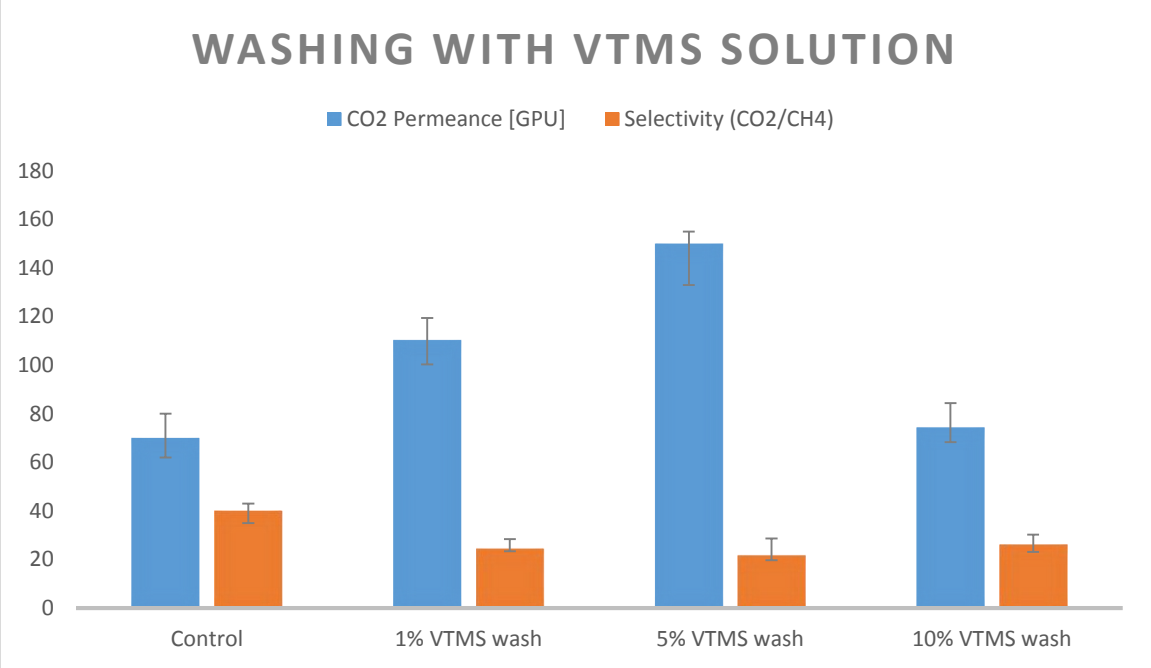

Figure 55: Performance of CMS hollow fibers after washing of precursor fibers with VTMS solution. All precursors were V-treated with 10% VTMS, and then washed with different concentrations of VTMS in hexane. Pure gas performances at 100 psi at 35 °C.

This is a proof of concept that V-treatment can be performed with 10% VTMS solution, and washing it further can improve the performance. The best result was found to be at washing with 5% VTMS solution. Performance improvement is also seen with a 1% VTMS wash. Note that the V-treatment optimization done by Bhuwania (Figure 48) showed that simply using 1% V-treatment is not effective in stopping collapse. If needed, the washing process may further be optimized to standardize the time and method of washing. The optimization of washing process has not been covered in this work, since other objectives existed for the project involving H_2S studies.

4.2.5 Concentration Optimization

As mentioned before, the least amount of organo-silica layer deposited on the outermost skin layer of the CMS hollow fiber is desirable for better transport properties. Similar to the optimization for V-treatment conditions for Matrimid®, an optimization of the VTMS weight percent was done on 6FDA:BPDA-DAM derived CMS fibers as well, since this would be needed for the H_2S work noted above. Four different concentrations of VTMS in hexane were used to treat the precursor hollow fibers, a cross section of which is shown in Figure 56. These fibers were pyrolyzed at 550 °C under UHP Argon, and their permeation results are demonstrated in the Figure 57.

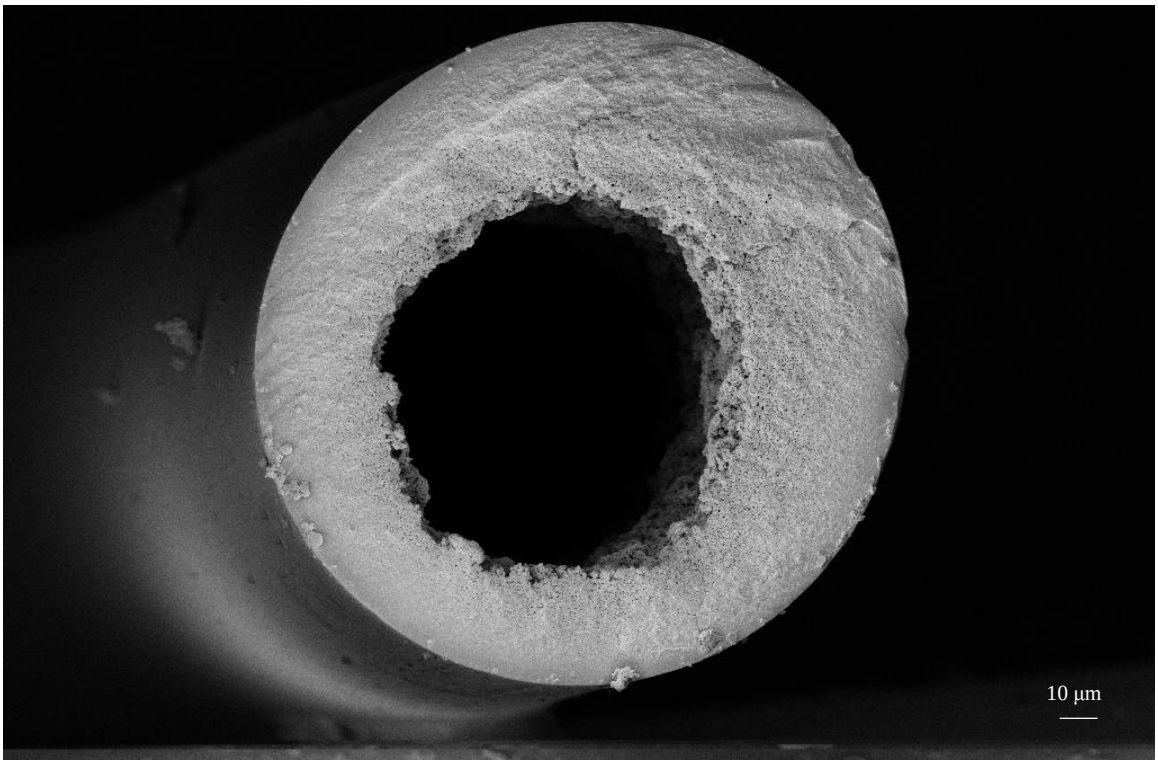

Figure 56: SEM image of cross section of a 6FDA:BPDA-DAM precursor hollow fiber

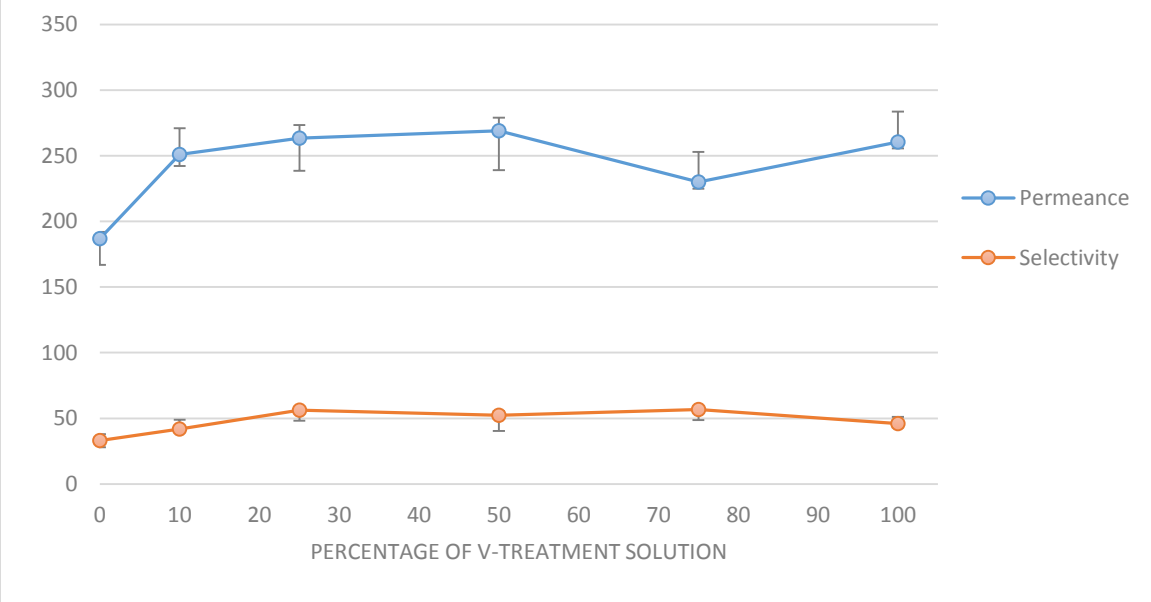

Figure 57: Optimization of V-treatment for 6FDA:BPDA-DAM derived CMS fibers, pyrolyzed at 550 °C under UHP Argon. Tested with pure gas feed at 100 psi at 35 °C.

This graph shows that all concentrations of VTMS gave similar permeation properties, and performed better than an untreated CMS fiber. The best combination of permeance and selectivity can be achieved by 25% or 50% weight percent of VTMS in hexane. Unlike the Matrimid® case, the permeance for 6FDA:BPDA-DAM fell in the same range for concentrations of 25% to 100% VTMS. While this result shows that the V-treatment does its job of stopping collapse it, it provides less enhancement, since the more rigid 6FDA:BPDA-DAM polymer with a small $T_g - T_d = 68$ °C, intrinsically shows less collapsing tendency than Matrimid with $T_g - T_d = 150$ °C. This can be qualitatively demonstrated by the SEM images.

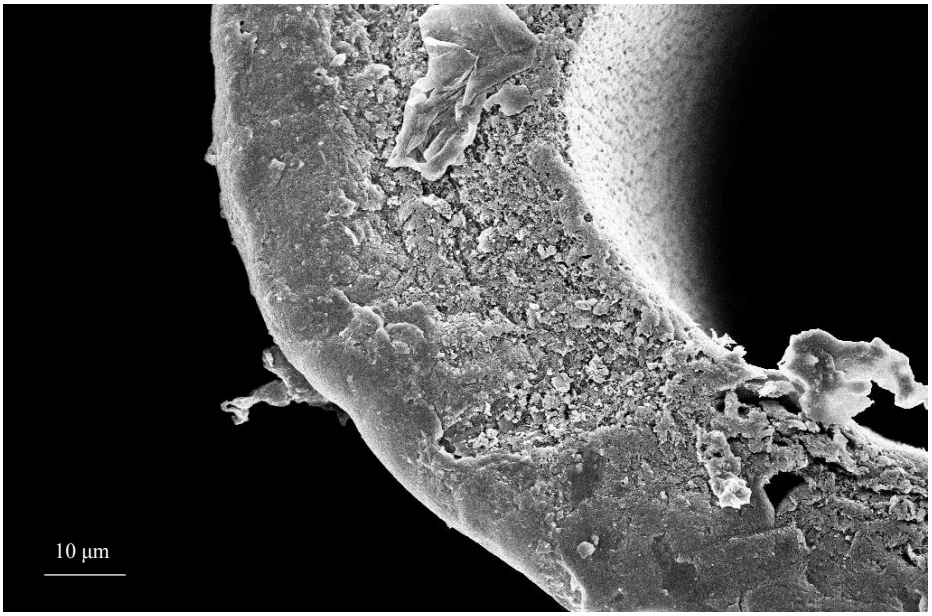

Figure 58: SEM image of untreated 6FDA:BPDA-DAM hollow fiber pyrolyzed at 550 °C under UHP Argon

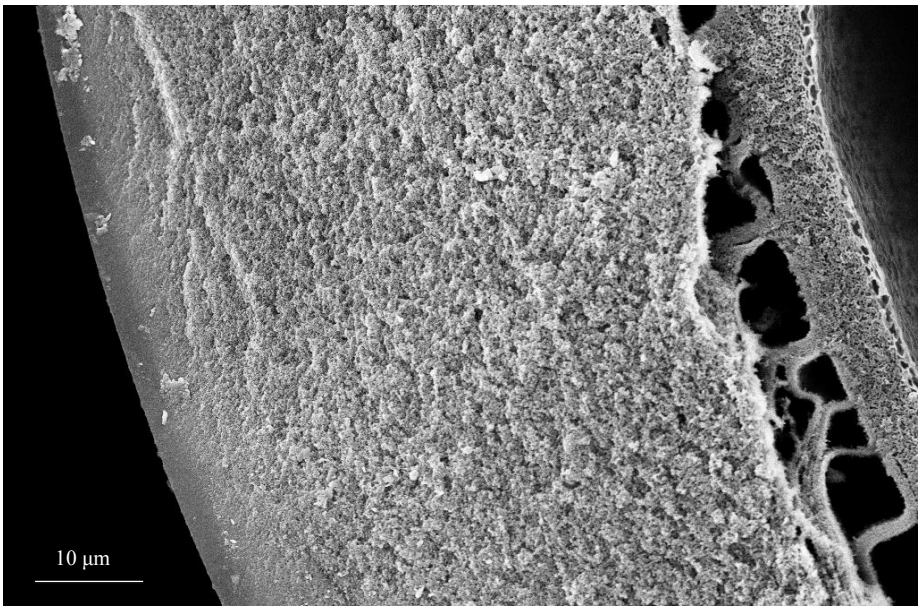

Figure 59: SEM image of 25% V-treated 6FDA:BPDA-DAM hollow fiber pyrolyzed at 550 °C under UHP Argon

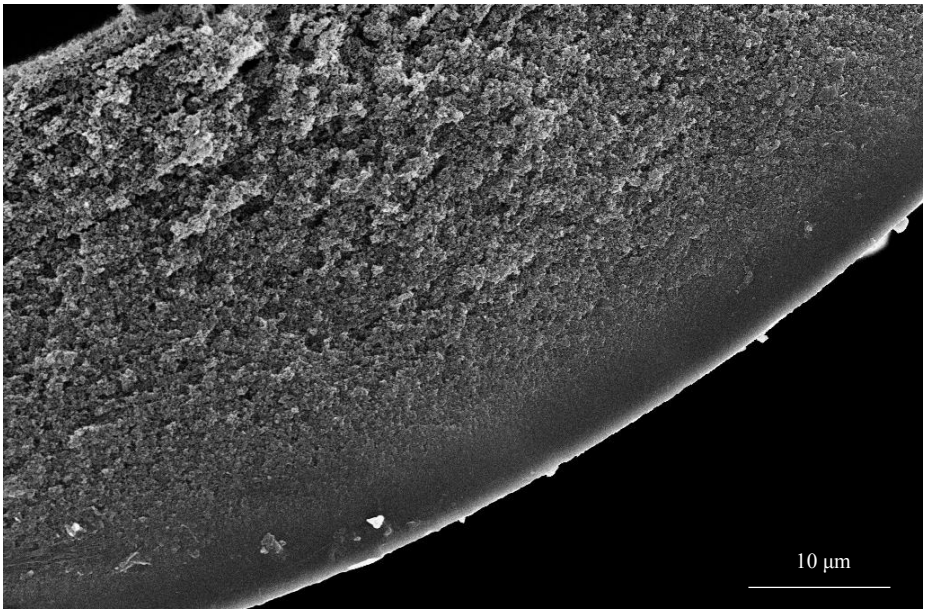

Figure 60: SEM image of 50% V-treated 6FDA:BPDA-DAM hollow fiber pyrolyzed at 550 °C under UHP Argon

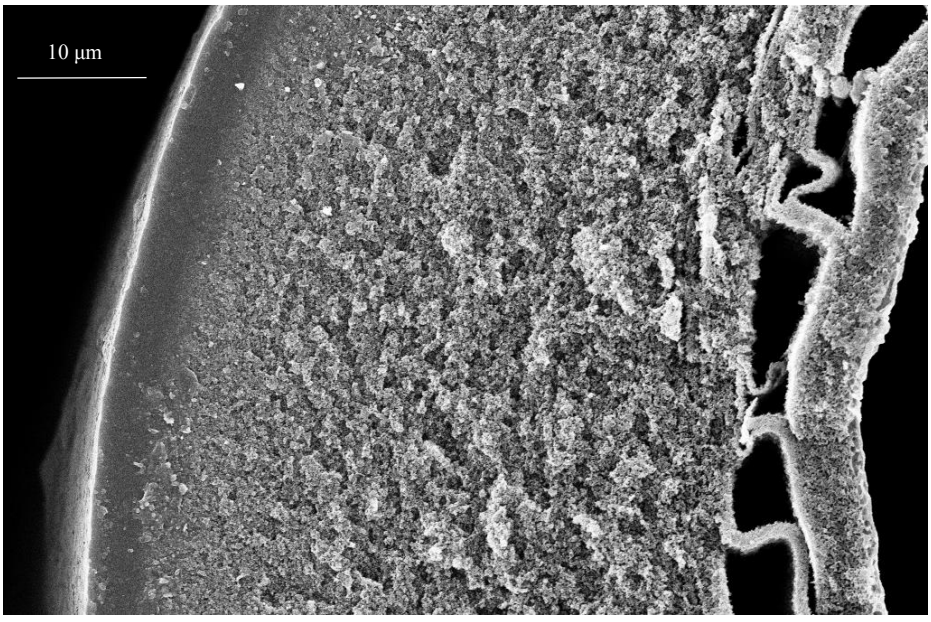

Figure 61: SEM image of 75% V-treated 6FDA:BPDA-DAM hollow fiber pyrolyzed at 550 °C under UHP Argon

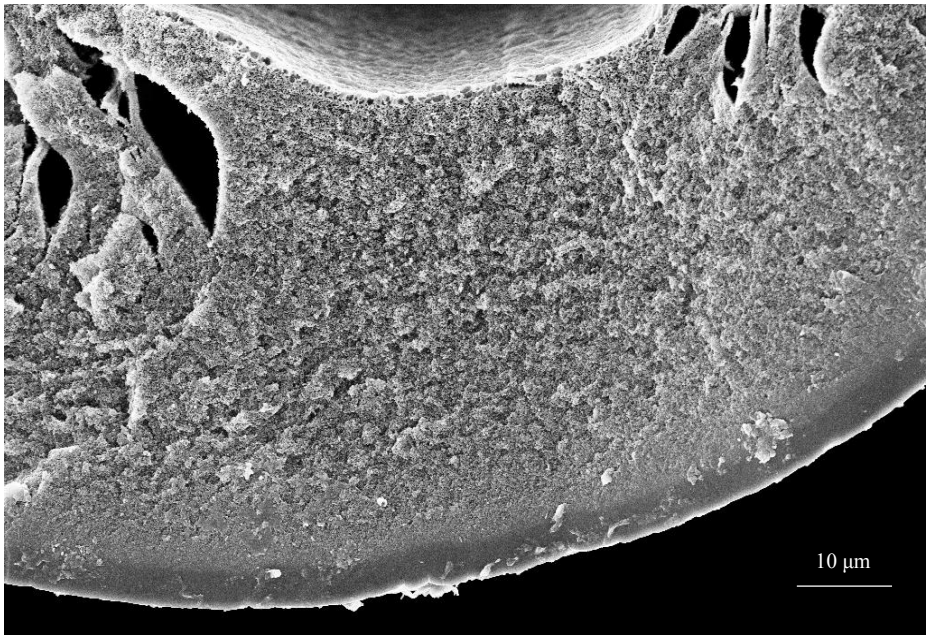

Figure 62: SEM image of 100% V-treated 6FDA:BPDA-DAM hollow fiber pyrolyzed at 550 °C under UHP Argon

The skin layer thickness in all the above figures for V-treated samples is between 3-4 microns, which successfully demonstrates the anticollapse. Separation thickness of an untreated fiber is ~16 microns.

A similar optimization of V-treatment solutions was done on CMS fibers from 6FDA:BPDA-DAM which were pyrolyzed with 30 ppm O_2 in Argon atmosphere. The permeance and selectivity trends are shown in Figure 63. The trend is similar to the optimization performed on 6FDA:BPDA-DAM pyrolyzed in UHP Argon. The permeance increased for V-treated fibers as compared to untreated fibers, and is within the range of error for any amount of VTMS used. The selectivity remained relatively unchanged.

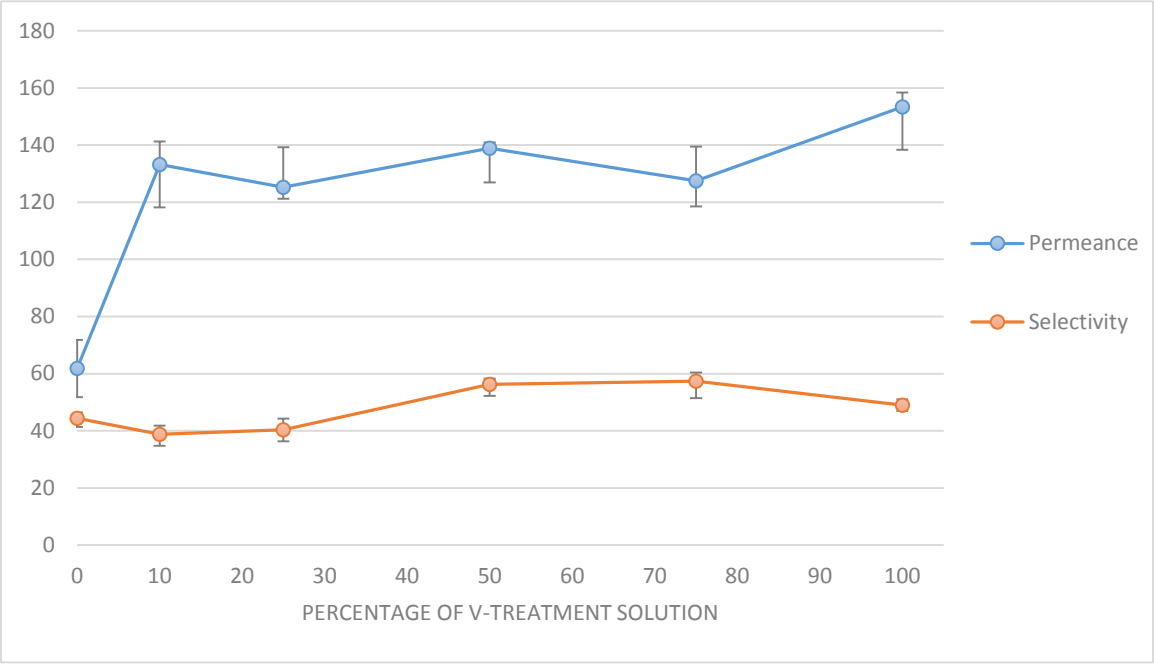

Figure 63: Optimization of V-treatment for 6FDA:BPDA-DAM derived CMS fibers, pyrolyzed at 550 °C with 30 ppm O_2 in Argon. Tested with pure gas feed at 100 psi at 35 °C.

It should be noted that this optimization yields different results from the one performed on CMS from Matrimid®. In this case, there is no optimum value of V-treatment concentration where the permeance is highest, like in the case of Matrimid® CMS. This suggests that the excess silica layer on CMS from 6FDA:BPDA-DAM does not vary with the concentration of VTMS used during the V-treatment, and may be getting removed during the process of pyrolysis. To understand why, one must go back to the structures of Matrimid® and 6FDA:BPDA-DAM.

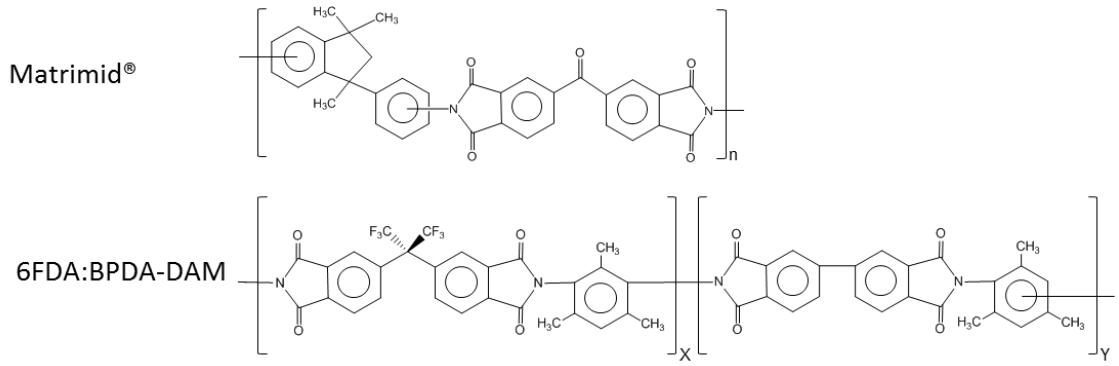

Figure 64: Comparing the structures of Matrimid® and 6FDA:BPDA-DAM polyimides.

A major reason that CMS from 6FDA:BPDA-DAM is intrinsically more open is due to the bulky $–CF_3$ groups, which are absent in Matrimid®. While Matrimid® evolves volatiles such as CO, CO_2, etc., 6FDA:BPDA-DAM also evolves fluorinated compounds, such as CHF_3 and trace HF in addition to CO, CO_2. This evolution of HF might be etching the organo-silica membrane in CMS fibers from 6FDA:BPDA-DAM making it sufficiently porous to add negligible resistance, that otherwise proves detrimental to the permeance of CMS fiber membranes from Matrimid®.

It is therefore concluded that any concentration of V-treatment is effective for increasing gas permeances. To allow ease of preparation, a concentration of 50% VTMS solution in hexane is chosen for use hence forward in this project for V-treatment of 6FDA:BPDA-DAM hollow fibers.

However, while the V-treatment clearly stops the collapse of the substructure and decreases the separation skin thickness by 5X, it causes an increase in permeance only by about 1.5X. Investigating this disparity in the change in separation thickness vs. permeance was outside the scope of this project, and must be studied further.

4.2.6 **Time optimization:**

So far, the V-treatment process involved the soak of polymer fibers in the VTMS solution for 24 hours. However, when a calculation was performed for diffusion rates, the estimated time it took for VTMS to enter the fiber through the skin turned out to be very short. A simple mass transfer calculation for two cases suggested that it took less than 1 second for the VTMS to actually enter the skin layer. The approximate numbers for diffusion coefficients in these calculations were based on the typical diffusivities in polymers [102].

Case A: Best case scenario. Here the VTMS has access to the fiber from both the shell side and the bore side.

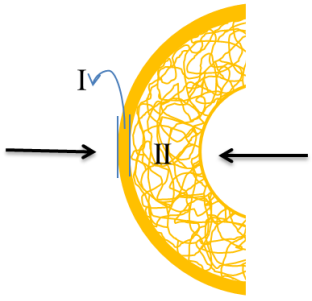

For two sided uptake, the time required for the mass transfer is:

$$t_{0.9} = 4 \times t_{1/2}$$

$$t_{1/2} = \left(0.05 \times \frac{l^2}{D}\right)$$

$$t_{0.9} = \left(0.2 \times \frac{l^2}{D}\right)_I + \left(0.2 \times \frac{l^2}{D}\right)_{II} = 0.66\ s$$

Where,

$$l_I = 1\ \mu$$

$$l_{II} = 40\ \mu$$

$$D_I = 10^{-7}\ cm^2/s$$

$$D_{II} = 5 \times 10^{-6}\ cm^2/s$$

The time required in this case is lesser since the VTMS has access to both the sides of the membrane, and has to travel only half the distance to saturate the membrane. This is the best case scenario for the mass transfer of VTMS, with high values of diffusion coefficients.

Case B: Worst case scenario. Here the VTMS has access only to the shell side of the membrane, the diffusion coefficient through the dense skin is a few orders of magnitude lower.

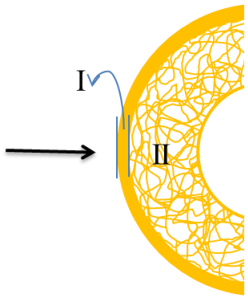

For single sided uptake, the time required for mass transfer in this case is:

$$t_{0.9} = 4 \times t_{1/2}$$

$$t_{1/2} = \left(0.05 \times \frac{(2l)^2}{D}\right)$$

$$t_{0.9} = \left(4 \times 0.05 \times \frac{(2l)^2}{D}\right)_I + \left(4 \times 0.05 \times \frac{(2l)^2}{D}\right)_{II} = 12\ s$$

Where,

$$l_I = 1\ \mu$$

$$l_{II} = 50\ \mu$$

$$D_I = 10^{-9}\ cm^2/s$$

$$D_{II} = 5 \times 10^{-6}\ cm^2/s$$

What we see though is that even in the theoretical worst case scenario, the time taken for the VTMS to diffuse through the wall of the hollow fiber is less than 1 minute. Therefore, experimental validation of this was done to find the minimum time required for the VTMS soak in order to show no collapse.

The procedure followed was the regular V-treatment procedure, with the only difference being the time allowed for soaking the polymer fibers in the VTMS solution. The fibers were immersed in the solution for 5 minutes at room temperature, which is clearly much less than the 24 hours of time used previously. They were then removed from the solution, wiped with Kimwipes and exposed to humidity for 24 hours. Drying in vacuum at 150 °C was done before pyrolyzing the fibers at 550 °C. SEM images in Figure 65 show the morphology of these CMS hollow fiber membranes.

The porous substructure of the CMS hollow fiber is retained, indicating that 5 minutes is enough time for the VTMS solution to diffuse through the hollow fibers and perform its function of anti-collapse agent.

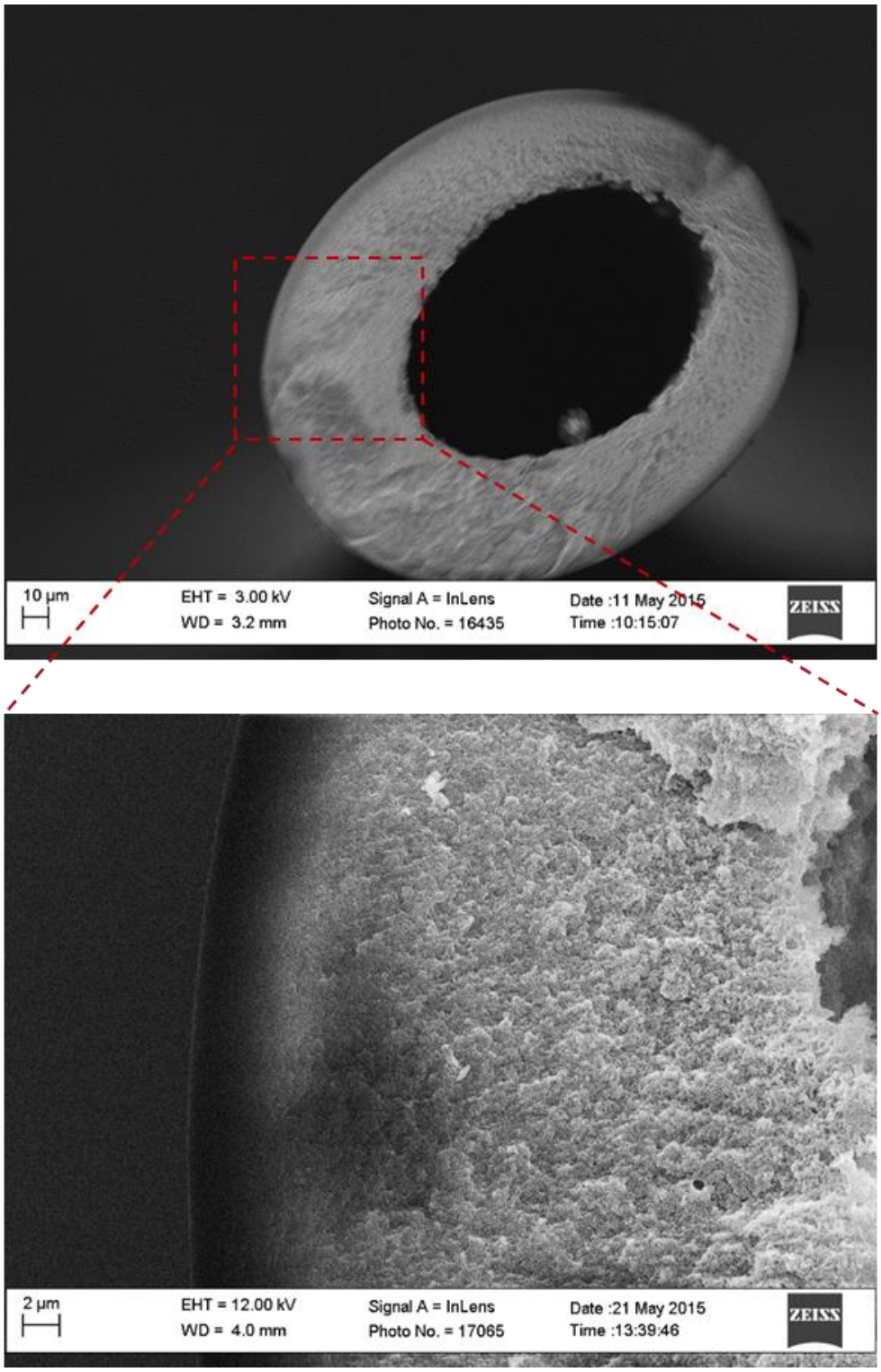

Figure 65: SEM images of 6FDA:BPDA-DAM CMS fibers pyrolyzed at 550 °C under UHP Ar atmosphere, after soaking in VTMS solution for 5 minutes.

4.2.7 Scale up

It is our goal to ultimately use the V-treatment process on an industrial scale to treat long continuous hollow fibers, where the VTMS will not have direct access to the bore side of the fibers. It is important to know whether the VTMS can diffuse through the dense skin layer of polymer hollow fibers of whether it requires bore side diffusion. If the VTMS cannot diffuse through the skin layer, the V-treatment will have to be done on individual fibers that have open bores available for the soak, which is industrially cumbersome.

To determine if the VTMS can diffuse through the skin layer, a "closed end" study was performed on both 6FDA:BPDA-DAM and Matrimid®. In this study, the V-treatment of the precursor hollow fibers was done, by soaking the fiber for 5 minutes while keeping the bore of the fiber unavailable to the V-treatment solution. After the V-treatment was done, the fibers exposed to 100% humidity in a glove bag for 24 hours and dried at 150 °C in vacuum. The two experimental setups looked like this:

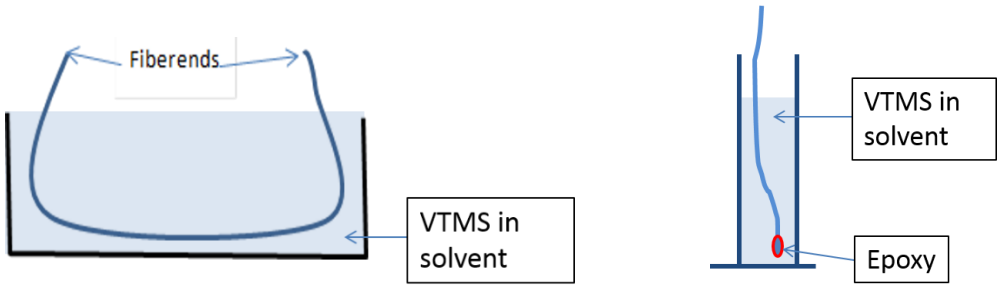

Figure 66: Experimental set up to verify whether the VTMS can diffuse through the skin of the hollow fiber membranes

The SEM images of the V-treated CMS hollow fiber show the morphology of the parts that were immersed in the VTMS solution and the parts that were outside the solution.

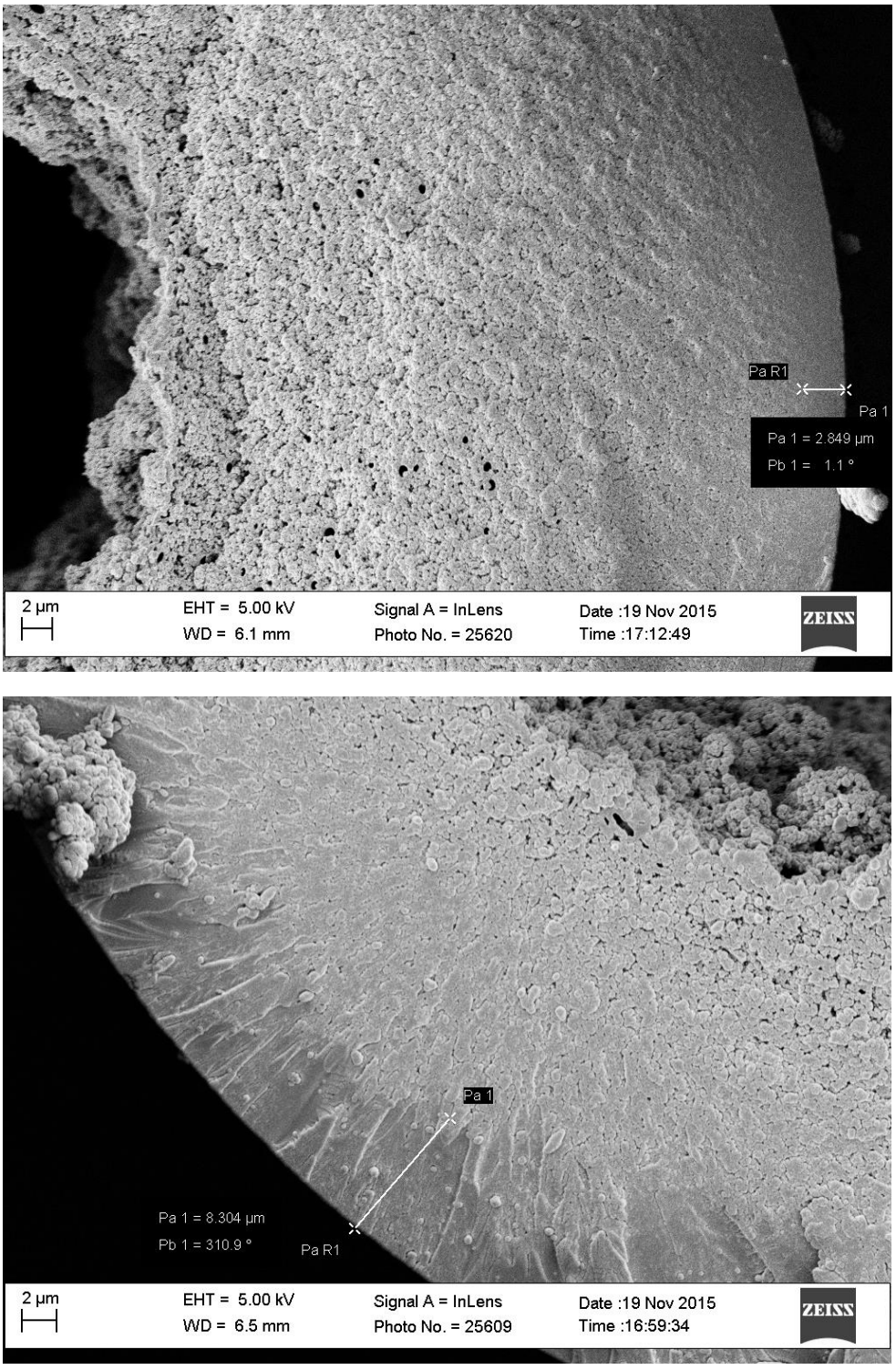

Figure 67: Scale up feasibility. SEM images of CMS hollow fiber membrane from 6FDA:BPDA-DAM at 550 °C under UHP Argon atmosphere : (top) part of the fiber immersed in the VTMS solution with thin skin; (bottom) part of the fiber outside the VTMS solution with partially collapsed substructure.

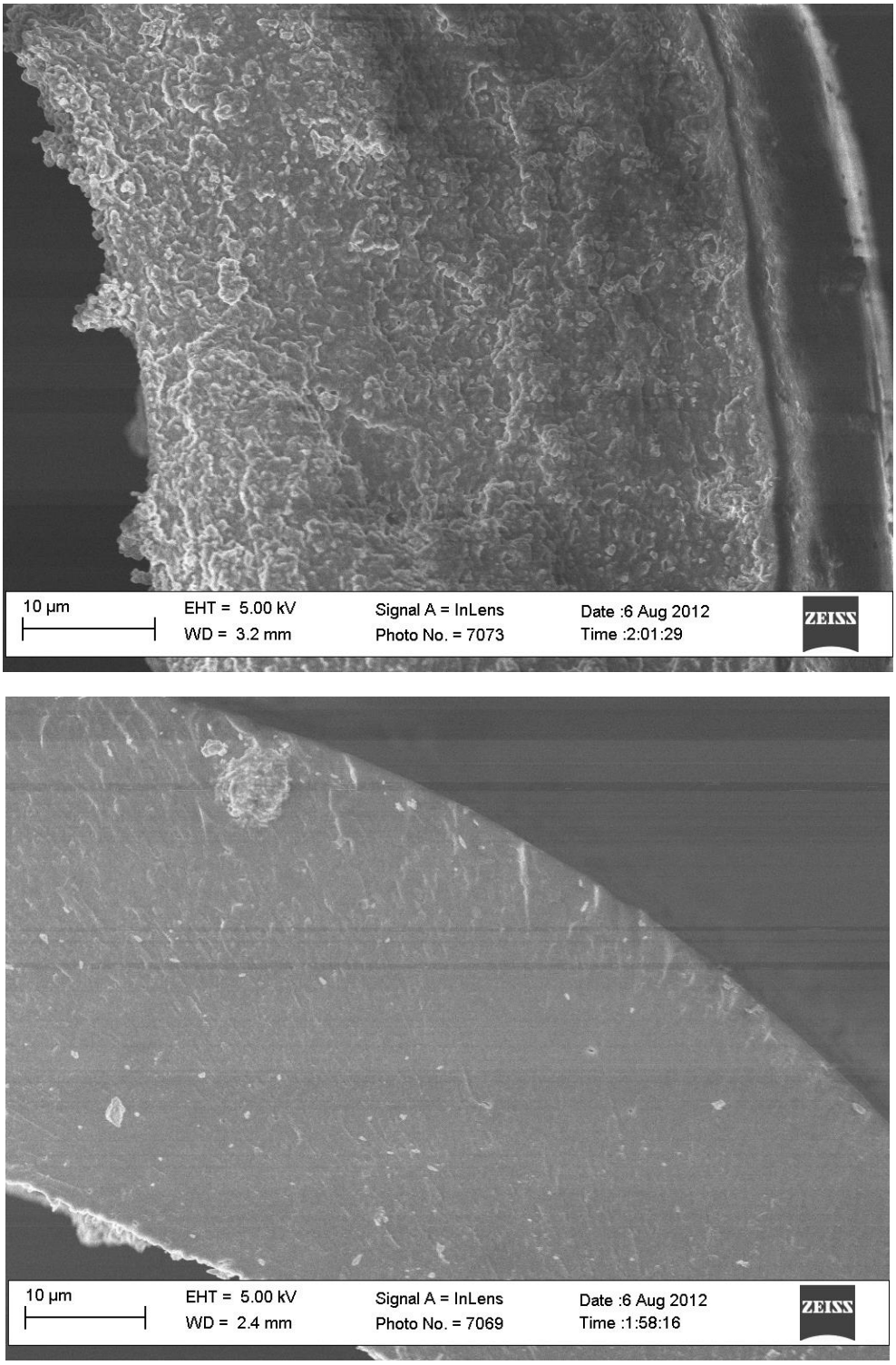

Figure 68: Scale up feasibility. SEM images of CMS hollow fiber membrane from Matrimid at 500 °C under UHP Ar atmosphere: (top) part of the fiber immersed in the VTMS solution showing thin skin; (bottom) part of the fiber outside the VTMS solution showing collapsed substructure.

The SEM images show that the there was no collapse in the part of the fiber soaked inside the solution, and pores collapse in the part inside the solution. To quantitatively verify this result, the transport properties of the part of the fibers that underwent V-treatment were also tested for Matrimid®. Figure 69 shows the transport properties of such a close ended V-treated fibers.

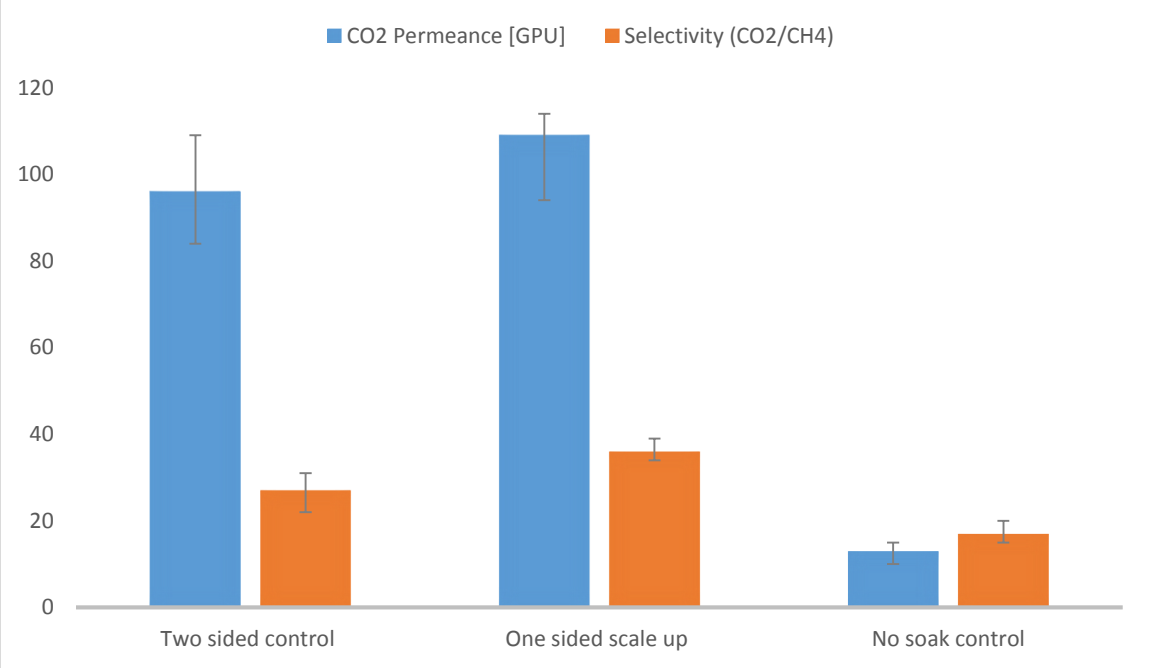

Figure 69: Performance of Matrimid® CMS hollow fibers V-treated with 10% VTMS, pyrolyzed at 500 °C with UHP Argon, tested with mixed gas (50% CO_2, 50% CH_4) at 100 psi. Control was completely immersed in VTMS solution, while bore of the scale up fiber was not immersed in VTMS solution.

The CO_2 permeance of the both the fibers used for scale up are similar to the properties of the control which was completely immersed in the VTMS solution. This shows that the V-treatment works on close ended fibers in terms of stopping the

substructure collapse. This is a crucial result in terms of confirming the scalability of V-treatment process.

Also the scale up is done in such a way that it does not have to add any extra step at the V-treatment parts as it can be integrated into the solvent exchange step of the production process. This is a huge gain industrially, where number of steps proportionally increased the capital costs and costs of production.

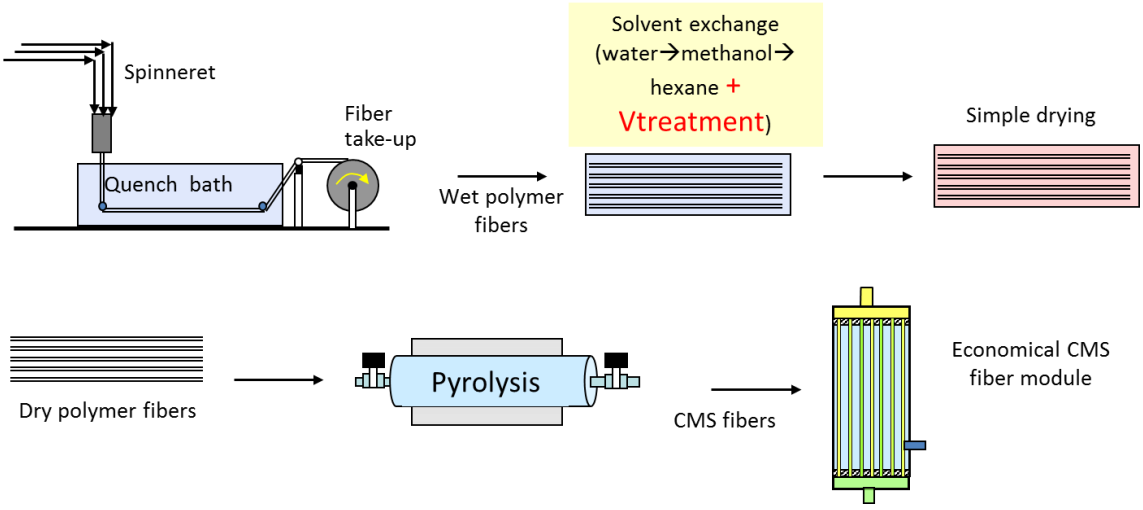

Figure 70: Schematic of what the integrated V-treatment process without adding extra process steps and time

4.3 Summary

In summary this chapter discusses the V-treatment process performed and optimized on Matrimid® and 6FDA:BPDA-DAM hollow fibers. Understanding the mechanism of V-treatment was begun with hollow fiber membranes by varying the time and temperature to inspect for "grafting". It was identified that the V-treatment does not change the polymer at a particular temperature or require a set length of time. The work

leads to a better understanding of the mechanism for V-treatment. An organo-silica layer deposited on the surface of the CMS fibers, adding a non-selective resistance to the gas transport through the membrane. Two strategies were considered for reducing the amount of silica deposited on the outermost skin: KOH etching and washing with VTMS containing solvent. A proof of concept was demonstrated to show that washing with VTMS solution does increase the permeance through the membrane for Matrimid® precursors. A V-treatment concentration optimization was performed on 6FDA:BPDA-DAM based CMS fibers, and it was shown that any concentration of VTMS basically stops collapse in the fiber and increases the permeances. Surprisingly, the concentration of VTMS appears less important, since the entire range of concentration from 10% to 100% showed similarly attractive properties for gas transport. The time required for VTMS to diffuse through the skin layer of the polymer was estimated approximately and it was experimentally investigated. On the basis of this work, it appears that the V-treatment process is industrially scalable.

CHAPTER 5 UNDERSTANDING INTERACTION OF H_2S WITH CMS

As noted earlier, the chief application of gas separation membranes is currently for bulk CO_2 removal in the natural gas industry. Nevertheless in some cases, CMS membranes will also encounter hydrogen sulfide. Since H_2S is known to be a very aggressive gas and is toxic in nature, little literature is available regarding H_2S separation with membranes. Based on the above facts, it was attractive to study the interaction of CMS with H_2S to determine its effects on the CMS membranes for general acid gas removal.

5.1 Conditioning methods

Kemmerlin was the first Koros group member to explore CMS membranes for separation of H_2S and CO_2 from CH_4 [32], and this work indicated significant changes in their transport properties upon exposure to different types of H_2S feeds. These long-lived changes in transport properties are termed as "H_2S conditioning." Kemmerlin's two types of protocols for studying H_2S conditioning are outlined below, and used in this work for consistency.

5.1.1 Mixed gas H_2S Conditioning

Mixed gas H_2S conditioning represents industrially relevant natural gas feed conditions containing H_2S and CO_2 impurities, to indicate the impact on a CMS membrane. In this work, an extended mixed gas conditioning protocol involved a 24 hour exposure of

the CMS membrane to a mixed gas feed of H_2S, CO_2 and CH_4 at a high pressure. This was achieved by subjecting the shell side (upstream) of the membrane to the high pressure feed gas, while pulling vacuum on the bore side (downstream) of the membrane. Subsequently, an effort was made to remove all of the feed components by raising the temperature of the permeation box containing the module to 50 °C and pulling vacuum on both the shell and the bore side for 24 hours. Once the module had been completely desorbed, the permeation system was cooled down to 35 °C and a permeation test was begun with CO_2 and CH_4 pure gas feeds to probe any time dependent changes reflecting recovery of performance to detect purely physical relaxation of the CMS matrix after removal of H_2S.

5.1.2 Pure gas H_2S conditioning

A pure gas H_2S conditioning protocol using a pure feed with nominally the same H_2S fugacity used in the mixed gas H_2S conditioning protocol was used to probe differences in the responses induced without CO_2 or CH_4 present during actual H_2S exposure. These two conditioning approaches were used to determine different effects on conditioned transport properties while keeping the control variable of H_2S activity essentially constant. The pure gas conditioning protocol involves a 24 hours soak at 150 psia of pure H_2S on the upstream (shell) side of the module while the downstream (bore) side of the module is still under active vacuum. Similar to the mixed gas conditioning protocol, after a 24 hours soak the temperature inside the permeation system was increased to 50 °C and the entire hollow fiber module (both shell and bore side) were kept under active vacuum for at least 72 hours to completely desorb any remaining H_2S that was not bonded to the membrane. After this desorption step, the temperature inside the permeation

system was returned to 35 °C and the system was allowed to reach steady state equilibrium. After the system reached steady state, another pure gas permeation experiment was begun. Detailed transport results for these two types of conditioning exposures will be presented later after providing some background to show evidence for likely chemical changes induced by exposure of CMS to H_2S.

5.2 Matrimid®

CMS derived from Matrimid® was used for preliminary study of the effect of H_2S on CMS membranes by Kemmerlin and this work. While admittedly not exhaustive, this work indicates that H_2S will need considerable additional in depth studies to avoid potential surprises in practical separations involving this aggressive component.

5.2.1 Permeation

Permeation properties of Matrimid® CMS showed that H_2S affected CMS membranes. The work in this section used V-treated Matrimid® CMS hollow fibers so that a higher value of starting permeance can be exploited to address this issue. The work has later been extended to 6FDA:BPDA-DAM derived CMS membranes, in both untreated and V-treated forms.

5.2.1.1 Mixed gas H_2S conditioning

This part of the work cited from Kemmerlin's work, used Matrimid® fibers that underwent an additional extended solvent exchange, to "heal" any minor surface defects

[32]. A mixed gas feed of 20% H_2S, 20% CO_2 and 60% CH_4 was used, representing a very aggressive natural gas feed containing H_2S and CO_2 as impurities. An exposure of the CMS membrane in the mixed gas was done at a high pressure of 1135 psia. After each 24 hours of exposure to mixed gas, the membrane was evacuated at 50 °C and subsequent testing with pure CO_2 at 150 psia with shell side feed 35 °C. It was observed that the pure gas CO_2 permeances through the CMS membrane derived from Matrimid® decreased with the time of exposure to H_2S. However, after the permeance value dropped for a few days, the CO_2 permeance gradually reached a steady state value. The normalized permeation data is reported in the Figure 71 on the y-axis, plotted against the time of exposure to H_2S in hours on the x-axis [32].

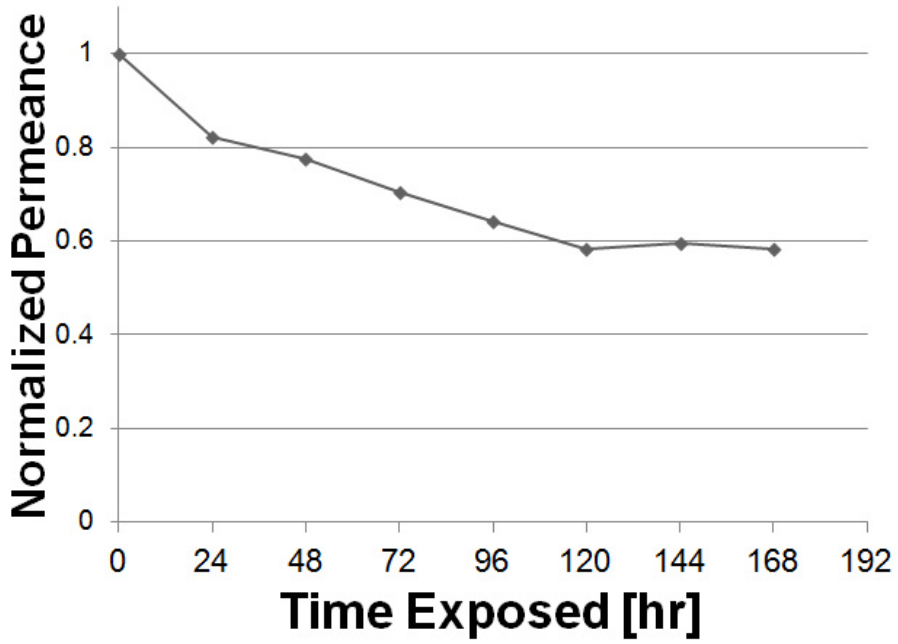

Figure 71: Pure gas CO_2 normalized permeation change as a function of time exposed to the extended conditioning mixed gas feed (20% H_2S, 20% CO_2 and 60% CH_4 at 1135 psi and 35 °C) Matrimid® CMS hollow fiber membranes produced at 500 °C with UHP Argon pyrolysis atmosphere [32]

The preceding data from Matrimid® derived CMS shows that the H_2S conditioning does not destroy the membrane performance, since the CO_2 permeance stabilizes at a value 40% lower than the starting value. The CO_2/CH_4 selectivity changed from an initial state value of 16.4 to a final state value of 26.7 after the performance of the membrane stabilized. This graph gives a benchmark value for steady state in CMS hollow fibers derived from Matrimid® at 500 °C.

5.2.1.2 Pure gas H_2S conditioning

H_2S conditioning at 150 psia and 35 °C for 24 hours was performed by Kemmerlin on CMS fibers made from Matrimid® without any V-treatment, pyrolyzed at 550 °C under UHP Argon. After every 24 hours, a pure gas CO_2 permeance test was performed at 150 psi with shell side feed to test the change in gas transport properties of the membrane. To benchmark against Kemmerlin's results, the same type of non V-treated 500 °C CMS were studied in this work. The change in the permeance is shown in Figure 72, where the y-axis plots the normalized permeance drop of CO_2 and the x-axis is the time in hours of exposure to H_2S. For comparison, the results from mixed gas H_2S conditioning feed (20% H_2S) are also shown in the Figure 72.

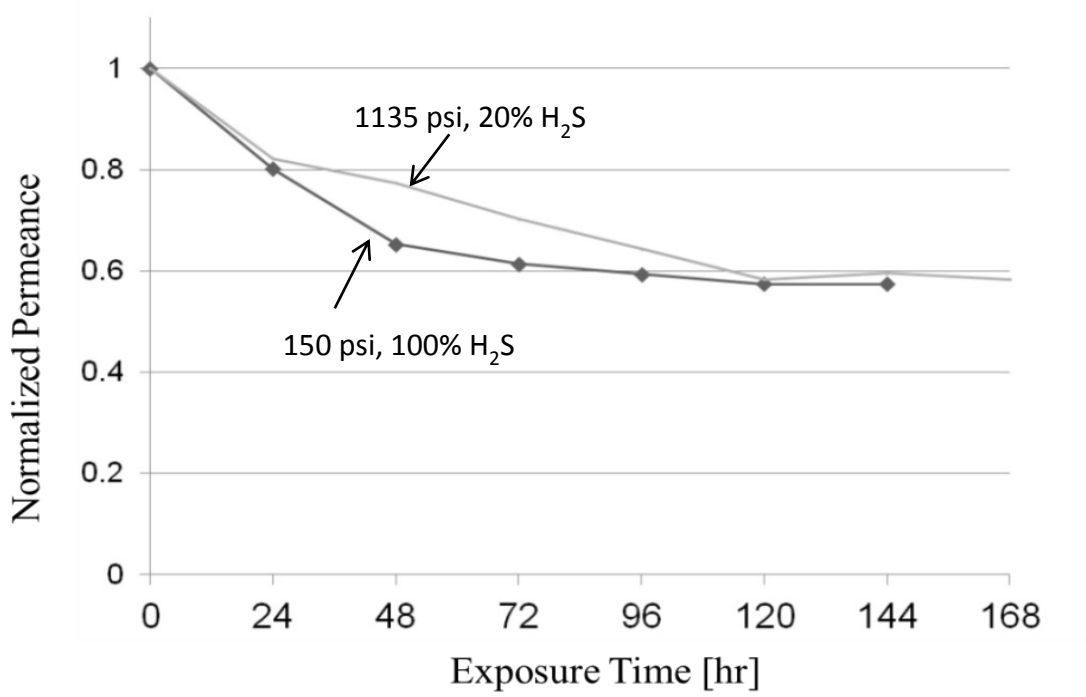

Figure 72: Pure gas normalized CO_2 permeation change as a function of time exposed to the rapid conditioning pure gas feed. Matrimid® CMS hollow fiber membranes produced via pyrolysis at 500 °C with 2 ppm O_2 in Ar pyrolysis atmosphere, tested with pure gas feed at 150 psi [32].

This above graph verifies that pure gas H_2S conditioning of CMS membranes decreases the permeance to essentially the same steady state value, but more rapidly than the lower concentration mixed gas H_2S conditioning protocol using a similar H_2S feed fugacity. This implies that a steady state exists, where the transport properties no longer change as a function of H_2S exposure. Using the above information, the pure H_2S conditioning protocol was selected for use in this project for most of the experiments, to reduce experimental time in this exploratory work of the new H_2S area.

In addition, V-treated samples were also studied since it was important to determine whether the presence of the residual silica from the V-treatment would further complicate the H_2S conditioning effect seen even for non-V-treated CMS. Matrimid® fibers were V-

treated with 10% VTMS solution and pyrolyzed at 500 °C with UHP Argon. The permeance was tested before and after exposure to H_2S with pure gas H_2S conditioning to determine the change in permeance. The results of this experiment are illustrated in Figure 73 and compared to those for untreated CMS derived from Matrimid®, where the x-axis is the CO_2 permeance and the y-axis is the CO_2/CH_4 selectivity.

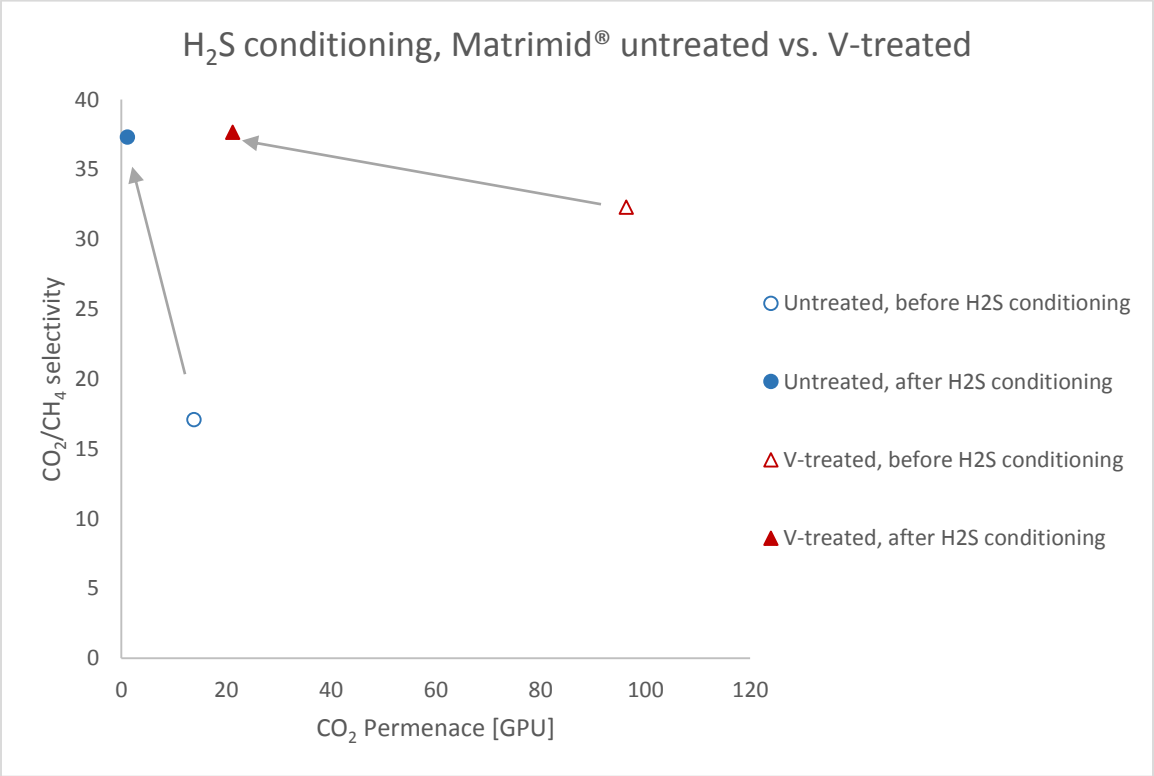

Figure 73: CO_2 permeance when exposed to the pure gas H_2S conditioning 10% V-treated Matrimid® CMS hollow fiber membranes produced via pyrolysis at 500 °C with UHP Argon pyrolysis atmosphere, tested with mixed gas feed (50% CO_2, 50% CH_4) at 100 psi at 35 °C

The above plot shows that the CO_2 permeance drops after conditioning, even in this case with V-treated Matrimid fibers. However, the *percentage* of drop is similar in the case

of both untreated and V-treated CMS fibers, and higher than what Kemmerlin has reported. This is attributed to the difference in solvent exchange procedure, where this work used a regular solvent exchange and Kemmerlin used an extended repeated solvent exchange process. It does not indicate that the CO_2 permeance dropped more due to the presence of VTMS, when compared to the percentage of drop in the untreated fibers in the same plot. Therefore it is concluded that the presence of residual silica from the V-treatment does not add extra complication per se in the H_2S conditioning.

Hypothesis:

All the above experiments from the H_2S conditioning show that the H_2S affects the CMS. This exposure to H_2S causes a loss in the permeance (and permeability) through the CMS membrane. Gas transport in CMS membranes is still modeled via the solution-diffusion model as described in Chapter 2. In the solution diffusion model, permeability is defined as the product of diffusivity and solubility.

$$P = D \times S$$

The change seen in the gas transport properties through these membranes represent the effect of H_2S exposure on both the solubility and diffusivity of the gas molecules through CMS. The exact manner in which the H_2S conditioning of CMS membranes remained unknown, but we hypothesized that H_2S may react at both the micropore sorption sites and the ultramicropore sieving sites. This results in a drop in both the diffusivity and solubility of the gas in the membrane. To test this hypothesis, a sorption experiment was done on CMS derived from Matrimid®.

5.2.2 Sorption

Equilibrium sorption tests were performed to understand if the H_2S affects the sorption capacity of CMS. A pressure decay sorption set up was used for these experiments, and sorption of CO_2 and CH_4 was done the CMS membranes before and after exposure to H_2S.

CMS hollow fiber samples were prepared by pyrolyzing Matrimid® hollow fibers at 500 °C in UHP Argon. These fibers were crushed and placed in a sorption cell for a pressure decay sorption in the H_2S lab. Sorption tests of CO_2 and CH_4 were carried out on the sample, and then the rapid H_2S conditioning protocol performed. This included soaking the sample in 150 psi of H_2S for 72 hours, and pulling vacuum on the sample at 50 °C for 72 hours. After the conditioning, CO_2 and CH_4 sorption were tested again to check for change in sorption capacity. The sorption isotherms are shown in Figure 74. The final pressure of the gas is plotted on the x-axis against the sorbed concentration of the gas on the y-axis.

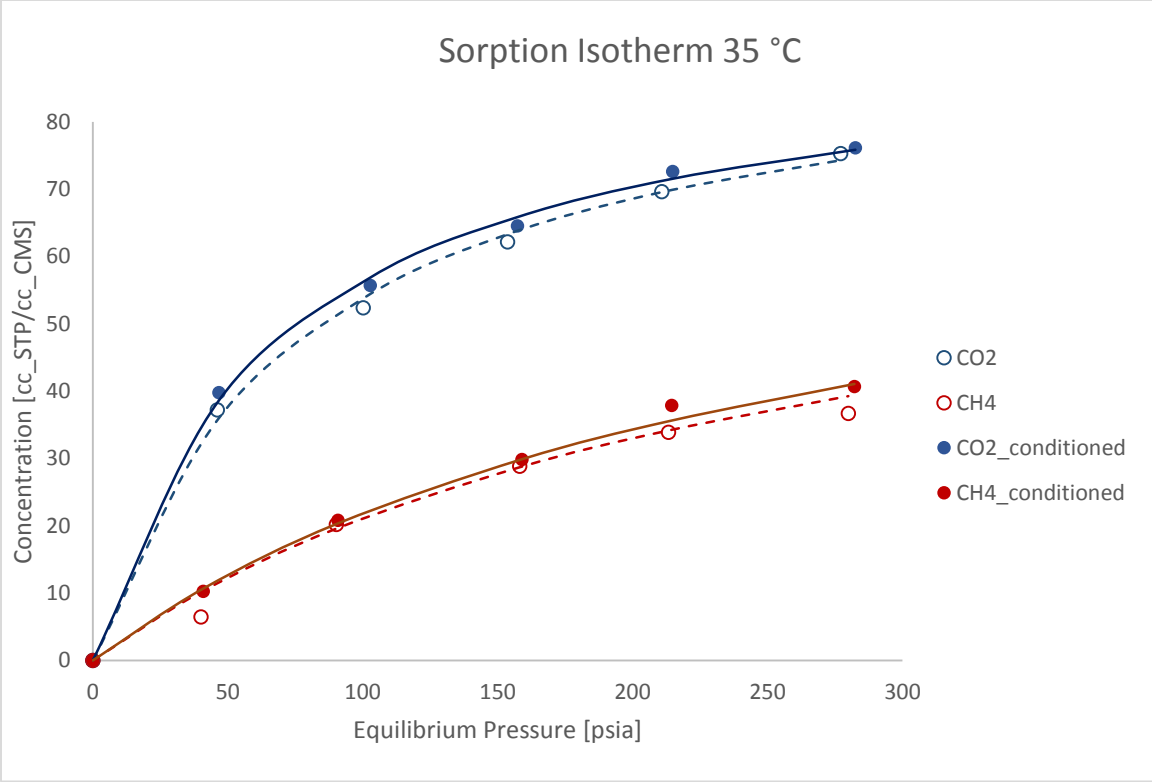

Figure 74: Sorption isotherms of CO_2 and CH_4 before and after H_2S conditioning on CMS from Matrimid® at 500 °C under UHP Argon. Tests were performed with pure gases at 35 °C

Langmuir sorption parameters for the sorption isotherms are listed for both the gases before and after conditioning in Table 8.

Table 8: Langmuir sorption parameters for gases before and after H_2S conditioning of CMS derived from Matrimid® at 500 °C under UHP Argon. Tests were performed with pure gases at 35 °C

Gas	C_h' (cc(STP)/cc_CMS)	b ($psia^{-1}$)
Before H_2S conditioning		
CO_2	94.77	0.0131
CH_4	73.23	0.0039
After H_2S conditioning		
CO_2	93.75	0.015
CH_4	75.33	0.0038

Figure 76 shows that the sorption isotherms for CH_4 and CO_2 over CMS that is unexposed to H_2S are very similar to those after exposure to 150 psi of H_2S for 72 hours. This implies that H_2S does not react significantly with the basal planes of CMS structure to permanently "clog" the micropore galleries between the ultramicropores. However, a decrease in permeance due to H_2S conditioning was observed, and we therefore hypothesize that although H_2S did not react at the basal planes, it chemisorbs at the reactive edges of ultramicropores of CMS, reducing the permeance by changing the diffusion coefficients of the penetrants. This is shown schematically in Figure 77, where (a) shows the slit-like structure of CMS, and (b) illustrates the ultramicropores conditioned with H_2S.

Since sulfur is a large atom, this reaction in the ultramicropores causes a large drop in the permeance and a rise in selectivity.

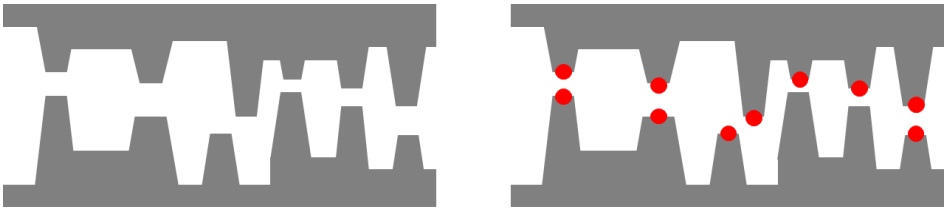

Figure 75: Schematic illustrating the slit-like ultramicropores of CMS (a) initial state and (b) H_2S conditioned state

5.2.3 FTIR

As noted earlier, Kemmerlin showed that H_2S strongly affects the separation and productivity of CMS membranes [32]. His preliminary work sought to determine whether the nature of the interaction was purely physical or primarily chemical. To probe this issue, FTIR was performed on CMS structures before and after exposure to H_2S. Specifically, two CMS samples made from Matrimid® pyrolyzed at 500 °C under UHP Argon and compared. One sample had been conditioned with H_2S using the pure gas conditioning protocol noted above, and the other hadn't been conditioned by exposure to any H_2S feed.

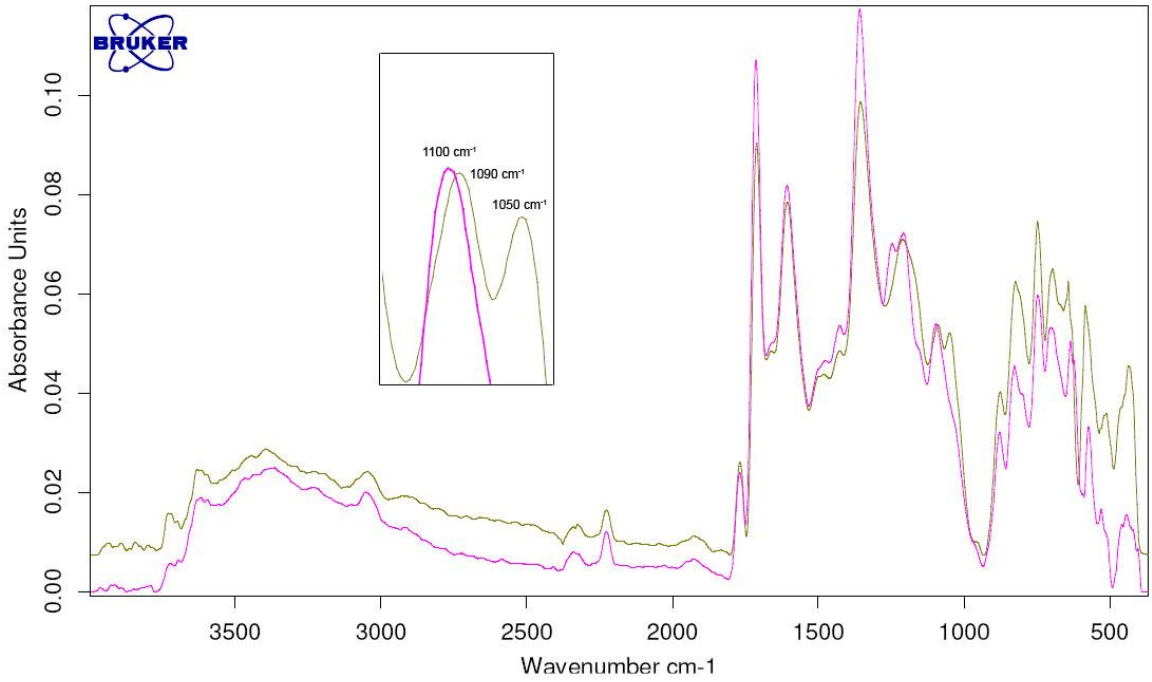

Figure 76: IR spectra of unconditioned (pink) and pure gas conditioned (green) CMS membranes pyrolyzed at 500 °C under UHP Argon. Inset shows key difference, with extra peak present at 1050 cm^{-1} [32].

Kemmerlin suggested that the extra peak in the inset possibly corresponded to the presence of sulfoxide functional group, S=O, that was not present in the unconditioned sample; however, vibrational frequencies for S=O and C=S are relatively close so some ambiguity remains. While the H_2S may be chemisorbing on doped oxygen to form an S=O bond, UHP Argon was used for pyrolysis with only around 0.5 ppm oxygen in the pyrolysis atmosphere. On this basis, it seems also possible that sulfur may be reacting with the carbon structure to create C=S groups analogous to oxygen doping.

5.3 6FDA:BPDA-DAM

5.3.1 Permeation

A similar study to that described for the Matrimid® derived CMS was performed for CMS hollow fibers derived from 6FDA:BPDA-DAM.

5.3.1.1 Mixed gas H_2S conditioning

The extended mixed gas H_2S conditioning protocol was used to better document and probe the effect of the H_2S over long periods of time, and gas transport properties are reported from this study in this section. An effort was also made to understand if more open CMS membranes exhibited the same declining permeance even in environments that have relatively *low* partial pressure of H_2S. To probe this issue, much milder feed gas conditions were used, still with significant H_2S content of relevance to actual natural gas. A mixed gas feed containing 0.5% H_2S, 20% CO_2 and 79.5% CH_4 was used, at a pressure of 100 psi compared to the previous section with 1135 psia of 20% H_2S. It was hypothesized that for such a mixed gas feed with a low concentration of H_2S, CO_2 competitive sorption may prevent the H_2S from conditioning the CMS membrane. In glassy polymers, competitive sorption of different penetrant species such as CO_2 and CH_4 present in a gas mixture are known to compete for fixed amount of Langmuir sorption sites associated with segmental packing defects in such glassy matrices. It was thought that such a physical competition effect might be at play in the case with H_2S in the glassy CMS matrix.

If such a physical chemical competition were the dominant factor, a low concentration of H_2S may prevent H_2S from conditioning the CMS membrane. The CO_2

and CH_4 permeances would be relatively less affected, and the poisoning effect would not be observed to such high degree.

Procedure: Fresh CMS hollow fiber membranes pyrolyzed from 6FDA:BPDA-DAM at 550 °C under UHP Argon atmosphere were epoxied into a module with 24 hour epoxy. These modules were exposed to feed gas containing 0.5% H_2S, 20% CO_2 and 79.5% CH_4 on the shell side, at a feed pressure of 100 psia for 24 hours. Vacuum was pulled on the permeate side (bore side) of the membrane to remove all the permeating gas. A retentate flow incorporated to maintain a stage cut of less than 1% so that the feed composition remained unchanged.

After 24 hours, a mixed gas permeation measurement was done by injecting the permeate gas into the GC to get the composition. The normalized CO_2 permeation data is reported in Figure 77. Multiple tests were done to confirm the trend, with variability less than 5%.

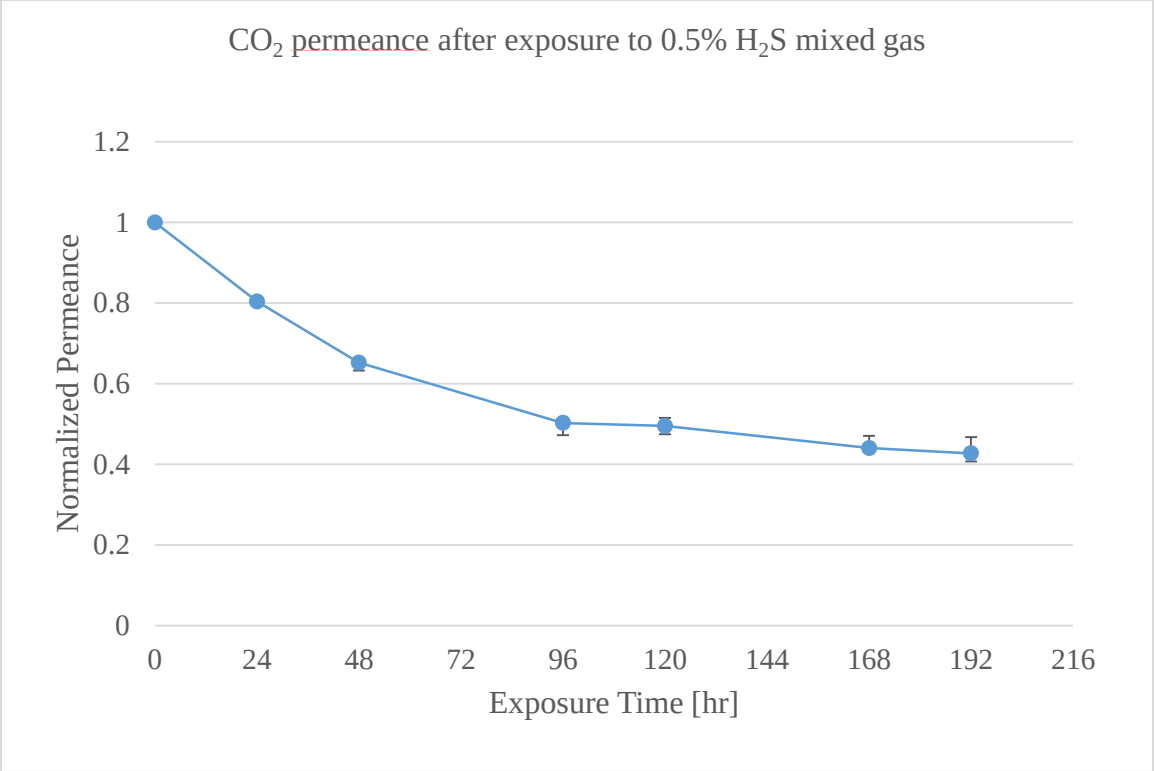

Figure 77: Normalized CO_2 permeance as a function of exposure to 0.5% H_2S. CMS fibers made from 6FDA:BPDA-DAM, pyrolyzed at 550 °C under UHP Argon. Tested with mixed gas (0.5% H_2S, 20% CO_2 and 79.5% CH_4) at 35 °C

Figure 77 suggests that even a low partial pressure of H_2S can adversely affect the 6FDA:BPDA-DAM derived CMS membranes, reducing the membrane permeance slowly but steadily. This means that given enough time, the CO_2 permeance may decrease even further to a steady state. Presumably this steady state will be the same as the one reached through rapid conditioning of the CMS membrane. More long term tests with 0.5% H_2S mixed gas were out of the scope of this work, and will be performed at Shell Global Solutions, Houston, TX.

5.3.1.2 Pure gas H_2S Conditioning

As it was seen that even small amounts of H_2S caused a drop in permeance of gases through the membrane, it was of interest to establish the permeance of conditioned CMS membranes after reaching steady state. The pure gas H_2S conditioning protocol allowed the simulation of a long term H_2S exposure in a shorter time, to reduce experimental time.

5.3.1.2.1 Untreated CMS fibers

Again, to minimize the time consuming studies in this exploratory work, the 6FDA:BPDA-DAM derived CMS hollow fiber membranes were exposed to the harsh condition of 150 psia of 99.6% H_2S to simulate an accelerated effect of H_2S mixed gas on the membrane.

As mentioned before, CMS derived from 6FDA:BPDA-DAM is intrinsically more open than CMS derived from Matrimid®, showing much higher CO_2 permeance at similar pyrolysis conditions. As in the case of Matrimid® derived CMS, when conditioned with the pure gas H_2S conditioning protocol described in section 5.1, the transport properties through the 6DA:BPDA-DAM derived CMS also changed. A curve demonstrating the fall of CO_2 permeance due to exposure to H_2S is shown in Figure 78 for a 6FDA:BPDA-DAM derived CMS created under UHP Argon at 550 °C without V-treatment.

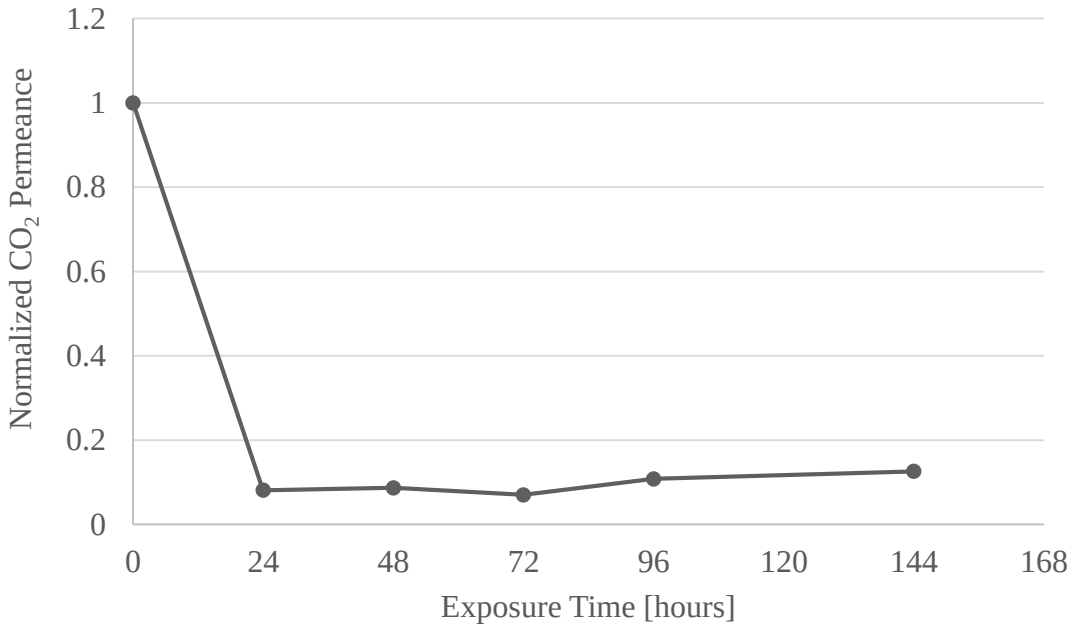

Figure 78: Normalized CO_2 permeance change as a function of time exposed to the 150 psi H_2S pure gas feed. 6FDA:BPDA-DAM CMS hollow fiber membranes produced via pyrolysis at 550 °C under UHP Argon atmosphere. Permeance tested at 35 °C with 100 psi of pure CO_2.

Table 9: Permeance and selectivity of CMS membrane before and after H_2S conditioned via the pure gas conditioning protocol. Permeances were tested with mixed gas (20% H_2S, 20% CO_2, 60% CH_4) at 100 psi and 35 °C.

	$(P/l)_{CO2}$ [GPU]	$(P/l)_{H2S}$ [GPU]	$\alpha_{(CO2/CH4)}$	$\alpha_{(H2S/CH4)}$
Before conditioning	109	-	33	-
After conditioning	6.8	1.7	58	15

Unlike Matrimid® where the steady state stabilization took 72 hours to reach, a large drop in permeance was seen in the first 24 hours of rapid H_2S conditioning for 6FDA:BPDA-DAM based CMS hollow fibers. Hence pure gas H_2S conditioning on 6FDA:BPDA-DAM will be done for 24 hours before pulling vacuum and testing. The

CO_2/CH_4 selectivity changed from 35 in the initial state to 58 in the final conditioned state. It also appears that the 72 hours of vacuum that was used after the exposure to H_2S could be causing some aging, i.e. decrease in CO_2 permeance due to settling of carbon sheets to achieve an equilibrium state. To verify if the drop in permeance was completely due to the exposure to H_2S or if vacuum aging played a big role, it was necessary to decouple these two effects on the 6F CMS fibers and is discussed later in section 5.4.

5.3.1.2.2 Oxygen doped 6F CMS fibers

It has been shown by Kiyono from the Koros group, that O_2 doping on CMS membranes can be used to tune the permeance and selectivity of the membrane. An optimal condition of O_2 doping for CO_2/CH_4 separation was achieved by pyrolyzing 6FDA:BPDA-DAM fibers with 30 ppm O_2 in UHP Argon at 550 °C. The effect of H_2S conditioning was also tested on these oxygen doped fibers, without any V-treatment complications.

Procedure: The 30 ppm doped 6FDA:BPDA-DAM CMS fibers at 550 °C were packed into a module and epoxied with 24 hour epoxy. They were subjected to the H_2S conditioning with the pure gas H_2S conditioning protocol, and permeances of CO_2 and CH_4 were tested before and after the conditioning. The results of this experiment are as shown in Figure 79.

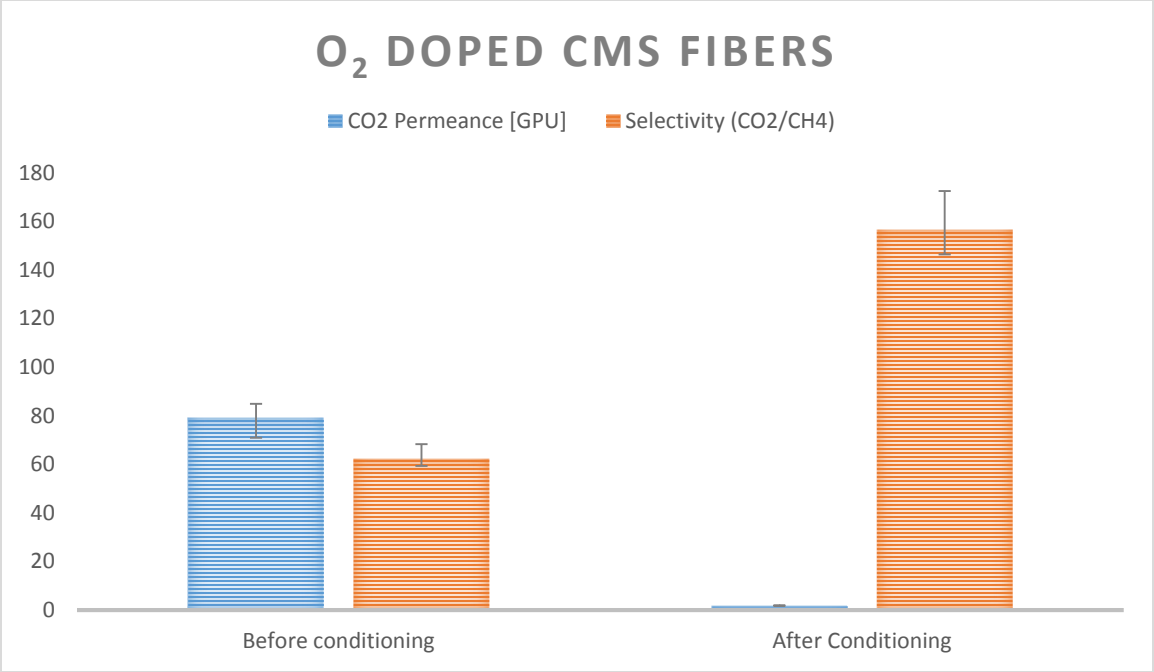

Figure 79: H_2S conditioning applied to V-treated 6FDA:BPDA-DAM derived CMS hollow fibers, pyrolyzed at 550 °C in 30 ppm O_2, cured with 24 hr epoxy – Duralco 4461. Tested with mixed gas (50% CO_2, 50% CH_4) at 100psi at 35 °C

As compared to Bhuwania's results for untreated 6F CMS fibers, the permeance starts out lower than expected before the H_2S exposure. However, the values of permeances and selectivity before conditioning were reasonably similar to Bhuwania's after taking into account the aging caused by at least 48 hours of exposure to ambient air (for curing the H_2S resistant epoxy.) It should be noted though, that the CO_2 permeance dropped very dramatically after H_2S conditioning. Moreover, the CH_4 permeance after conditioning was so low that it could not be measured accurately without error. These tests were repeated with longer conditioning times (3 days) and gave similar results.

This is a disappointing result, but perhaps not an extremely surprising one. The hypothesis for this major drop in permeance for oxygen doped CMS fiber is that the ultramicropores which were tuned by the doped oxygen now get double doped after H_2S

conditioning. In this context, a reaction like Kemmerlin suggested involving an S=O moiety may be created; however, at much greater prevalence due to the preexisting –C=O from the O_2 doping. A cartoon of this idea looks as follows:

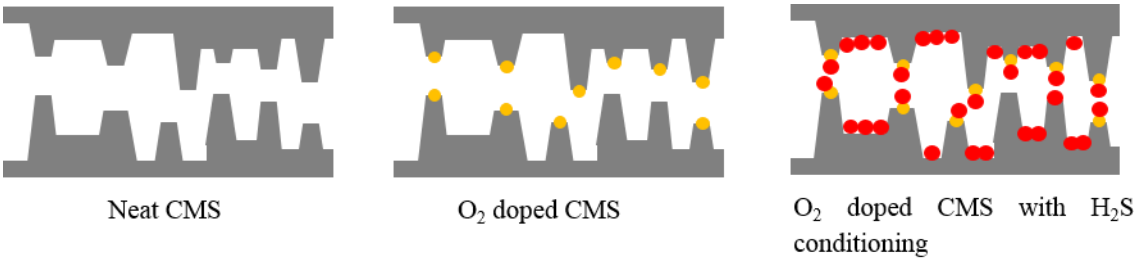

Figure 80: Hypothesis for oxygen doped fibers with H_2S conditioning. Left: Neat CMS membrane; Middle: O_2 doped CMS membrane; Right: O_2 doped CMS membrane after H_2S conditioning (double doping.)

From the drastic drop in permeance, it seems like the 6F CMS structure gets "double doped", which leads to clogging of the ultramicropores and therefore leading to reduced permeances. Also note that the H_2S is shown to be reacted on the basal planes of the CMS as well. This will be discussed further in Section 5.3.2. On this basis, in Chapter 6, an approach to prevent H_2S conditioning instead of using oxygen doped 6F in a H_2S feed mixed gas stream will be considered. Before considering such a topic, however, the complexities introduced by V-treatment will be considered for non O_2 doped fibers.

5.3.1.2.3 V-treated CMS fibers

V-treatment was used to reduce substructure collapse in the CMS hollow fibers derived from 6FDA:BPDA-DAM. This enables starting with a higher level CO_2 permeance level, so that deteriorating effect of H_2S may still lead to reasonable end permeances.

6FDA:BPDA-DAM V-treated CMS fibers were also exposed to pure gas H_2S conditioning protocol, and the CO_2 permeance and CO_2/CH_4 selectivity before and after conditioning are reported in Figure 81.

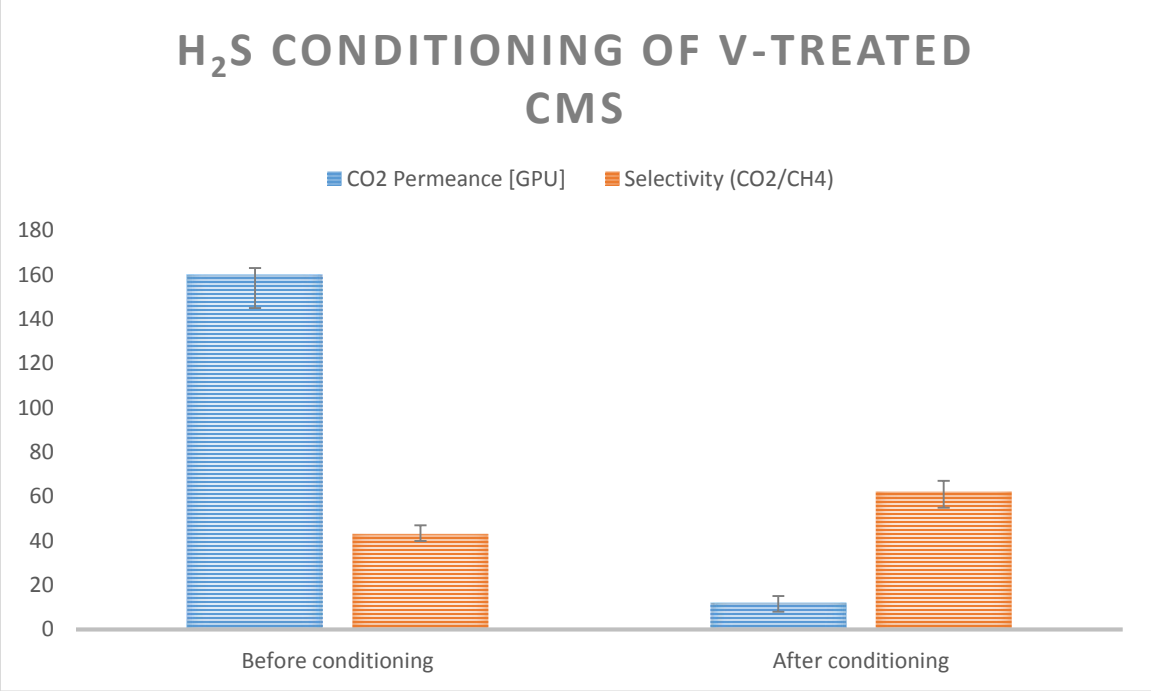

Figure 81: CO_2 Permeance and CO_2/CH_4 selectivity of CMS derived from V-treated 6FDA:BPDA-DAM fibers before and after conditioning. CMS fibers were pyrolyzed at 550 °C in UHP Argon, cured with 24 hr epoxy – Duralco 4461. Tested with mixed gas (50% CO_2, 50% CH_4) at 100psi at 35 °C

Hypothesis:

All the above experiments from the pure gas H_2S conditioning show that the H_2S also affects the CMS derived from 6FDA:BPDA-DAM. This exposure to H_2S causes a loss in the permeance (and therefore permeability) through the CMS membrane. As in the case of Matrimid®, gas transport in CMS membranes is modeled via the solution-diffusion

model as described in Chapter 2. Permeability is defined as the product of diffusivity and solubility in the solution diffusion model.

$$P = D \times S$$

Effect of H_2S exposure on both the solubility and diffusivity of the gas molecules through CMS is represented by the change seen in the gas transport properties through these membranes. The *exact* manner in which the H_2S conditioning of CMS membranes remains unknown, but the hypothesis explored here, as was done for Matrimid® CMS, is that H_2S reacts at both the micropore sorption sites and the ultramicropore sieving sites. This results in a drop in both the diffusivity and solubility of the gas in the membrane. To test this hypothesis, a sorption experiment was done on CMS derived from 6FDA:BPDA-DAM.

5.3.2 Sorption

As in the case of Matrimid® derived CMS, equilibrium sorption tests were also performed in this case to understand if the H_2S affects the sorption capacity of CMS derived from 6FDA:BPDA-DAM. A pressure decay sorption set up was used for these experiments, and sorption of CO_2 and CH_4 was done the CMS membranes before and after exposure to H_2S.

To inspect if the mechanism of H_2S conditioning is different for 6F CMS, a sorption test was performed. The experiment was done with CMS derived from 6FDA:BPDA-DAM fibers (pyrolyzed at 550 °C in UHP Argon), where sorption isotherms were obtained for CO_2 and CH_4, both before exposure and after exposure to H_2S via a pure gas H_2S conditioning protocol. In this test, with the pure gas H_2S conditioning protocol, sample was soaking for 3 days in pure H_2S, after which vacuum was applied for 3 days. Sorption tests

of CO_2 and CH_4 were carried out using a pressure-decay sorption system. The sorption isotherms are shown in Figure 82.

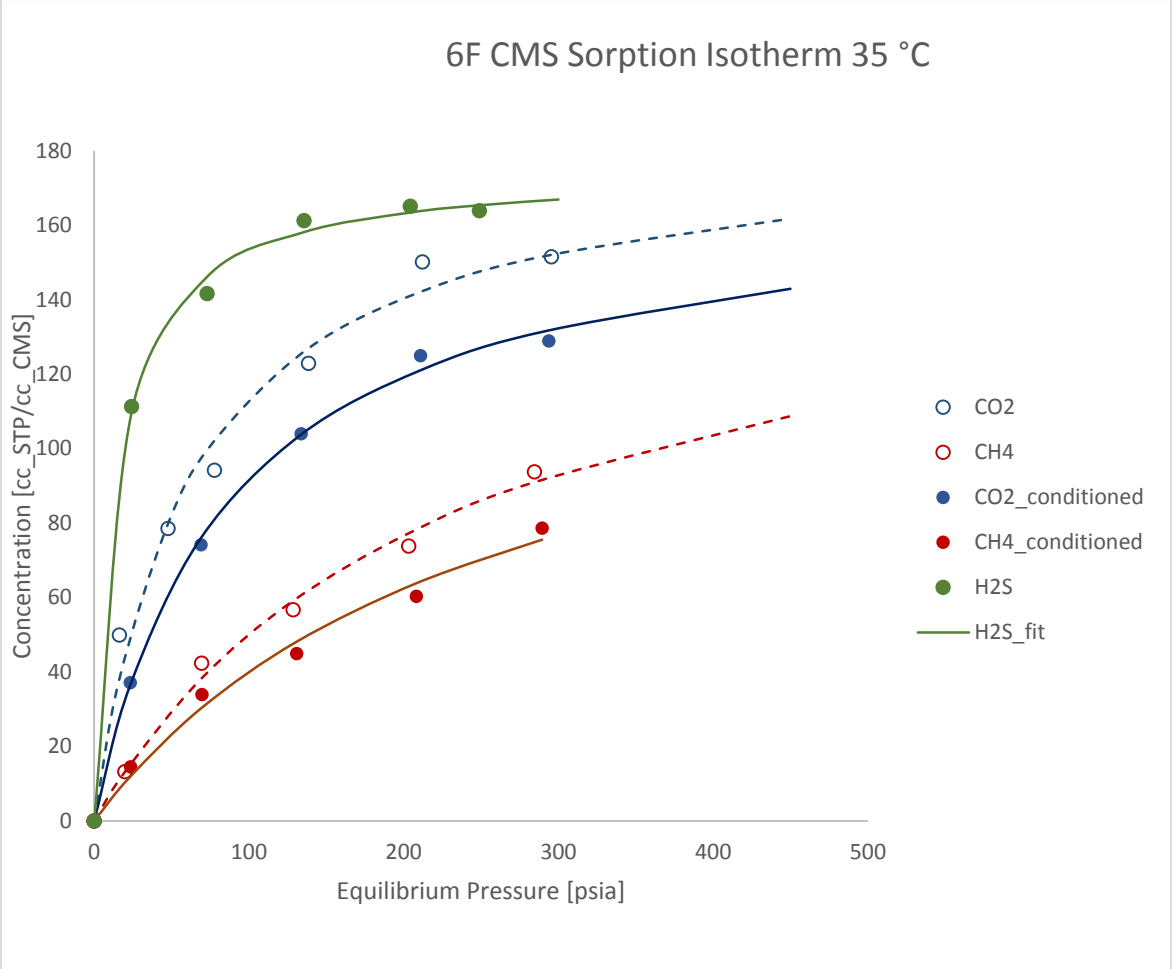

Figure 82: Sorption isotherm for CO_2 and CH_4 before and after H_2S conditioning, and isotherm of H_2S. CMS sample was pyrolyzed at 550 °C in UHP Argon. Tests performed with pure gases at 35 °C

Unlike the case of Matrimid®, the above CO_2 isotherms show that sorption of CO_2 before H_2S conditioning was higher in value than its sorption isotherm after H_2S conditioning and pulling vacuum. The Langmuir hole filling capacity and affinity constants are reported in the table below.

Table 10: Langmuir sorption parameters for CMS derived from 6FDA:BPDA-DAM, pyrolyzed at 550 °C under UHP in Argon

Gas	C'_H cc(STP)/cc(CMS)	b $psia^{-1}$
Before H_2S conditioning		
CO_2	164.4	0.016
CH_4	127.6	0.0044
After H_2S conditioning		
CO_2	149.1	0.012
CH_4	109.3	0.0039
H_2S	174.93	0.0696

Unlike in the case of Matrimid® derived CMS, in this case the sorption curves for CH_4 and CO_2 over CMS that is unexposed to H_2S are not similar to those after exposure to 150 psi of H_2S for 72 hours and vacuum of 72 hours. Unfortunately, at that time it wasn't clear how much aging can affect sorption capacity. Rungta has shown that vacuum aging can significantly affect the sorption capacity of the CMS membranes. This reduced sorption can be either attributed to aging phenomenon, or it could suggest that the H_2S gets sorbed at the basal planes of 6F CMS structure. A cartoon of the hypothesis looks like this:

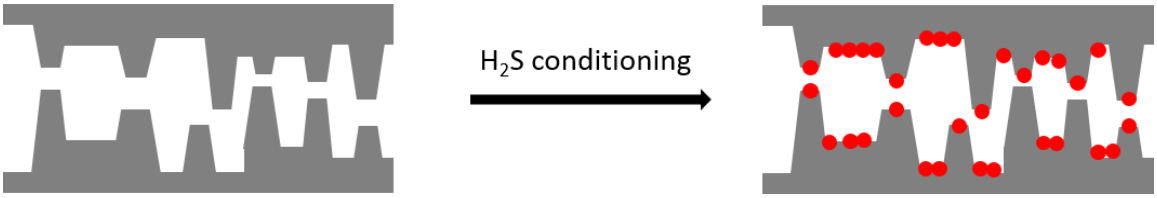

Figure 83: Hypothesis of H_2S interaction with CMS derived from 6FDA:BPDA-DAM

The hypothesis is that the sorption may be due to the highly accessible pyridinic and pyrrolic nitrogens in the 6FDA:BPDA-DAM CMS structure, indicated in the schematic in Figure 84. These types of nitrogen are basic in nature, and as a result the acidic H_2S has high affinity to them. This acid-base interaction may cause the H_2S to be strongly chemisorbed at the basal planes in addition to the reactive ultramicropore edges. It may be that such functionalities are less accessible, or not as prevalent in the more compact Matrimid®.

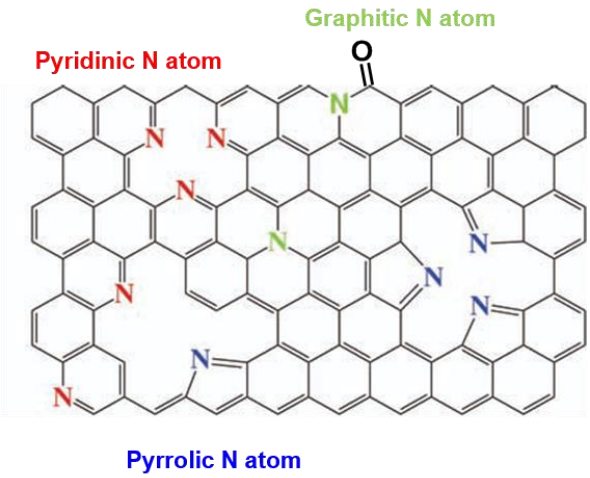

Figure 84: Schematic of different types of Nitrogen atoms present in the CMS structure derived from 6DA:BPDA-DAM

It was also verified that even after exposure to high pressures of CO_2, the curves before and after conditioning do not meet. This supports the hypothesis that the H_2S sorbed in the basal planes isn't simply physically sorbed, but appears to be chemically interacting with the CMS structure.

Sorption selectivity and mobility selectivity values of the membranes after H_2S conditioning were calculated using Eq. (8) and are provided in Table. Based on these numbers, the H_2S/CH_4 mobility selectivity is marginally higher than those found in glassy polymers [24].

Table 11: Sorption and mobility selectivity in 6FDA:BPDA-DAM derived CMS hollow fibers at 35°C at 100 psi, before and after. Values are calculated from pure gas permeation and sorption data

Conditioning	S_{CO2}/S_{CH4}	D_{CO2}/D_{CH4}	S_{H2S}/S_{CH4}	D_{H2S}/D_{CH4}
Before	2.59 ± 0.3	12.43 ± 1.7	-	-
After	2.75 ± 0.2	16.36 ± 1.5	4.96 ± 0.5	2.35 ± 0.2

These values show that CMS fibers behave much more like typical glassy polymers when permeability and selectivity values are compared.

5.3.3 TPD

To probe the above issues more deeply, besides the exposure and FTIR studies by Kemmerlin, in this study a temperature programmed desorption was carried out on H_2S conditioned CMS samples to assess the reversibility of the H_2S conditioning effect. The samples used for this work had been conditioned in 150 psi of H_2S for 3 days, rather than only one day as in Kemmerlin's work. They were then evacuated for 3 days at < 1 millitorr

at 50 °C to desorb any unreacted H_2S for 3 days before the TPD was performed. The TPD used a TCD detector which detects the thermal conductivity of molecules desorbed from the sample of CMS. The carrier gas used in this case was Helium, since it has a significantly different thermal conductivity compared to that of H_2S, or other higher molecular weight species, thereby making it possible to detect such species. Although a facility was not available to identify any evolved gas in terms of chemical identity, the goal was to determine if any evidence could be found indicating that H_2S exposure was thermally reversible. Along with this type of TPD study, an associated transport study was also done (described later) to assess recovery of transport properties after such a more aggressive removal of sorbed or chemisorbed species from the prior H_2S exposure could be detected.

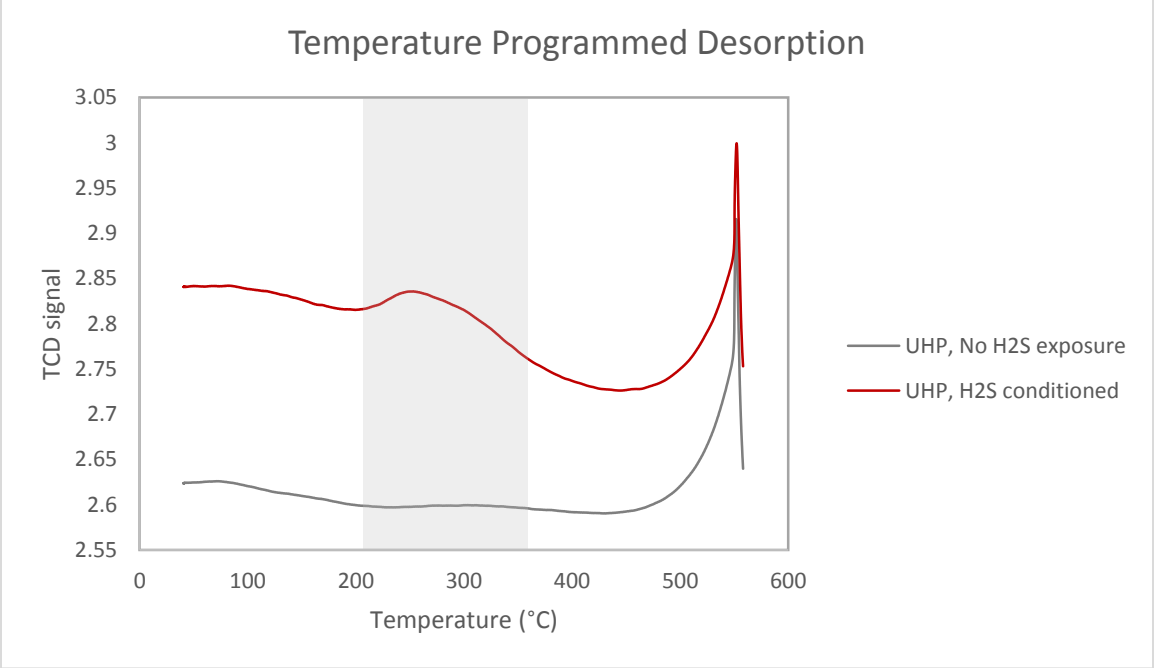

Figure 85: Thermally programmed desorption, possibly showing evolution of H_2S in the conditioned sample, compared to no evolution of gas in the unconditioned sample. CMS sample was pyrolyzed at 550 °C in UHP Argon.

Figure 85 shows deviation of thermal conductivity signal from that of the carrier gas on the y-axis, versus the temperature at which a species is evolved on the x-axis. A peak is seen at about 252 °C, indicating the evolution of a gas at that temperature. Since this evolution is only seen in the sample that was conditioned with H_2S, it possibly suggests that a sulfur containing species being evolved, possibly H_2S itself. Further work will be needed using a residual gas analyzer to prove that evolved component is H_2S; however, access to such a device was not available in the current study.

5.4 Decoupling vacuum from H_2S conditioning

Both the mixed gas H_2S conditioning and the pure gas H_2S conditioning protocols consisted of pulling vacuum for lengthy times after the H_2S soak was completed. However, it is known that vacuum ages the CMS membranes and results in a drop in permeance, much like physical aging in polymers. The drop in permeance in the CMS membrane from the conditioning protocols could be a combination of both the H_2S interaction with the CMS as well as the vacuum aging.

To identify how much the vacuum aging was affecting permeance and selectivity through 6FDA:BPDA-DAM derived CMS fibers pyrolyzed at 550 °C in UHP Argon, a control test was performed. CO_2 and CH_4 permeances were tested on CMS fiber modules 2 days after pyrolysis, to maintain consistency with other testing protocols which use the 24 hour epoxy. The results of the experiment are listed in Figure 86.

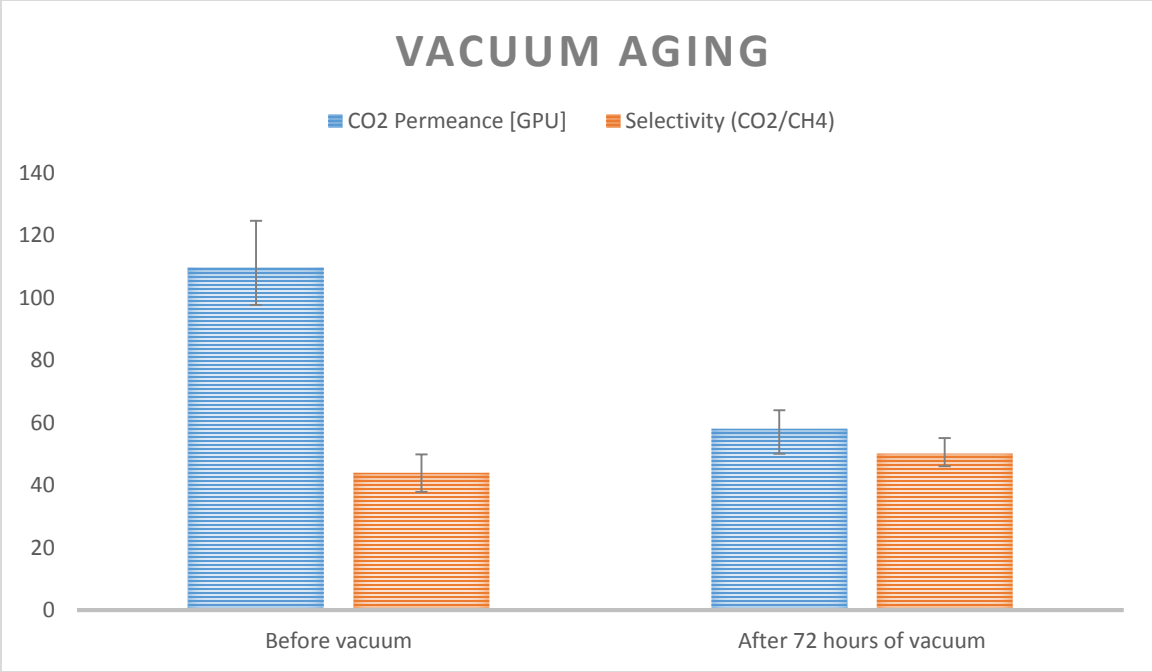

Figure 86: Effect of pulling vacuum on CO_2 permeance of 6FDA:BPDA-DAM derived CMS fibers pyrolyzed at 550 °C in UHP Argon. Tested with mixed gas (50% CO_2, 50% CH_4) at 100 psi and 35 °C

The results in Figure 86 indicate that pulling vacuum on the modules for 72 hours causes about 50% drop in the permeance. Vacuum aging may, therefore, be a big factor in the loss of permeance shown after H_2S conditioning. To decouple these effects, one can purge CO_2 through the module after the H_2S soak instead of pulling vacuum in order to desorb any excess/unreacted H_2S from the membrane. Since it is known that CO_2 active exposure minimizes physical aging [90], this approach could be pursued.

First however, to further decouple the vacuum aging from effect of H_2S itself, or to see if vacuum is causing at least a part of the drop in permeance in "H_2S conditioning", another experiment was done: Two parallel modules were tested for CO_2 and CH_4 permeance. One of them was subjected to the regular pure gas H_2S conditioning protocol (exposure to 150 psi of pure H_2S for 72 hours, vacuum at 50 °C for 72 hours.) The other

one was subjected to an analogous "CO_2 conditioning" protocol (exposure to 150 psi of pure CO_2 for 72 hours, vacuum at 50 °C for 72 hours, vacuum for 50 °C for 72 hours.) The results of these two experiments were compared to determine whether the drop in permeance was wholly due to H_2S. The gas permeation results of this experiment are shown in Figure 87.

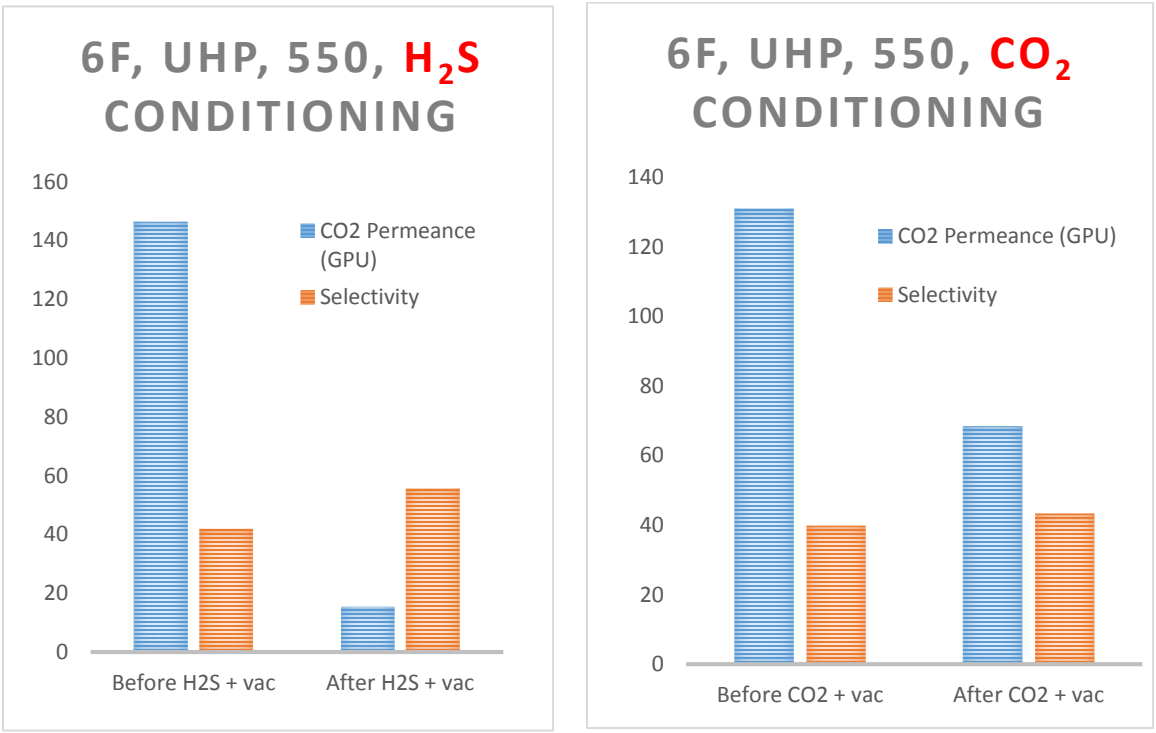

Figure 87: Decoupling of vacuum aging from H_2S conditioning for 6FDA:BPDA-DAM derived CMS fibers pyrolyzed at 550 °C in UHP Argon. CO_2 permeance measured with mixed gas (50% CO_2, 50% CH_4) at 100 psi, 35 °C.

These graphs show that with H_2S conditioning, the CO_2 permeance drops by 80%. However, with the CO_2 conditioning, the CO_2 permeance drops by 50%. This suggests that 50%, or half of the drop in permeance in both the conditioning methods was caused by

pulling vacuum. Here the assumption is that CO_2 purging causes no drop in permeance, as shown by Bhuwania in his aging stability study [90].

Hence, the H_2S conditioning protocol was changed and the vacuum step was replaced with purging with CO_2 at 50 °C.

5.5 Discussion

All these above experiments provide insight into the nature of interaction of H_2S with CMS membranes. A drop is seen in the permeance of both Matrimid® and 6FDA: BPDA-DAM derived CMS membranes. This fact, coupled with the FTIR result indicated that the H_2S is reacting with some part of the carbon structure of the CMS membrane. Sulfurization of carbons or reactions of H_2S with charcoals have been described in the literature as a way to change surface properties of carbon blacks or charcoals [103-105]. Highly stable structures are reported to be formed, suggesting that the sulfur may react at the aromatic rings of the carbon layers. Some of the carbonyl groups present in the ultramicropores may be susceptible to transformation into thiopyrones according to the following simplified scheme:

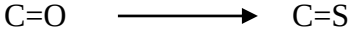

Meyer et. al. have also reported that sulfide react with ketones in the presence of ammonia or amines at room temperature without the application of pressure [106].

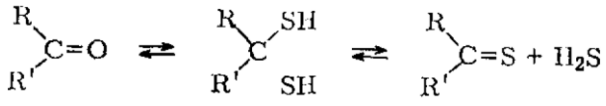

This is consistent with the FTIR peak at 1050 that is likely to reflect the –C=S bond. This appears to be a stable structure that will not decompose at low temperatures.

Recall, however, desorption of a species at 252 °C in the TPD shown in Figure 85 suggests that H_2S may be evolved from the CMS sample at that temperature. This is suggestive of an additional reversible interaction of H_2S with carbons. As shown in Figure 84, the carbon structure of the CMS membranes consists of pyridinic and pyrrolic nitrogens, which can behave like Lewis bases. As H_2S is an acidic gas, it can react with the basic nitrogens, similar to the reaction with a primary or secondary amine via an instantaneous proton transfer mechanism [107], i.e.

$$H_2S + R_2NCH_3 \rightleftarrows R_2NCH_3^+ + HS^-$$

This is similar to the amine absorption used in scrubbing the acid gases from a natural gas stream [108]. Amine absorption is also a reversible reaction, and the H_2S can be recovered by heating the product, as is done in thermal regeneration of amines (described in section 1.1.1). It appears likely that the H_2S undergoes a similar reaction in the CMS membranes at the ultramicropores and possibly in the micropores as well.

The sorption isotherms of CO_2 and CH_4 in Figure 74 and Figure 82 have been fitted to Langmuir regime, as sorption in CMS membranes is typically described by the Langmuir isotherm. However, the data in the sorption isotherms possibly look like dual mode sorption that typically describes sorption in polymeric membranes. The calculated Langmuir hole filing capacity is also higher for both Matrimid® and 6FDA: BPDA-DAM derived CMS membranes compared to those seen by Steel and Koros, and Kiyono and Koros. This is because unlike Steel's work and Kiyono's work, this study starts with a more open structure of CMS that is not allowed to age very much under vacuum.

Rungta and Xu showed that like glassy polymers, CMS membranes can exhibit time based behavior as well. Long periods of storage or pulling vacuum provide the carbon chains enough time to settle down, and their performances converge. This is called aging of the CMS membrane, after which their saturation capacity decreases so the final samples tend to exhibit more Langmuir behavior. The sorption experiments in the current work suggest that the gases sorb not only into the micropores, but possibly also in the larger ultramicropores which is analogous to the sorption in the dense polymer matrix of polymeric membranes. As the CMS membrane ages, the carbon sheets settle and ultramicropores come closer together. The material may lose its extra sorption capacity associated with the larger ultramicropores in the dense matrix, and therefore starts showing Langmuir behavior.

The sorption selectivity for H_2S/CH_4 in CMS is higher than in the case of neat glassy polymers, potentially making CMS good starting materials for H_2S/CH_4 separation. However, H_2S reacts with CMS membrane in such a fashion that it lowers the gas transport properties in the membranes, deteriorating the membrane. If this poisoning of the membrane can be prevented by engineering the structure of the membrane, CMS has the potential to be a robust membrane for gas separation. Approaches of tackling this H_2S conditioning problems are discussed in the next chapter.

5.6 Summary

The effect of pure gas and mixed gas H_2S was investigated on CMS hollow fiber membranes derived from Matrimid® and 6FDA:BPDA-DAM. It is seen that the gas permeation drops dramatically and CO_2/CH_4 selectivity increases when the CMS membrane is exposed to pure gas H_2S, for both untreated and V-treated fibers.

Benchmarking of separation performance in presence of H_2S were considered. Effect of this conditioning on the sorption capacities of CO_2 and CH_4 were demonstrated, showing that the sorption capacity decreased after H_2S conditioning in the case of CMS derived from 6FDA:BPDA-DAM. The sorption and diffusion selectivity for CO_2/CH_4 and H_2S/CH_4 has been also shown in this chapter. A possible mechanism for the nature of interaction of H_2S with the CMS membrane was proposed.

CHAPTER 6 MITIGATION OF HYDROGEN SULFIDE CONDITIONING

This chapter considers approaches to mitigate H_2S conditioning of the CMS structure. The experiments were performed on both Matrimid® and 6FDA:BPDA-DAM derived CMS.

For the Matrimid® derived CMS, the H_2S was shown in Chapter 5 to primarily react with the reactive edges at the ultramicropores (based on sorption, permeation and diffusion after exposure to H_2S). This insight led to the idea of altering reactive edges with another moiety that might make them inert, unlike the case with oxygen doping. Clearly this must be considered an exploratory study, but some promising leads were found in the literature.

Specifically, it has been shown in the literature that chlorination of carbons at 400-600°C results in fixation of chlorine giving rise to rather stable compounds. Papirer [109] and Puri [110] have shown that Cl_2 can strongly irreversibly bond with carbon blacks and charcoals at high temperatures. The carbons were treated with a mixture of nitrogen and chlorine gas at temperature of 450 °C and then stored under atmospheric conditions, to give very stable carbon chlorine structures. The added chlorine was shown to be only partially eliminated with heating at high temperature (1200 °C) or boiling with concentrated alkaline hydroxide solution. Although these chlorine modified carbons were not tested for H_2S exposure, it appeared worthy of study for our work with CMS.

These earlier studies motivated work for this project with an idea to possibly use trace amounts of chlorine in the pyrolysis sweep gas contacting the polymeric hollow

fibers, similar to that of O_2 in oxygen doping. It was hypothesized that such treatments may stabilize the CMS against H_2S conditioning, and also provide an alternative to O_2 doping for ultramicropore size tunings.

6.1 Matrimid®

Matrimid® polymer fibers were pyrolyzed with UHP Argon with a final pyrolysis temperature of 500°C, and then the flow gas was switched to 15 ppm Cl_2 in Argon for a soak time of 2 hours. As mentioned before, the temperature of 500 °C was chosen because the Matrimid® CMS structure is intrinsically highly "open" at this temperature. The selectivity suffers due to this openness, but this temperature corresponds to the highest permeance for a collapsed Matrimid® CMS hollow fiber. As noted above, it was hypothesized that Cl_2 fixation would react at the ultramicropores, and reduce the average size of the ultramicropores, thereby providing a more stable variant of the O_2 doping, which was shown in Chapter 5 to lead to apparent "double doping" in the presence of H_2S. This undesirable double doping greatly reduced CO_2 permeation, despite leaving CO_2/CH_4 selectivity at an attractive value. A schematic representation of the carbon structure is shown in Figure 88. As shown, the process was viewed to be analogous to oxygen doping, but with more reactively inert edges.

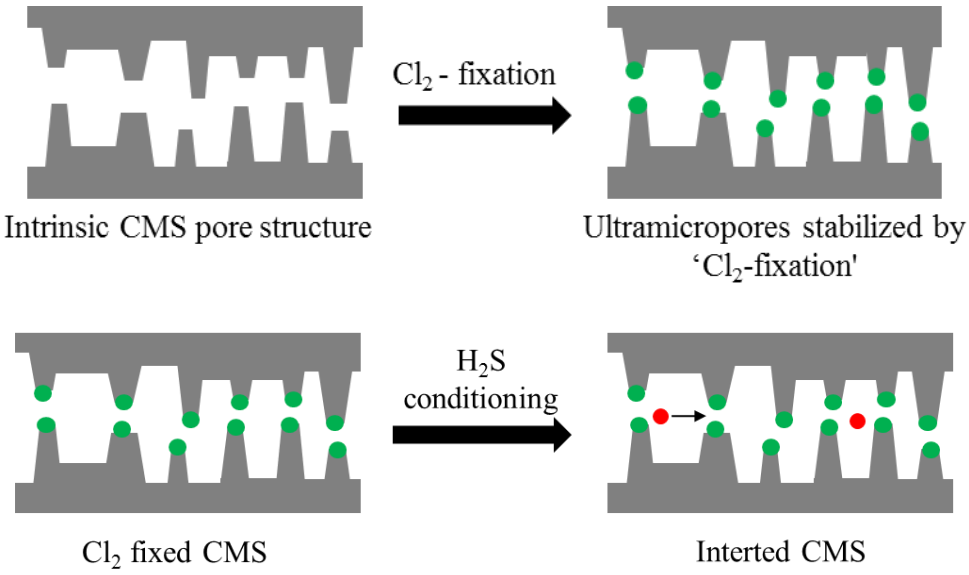

Figure 88: Schematic of chlorine fixation hypothesis at the ultramicropores of the CMS structure derived from Matrimid®

As indicated, the vision was for the Cl_2 to be bonded at the reactive ultramicropores edges and make the edges inert to other reactions, while still allowing ultramicropore sizes enough for gas diffusion. The resulting membrane was, therefore tested for CO_2 and CH_4 mixed gas feed after the Cl_2 fixation. The permeance and selectivity data are summarized in the plot in Figure 89.

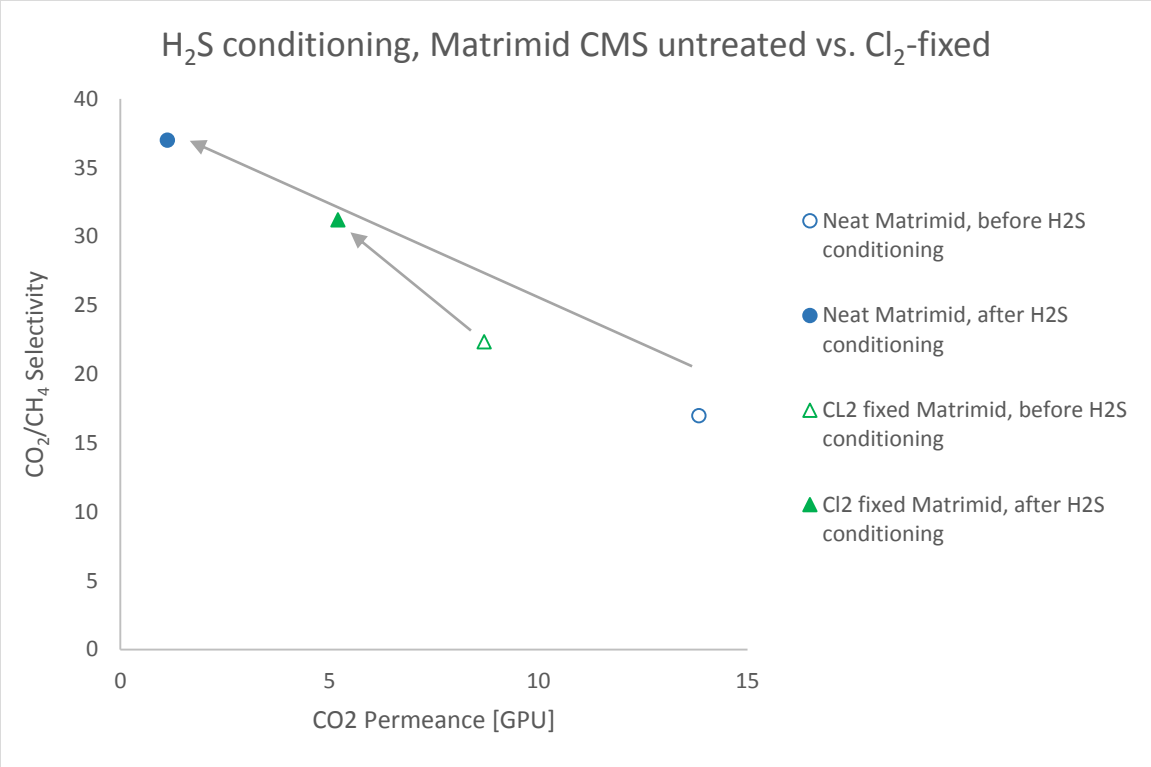

Figure 89: Influence of chlorine fixation on the effect of H_2S conditioning on CMS derived from Matrimid®. All membranes were pyrolyzed at 500 °C, comparing 15 Cl_2 in Argon (red) with UHP Argon (blue) atmosphere. Tested with mixed gas (50% CO_2, 50% CH_4) at 100 psi and 35 °C

As expected based on the previous discussion, the Cl_2 fixed fibers started with a lower CO_2 permeance (40% lower) than that of the neat CMS fiber. The CO_2 permeances for both the neat CMS fibers and Cl_2 fixed CMS fibers dropped after H_2S conditioning. Moreover the CO_2/CH_4 selectivity increased due to the Cl_2 exposure. However, the drop in permeance in the *neat fiber was much more drastic* than the drop in the Cl_2 doped fiber, which ended up at a roughly 4X higher permeance value. This preliminary result supported the hypothesis that the chlorine was fixed at the ultramicropores which reduced the starting permeance, but prevented complete H_2S conditioning.

The resultant changes can be envisioned in the form of shift of distribution of the ultramicropore size. Ideally, the chlorine fixation of CMS alters the ultramicropore distribution of the structure as shown in Figure 90.

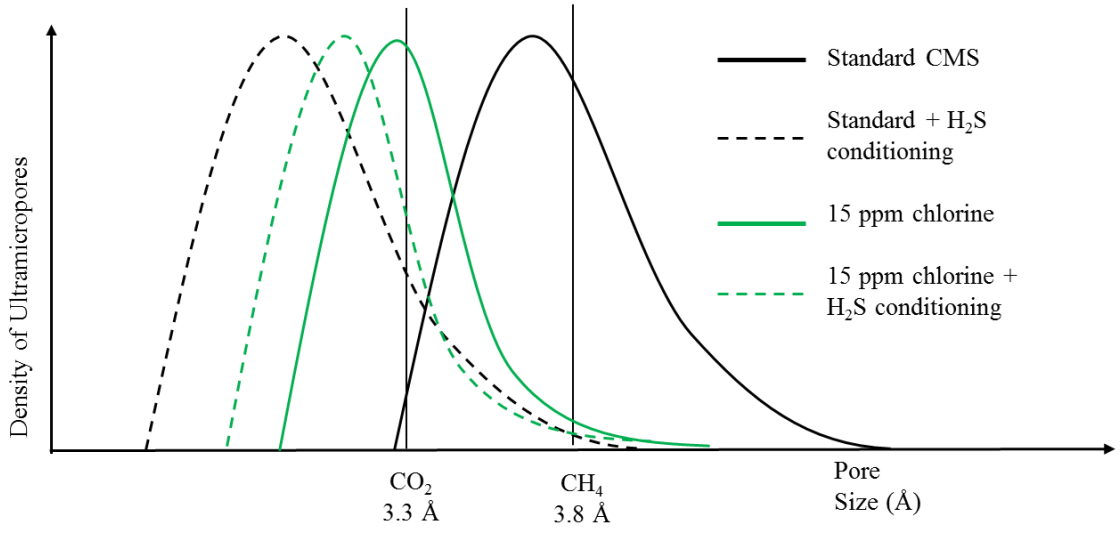

Figure 90: Envisioned change in Matrimid® CMS ultramicropore distribution due to chlorine fixation and H_2S conditioning

While this chlorine fixation/doping is hypothesized to lead to a tightening of the ultramicropores, reducing the average ultramicropore size. A chlorine atom is a little smaller than a sulfur atom (atomic radii of sulfur and chlorine are 1.04 Å vs. 0.99 Å respectively [111, 112]), so if as a preliminary hypothesis, the ultramicropore size after chlorine doping would still be bigger than that in case of sulfur chemisorption or reaction at those sites. This hypothesis led to a hope that higher permeances might result, with still attractive increases in selectivity of CMS hollow fiber membranes in the presence of H_2S. Clearly, the result did show some benefits with an ability to mitigate the deteriorating effect

of H_2S conditioning. On this basis, the chlorine fixation treatment was therefore extended to the more open CMS structure derived from 6FDA:BPDA-DAM, with the expectation that the large negative effects of H_2S on the 6FDA:BPDA-DAM derived CMS might be mitigated.

6.2 6FDA:BPDA-DAM

Based on the above basis, it was hoped that the end value of permeance after H_2S conditioning in this case would be high enough for industrial relevance and attractive selectivities would also be observed. With a vision of combining both the advantage of the anti-collapse V-treatment and inerting to H_2S, 6FDA:BPDA-DAM based CMS with and without V-treatment were explored.

6.2.1 Untreated

In case of non V-treated 6FDA:BPDA-DAM, the same idea was utilized to neutralize reactive ultramicropore edges that were open to H_2S. Specifically, 6FDA:BPDA-DAM fibers were pyrolyzed at 550 °C with 15 ppm Cl_2 in Argon. H_2S conditioning was done with an aggressive exposure for 72 hours of 150 psi pure H_2S with a vacuum on the permeate side. Following this exposure, as described in Chapter 5, CO_2 was purged for 72 hours at 50 °C through the membrane to sweep out H_2S. After this process, pure CO_2 and CH_4 permeation tests were pursued to probe the impact of the exposure. The results are shown in Figure 89 and Table 12.

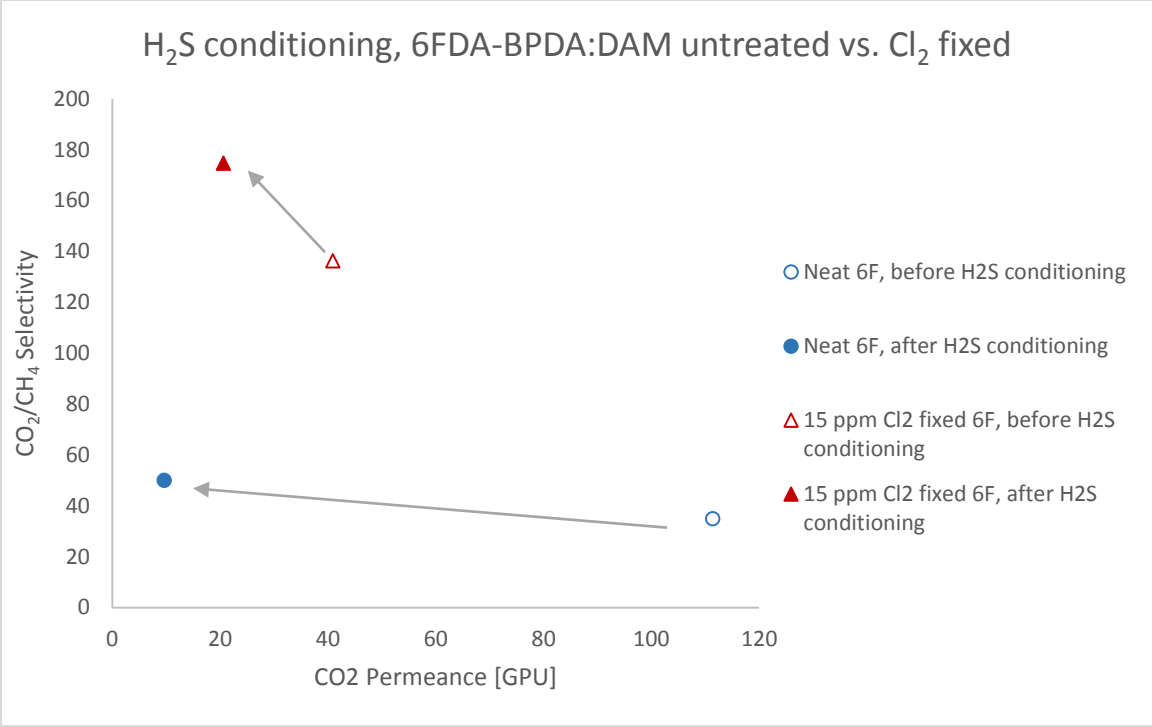

Figure 91: Influence of chlorine doping on the effect of H_2S conditioning in CMS derived from 6FDA:BPDA-DAM pyrolyzed at 550 °C, comparing 15 Cl_2 in Argon (red) with UHP Argon (blue) atmosphere. Tested with mixed gas (50% CO_2, 50% CH_4) at 100 psi feed pressure and 35 °C

Table 12: Permeance and selectivity of chlorine fixed CMS membrane before and after H_2S exposure via the pure gas conditioning protocol. Tested with mixed gas (20% H_2S, 20% CO_2, 50% CH_4) at 100 psi and 35 °C

	$(P/l)_{CO2}$ [GPU]	$(P/l)_{H2S}$ [GPU]	$\alpha_{(CO2/CH4)}$	$\alpha_{(H2S/CH4)}$
Before conditioning	40.63	-	127	-
After conditioning	19.2	2.02	174	18.4

Figure 91 shows that when the neat 6FDA:BPDA-DAM CMS was exposed to the pure H_2S at 150 psi, the CO_2 permeance dropped by 90% of its original value with some

increase in ideal CO_2/CH_4 selectivity. As expected, when the 550 °C 6FDA:BPDA-DAM derived CMS was exposed to chlorine during the pyrolysis, a lower pre-H_2S exposure CO_2 permeance and higher CO_2/CH_4 selectivity resulted. This was expected, since the chlorine atoms were expected to react at the ultramicropores, reducing their size. This change would (and did) lead to lower diffusion coefficients for CO_2 and CH_4, but higher CO_2/CH_4 selectivity - also as observed. When the chlorine "fixed" membrane was exposed to H_2S via the standard 150 psia pure gas H_2S conditioning protocol, the CO_2 permeance still dropped by 50% and the ideal CO_2/CH_4 selectivity increased even further after H_2S conditioning. While the CO_2 permeance of 20 GPU and ideal CO_2/CH_4 selectivity of 175 were greatly superior to the "unfixed" H_2S exposed CO_2 permeance of 9 GPU and CO_2/CH_4 selectivity of 50, the preferred outcome (no loss of CO_2 permeance from 40 GPU) was clearly not achieved. To provide the simplest possible explanation of these observations, while maintaining the same general framework used in this work, two possible additional suggestions were considered:

i. The 15 ppm Cl_2 in Argon pyrolysis atmosphere was inadequate to inert the existing reactive edges. In this case, non-inerted ultramicropore edges could still be open to attack by the aggressive H_2S (Figure 92). In this case, a higher Cl_2 concentration could potentially inert such edges, and if the smaller size of the chlorine atom versus sulfur could provide a smaller permeance loss with a still attractive CO_2/CH_4 selectivity less than 175 observed for the 15 ppm Cl_2 case.

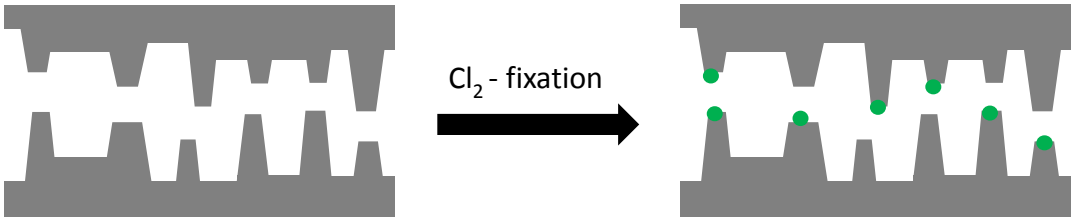

Intrinsic CMS pore structure

Ultramicropores stabilized by 'Cl_2-fixation'

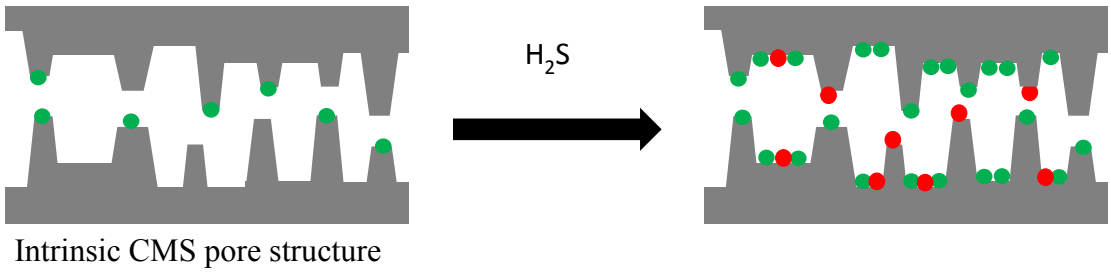

Figure 92: Chlorine fixation may leave some ultramicropores open for H_2S attack during conditioning

ii. The 50% drop in permeance could possibly be due to interaction of H_2S with chlorine moieties in the CMS, present in sufficiently large quantities that were not actually "inerted" as had been envisioned to occur. In fact, H_2S and chlorine do not typically react in gas phase, therefore if this case applied, it was expected to result from a strong physical interaction of some sort between them. If this second effect were dominant, higher Cl_2 doping of previously undoped edges would tend to lead to further CO_2 permeance reductions – with difficult to predict changes in CO_2/CH_4 selectivity.

To test these hypotheses, a higher and a lower Cl_2 concentration during the pyrolysis was explored, still without any V-treatment considered. An additional control experiment was done to check whether a similar tendency was seen with O_2 doped CMS membranes. With this in mind, H_2S conditioning was performed on 30 ppm O_2 doped CMS from 6FDA:BPDA-DAM pyrolyzed at 550 °C. The comparison of performance of O_2 doped membrane vs. Cl_2 fixed membrane to the H_2S is shown in Figure 93.

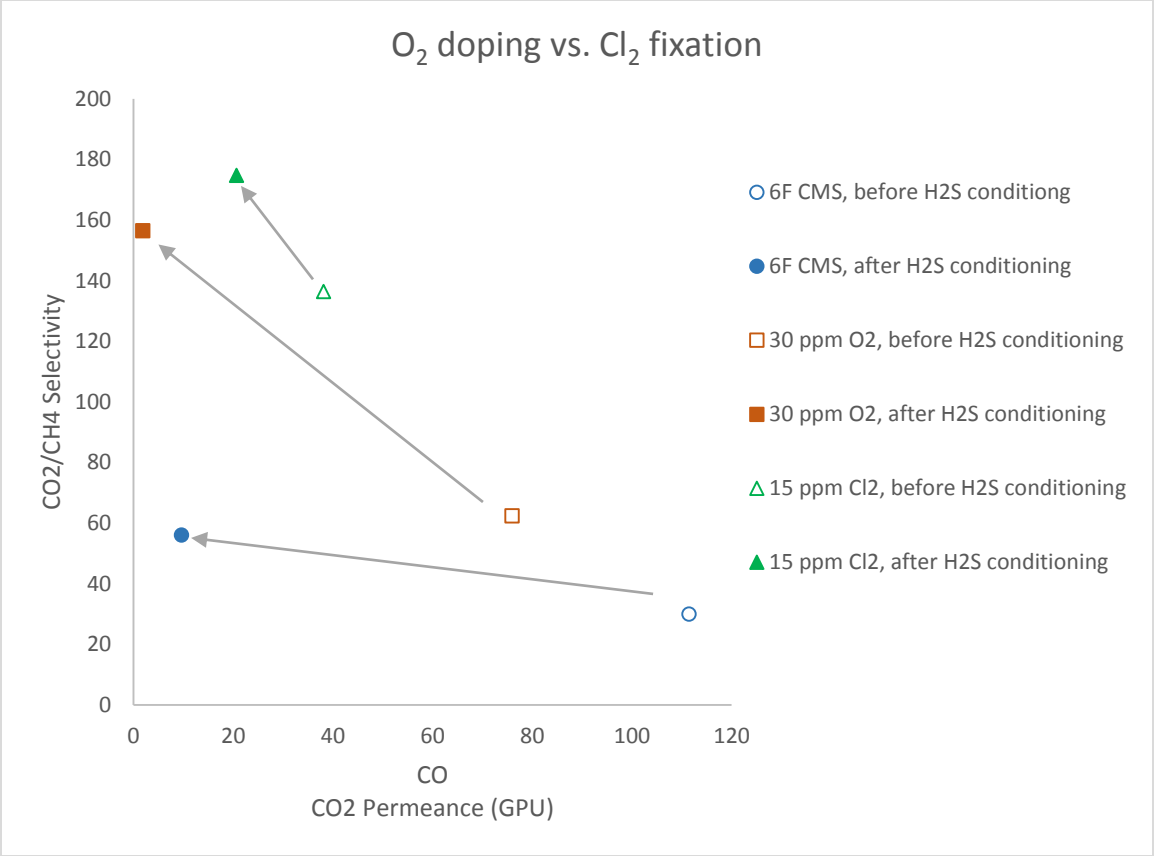

Figure 93: Comparison of H_2S conditioning on O_2 doped fibers vs. chlorine fixed CMS membranes pyrolyzed from 6FDA:BPDA-DAM at 550 °C. Tested with mixed gas (50% CO_2, 50% CH_4) at 100 psi and 35 °C

After H_2S conditioning of O_2 doped fibers, the permeance of the membranes was almost entirely lost and the selectivity increased. These results suggest that indeed, a "double-doping", active in the presence of O_2 doped site is likely (as was noted in the Matrimid® derived CMS.) This means that H_2S conditioning made the oxygen doped membrane "double-doped" and therefore effectively plugged the membrane to gas flow.

The cartoon of what is envisioned to happen in the case of O_2 doping is shown in Figure 94.

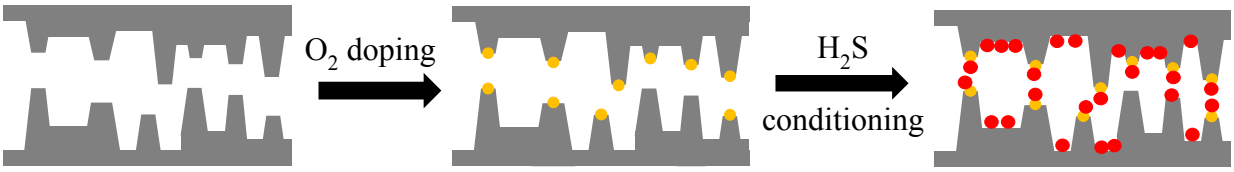

Figure 94: Schematic of oxygen doped 6FDA:BPDA-DAM CMS undergoing H_2S conditioning to forma a doubly doped fiber

This double doping shifts the ultramicropore distribution so that the permeance decreases and selectivity increases after H_2S conditioning.

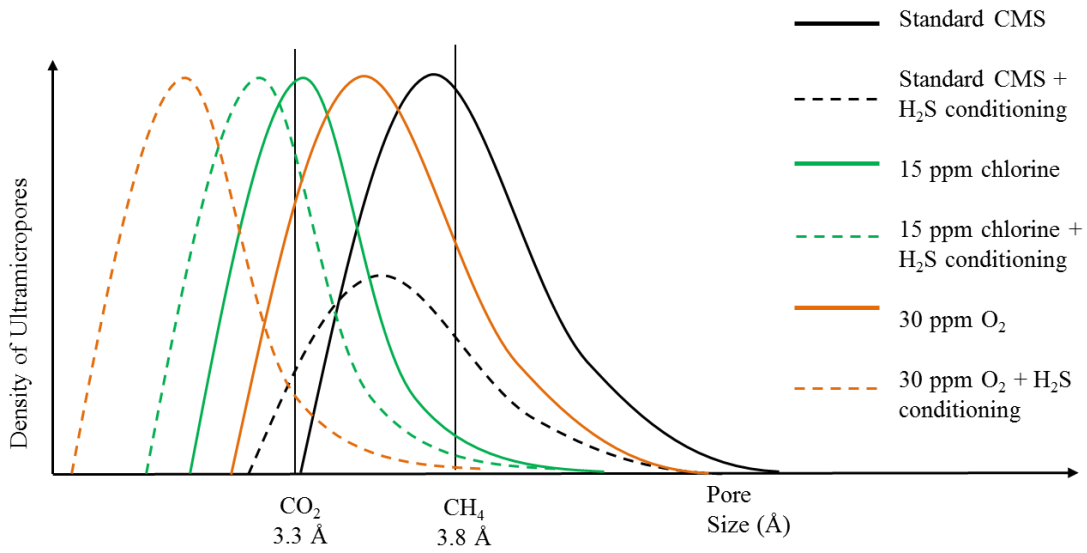

Figure 95: Envisioned change in ultramicropore distribution with H_2S conditioning of standard CMS sample (pyrolyzed in UHP Ar), chlorine fixed sample (pyrolyzed with 15 ppm Cl_2 in Ar) and oxygen doped sample (pyrolyzed with 30 ppm O_2 in Ar)

It is expected that with optimizing the chlorine fixation, the ultramicropores could be tuned into the "sweet spot" where H_2S will not condition the membrane.

6.2.1.1 Varying the chlorine concentration

In an effort to determine the amount of chlorine that is adequate to neutralize most ultra micropores without overdoping the membrane, 5 ppm and 30 ppm chlorine in Argon were chosen for the optimization. These concentrations were selected as they are comparable to the oxygen doping concentration optimization done by Kiyono [72]. In the O_2 doping experiments we had seen that 30 ppm O_2 in Ar was optimum for a good selectivity with reasonable permeance, while 50 ppm O_2 in Argon caused over-doping. The aim was to obtain the most optimal gas permeation results, while preventing H_2S conditioning.

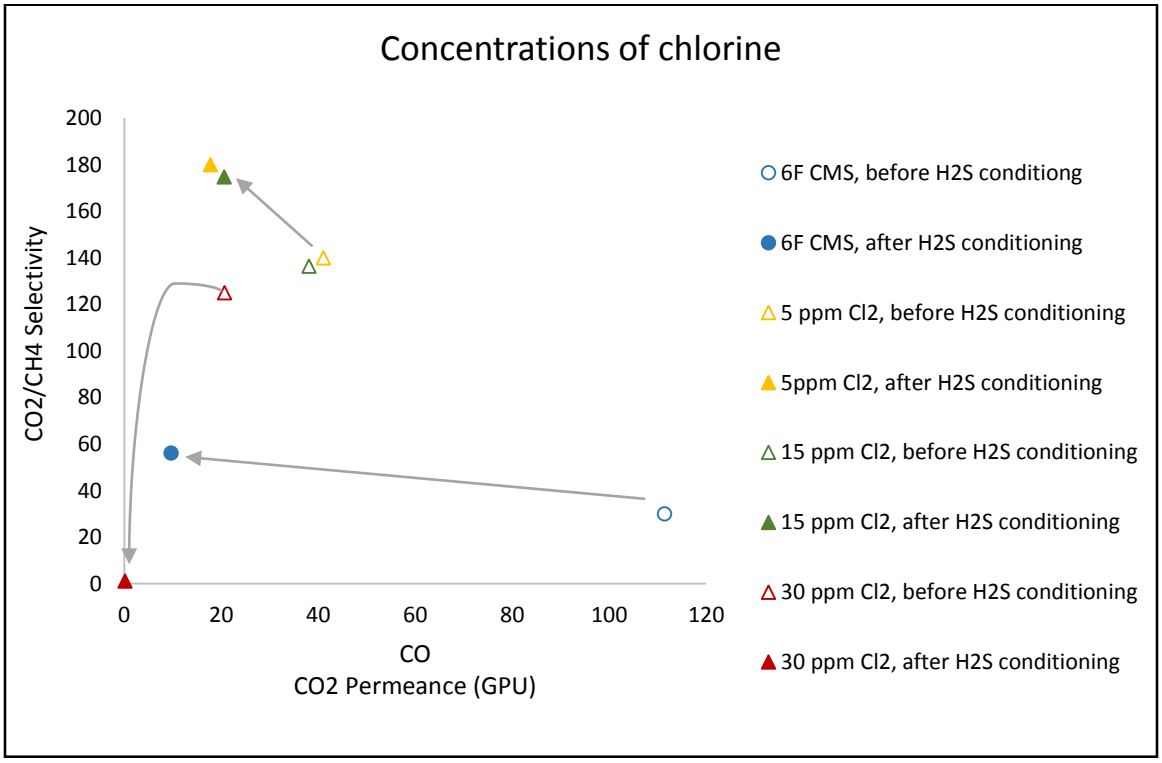

Figure 96: Comparison of CO_2 permeance and CO_2/CH_4 selectivities of CMS membranes derived from 6FDA:BPDA-DAM pyrolyzed at 550 °C, in different concentrations of Cl_2 in Argon atmosphere. Tested with mixed gas (50% CO_2, 50% CH_4) at 100 psi and 35 °C

Figure 96 shows the comparison of mixed gas performance of different concentrations of chlorine in the pyrolysis atmosphere. The open markers denote performance of CMS fiber before H_2S exposure, and the solid markers denote performance of fibers after H_2S conditioning. It is seen that 5 ppm and 15 ppm chlorine fixed fibers show similar performances before and after H_2S conditioning. However, they still lose about 50% of the permeance based after H_2S conditioning. This is also different from the oxygen doping, since unlike the H_2S conditioning of oxygen doped CMS, a huge loss in permeance is seen in chlorine fixation. For the fibers pyrolyzed with 30 ppm of chlorine, the starting permeance is low as expected. The dramatic and highly undesirable loss in both CO_2 permeance and CO_2/CH_4 selectivity for the 30 ppm chlorine treated sample after H_2S conditioning was surprising, but it was *repeated and found to be correct*. Indeed, all these experiments were repeated to confirm the results within experimental error.

It was hoped that the chlorine fixation would stop H_2S conditioning in the beginning of this project; however, the H_2S conditioning clearly still affects the permeances of chlorine treated fibers, regardless of the concentration of chlorine used. This meant that the H_2S is still interacting with the chlorine treated fibers. These facts notwithstanding, even the losses in sorption coefficients for the "un-fixed" samples were small (1.2X drop) vs. the close to 6X drop in permeance, so most of the effects of H_2S are reflected by changes in the ultramicropores which control diffusion and diffusion selectivity.

To consolidate the state of understanding, based on the preceding results, a preliminary summary is useful. The ultramicropore structure is envisioned to change as follows. At low concentrations of chlorine fixation (5 ppm and 15 ppm), only the largest ultramicropores are affected. Such a change affects, as seen by the diffusion of both CO_2

and CH_4, but the change is more drastic for CH_4 and hence an increase is seen in the selectivity. As the concentration of chlorine in the pyrolysis atmosphere is increased to 30 ppm, small ultramicropores may also start to be closed down. When this highly closed CMS structure is exposed to H_2S conditioning, it becomes blocked by the H_2S by an interaction (explored in Section 6.4), reducing both the permeance and the selectivity through the membrane. It is believed that the high chlorine + H_2S exposed case leaves only a miniscule number of low selectivity paths open.

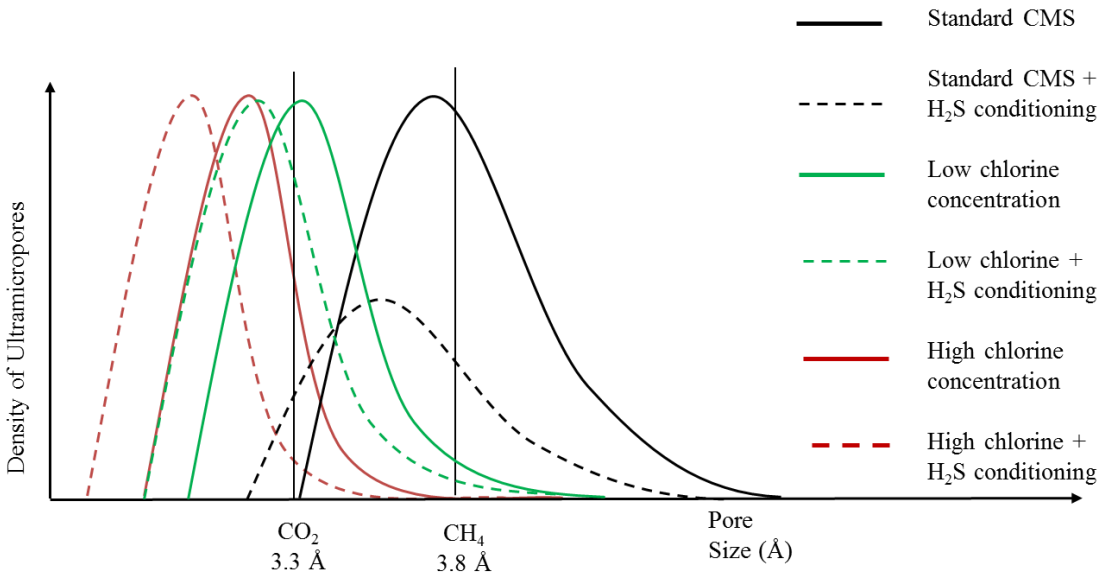

Figure 97: Envisioned change in ultramicropore distribution with chlorine fixation and H_2S conditioning

Also note that most of the chlorine fixed CMS fibers end up with similar final permeance after H_2S conditioning as the ones with no chlorine fixation; however, *much higher CO_2/CH_4 selectivity is seen for the Cl_2 treated samples*. These facts suggest that additional work is needed at still lower Cl_2 doping conditions to optimize performance of

CMS materials in the presence of aggressive H_2S containing feeds. This work at sub-5 ppm levels of CO_2 and/or O_2 will be the topic of on-going work supported by Shell. To guide such work, however, additional checks of the central basis of the above arguments was felt to be wise. This work comprises the remaining of the discussion this chapter. Specifically, as discussed for the case of Matrimid®-derived CMS, changes in sorption for CO_2 and CH_4 due to H_2S exposure was expected to be much smaller than the orders of magnitude change in permeance. Proving this would verify that most of the H_2S effects are due to effects on the ultramicropores, which has been the basis of the preceding arguments. This is possibly due to the chlorine not entirely reacting with the CMS membrane, leaving open at least some spots for H_2S to come in a react with.

6.2.1.2 Sorption

A sorption experiment was done to verify whether the H_2S affected the sorption capacity of the CMS membranes, as in the case of neat CMS from 6FDA:BPDA-DAM. The equilibrium sorption test was performed using the same procedure as in Chapter 5, using sorption decay set up to measure CO_2 and CH_4 sorption isotherms before and after H_2S conditioning of chlorine "fixed" CMS membranes, reported in Figure 98. It was seen that unlike the case of neat CMS, Cl_2 stops the 6FDA:BPDA-DAM CMS from losing sorption capacity in the presence of H_2S.

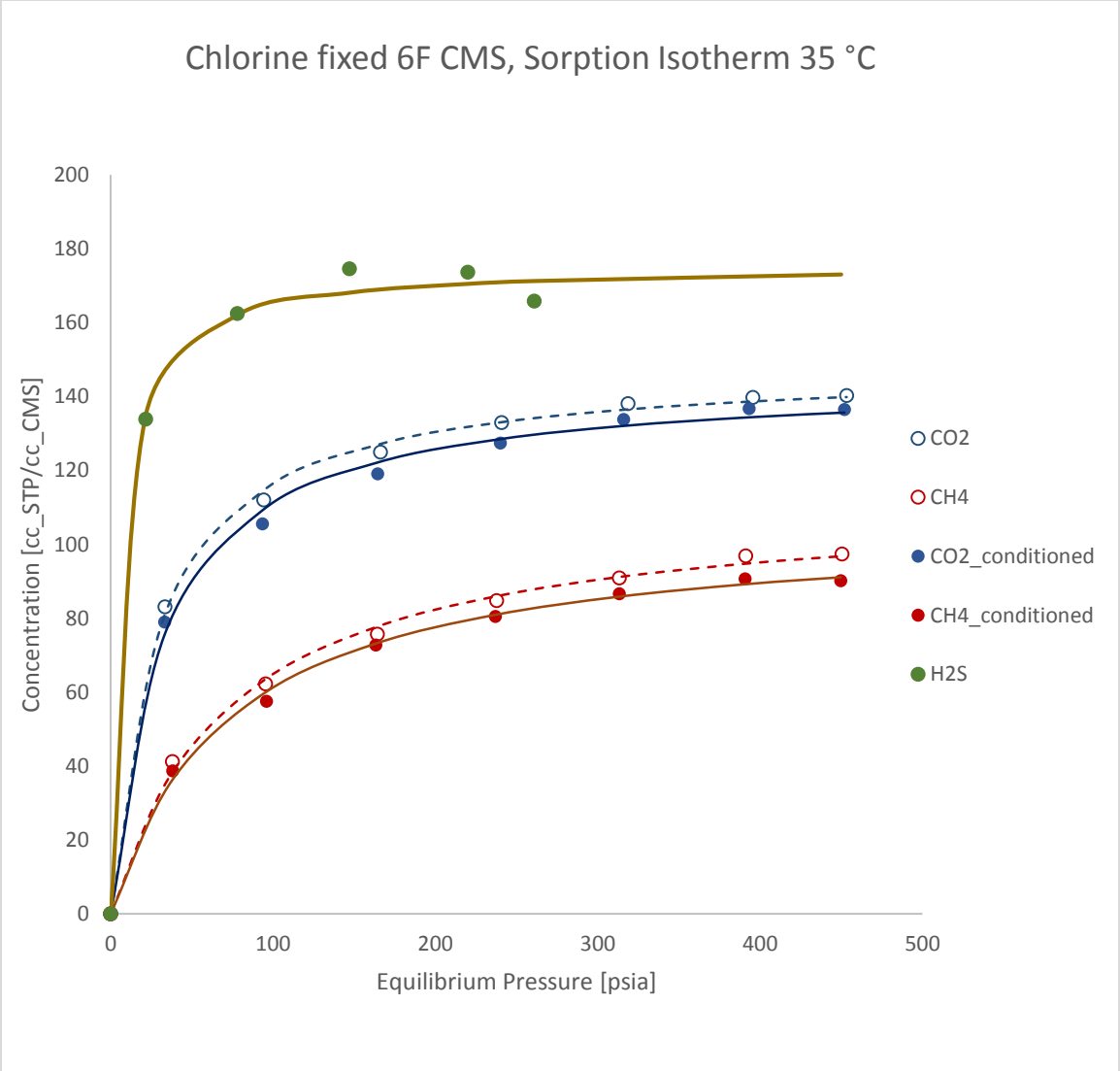

Figure 98: Sorption isotherms of CO_2 and CH_4 before and after H_2S conditioning on 6FDA:BPDA-DAM fibers pyrolyzed with 15 ppm Cl_2 at 550 °C. Tests performed with pure gases at 35 °C

The hole filling capacity and affinity constants of the gases, summarized in the Table 13, show that the sorption properties of the constants don't appreciably change after H_2S conditioning is performed.

Table 13: Langmuir sorption parameters for CMS derived from 6FDA:BPDA-DAM, pyrolyzed at 550 °C under 15 ppm Cl_2 in Argon. Tests performed at 35 °C

Gas	C'_H cc(STP)/cc(CMS)	b $psia^{-1}$
Before H_2S conditioning		
CO_2	148.4	0.036
CH_4	112.7	0.014
After H_2S conditioning		
CO_2	146.9	0.033
CH_4	109.87	0.014
H_2S	175.523	0.154

These results suggest that H_2S conditioning, indeed, has only secondary effects on the gas sorption character when Cl_2 is or is not present in the structure. These isotherms are better fitted to Langmuir model with ($R^2 \sim 0.99$) than the ones without chlorine fixation, perhaps indicating that there are fewer small spaces between the strands of the carbon chains for the molecules to sorb into. This may be possible due to the more bulky chlorines partially blocking the ultramicropores between these strands; however, at this point, the key information is that the Cl_2, O_2 and H_2S effects are primarily active in the ultramicropore domains.

Sorption selectivity and mobility selectivity values of the Cl_2 fixed CMS membranes after H_2S conditioning were calculated using Eq. (8) and are provided in Table 14. Based on these numbers, the CO_2/CH_4 mobility selectivity is much higher than CMS

pyrolyzed without chlorine (compare with values from Table 11), while the CO_2/CH_4 sorption selectivity is lower. Similarly, H_2S/CH_4 mobility selectivity is higher than those found in glassy polymers as well as those compared to CMS pyrolyzed without chlorine (compare with values from Table 11), and sorption selectivity is about the same.

Table 14: Sorption and mobility selectivity in 6FDA:BPDA-DAM derived Cl_2 fixed CMS hollow fibers at 35°C. Values are calculated from pure gas permeation and sorption data

Conditioning	S_{CO2}/S_{CH4}	D_{CO2}/D_{CH4}	S_{H2S}/S_{CH4}	D_{H2S}/D_{CH4}
Before	1.77 ± 0.2	75.27 ± 5.4	-	-
After	1.76 ± 0.1	94.78 ± 7.5	2.56 ± 0.2	7.42 ± 1.0

The fact that mobility selectivity is higher for both CO_2/CH_4 and H_2S/CH_4 after conditioning, in addition to lowered permeance through chlorine fixed CMS membrane compared to CMS membrane without chlorine fixation, further supports the hypothesis that the chlorine is doped in the ultramicropores of the CMS membranes.

6.2.2 V-treated

To also prepare the way for later studies, the Cl_2 fixing/doping work was extended to V-treated 6FDA:BPDA-DAM derived CMS fibers. The expectation was for the ending permeance to be higher than what is seen for untreated CMS by suppressing the support layer collapse. Based on work in Chapter 4, 50% V-treated 6FDA:BPDA-DAM fibers were pyrolyzed with 15 ppm Cl_2 at 550 °C. Is was expected that the starting CO_2 permeance would be twice as high as the untreated CMS fibers before H_2S conditioning. The permeation properties were measured before and after exposure to H_2S, and are

summarized in Figure 99. For comparison, permeation properties of CMS from 6FDA:BPDA-DAM pyrolyzed with UHP Argon and with 15 ppm Cl_2 are shown.

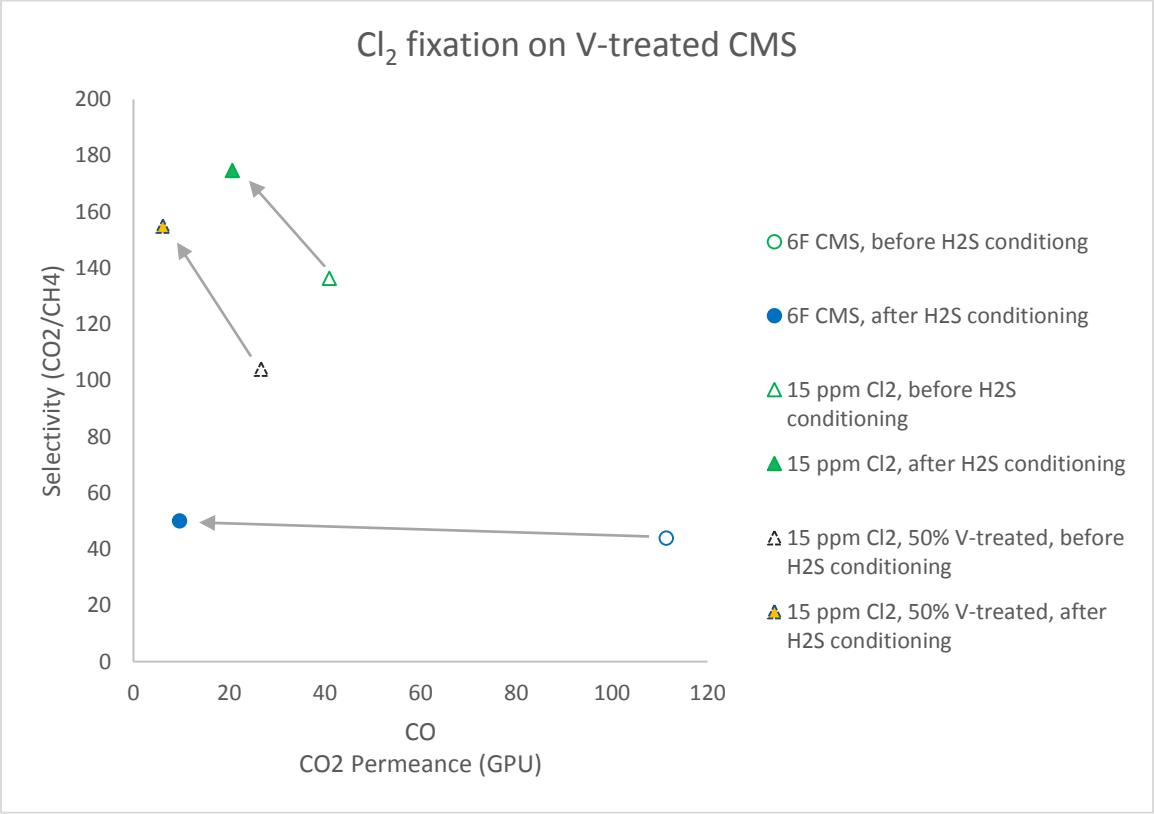

Figure 99: Permeation performance of 50% V-treated 6FDA:BPDA-DAM CMS fibers pyrolyzed with 15 ppm Cl_2 in Argon at 550 °C. Tested with mixed gas (50% CO_2, 50% CH_4) at 100 psi and 35 °C

Table 15: Permeance and selectivity of chlorine fixed CMS membrane after H_2S exposure via the pure gas conditioning protocol. Tested with mixed gas (20% H_2S, 20% CO_2, 50% CH_4) at 100 psi and 35 °C

	$(P/l)_{CO2}$ [GPU]	$(P/l)_{H2S}$ [GPU]	$\alpha_{(CO2/CH4)}$	$\alpha_{(H2S/CH4)}$
Before conditioning	26.64	-	104	-
After conditioning	5.9	0.73	187	22.81

Again unexpectedly, the starting permeance of 50% V-treated fibers pyrolyzed in 15 ppm Cl_2 was *even lower* than the non V-treated CMS under 15 ppm Cl_2. This outcome could possibly be due to two effects: 1) the chlorine hinders the function of V-treatment, thereby still allowing the porous substructure of the hollow fiber to collapse, or, 2) The chlorine reacts with the silica gel to form an additional resistance that leads to lowered permeance and selectivity. To determine if the chlorine fixation was hindering with collapse of the porous substructure, SEM images were examined to observe the morphology and compared to CMS fibers prepared without any V-treatment.

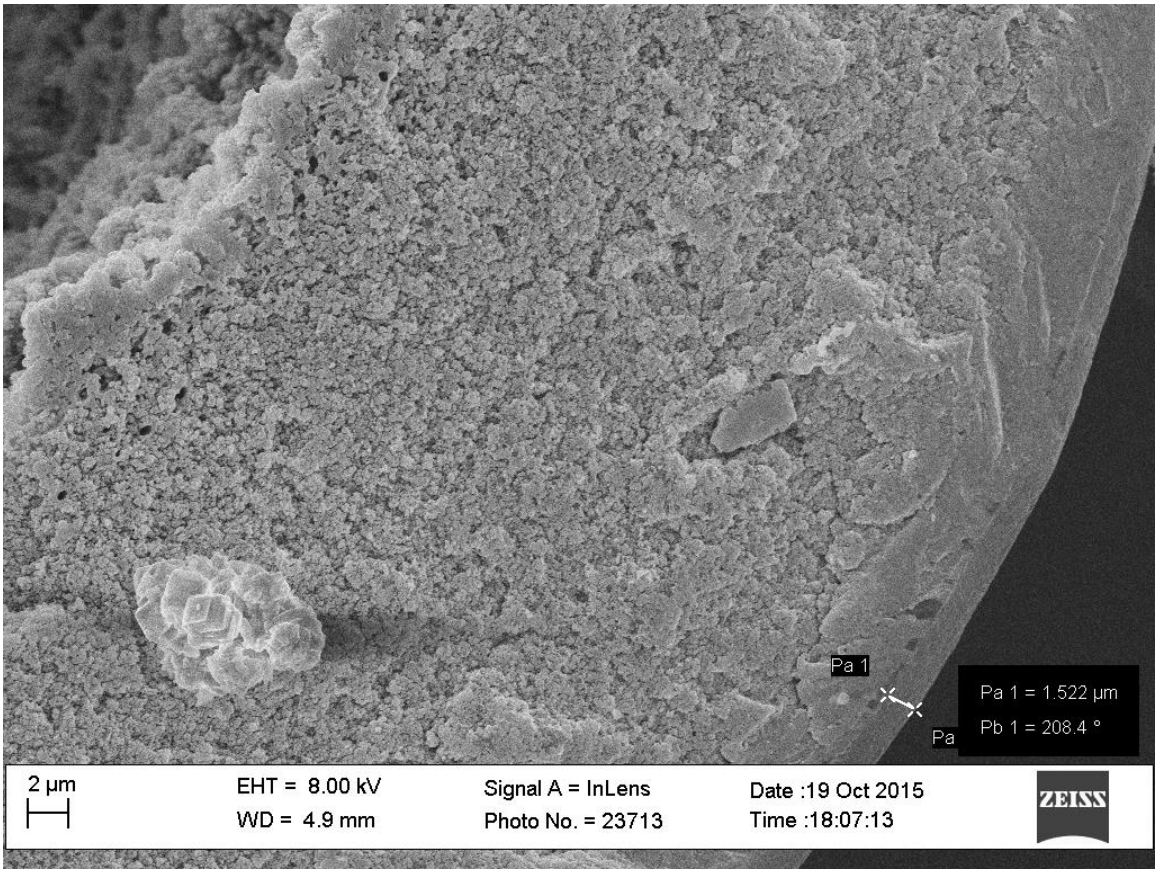

Figure 100: SEM image of 50% V-treated 6FDA:BPDA-DAM CMS fibers pyrolyzed with 15 ppm Cl_2 in Argon at 550 °C. The fiber shows intact porous substructure, indicating that the V-treatment still works in the presence of chlorine.

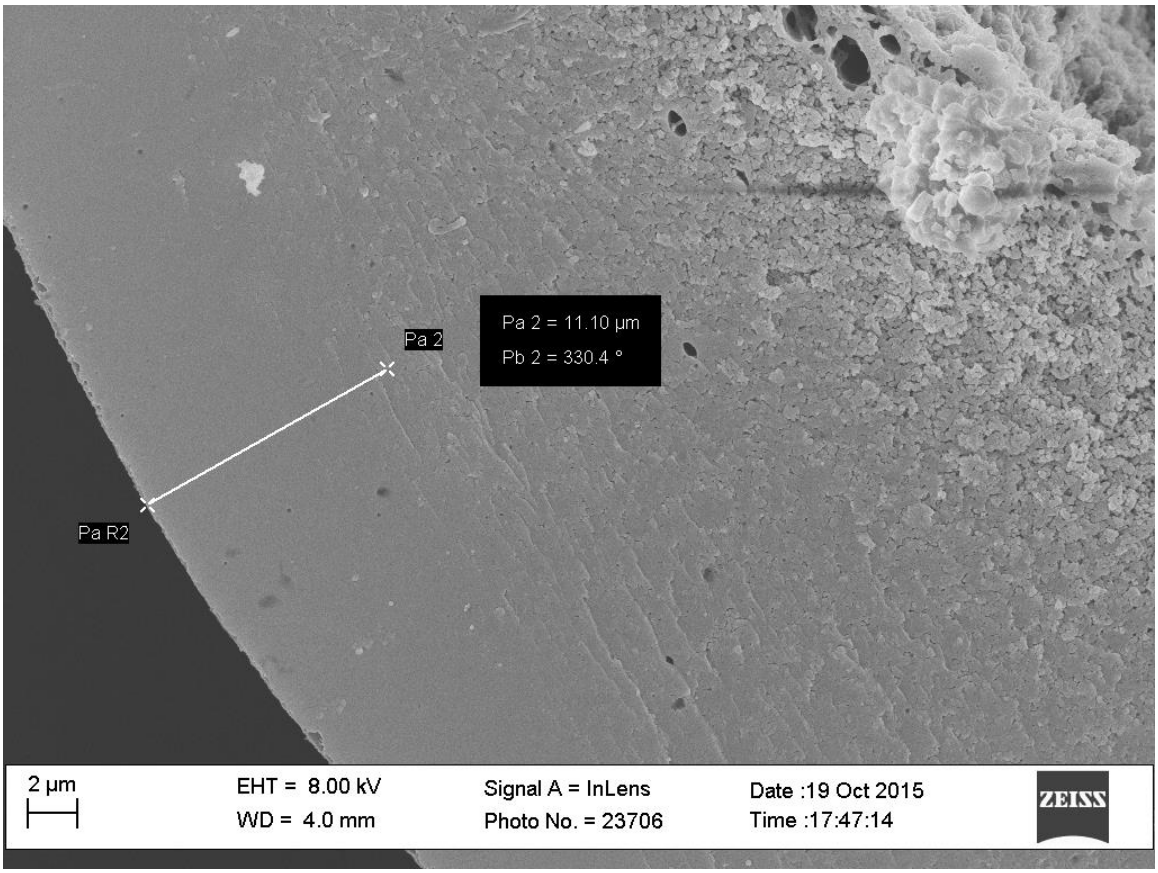

Figure 101: SEM image of 6FDA:BPDA-DAM CMS fibers without V-treatment pyrolyzed with 15 ppm Cl_2 in Argon at 550 °C. The fiber shows collapsed porous substructure.

The morphology of 50% V-treated CMS hollow fiber pyrolyzed in presence of chlorine showed that the substructure *had not collapsed*. The skin layer was thin as expected, with a separation thickness of ~1.6 µm (Figure 100) as compared to the skin thickness of ~11 microns for untreated CMS fibers (Figure 101). This means that the chlorine does not interfere with the V-treatment mechanism.

Since the CO_2 permeance observed through this membrane is less than half of what is expected at this skin thickness, it appears that the Cl_2 is likely to be interacting with the organo-silica material present after pyrolysis. To understand this, we return to the structure

of VTMS and the highly porous organo-silica gel structure left after the pyrolysis, previously mentioned in Figure 45.

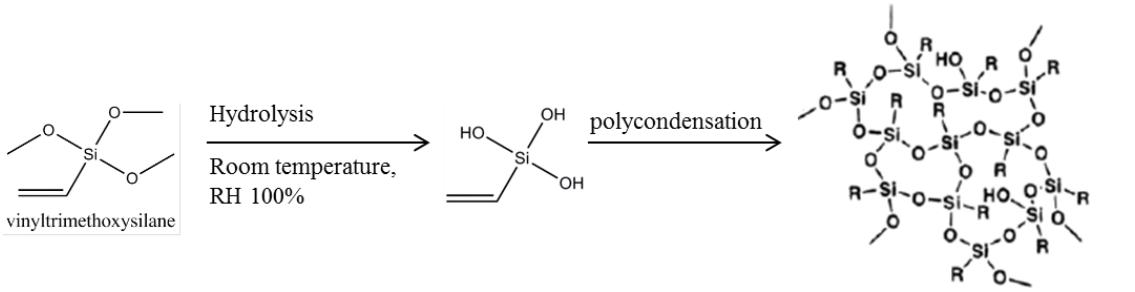

The organo-silica gel retains the vinyl groups from the VTMS, which Bhuwania showed helps give useful flexibility. In fact, however, the chlorine present in the pyrolysis atmosphere is free to react with the remaining vinyl part of the sol gel, possibly making a vinyl chloride like compound. While this does not affect effectiveness of the sol gel to provide support to the pores of the substructure, it could certainly affect the gas transport through the membrane. There is no difference seen in the flexibility of the resultant fibers, but the undesirable loss in permeance certainly requires attention. It may be, in fact, that Cl_2 or O_2 doping at lower levels mentioned as desirable to optimize CMS permeance and selectivity in the context of Figure 93 – Figure 96 may also minimize the impact on the V-treatment residual silica layer.

6.3 Characterization

As a final issue, while the effect of chlorine was definitely seen in the permeation experiments, it was felt to also be useful to show that the chlorine was actually present and bonded to the CMS. Clearly the ppm levels of chlorine used in all the chlorine fixation experiments made bonded chlorine analysis challenging. Such a low concentration made it both difficult to detect the presence of chlorine and also to see the bonding nature through characterization techniques. In any case, some techniques were attempted to characterize the presence of chlorine in the CMS membranes.

TPD: A thermally programmed desorption was conducted to see whether the chlorine reacted at the carbon comes off at high temperatures. A plot of the TCD signal from the thermal conductivity detector versus the temperature of the sample is shown in Figure 102.

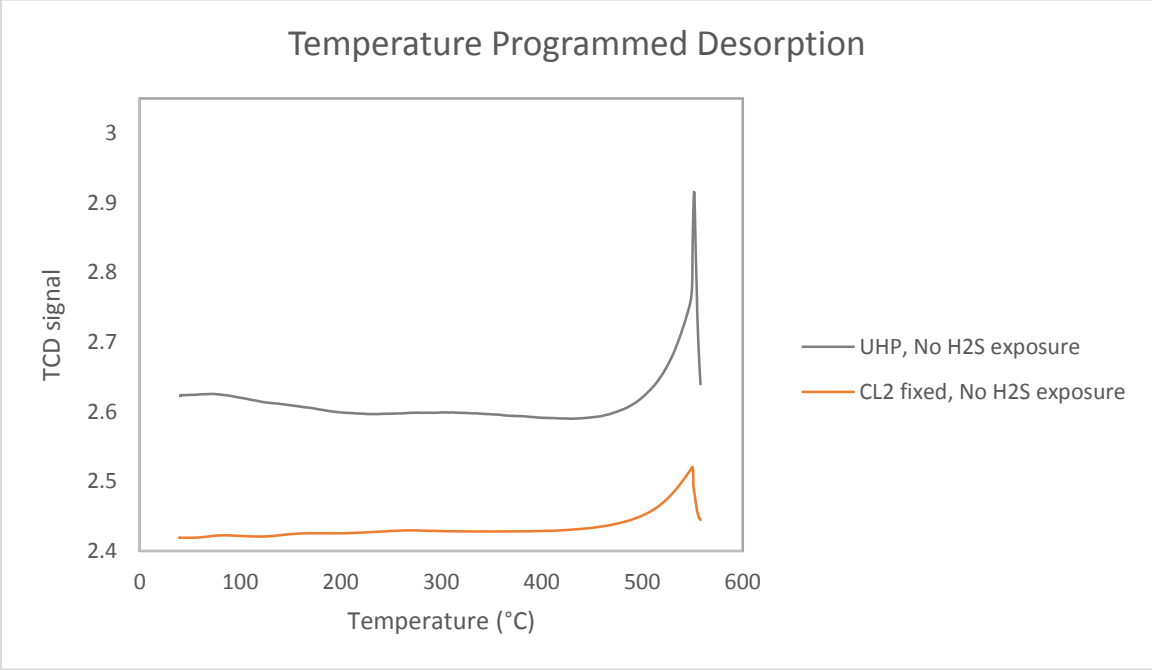

Figure 102: Thermally programmed desorption to verify that no chlorine or chlorine compounds decompose from the carbon structure with heating up to the temperature of its original formation (550 °C). Two samples being compared are CMS pyrolyzed with UHP Ar (gray) and 5 ppm Cl_2 in Argon

The above plot shows deviation of thermal conductivity signal from that of the carrier gas on the x-axis, versus the temperature at which a species is evolved. Both the samples show that no species of gases were evolved when the CMS samples were heated from room temperature until close to the final pyrolysis temperature, 550 °C in this case. The peak seen at about 550 °C was from the evolution of pyrolysis products at that temperature, which is known to be ongoing as temperature rises to the original temperature of pyrolysis, and this evolution is observed in both the samples. This makes sense, since the CMS sample can still pyrolyze at this final temperature. The TPD is not calibrated for pyrolysis by products, therefore the figure should not be interpreted quantitatively. It is

inferred from the plot that the reacted chlorine, as expected, is very stable throughout the TPD, confirming what is found in the literature.

FTIR: Two CMS samples from 6FDA:BPDA-DAM CMS fibers pyrolyzed at 550 °C were analyzed with FTIR: one pyrolyzed with no chlorine and the other with 15 ppm of chlorine. Since this thesis is considering work done on hollow fibers, it was necessary to crush the fibers and form a KBr pellet of the CMS fibers. The comparison of FTIR spectra looked as follows:

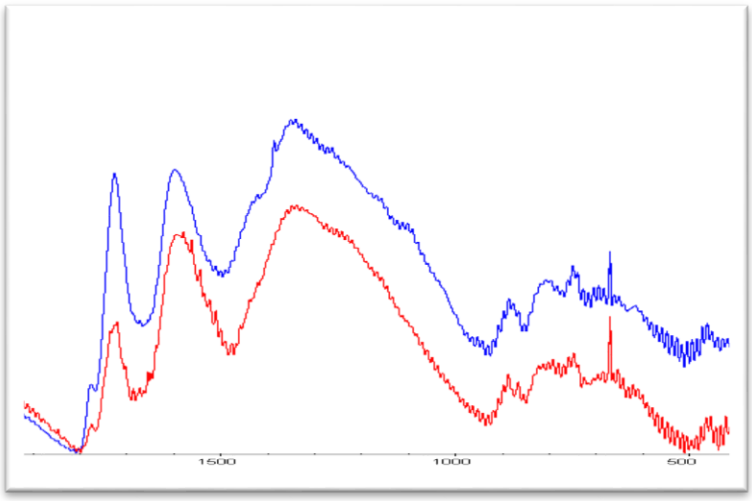

Figure 103: FTIR spectra of CMS samples 6FDA:BPDA-DAM CMS fibers pyrolyzed at 550 °C with 15 ppm chlorine fixation (blue) and without (red)

If the chlorine was reacting extensively with the aromatic carbon, an extra C-Cl peak would be expected at around 743 cm^{-1} wavenumber; however, it is not really possible to see any difference between the spectra of the two samples. There are many broad peaks in the spectrum and the region of interest has many overlapping peaks. Therefore FTIR

was inconclusive in proving or disproving the reaction of chlorine with the carbon structure.

NMR: Solid state NMR spectra were measured for three samples to compare whether chlorine bonding could be detected. CMS hollow fiber membranes were prepared at 550 °C under UHP Argon and 15 ppm chlorine in Argon. The CMS hollow fiber samples were crushed into powder form for ^{13}C spectra and a spectrum was also obtained for 6FDA:BPDA-DAM polymer precursor to try to determine any shifts in peaks.

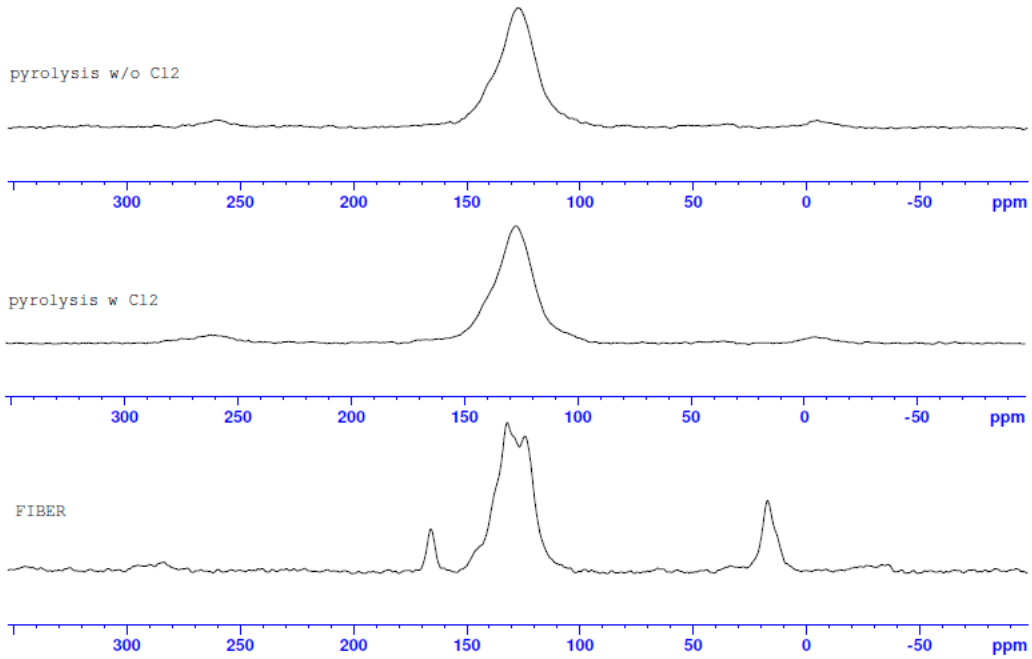

Figure 104: ^{13}C solid state NMR spectra for neat CMS derived from 6FDA:BPDA-DAM pyrolyzed at 550 °C with UHP Argon (top), chlorine fixed CMS pyrolized at 550 °C with 15 ppm in Argon (middle) and pure polymer precursor from 6FDA:BPDA-DAM

The NMR spectra shown in Figure 104 do not indicate any strong difference in the spectrum for CMS with chlorine when compared to CMS without chlorine. This lack of difference is attributed to the low concentration of chlorine that is present in the sample itself. We expect the sample to have ppm level of chlorine, and this amount is not enough to be manifested in solid state NMR.

XPS: This is a surface technique that analyzes the top few nanometers of the surface of a structure, as well as the bonding state of certain elements in the structure. When XPS was performed on CMS pyrolyzed with 15 ppm chlorine, a survey scan that was obtained to show all elements detected by the XPS.

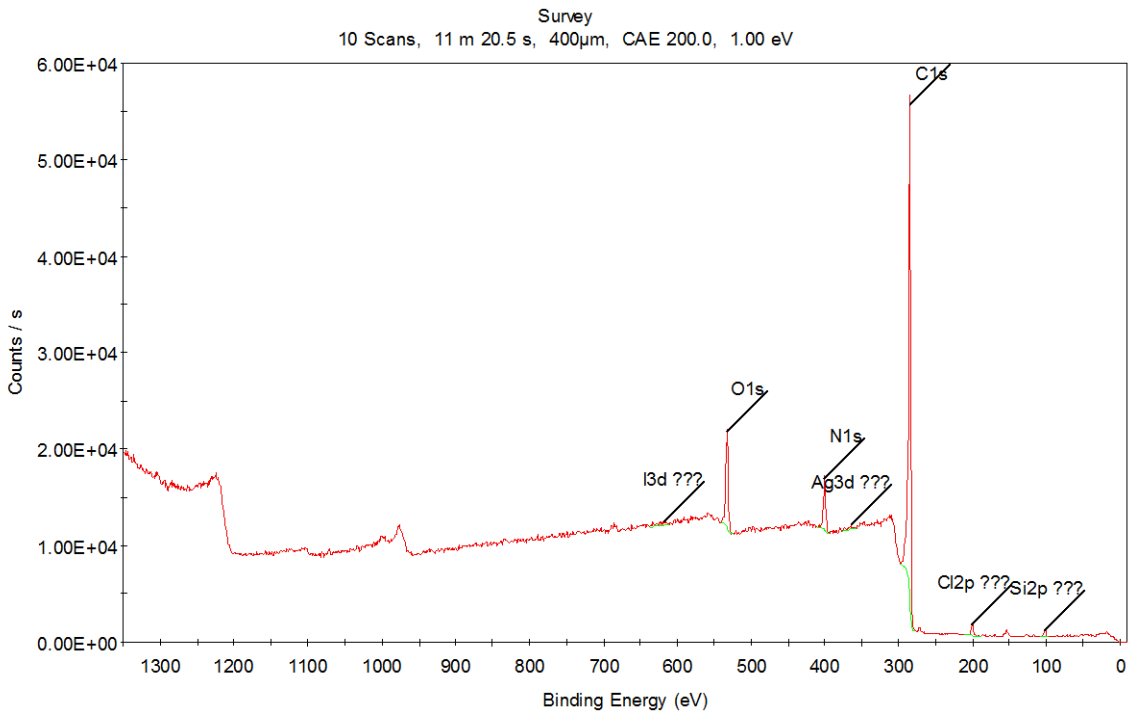

Figure 105: XPS spectroscopy - survey scan of CMS hollow fiber derived from 6FDA:BPDA-DAM pyrolyzed in 15 ppm Cl_2 in Argon at 550 °C

The survey scan in Figure 105 clearly showed large peaks for carbon, nitrogen and oxygen, and a small chlorine peak. A separate chlorine scan was done to positively identify the peak of chlorine. Since this is a surface technique, it was analyzed on both CMS asymmetric hollow fiber membranes as well as powdered CMS sample pyrolyzed in the presence of chlorine.

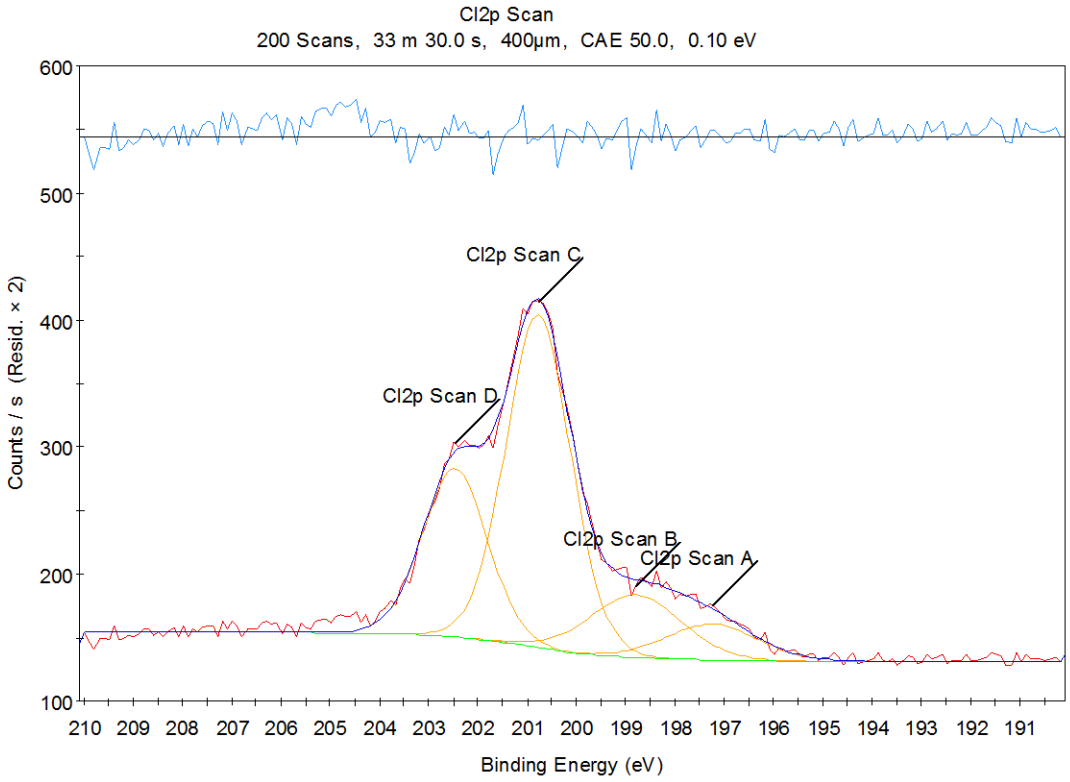

Figure 106: XPS spectroscopy - chlorine scan for CMS hollow fiber derived from 6FDA:BPDA-DAM pyrolyzed in 15 ppm chlorine in Argon at 550 °C

The plot in Figure 106 has been acquired with 200 scans, flood gun on and 400 micron area. It can be seen that there is an apparent chlorine peak at 200.1 eV, which corresponds to the chlorine 2p binding energy which shows Cl2p spin orbital splitting. A deconvolution of peaks was done to fit the $Cl2p_{3/2}$ and $Cl2p_{1/2}$ peaks at 200.77 eV and 202.46 eV (with $\Delta = 1.69$ eV). These correspond to Cl atoms covalently bonded to sp2 and sp3 carbons [109]. The other set of peaks fitted at 197.24 eV and 198.8 eV correspond to Cl2p peaks of elemental chlorine with orbital splitting for chloride.

TPD for H_2S: A temperature programmed desorption was carried out on H_2S conditioned CMS samples that were pyrolyzed in chlorine atmosphere. These samples had seen 150 psi of H_2S for 3 days, and then were vacuum was pulled to desorb any unreacted H_2S for 3 days at 150 °C before the TPD was performed. The TPD used recorded the thermal conductivity of a desorbed molecule form the sample of CMS. The carrier gas used in this case was Helium, since it has a significantly different thermal conductivity than H_2S.

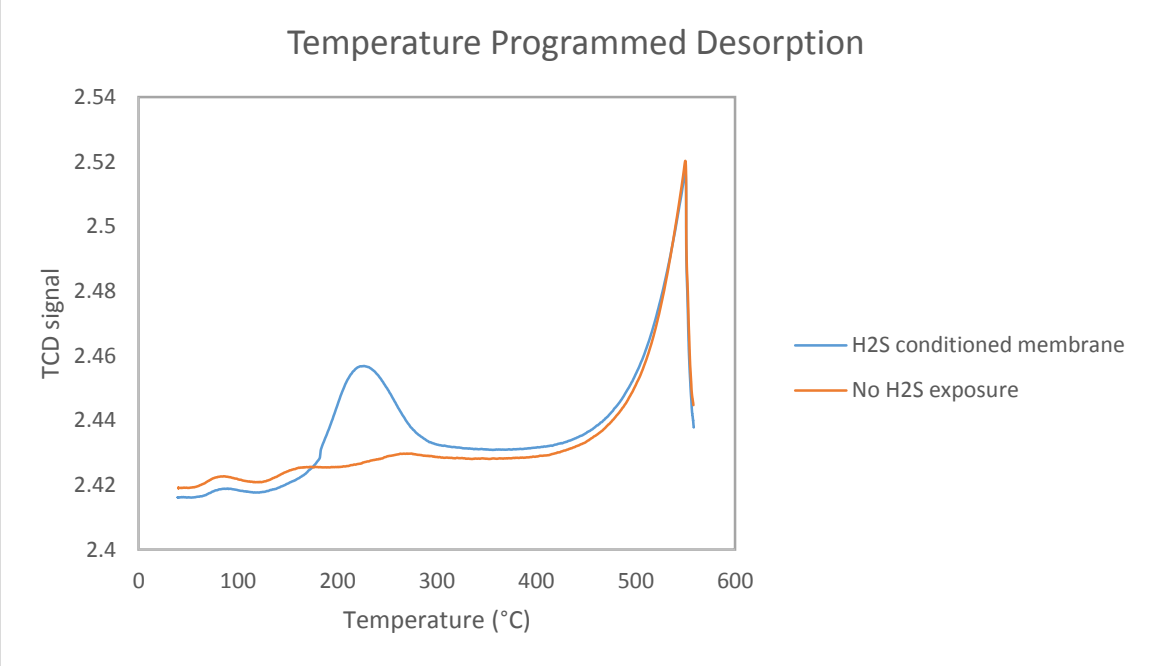

Figure 107: Thermally programmed desorption, showing evolution of H_2S in the H_2S conditioned sample (blue), compared to no evolution of the gas in the unconditioned sample (orange). Both membranes prepared with 6FDA:BPDA-DAM pyrolyzed with 15 ppm Cl_2 in Argon at 550 °C.

A peak is seen at 226 °C in the sample that was conditioned with H_2S, indicating that a gas species is evolving from the sample. While this looks similar to Figure 85 showing a gas evolving from a CMS membrane without chlorine fixation, it should be

noted that in this case the gas species evolves at a lower temperature vs. that seen at 252.2 °C in Figure 85. The evolved gas was tested for the presence of H_2S using lead acetate strips [113, 114], and the results are shown in Figure 108. TPD of the unconditioned sample did not change color of the lead acetate strip, while the H_2S conditioned sample turned the lead acetate strip black clearly indicating the evolution of H_2S gas.

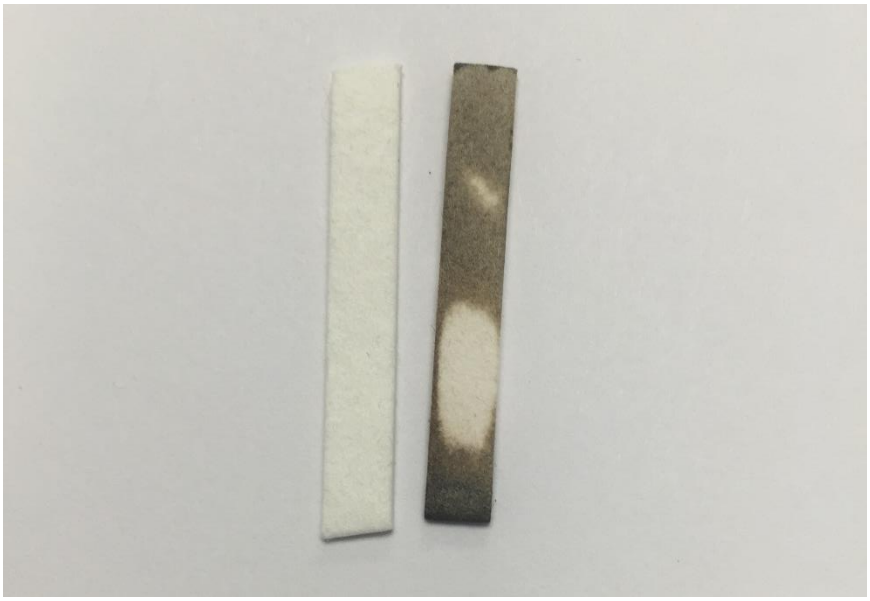

Figure 108: Lead acetate test for gas evolved from TPD from the unconditioned sample (left) and H_2S conditioned sample (right). Both CMS samples were pyrolyzed at 550 °C with 15 ppm Cl_2 in Ar atmosphere.

6.4 Discussion

It is seen from XPS of the chlorine fixed CMS, it can be conclusively said that the chlorine successfully reacts with the carbons at some part. The method was built based on scientifically known facts that (i) chlorine reacts with active carbon edges at high temperature during pyrolysis with the optimum between 400-600 °C [110, 115], and (ii) the reaction of chlorine with amorphous carbons is endothermic in the temperature range

of interest. It is known from literature that the amount of chlorine fixed on carbon blacks increases with increase in temperature. Papirer et al. reported Cl bonded to carbon blacks in the form of CCl, CCl_2 and CCl_3 groups [109]. In the case of carbon molecular sieves, the chlorine is envisioned to be bonded to the aromatic carbon in the strands of the CMS via electrophilic substitution reaction. A simplified scheme of the reaction is as follows:

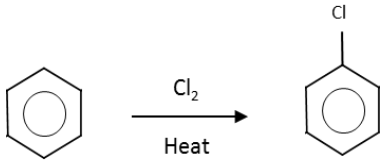

This reaction is likely practically irreversible around the pyrolysis temperature of CMS samples, and occurs at the ultramicropores.

$$C + Cl \longleftrightarrow C - Cl_{\text{complex}}$$

As noted earlier, another factor supporting the view that the chlorine primarily reacts at is ultramicropores is supported by the sorption isotherms of chlorine fixed CMS. It is seen that from Figure 98 that the sorption isotherms of CO_2 and CH_4 have a traditional Langmuir appearance and do no change significantly before and after conditioning with H_2S. This may suggest that unlike the neat CMS membranes, strands of the carbon chains comprising remaining ultramicropores in this case are much closer together, making reactive sites less accessible. Specifically, perhaps the chlorine fixation leads to the space within the ultramicropores being occupied by chlorine atoms, perhaps excluding gas sorption in this domain of the material. This is consistent with the fact that the sorption data under similar experimental conditions shows a better Langmuir fit than neat unaged

CMS membrane, which may be able to accommodate some sorption in the larger ultramicropores, prior to aging or chlorine exposure.

In the CMS structure itself, the ultramicropores are reasonably envisioned to comprise many strands of long rigid carbon entities arranged into defect-containing sheets, which are arranged randomly with each other (Figure 15 in Chapter 2). The chlorine is believed to react at the reactive edges of such ultramicropores to tune the CMS structure. The ability to exercise entropic control of diffusing components such as CO_2 vs. CH_4 is believed to be the key distinguishing feature of CMS [116], by reducing the degrees of freedom of the penetrant gas molecules, for instance CH_4 vs. CO_2, or CH_4 vs. N_2. When proper amount of chlorine is used, this tuning leads to lowering the permeability of the membrane with rise in selectivity. However, if excess chlorine is doped in combination with H_2S conditioning, both permeability and selectivity is seen to be lower than desired. This argument is, again, consistent with the need to use a possibly much lower concentration of chlorine (or O_2) in pyrolysis as discussed previously.

Additionally, the Langmuir constants for the gases can be compared from Table 10 and Table 13.

Table 16: Comparison of Langmuir constants after H_2S conditioning for pure gases. 6FDA:BPDA-DAM derived CMS samples from 550 °C pyrolysis

Gas	C'_H cc(STP)/cc(CMS)	b $psia^{-1}$
Before conditioning		
Unfixed CMS		
CO_2	164.4	0.016
CH_4	127.6	0.0044
Chlorine fixed CMS		
CO_2	148.4	0.036
CH_4	112.7	0.014
After conditioning		
Unfixed CMS		
CO_2	149.1	0.012
CH_4	109.3	0.0039
H_2S	174.93	0.0696
Chlorine fixed CMS		
CO_2	146.9	0.033
CH_4	109.87	0.014
H_2S	175.523	0.154

The affinity constant of H_2S is seen to be higher in the case of Cl_2 fixed CMS (b = 0.154), than the affinity constant of in case of CMS pyrolyzed without Cl_2 (b = 0.0696). It can be seen that while the hole filling capacities for both CO_2 and CH_4 start out higher for the unfixed CMS membrane, and these capacities decrease somewhat after the conditioning. However in the case of chlorine fixed CMS, this parameter is essentially unchanged before and after conditioning.

At this point it is not possible to definitively say much more about the nature of the chlorine treated CMS. Nevertheless, some reasonable "speculations" are felt to be justified and are offered here in this spirit to stimulate work by subsequent researchers who may pursue the chlorine treatment approach. The permeance and selectivity of CMS made with 30 ppm of chlorine was seen to drastically drop *after* H_2S conditioning, shown in Figure 96. It is felt to be unlikely that H_2S "double dopes" on chlorine by an actual formation of carbon-sulfur-chlorine bond.

Although sulfenyl chloride compounds are known, these are reactive and therefore unstable compounds. Moreover, a gas phase reaction of chlorine with H_2S is not reported. It does seem possible, however, for H_2S to hydrogen bond with the chlorine atoms attached at the selective ultramicropores, essentially blocking the way. A simplified schematic of this is shown in Figure 109. Moreover, this mechanism would explain the TPD results (on page 193).

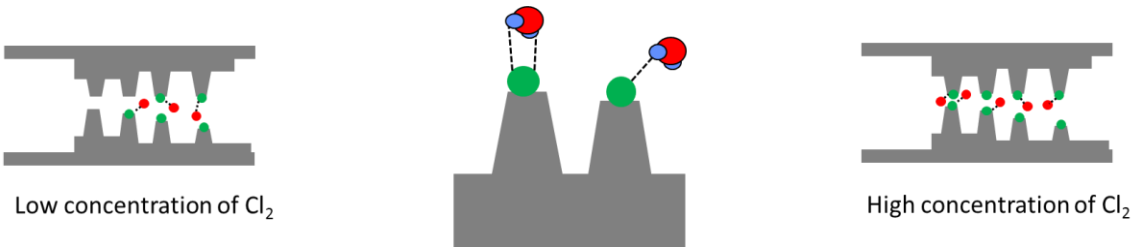

Figure 109: Simplified representation of H_2S hydrogen bonding with the chlorine fixed at the ultramicropores

This mechanism would suggest that after the TPD event, CO_2 and CH_4 permeance would rise, counter to what is usually seen upon thermal treatment that causes reduction of micropores and tightening of ultramicropores. Evidence for exactly this type of counter

intuitive response has been observed when an H_2S conditioned module was heated to 180 °C. Close to 60% of the initial unconditioned CO_2 permeance and selectivity was regained by this method. These results must be reproduced in future work to show the feasibility of this method for testable modules.

This hydrogen bonding affects the permeance of the CMS prepared with lower concentrations of chlorine as well, but at 30 ppm Cl_2 it appears to practically block all ultramicropores, thereby allowing essentially no transport of gases through the membrane. This could be a reason the permeance and selectivity both drop in the case of 30 ppm chlorine fixed CMS after H_2S conditioning.

Therefore, while chlorine fixation offers a tool in some cases, like O_2 doping it must be used carefully. It is in fact, unclear whether chlorine fixation is preferable tuning agent vs. O_2. Indeed, if O_2 can be used, it is probably a *more practical* tool given the complications of working with dilute Cl_2 vs. dilute O_2. In any case, if one starts with a much more open structure of CMS based on other 6FDA derived polymers, the H_2S conditioning may not have such a huge negative effect, and can either be employed despite the lost permeance or be tuned more carefully with chlorine fixation, and this appears to be the wisest path forward for future research.

6.5 Summary

An attempt was made to mitigate the negative effects of H_2S conditioning by doping the CMS membrane with chlorine. CMS fibers from both Matrimid® and 6FDA:BPDA-DAM were pyrolyzed in the presence of parts per millions of chlorine, and the reaction of chlorine with carbon was confirmed with XPS. Chlorine fixation by this method reduces the sorption coefficient of the CO_2 and CH_4 in the CMS membrane as compared to the

unfixed membrane, and increases the affinity of H_2S to the membrane. Chlorine fixation causes the permeance of gases through the membrane to drop as expected, with increase in CO_2/CH_4 selectivity. However, it was found that chlorine fixation does not completely diminish the effect of H_2S conditioning. A possible mechanism for the nature of interaction of H_2S with the chlorine fixed CMS was proposed.

CHAPTER 7 CONCLUSIONS AND FUTURE DIRECTIONS

Carbon molecular sieve (CMS) membranes, formed via the high temperature pyrolysis of polymeric precursor membranes, show excellent potential for CO_2 and H_2S acid gas separation from CH_4. In this project, the effect of sour gas on CMS membrane properties has been studied in detail for the first time. In collaboration with Shell Global Solutions, improved understanding of the interaction of H_2S with CMS was pursued with a goal of providing high CO_2 permeance while maintaining attractive selectivities for both CO_2 and H_2S relative to CH_4.

The research focused on identifying and optimizing key parameters to tune the CMS ultramicropore structure and morphology. Hollow fiber membranes were used to extract transport properties of CMS before and after exposure to high concentrations of H_2S. The specific aims were:

1. V-treatment: Engineer the asymmetric hollow fiber membranes to achieve superior separation properties before and after H_2S exposure.
2. H_2S conditioning: Obtain a fundamental understanding of interaction of H_2S with carbon molecular sieves.
3. Stabilization against H_2S: Engineer CMS hollow fiber membranes to resist aggressive sour gas feed conditions and characterize the membranes, to optimize separation performance.

7.1 Summary and conclusions

7.1.1 Optimization of V-treatment for scale up

For stopping CMS fiber substructure collapse, V-treatment process was identified on Matrimid® and 6FDA:BPDA-DAM hollow fibers. The process of V-treatment was developed by Bhuwania, but this work explored the key parameters leading to a better understanding of the mechanism and its potential for practical implementation. An optimization of the exposure time, exposure temperature, and concentration of treatment agent was performed and shown to prevent collapse under specific conditions. It was determined that the VTMS does not need direct access to the bore of the hollow fiber, and since it can diffuse through the skin layer and be effective in stopping the substructure collapse. Also, the time required for the V-treatment solution to diffuse through the skin was estimated and experimentally verified to be less than 5 minutes. These two factors together successfully reduce the total time required by the V-treatment, while adding *no extra steps* to the fiber formation process. This is particularly important for the scale up of the process, as V-treatment can be integrated in the solvent exchange step.

It was also proven that the V-treatment does not react with the polymer at a practical treatment temperatures, leading to a better understanding of V-treatment mechanism. Specifically, the process of V-treatment leads to an organo-silica layer deposited on the surface of the CMS fibers, adding a non-selective resistance to the gas transport through the membrane. In this work, two strategies were considered for reducing the amount of silica deposited on the outermost skin: KOH etching and washing with VTMS containing solvent. A proof of concept showed a practical means of minimizing the external deposit by washing with 5% VTMS solution, thereby increasing the permeance through the

membrane for Matrimid® derived CMS. A V-treatment concentration optimization was performed on 6FDA:BPDA-DAM based CMS fibers, and it was shown that any concentration in the range of 10% - 100% of VTMS in hexane ultimately prevented substructure collapse in the CMS hollow fiber. However, the permeance increase is not proportional to the corresponding decrease in separation layer thickness. A 5% VTMS post exposure wash was shown to be unnecessary for the case of the 6FDA:BPDA-DAM derived CMS. It is speculated that trace HF emissions during pyrolysis may make the deposited organo -silica layer sufficiently porous to add negligible added resistance — a benefit of the 6FDA containing precursor.

7.1.2 Benchmarking CMS performance in the presence of H_2S

The effect of pure gas and mixed gas H_2S was investigated on CMS hollow fiber membranes derived from Matrimid® and 6FDA:BPDA-DAM. CMS membranes lost 90% gas permeance in the presence of both pure gas and mixed gas H_2S conditioning feeds, and slightly increased CO_2/CH_4 selectivity. It was shown by a combination of FTIR, sorption change and loss of flux that H_2S chemically reacted with CMS even at room temperatures (35 °C). After H_2S conditioning, S_{H2S}/S_{CH4} sorption selectivity of CMS membranes is lower than that seen in glassy polymers with added functionalities that can interact with H_2S (CMS ~ 5, PEGMC glassy polymer ~ 8). On the other hand, the diffusion selectivity D_{H2S}/D_{CH4} is higher than that of essentially all known glassy polymers (CMS ~ 2.46, glassy polymers ~ 1) and rubbery polymers (~1).

It was also determined that in Matrimid® derived CMS, the H_2S reacts primarily in the ultramicropores, reducing the diffusion through the membrane with little change in

sorption. This trend leads not only to reduced permeance (90% drop) but also increased selectivity (2x). However, in the 6FDA:BPDA-DAM derived CMS, H_2S appears to react both in the micropores and the ultramicropores, reducing both the sorption capacity (10-15% drop) and the permeance (90% drop), with CO_2/CH_4 selectivity increase (1.3x). This difference in interaction of H_2S with Matrimid® and 6FDA:BPDA-DAM was possibly due to the extra availability of pyridinic nitrogens in the CMS derived from 6FDA:BPDA-DAM. The diffusion selectivity D_{CO2}/D_{CH4} of the CMS membrane increased as a result of H_2S conditioning. It was shown that H_2S can be partially removed from the CMS using thermally programmed desorption, and testing the evolved gas by lead acetate strips. A possible mechanism for the nature of interaction of H_2S with the CMS membrane was proposed in this work.

7.1.3 Development of novel mitigation tool

To mitigate this negative effect of H_2S conditioning, chlorine fixation was developed as a potential tool. This involved reacting chlorine with the carbon structure while the CMS was being formed, i.e. during the pyrolysis. Both Matrimid® and 6FDA:BPDA-DAM were pyrolyzed in the presence of parts per millions of chlorine, and the reaction of chlorine with carbon was confirmed with XPS. So called Cl_2-fixation alters the properties of 6FDA:BPDA-DAM derived CMS by tuning both ultramicropores and micropores. This is seen by an expected drop of CO_2 permeance (by 65%), and increase in selectivity (3.5x). Sorption selectivities S_{CO2}/S_{CH4} and S_{H2S}/S_{CH4} for the neat CMS membranes without chlorine fixation (2.75 and 4.96 respectively) were seen to be higher than those of chlorine fixed CMS membranes (1.76 and 2.56 respectively). Chlorine

fixation essentially reduces the access of CO_2 and H_2S to the pyridinic nitrogens, seen from the lower sorption selectivities for both CO_2 and H_2S over CH_4.

Chlorine fixation led to an increase the apparent affinity of H_2S to the membrane shown by doubling of the Langmuir affinity constant. The membrane also became more selective due to the molecular size sieving, since the chlorine tunes the sieving ultramicropores reducing their size. However, 50% of the starting permeance was still lost after H_2S conditioning, indicating that the membrane was only partially resistant to H_2S. The final value of CO_2 permeance after H_2S conditioning of this 15 ppm chlorine fixed fiber was 20.63 GPU with a CO_2/CH_4 selectivity of 179. The permeance is marginally better than the performance of CMS without chlorine fixation, however the selectivity is 3.5x higher. The H_2S was envisioned to strongly hydrogen bond with the chlorine atoms at the ultramicropores, thereby reducing the access of the penetrant gases like CO_2 and CH_4 to ultramicropores. Thermally programmed desorption was carried out to demonstrate that heating H_2S conditioned membrane could remove the H_2S from such a chlorine fixed CMS membrane, and was confirmed with a lead acetate test. While the chlorine fixation proved to be a tool for tuning the separation properties of the CMS, it did not completely stop the deteriorating effect of H_2S conditioning.

Also in an attempt to address the reduced flux of this membrane, chlorine fixation is combined with a permeance increasing technology, V-treatment. When a V-treated, chlorine fixed membrane was prepared, the permeance was not seen to rise as much as expected, but it was verified with SEM that the porous substructure was prevented from collapse. The observed lowered permeance, therefore, was attributed to the possible reaction between the silica gel and chlorine to form a vinyl chloride type of compound,

which provides additional resistance to gas transport. To avoid complications in the manufacture of the CMS membranes, it is best to find a way around chlorine fixation unless necessary.

Overall, this work has improved the basic understanding of the interaction of sour gas with CMS, which is a big step toward trying to mitigating the negative effects of sour gas. While this work hasn't provided a completely H_2S resistant CMS membrane, it suggests paths to follow for high performance membranes in sour gas applications. While CMS membrane may not completely replace amine absorption, they can supplement the absorption columns by removing the bulk of the impurities and providing a much cleaner starting feed stream for amine absorption. Overall, it makes a relatively clean fuel, natural gas, even cleaner to produce and therefore more accessible. In the long term, this will hopefully mean that natural gas is used much more as a fossil fuel than coal or other petroleum based fuel that leave a higher carbon footprint on the earth.

7.2 Recommendations

The first two research objectives of this work have been successfully achieved. Substantial contributions were made in the field of CMS membranes, on the front of higher throughput membranes for CO_2/CH_4 separation and understanding the behavior of CMS in $CO_2/H_2S/CH_4$ feed gases. Although the chlorine fixation made the CMS partially resistant, it had some disadvantages of its own. Much more work has to be done on this front. A few recommendations for future work are listed below.

7.2.1 Optimization of chlorine fixation and exploring other dopant molecules

More work to optimize the amount of chlorine required to achieve the best combination of permeance and selectivity, while also ensuring that all the reactive edges are neutralized might be useful. If this path is pursued, chlorine fixed membranes should be subjected to long tests of realistic harsh conditions. Other dopant molecules can also be evaluated for mitigating the H_2S conditioning. Bromine is a suitable candidate, but it may reduce permeances to unacceptable levels.

7.2.2 Other 6FDA based precursors

Although 6FDA:BPDA-DAM is an intrinsically open precursor, the chlorine fixation significantly reduces the average size of its ultramicropores. Using other 6FDA based polymer precursors that provide a much more open CMS structure will be particularly useful since helpful for tuning the properties of the membrane with chlorine. As a starting point, CMS membranes based on 6FD-mPDA/DABA may be used, which have exhibited permeability more than 14000 Barrer and CO_2/CH_4 selectivity above 50 [117]. In fact, a more open intrinsic structure may enable an effective "H_2S doping" for an intrinsically more open CMS from such a precursor to give industrially attractive permeance in presence of H_2S.

7.2.3 Detailed investigation of H_2S interaction with CMS

A second sorption isotherm for H_2S on CMS should be measured after the H_2S has completely conditioned the CMS membrane (during which the first sorption isotherm is measured). The Langmuir sorption capacity and affinity constant are both expected to reduce in the second sorption isotherm.

Furthermore, Section 5.5 indicates that H_2S might be undergoing an acid base reaction with the pyridinic nitrogens in the CMS structure obtained from 6FDA:BPDA-DAM. It is shown in literature that when polyimides are decomposed, N_2 can be evolved as a decomposition gas at high temperatures [118] (shown in Figure 110). If this N_2 evolves from the pyridinic nitrogens in the CMS structure, they can be eliminated in order to reduce interaction with H_2S in sour gas. As a starting point, techniques that may allow monitoring evolved gases from pyrolysis in situ can be used to detect the evolution of N_2.

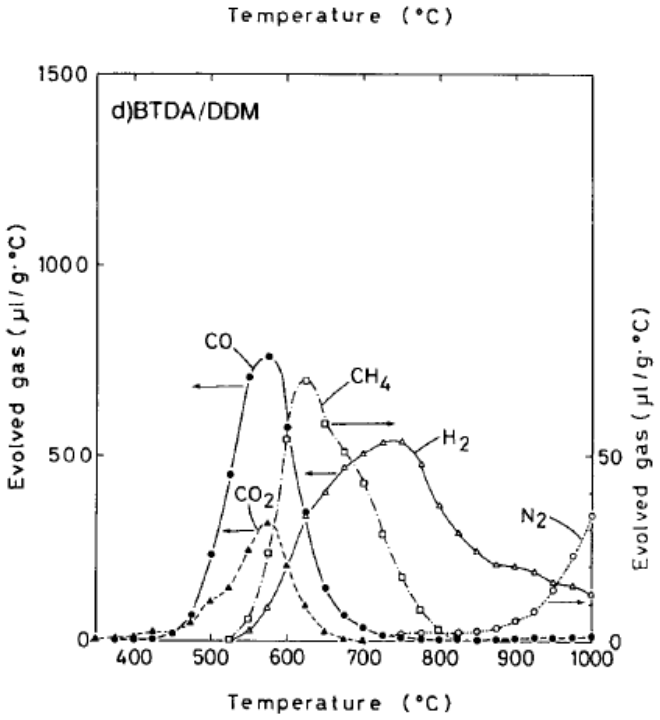

Figure 110: Evolution of decomposition gases with change in pyrolysis temperature

Using higher pyrolysis temperatures (> 900 °C) to eliminate the pyridinic nitrogens in the CMS structure that provide affinity to the H_2S should be explored. Removal of those nitrogens might prove to be favorable for our case, reducing the "poisoning" of membranes.

This, again, with a more open precursor may lead to attractive and relatively H_2S resistant CMS membranes.

7.2.4 Regenerating the performance at high temperature

The thermally programmed desorption shows that H_2S can be removed from the CMS structure by heating above 220 °C. Regeneration described in Section 6.4 showed that the lost permeance of CO_2 due to H_2S conditioning can be partially regained. Further tests should be performed to check whether testable modules can regain permeance, to show that H_2S conditioning on chlorine fixed CMS is reversible. Modules will have to be made using high temperature resistant epoxy so as to not fail at the regeneration temperatures.

7.2.5 Chlorine fixation and V-treatment

The performance of V-treated membranes pyrolyzed under Cl_2 atmosphere should be studied in detail. Whether the performance drop seen in section 6.2.2 is due to the chemical nature of the silica gel or whether it is a physical aging issue, can be further investigated. As a starting point, characterization techniques such as solid state NMR and XPS can help in understand this aspect.

7.2.6 Crosslinkable polymers for CMS formation

Kraftschik from the Koros group developed a novel crosslinking method for crosslinking 6FDA-based polyimides, which showed favorable sour gas separation performance. His PEGMC and PDMS post-treated membranes may be used as precursors for formation of CMS membranes. This may combine the high sorption selectivity of these membranes and

the high diffusion selectivity of CMS membranes to give attractive separation performance for H_2S/CH_4.

APPENDIX

This part of the thesis enlists experiments that is not key to the thesis, but were explored in interest of exploring new ideas with potential which eventually were not successful.

A.1. V-treatment of Dense Films

To supplement hollow fiber work by Bhuwania, with detailed insights on CMS permeability, solubility and diffusivity, this work considered V-treatment of dense films.

A.1.1. Soak in VTMS solution

A dense film of the desired polymer was cast using solution casting method. The polymer was first dried for 12 hours to remove any absorbed moisture, under vacuum at 120 °C. A 2 wt% solution was made from the dried powder by dissolving it in dichloromethane (>99.6%, Sigma Aldrich) in a 40 mL vial, and placed on a roller at room temperature for 12 hours to ensure complete mixing. The solution was then filtered using a 0.45 μm PTFE filter (Micropore Corporation) attached to 30 mL syringe and poured onto a Teflon disk at room temperature, as shown in Figure 111. The whole assembly of solution casting was kept on a leveled stage to ensure uniform thickness, inside a glove bag in a fume hood. A crystallization disk was used to cover the Teflon disk to enable a slower rate of evaporation, and two jars with excess dichloromethane were placed in the glove bag. The glove bag was sealed and purged with nitrogen, and it was allowed to saturate with dichloromethane by waiting at least for 2 hours before casting. Once the casting solution was poured, the dichloromethane from the polymer solution was allowed to completely evaporate over 3-4 days. Finally a vitrified film was removed and dried under vacuum at 120 °C for 12 hours to remove any residual solvent.

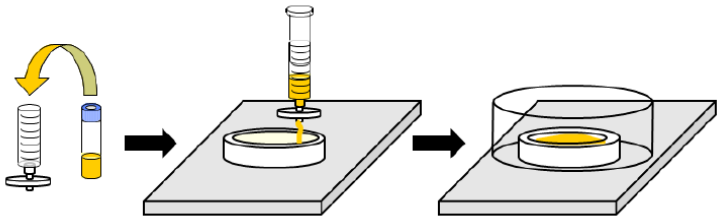

Figure 111: Schematic of solution casting method for formation of dense films [65]

The same procedure of V-treatment that was used on hollow was followed for dense films to find weight gain, as follows:

1. Once the dense film is formed and dried, 3 identical circular pieces were cut out using a die, and labeled as samples A, B, C.
2. The thickness of the films was measured at various points across the surface, and the average thickness was calculated.
3. The film was weighed (g), and the weight was recorded as the "Weight before soak".
4. The film was then soaked in 10 g of 10% VTMS solution in hexane in a vile, for 24 hours.
5. After 24 hours of soak, the film was removed from the solution and wiped dry with Kimwipes. The film was weighed again, and the weight was recorded as "Weight after soak".
6. The soaked film was exposed to 100% RH air for 24 hours, then and dried under vacuum at 150 °C for 24 hours.
7. The films were removed from the vacuum oven, and then weighed again. This weight was recorded as "Weight after humidity and drying".

8. The "Overall VTMS take up" was calculated in gram by subtracting "Weight before soak" from the "Weight after Humidity and soak", and then the percentage weight gain is calculated.

This experiment was performed on both Matrimid® and 6FDA:BPDA-DAM dense film, and the results of the take up are listed in Table 17.

Table 17: Take up of VTMS in 6FDA:BPDA-DAM and Matrimid® dense films

	6FDA:BPDA-DAM			Matrimid®		
	A	B	C	A	B	C
Avg thickness (mil)	425	461.67	431.67	348	358	326
Weight before soak (g)	0.0359	0.0374	0.0374	0.027	0.0255	0.0274
Weight after soak (g)	0.0455	0.0503	0.0496	0.0307	0.034	0.0346
Weight after exposure to humidity and drying (g)	0.04	0.0397	0.0391	0.04	0.0397	0.0391
Overall VTMS take up (g)	0.0041	0.0023	0.0017	0.013	0.0142	0.0117
Percentage take up	11.42	6.15	4.55	48.15	55.68	42.70

V-treatment on dense film precursors showed a lower percentage of weight gain in the 6FDA:BPDA-DAM dense film, which are somewhat reasonable. The result for uptake in Matrimid® is more surprising, since it shows a very high uptake of VTMS and is unaccompanied by change in the morphology of the dense film. This result is surprising and need to be rechecked and clarified for both the materials.

Therefore, a different way of incorporating the presence of VTMS in the dense films was explored, and is explained in the next section.

A.1.2. VTMS in casting solution

The idea was to overcome the diffusion barrier of thick dense films by casting the dense films with VTMS solution *present in the casting solution*. After all the solvent evaporated in the film casting process however, the films showed a complex morphology (Figure 112) and were not transparent.

Figure 112: Striations on Matrimid phase separated films after casting them with VTMS in casting solution.

The observed morphology appears to reflect phase separation occurring during the process of film casting. As the solvent dichloromethane (DCM) evaporated from the casting solution, the less volatile non-solvent in this case, VTMS, led to phase separation. This outcome violated our purpose of using dense films, which was to exploit the feature

of uniform thickness of dense films to understand the effect of V-treatment on change in permeability. Therefore, V-treatment of Matrimid® with the VTMS in the casting solution was shown to not be the best way to go forward, and the focus was shifted back to hollow fibers.

REFERENCES

1. Koros, W.J. and W.C. Madden, *Encyclopedia of Polymer Science and Technology* 3rd ed. 2004: John Wiley & Sons.
2. *International Energy Outlook 2010*, 2010, U.S. Energy Information Administration: Washington, D.C.
3. *International Energy Outlook 2011* 2011; Available from: http://www.eia.gov/forecasts/archive/ieo11/pdf/0484(2011).pdf.
4. *Hydrogen Sulfide, MSDS # 001029. [Material Safety Data Sheet]*. [cited 2010 26 April 2010]; Available from: http://www.airgas.com/documents/pdf/001029.pdf.
5. Baker, R.W. and K. Lokhandwala, *Natural Gas Processing with Membranes: An Overview.* Industrial & Engineering Chemistry Research, 2008. **47**(7): p. 2109-2121.
6. *Annual Energy Outlook 2015*. 2015; Available from: http://www.eia.gov/forecasts/aeo/pdf/0383(2015).pdf.
7. Hao, J., P.A. Rice, and S.A. Stern, *Upgrading low-quality natural gas with H2S- and CO2-selective polymer membranes: Part I. Process design and economics of membrane stages without recycle streams.* Journal of Membrane Science, 2002. **209**(1): p. 177-206.
8. Total, *Sour Gas: A History of Expertise* 2007
9. Amirkhanov, D., et al., *Hollow fibres for removal and concentration of hydrogen sulfide from gas mixtures by the membrane method.* Fibre Chemistry, 2001. **33**(1): p. 67-72.
10. Orme, C.J. and F.F. Stewart, *Mixed gas hydrogen sulfide permeability and separation using supported polyphosphazene membranes.* Journal of membrane science, 2005. **253**(1): p. 243-249.
11. Meyer, H.S., *Volume and Distribution of Subquality Natural Gas in the United States.* GasTIPS, 2000. **6**.
12. Ward, Z.T., et al., *Equilibrium Data of Gas Hydrates containing Methane, Propane, and Hydrogen Sulfide.* Journal of Chemical & Engineering Data, 2014. **60**(2): p. 424-428.
13. Legault, A., *Mainstreaming Efficient Industrial Separation Systems.* International Energy Agency (IEA) OPEN Energy Technology Bulletin, 2008(55).
14. Bhide, B.D., A. Voskericyan, and S.A. Stern, *Hybrid processes for the removal of acid gases from natural gas.* Journal of Membrane Science, 1998. **140**(1): p. 27-49.
15. Achoundong, C.S.K., *Engineering economical membrane materials for aggressive sour gas separations*, 2013, Georgia Institute of Technology: Atlanta, GA, USA.
16. Baker, R.W. and K.A. Lokhandwala, *Acid gas fractionation process for fossil fuel gasifiers*, 1996, Google Patents.
17. Lokhandwala, K.A.M.P., CA), Baker, Richard W. (Palo Alto, CA), *Sour gas treatment process including membrane and non-membrane treatment steps*, 1995, Membrane Technology and Research, Inc. (Menlo Park, CA): United States.
18. Klass, D.L. and C.D. Landahl, *Gas sweetening by membrane permeation*, 1985, Google Patents.

19. Cooley, T. and A. Coady, *Removal of H2S and/or CO2 from a light hydrocarbon stream by use of gas permeable membrane.* US Patent A, 1978. **4130403**: p. 19.
20. Eldridge, R.B., *Olefin/paraffin separation technology: a review.* Industrial & engineering chemistry research, 1993. **32**(10): p. 2208-2212.
21. Worrell, E., et al., *Energy use and energy intensity of the US chemical industry.* Lawrence Berkeley National Laboratory, 2000.
22. Chenar, M.P., et al., *Removal of hydrogen sulfide from methane using commercial polyphenylene oxide and Cardo-type polyimide hollow fiber membranes.* Korean Journal of Chemical Engineering, 2011. **28**(3): p. 902-913.
23. Baker, R.W., *Future Directions of Membrane Gas Separation Technology.* Industrial & Engineering Chemistry Research, 2002. **41**(6): p. 1393-1411.
24. Kraftschik, B.E., *Advanced Crosslinkable Polyimide Membranes for Aggressive Sour Gas Separations.* 2013.
25. Robeson, L.M., *Correlation of separation factor versus permeability for polymeric membranes.* Journal of Membrane Science, 1991. **62**(2): p. 165-185.
26. Robeson, L.M., *The upper bound revisited.* Journal of Membrane Science, 2008. **320**(1–2): p. 390-400.
27. Chen, C.-C., *Thermally crosslinked polyimide hollow fiber membranes for natural gas purification*, 2011, Georgia Institute of Technology: Atlanta, GA, USA.
28. Clausi, D.T., *Formation and characterization of asymmetric polyimide hollow fiber membranes for gas separations*. 1998.
29. *Nitrogen Membranes - Technology*. 2010 [cited 2010 3 December]; Available from: http://www.medal.airliquide.com/en/nitrogen-membranes/nitrogen-membranes-technology.html.
30. Baker, R.W., *Membrane Technology and Applications*. 2 ed. 2004, West Sussex: John Wiley & Sons, Ltd.
31. Xu, L., M. Rungta, and W.J. Koros, *Matrimid® derived carbon molecular sieve hollow fiber membranes for ethylene/ethane separation.* Journal of Membrane Science, 2011. **380**(1–2): p. 138-147.
32. Kemmerlin, R., *Carbon Molecular Sieve membranes for aggressive sour gas separations*, 2012, Georgia Institute of Technology: Atlanta, GA.
33. Hines, A.L., R.N. Maddox, and P. Hall, *Mass transfer: fundamentals and applications*. Vol. 434. 1985: Prentice-Hall Englewood Cliffs, NJ.
34. Cussler, E.L., *Diffusion: mass transfer in fluid systems*. 1997: Cambridge university press.
35. Koros, W.J., *Membranes: learning a lesson from nature.* Chemical engineering progress, 1995. **91**(10).
36. Koros, W.J. and G.K. Fleming, *Membrane-based gas separation.* Journal of Membrane Science, 1993. **83**(1): p. 1-80.
37. Steel, K.M., *Carbon membranes for challenging gas separations*, 2000, The University of Texas at Austin: Austin TX, USA.
38. Koros, W.J., *Barrier polymers and structures*. Vol. 423. 1990: Amer Chemical Society.
39. Pierson, H., *Handbook of Carbon, Graphite, Diamond, and Fullerenes, Processing, Properties and Applications*, 1993, Noyes publications New York:.

40. Singh-Ghosal, A. and W.J. Koros, *Energetic and Entropic Contributions to Mobility Selectivity in Glassy Polymers for Gas Separation Membranes.* Industrial & Engineering Chemistry Research, 1999. **38**(10): p. 3647-3654.
41. Fu, Y.-J., et al., *Development and characterization of micropores in carbon molecular sieve membrane for gas separation.* Microporous and Mesoporous Materials, 2011. **143**(1): p. 78-86.
42. Park, H.B., et al., *Relationship between chemical structure of aromatic polyimides and gas permeation properties of their carbon molecular sieve membranes.* Journal of Membrane Science, 2004. **229**(1): p. 117-127.
43. Chen, J., et al., *The structural characterization of a CMS membrane using Ar sorption and permeation.* Journal of Membrane Science, 2009. **335**(1): p. 1-4.
44. Steel, K.M. and W.J. Koros, *Investigation of porosity of carbon materials and related effects on gas separation properties.* Carbon, 2003. **41**(2): p. 253-266.
45. Campo, M., F. Magalhaes, and A. Mendes, *Comparative study between a CMS membrane and a CMS adsorbent: Part I—Morphology, adsorption equilibrium and kinetics.* Journal of Membrane Science, 2010. **346**(1): p. 15-25.
46. Ismail, A.F. and L. David, *A review on the latest development of carbon membranes for gas separation.* Journal of membrane science, 2001. **193**(1): p. 1-18.
47. Suda, H. and K. Haraya, *Gas permeation through micropores of carbon molecular sieve membranes derived from Kapton polyimide.* The Journal of Physical Chemistry B, 1997. **101**(20): p. 3988-3994.
48. Singh, A., *Membrane materials with enhanced selectivity: an entropic interpretation. Austin TX USA, The University of Texas at Austin*, 1997, Ph. D. thesis.
49. Williams, P., *Analysis of factors influencing the performance of CMS membranes for gas separation. Atlanta GA USA, Georgia Institute of Technology*, 2006, Ph. D. thesis.
50. Wijmans, J.G. and R.W. Baker, *The solution-diffusion model: a review.* Journal of Membrane Science, 1995. **107**(1-2): p. 1-21.
51. Kärger, J. and D.M. Ruthven, *Diffusion in Zeolites and other microporous solids John Wiley & Sons.* New York, 1992: p. 467.
52. Clausi, D.T. and W.J. Koros, *Formation of defect-free polyimide hollow fiber membranes for gas separations.* Journal of Membrane Science, 2000. **167**(1): p. 79-89.
53. Pinnau, I.A., TX), Koros, William J. (Austin, TX), *Defect-free ultrahigh flux asymmetric membranes*, 1990, Board Regents The University of Texas System (Austin, TX): United States.
54. Saufi, S.M. and A.F. Ismail, *Fabrication of carbon membranes for gas separation - a review.* Carbon, 2004. **42**(2): p. 241-259.
55. Koresh, J.E. and A. Sofer, *Molecular sieve carbon permselective membrane. Part I. Presentation of a new device for gas mixture separation.* Separation Science and Technology, 1983. **18**(8): p. 723-734.
56. Fuertes, A.B. and I. Menendez, *Separation of hydrocarbon gas mixtures using phenolic resin-based carbon membranes.* Separation and purification technology, 2002. **28**(1): p. 29-41.

57. Acharya, M. and H.C. Foley, *Spray-coating of nanoporous carbon membranes for air separation.* Journal of membrane science, 1999. **161**(1): p. 1-5.
58. David, L. and A. Ismail, *Influence of the thermastabilization process and soak time during pyrolysis process on the polyacrylonitrile carbon membranes for O 2/N 2 separation.* Journal of membrane science, 2003. **213**(1): p. 285-291.
59. Centeno, T.A. and A.B. Fuertes, *Carbon molecular sieve gas separation membranes based on poly (vinylidene chloride-co-vinyl chloride).* Carbon, 2000. **38**(7): p. 1067-1073.
60. Fuertes, A., D. Nevskaia, and T. Centeno, *Carbon composite membranes from Matrimid® and Kapton® polyimides for gas separation.* Microporous and Mesoporous materials, 1999. **33**(1): p. 115-125.
61. Jones, C.W. and W.J. Koros, *Caron molecular-sieve gas separation membranes-I. Preparation and characterization based on polyimide precursors.* Carbon, 1994. **32**(8): p. 1419-1425.
62. Kiyono, M., *Carbon Molecular Sieve membranes for natural gas separations*, 2010, Georgia Institute of Technology.
63. Kim, Y.K., et al., *The gas separation properties of carbon molecular sieve membranes derived from polyimides having carboxylic acid groups.* Journal of membrane science, 2004. **235**(1): p. 139-146.
64. Vu, D.Q., *Formation and characterization of asymmetric carbon molecular sieves and mixed matrix membranes for natural gas purification*, 2001, University of Texas at Austin: Austin, TX, USA.
65. Rungta, M., *Carbon molecular sieve dense film membranes for ethylene/ethane separations.* 2012.
66. Xu, L., *Carbon molecular sieve hollow fiber membranes for olefin/paraffin separations.* 2013.
67. Steel, K.M. and W.J. Koros, *An investigation of the effects of pyrolysis parameters on gas separation properties of carbon materials.* Carbon, 2005. **43**(9): p. 1843-1856.
68. Vu, D.Q., W.J. Koros, and S.J. Miller, *High pressure CO_2/CH_4 separation using carbon molecular sieve hollow fiber membranes.* Industrial & Engineering Chemistry Research, 2002. **41**(3): p. 367-380.
69. Rungta, M., et al., *Membrane-based ethylene/ethane separation: The upper bound and beyond.* AIChE Journal, 2013. **59**(9): p. 3475-3489.
70. Geiszler, V.C. and W.J. Koros, *Effects of polyimide pyrolysis conditions on carbon molecular sieve membrane properties.* Industrial & engineering chemistry research, 1996. **35**(9): p. 2999-3003.
71. Geiszler, V.C., *Polyimide precursors for carbon molecular sieve membranes*. 1997.
72. Kiyono, M., P.J. Williams, and W.J. Koros, *Effect of pyrolysis atmosphere on separation performance of carbon molecular sieve membranes.* Journal of Membrane Science, 2010. **359**(1–2): p. 2-10.
73. Grisdale, R., *The properties of carbon contacts.* Journal of Applied Physics, 1953. **24**(10): p. 1288-1296.
74. Kusuki, Y., et al., *Gas permeation properties and characterization of asymmetric carbon membranes prepared by pyrolyzing asymmetric polyimide hollow fiber membrane.* Journal of Membrane Science, 1997. **134**(2): p. 245-253.

75. Okamoto, K.-i., et al., *Olefin/paraffin separation through carbonized membranes derived from an asymmetric polyimide hollow fiber membrane.* Industrial & engineering chemistry research, 1999. **38**(11): p. 4424-4432.
76. Tin, P.S., et al., *Novel approaches to fabricate carbon molecular sieve membranes based on chemical modified and solvent treated polyimides.* Microporous and mesoporous materials, 2004. **73**(3): p. 151-160.
77. Fuertes, A.B., *Effect of air oxidation on gas separation properties of adsorption-selective carbon membranes.* Carbon, 2001. **39**(5): p. 697-706.
78. Soffer, A., et al., *Method of improving the selectivity of carbon membranes by chemical carbon vapor deposition*, 1997, Google Patents.
79. Singh, R. and W.J. Koros, *Carbon molecular sieve membrane performance tuning by dual temperature secondary oxygen doping (DTSOD).* Journal of Membrane Science, 2013. **427**: p. 472-478.
80. Chatterjee, G., A.A. Houde, and S.A. Stern, *Poly(ether urethane) and poly(ether urethane urea) membranes with high H2S/CH4 selectivity.* Journal of Membrane Science, 1997. **135**(1): p. 99-106.
81. Bos, A., et al., *Plasticization-resistant glassy polyimide membranes for CO2/CO4 separations.* Separation and Purification Technology, 1998. **14**(1-3): p. 27-39.
82. Medal Technology and Research, I., *Low-Quality Natural Gas Sulfur Removal/Recovery*, 1998, The Department of Energy: Morgantown, WV.
83. Mohammadi, T., et al., *Acid Gas Permeation Behavior Through Poly(Ester Urethane Urea) Membrane.* Industrial & Engineering Chemistry Research, 2008. **47**(19): p. 7361-7367.
84. Sridhar, S., B. Smitha, and T.M. Aminabhavi, *Separation of Carbon Dioxide from Natural Gas Mixtures through Polymeric Membranes—A Review.* Separation & Purification Reviews, 2007. **36**(2): p. 113-174.
85. Wind, J.D., D.R. Paul, and W.J. Koros, *Natural gas permeation in polyimide membranes.* Journal of Membrane Science, 2004. **228**(2): p. 227-236.
86. Kraftschik, B. and W.J. Koros, *Cross-linkable polyimide membranes for improved plasticization resistance and permselectivity in sour gas separations.* Macromolecules, 2013. **46**(17): p. 6908-6921.
87. Achoundong, C.S., et al., *Silane modification of cellulose acetate dense films as materials for acid gas removal.* Macromolecules, 2013. **46**(14): p. 5584-5594.
88. Xu, L., et al., *Olefins-selective asymmetric carbon molecular sieve hollow fiber membranes for hybrid membrane-distillation processes for olefin/paraffin separations.* Journal of Membrane Science, 2012. **423**: p. 314-323.
89. Rungta, M., L. Xu, and W.J. Koros, *Carbon molecular sieve dense film membranes derived from Matrimid® for ethylene/ethane separation.* Carbon, 2012. **50**(4): p. 1488-1502.
90. Bhuwania, N., *Engineering the Morphology of Carbon Molecular Sieve (CMS) Hollow Fiber Membranes.* 2013.
91. Damle, S. and W.J. Koros, *Permeation Equipment for High-Pressure Gas Separation Membranes.* Industrial & Engineering Chemistry Research, 2003. **42**(25): p. 6389-6395.

92. Koros, W.J. and D. Paul, *Design considerations for measurement of gas sorption in polymers by pressure decay.* Journal of Polymer Science: Polymer Physics Edition, 1976. **14**(10): p. 1903-1907.
93. Gulbransen, E.A. and K.F. Andrew, *Kinetics of the Oxidation of Chromium.* Journal of the electrochemical Society, 1957. **104**(6): p. 334-338.
94. Lillerud, K. and P. Kofstad, *On high temperature oxidation of chromium I. Oxidation of annealed, thermally etched chromium at 800–1100 C.* Journal of the electrochemical society, 1980. **127**(11): p. 2397-2410.
95. Ning, X., *Carbon Molecular Sieve Membranes for Nitrogen/Methane Separation.* 2014.
96. Bhuwania, N., et al., *Engineering substructure morphology of asymmetric carbon molecular sieve hollow fiber membranes.* Carbon, 2014. **76**: p. 417-434.
97. Baney, R.H., et al., *Silsesquioxanes.* Chemical Reviews, 1995. **95**(5): p. 1409-1430.
98. Feher, F.J., D.A. Newman, and J.F. Walzer, *Silsesquioxanes as models for silica surfaces.* Journal of the American Chemical Society, 1989. **111**(5): p. 1741-1748.
99. Douskey, M., et al., *Spectroscopic studies of a novel cyclic oligomer with pendant alkoxysilane groups.* Progress in organic coatings, 2002. **45**(2): p. 145-157.
100. Zhang, Q., et al., *Permeable silica shell through surface-protected etching.* Nano letters, 2008. **8**(9): p. 2867-2871.
101. Williams, K.R. and R.S. Muller, *Etch rates for micromachining processing.* Microelectromechanical Systems, Journal of, 1996. **5**(4): p. 256-269.
102. Bird, R.B., W.E. Stewart, and E.N. Lightfoot, *Transport phenomena. 1960.* Madison, USA, 1960.
103. Puri, B.R. and R.S. Hazra, *Carbon-sulphur surface complexes on charcoal.* Carbon, 1971. **9**(2): p. 123-134.
104. Papirer, E., V.T. Nguyen, and J.-B. Donnet, *Introduction of sulfur groups onto the surface of carbon blacks.* Carbon, 1978. **16**(2): p. 141-144.
105. Papirer, E., S. Li, and A. Vidal, *Formation of carbon black-sulfur surface derivatives by reaction with P 2 S 5.* Carbon, 1991. **29**(7): p. 963-968.
106. Mayer, R., et al., *Base-Catalysed Reactions of Ketones with Hydrogen Sulfide.* Angewandte Chemie International Edition in English, 1963. **2**(7): p. 370-373.
107. Jou, F.Y., A.E. Mather, and F.D. Otto, *Solubility of hydrogen sulfide and carbon dioxide in aqueous methyldiethanolamine solutions.* Industrial & Engineering Chemistry Process Design and Development, 1982. **21**(4): p. 539-544.
108. Rivas, O. and J. Prausnitz, *Sweetening of sour natural gases by mixed-solvent absorption: Solubilities of ethane, carbon dioxide, and hydrogen sulfide in mixtures of physical and chemical solvents.* AIChE Journal, 1979. **25**(6): p. 975-984.
109. Papirer, E., et al., *XPS study of the halogenation of carbon black—Part 2. Chlorination.* Carbon, 1995. **33**(1): p. 63-72.
110. Puri, B.R. and R.C. Bansal, *Studies in surface chemistry of carbon blacks Part IV. Interaction of carbon blacks with gaseous chlorine.* Carbon, 1967. **5**(2): p. 189-194.
111. Brockway, L. and H. Jenkins, *The Molecular Structures of the Methyl Derivatives of Silicon, Germanium, Tin, Lead, Nitrogen, Sulfur and Mercury and the Covalent Radii of the Non-Metallic Elements.* Journal of the American Chemical Society, 1936. **58**(10): p. 2036-2044.

112. Pauling, L., *Atomic radii and interatomic distances in metals.* Journal of the American Chemical Society, 1947. **69**(3): p. 542-553.
113. Sanderson, H., R. Thomas, and M. Katz, *Limitations of the lead acetate impregnated paper tape method for hydrogen sulfide.* Journal of the Air Pollution Control Association, 1966. **16**(6): p. 328-330.
114. Gilardi, E.F. and R.M. Manganelli, *A laboratory study of a lead acetate-tile method for the quantitative measurement of low concentrations of hydrogen sulfide.* Journal of the Air Pollution Control Association, 1963. **13**(7): p. 305-309.
115. Nakamura, A., et al., *Effect of chlorine treatment on adsorption properties of phenol–formaldehyde resin-derived char.* Carbon, 2000. **38**(9): p. 1361-1367.
116. Singh-Ghosal, A. and W. Koros, *Air separation properties of flat sheet homogeneous pyrolytic carbon membranes.* Journal of Membrane Science, 2000. **174**(2): p. 177-188.
117. Qiu, W., et al., *Gas Separation Performance of Carbon Molecular Sieve Membranes Based on 6FDA-mPDA/DABA (3: 2) Polyimide.* ChemSusChem, 2014. **7**(4): p. 1186-1194.
118. Inagaki, M., T. Ibuki, and T. Takeichi, *Carbonization behavior of polyimide films with various chemical structures.* Journal of applied polymer science, 1992. **44**(3): p. 521-525.

VITA

Shweta Karwa was born on February 19th, 1990 and brought up in Nashik, India. She completed her schooling in Nashik and Pune, and moved to Mumbai for her undergraduate studies. She attended Institute of Chemical Technology for undergraduate studies, where she completed her Bachelors in Intermediates and Dyestuff Technology in 2011. She enrolled in the School of Chemical and Biomolecular Engineering at Georgia Institute of Technology in Atlanta, GA as a PhD student under the guidance of Dr. William Koros. Her other interests include caving, traveling and outdoor activities. After completion of her PhD, she will join Shell Oil Company as a Research Engineer in Houston.